PALOS VERDES LANDFILL
REMEDIAL INVESTIGATION REPORT

APPENDIX E.2

HYDROGEOLOGIC MODELING REPORT
(DAMES & MOORE, INC.)

HYDROGEOLOGIC MODELING
FOR REMEDIAL INVESTIGATION/FEASIBILITY STUDY,
GROUNDWATER FLOW MODEL
PALOS VERDES LANDFILL
FOR
COUNTY SANITATION DISTRICTS
OF LOS ANGELES COUNTY

DAMES & MOORE, INC.
March 17, 1993

DAMES & MOORE

6 HUTTON CENTRE DRIVE, SUITE 700
SANTA ANA, CALIFORNIA 92707
(714) 433-2000

A:128\csdpvlf.fnl

DAMES & MOORE
3602 INLAND EMPIRE BLVD., SUITE C-110, ONTARIO, CALIFORNIA 91764
(909) 980-4000 FAX: (909) 980-1399

March 16, 1993
12482-010-128

COUNTY SANITATION DISTRICTS
OF LOS ANGELES COUNTY
1955 Workman Mill Road
Post Office Box 4998
Whittier, California 90607-4998

Attention: Ms. Mary Jo Jacobs
Project Manager

Submittal of Final Report for
Hydrogeologic Modeling at the
Palos Verdes Landfill, California

Ladies and Gentlemen:

Dames & Moore is pleased to submit our Final Report titled "Hydrogeologic Modeling for Remedial Investigation/Feasibility Study, Groundwater Flow Model, Palos Verdes Landfill, dated March 17, 1993. This study has been prepared under the direct supervision of Mr. N. Thomas Sheahan, a California Certified Engineering Geologist, and a California Registered Geophysicist. In preparing this report, Dames & Moore has employed the expertise of scientists and engineers with experience in the evaluation and execution of comprehensive groundwater modeling investigations. Both peer review and quality assurance/quality control review measures have been employed to ensure that this document adequately reflects the data available and that it is complete and appropriately interpreted. The data and information in this report and the professional opinions expressed are presented, within the limits prescribed by the client, in accordance with generally accepted professional engineering and scientific principles and practice. If you have any questions regarding this Final Report, please do not hesitate to give us a call.

Respectfully submitted,

DAMES & MOORE, INC.

N. Thomas Sheahan, C.E.G. #307
Managing Principal-in-Charge

Enclosures

HYDROGEOLOGIC MODELING
FOR REMEDIAL INVESTIGATION/FEASIBILITY STUDY,

GROUNDWATER FLOW MODEL

PALOS VERDES LANDFILL

FOR

COUNTY SANITATION DISTRICTS OF LOS ANGELES COUNTY

BY

DAMES & MOORE, INC.
6 HUTTON CENTRE DRIVE, SUITE 700
SANTA ANA, CALIFORNIA 92707

March 17, 1993

A:128\csdpvlf.fnl

COUNTY SANITATION DISTRICTS
OF LOS ANGELES COUNTY

GENERAL MANAGER

Charles W. Carry, P.E.
Chief Engineer

SUPERVISOR

Chi-Chung Tang, Ph.D., P.E.
Supervising Engineer

PROJECT MANAGER

Mary Jo Jacobs
Project Engineer

PROJECT TEAM

Mercedes Murillo, R.G., C.E.G.	**Lead Geologist**
John Hower	**Project Geologist**
Ethan Laden	**Project Engineer**
Steve Carr	**Senior Chemist**

A:128\csdpvlf.fnl

DAMES & MOORE PROJECT TEAM

PROJECT DIRECTOR

N. Thomas Sheahan, R.G., C.E.G., R.Gp.
Managing Principal-in-Charge

PROJECT MANAGER

Varut Guvanasen, Ph.D., P.E.
Senior Engineer

PROFESSIONAL STAFF

Ijaz Jamall, Ph.D., D.A.B.T.	Principal Toxicologist
Essi E. Esmaili, Ph.D., R.G.	Senior Geochemist
Nancy J. Darigo, R.G.	Senior Geologist
Alix Robertson, Ph.D.	Senior Statistician
David M. Johnson	Project Hydrogeologist
Theodore A. Johnson	Project Hydrogeologist
Anthony P. Kirk	Staff Geologist
John L. Daverin	Assistant Geologist

TECHNICAL AND ADMINISTRATIVE STAFF

Deanna M. Bauhard	Administrative Manager
Ann L. Shea	Librarian

A:128\csdpvlf.fnl

TABLE OF CONTENTS

TABLE OF CONTENTS (Continued)

APPENDICES

A. References
B. Technical References on Hydrogeologic Models
C. Plots of Sensitivity/Uncertainty Analysis Cases
D. Statistics of Sensitivity/Uncertainty Analyses
E. Statistics of Hydraulic Conductivity Analyses
F. Glossary of Selected Technical Terms
G. Hydrographs of Selected Wells
H. Distributions of Hydraulic Conductivity and Porosity Values
I. Gradient across the Palos Verdes Fault Zone

LIST OF TABLES

LIST OF FIGURES

LIST OF FIGURES (Continued)

HYDROGEOLOGIC MODELING

FOR REMEDIAL INVESTIGATION/FEASIBILITY STUDY, PALOS VERDES LANDFILL

GROUNDWATER FLOW MODEL

1.0 INTRODUCTION

The Palos Verdes Landfill (PVLF) is one of six landfills currently operated by the County Sanitation Districts of Los Angeles County (Sanitation Districts). Of these landfills, four are active and two are inactive, including the PVLF.

The Sanitation Districts are currently conducting a Remedial Investigation/Feasibility Study (RI/FS) of the PVLF under the oversight of the California EPA Department of Toxic Substances Control (DTSC). To assist in the preparation of the RI/FS, the Sanitation Districts have engaged the services of Dames & Moore to develop a groundwater flow model to simulate hydrogeologic conditions present at the site. Dames & Moore will also be developing a contaminant transport model to be used in conjunction with this flow model. These models will, in turn, be used by Dames & Moore in a subsequent health risk assessment study. The overall work being performed by Dames & Moore is described in our proposal to the Sanitation Districts dated July 22, 1991, and includes four main tasks.

- Task 1 -- Review of Existing Literature and Data

- Task 2 -- Groundwater Flow Modeling

- Task 3 -- Contaminant Transport Modeling

- Task 4 -- Baseline Risk Assessment

This report presents the results of Tasks 1 and 2 above, and focuses on the groundwater flow modeling. Tasks 3 and 4 will be presented in subsequent reports.

1.1 BACKGROUND

The inactive PVLF site is located at 25706 Hawthorne Boulevard, Rolling Hills Estates, California. It is situated topographically within the north-facing foothills of the Palos Verdes peninsula in the south-central portion of Los Angeles County. The PVLF consists of six parcels of land comprising a total area of approximately 291 acres. The area surrounding the PVLF is dominated by residential development with some scattered commercial and industrial uses including sand and gravel quarrying operations. Figures 1.1 and 1.2 show the model area (study area) and PVLF site area, respectively.

Prior to its use as a landfill, the site was the location of mining operations for diatomaceous earth. Conducted since the early 1900s, these mining operations were usually open-pit mines. The first landfill operations began on Parcel 1 in 1952. These continued on a small scale until 1957 when the Sanitation Districts began operation of a Class II municipal waste disposal unit. This parcel was closed in 1965 and subsequently developed as the South Coast Botanic Garden. Parcel 4 accepted inert wastes. Other parcels were opened as Class I and Class II disposal areas. Portions of parcels 2, 3, and 5, and all of parcel 6 were operated as Class I disposal sites receiving hazardous materials from April 1964 through October 1980. The remainder of the site continued receiving municipal waste until December 31, 1980, when the PVLF reached its final design capacity.

1.2 PURPOSE, SCOPE, AND OBJECTIVE

The Sanitation Districts and DTSC entered into an enforceable agreement on March 31, 1988, under which the Sanitation Districts agreed to perform a series of studies to investigate the nature and extent of environmental contamination that may potentially be emanating from the PVLF. The Sanitation Districts are currently conducting studies in accordance with a Hydrogeologic Characterization Plan (HCP) that defines four phases of work for investigation of the geologic and hydrogeologic conditions in the vicinity of the PVLF. The primary purpose of the groundwater flow modeling performed by Dames & Moore is to assist the Sanitation Districts in characterizing groundwater flow for a portion of the HCP, and to provide a hydrogeological framework for subsequent contaminant transport modeling and risk assessment at potential offsite receptors.

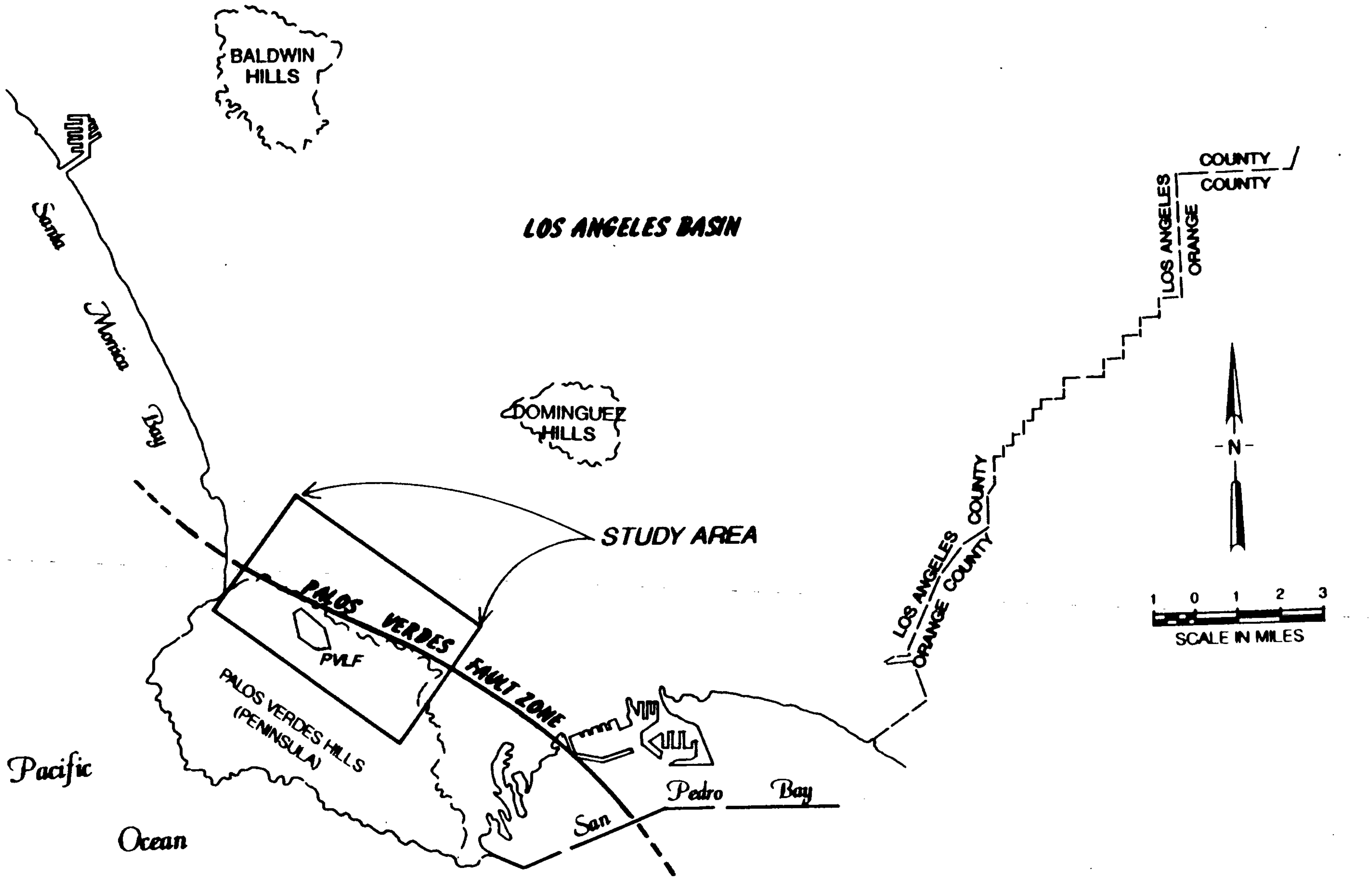

FIGURE 1.1
Project Location Map

DAMES & MOORE

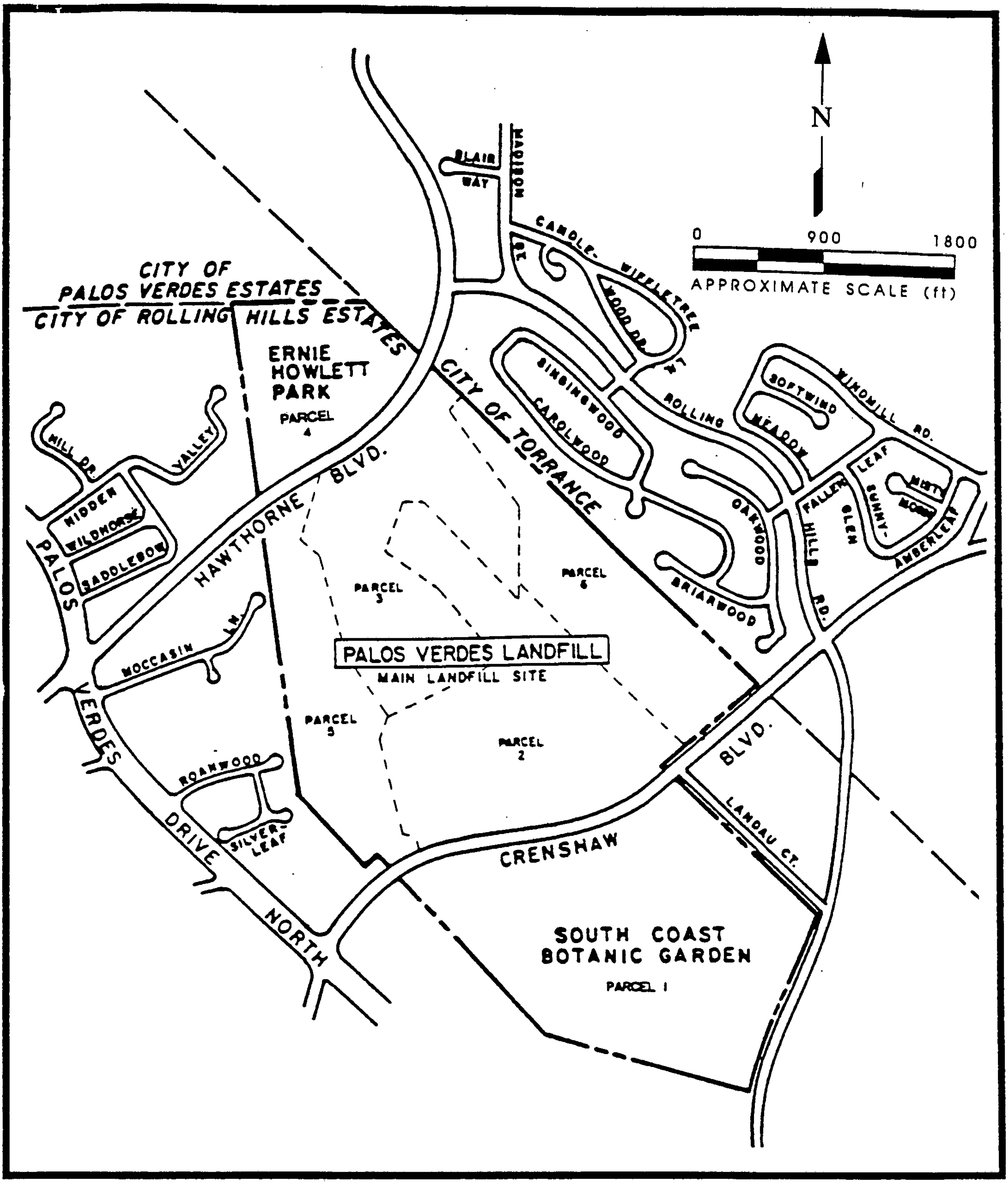

Figure 1.2
PVLF SITE MAP

Specific tasks involved in development of the groundwater flow model are listed below.

- Review available published and unpublished literature on the PVLF and study area.

- Review and provide data selection input for the Sanitation Districts' geologic model of the study area.

- Conceptualize the appropriate groundwater flow model.

- Select a groundwater flow model in consideration of:

  - Objective criteria;
  - Technical criteria;
  - Implementation criteria; and
  - Historical application criteria.

- Define the nature and relationships of aquifer properties.

- Evaluate the impact of Monterey Formation and related natural hydrocarbon deposits on groundwater flow.

- Develop and calibrate the detailed groundwater flow model including:

  - Code verification;
  - Model construction; and
  - Model verification/calibration.

- Perform sensitivity/uncertainty analysis of the calibrated groundwater flow model.

- Prepare a report of findings.

This portion of the study has as its main objective to develop a groundwater flow model representative of the hydrogeologic conditions within the study area, and to simulate groundwater flow in the subsurface for a better understanding of this flow system. The groundwater flow model is intended to form the basis for subsequent contaminant transport modeling and baseline health risk assessment at the PVLF, both of which will be performed in the future and discussed in separate reports.

This report is organized in the following fashion: Section 1.0 introduces the report and presents the Purpose, Scope, and main Objective of the study; Section 2.0 provides a review of the existing literature and data used for this study; Section 3.0 provides a discussion of the geologic setting of the study area; Section 4.0 discusses the MCS-based geologic model developed by the Sanitation Districts; Section 5.0 presents the hydrogeologic setting of the study area; Section 6.0 discusses the development, calibration, and sensitivity/uncertainty of the groundwater flow model; and Section 7.0 presents the findings and conclusions of this portion of the study. Figures and tables are presented throughout the body of the report. Support documentation is presented in the appendices.

2.0 REVIEW OF EXISTING LITERATURE AND DATA

A detailed review of existing information both at the PVLF site and the study area was performed in order to incorporate pertinent information into this model concerning the geology, hydrogeology, and groundwater resources. The following paragraphs describe the sources of this information, and the technical references for groundwater modeling which were used to compile input data for the groundwater flow model.

A wide variety of data sources were utilized in the development of this report. Appendix A contains a comprehensive list of these data sources. Much of the information on or immediately adjacent to the PVLF was obtained by the Sanitation Districts through various field investigations. A GEOREF computer literature search was performed by Dames & Moore and the Sanitation Districts for information from published sources. Both public and proprietary information on water wells in the study area was researched by Dames & Moore through contacts with various public agencies and some private companies.

Woodring and others (1936; 1946) completed geologic mapping and stratigraphic characterization of the Palos Verdes peninsula. These works are commonly recognized as definitive studies of the region. Cleveland (1976) produced a geologic map of the northeastern side of the Palos Verdes area, adjacent to the area overlain by the landfill. Further assessment of the lithologic and stratigraphic divisions of the Monterey Formation and its environments of deposition were completed by Rowell (1981; 1982), and Conrad and Ehlig (1986; 1987).

The regional structure of the Palos Verdes peninsula and the Palos Verdes fault zone has been included in previous studies by Yerkes et. al. (1965), Ziony, et al (1974), Greene, et al (1979), and Davis, et al (1989). In a regional study of the Los Angeles Basin, Hauksson (1990) analyzed focal mechanisms of earthquakes possibly caused by movement along the Palos Verdes fault zone. More specific analyses of the onshore portion of the Palos Verdes fault zone have been completed by Marine Environmental Science Associates (1983), Woodward-Clyde Consultants (1987), Fischer, et al (1987), and Patterson and Freeman (1990). Fleisher (1971) described gravitational slump folding in a portion of the Monterey Formation in the Palos Verdes area.

A considerable amount of information on the study area hydrogeology has been compiled by Poland (1959), and the California Department of Water Resources (CDWR - 1961). Additional information was obtained from well logs on file at the Los Angeles County Department of Public Works (LACDPW) and California Division of Oil and Gas (CDOG). Other data on groundwater wells in or near the study area were obtained through personal communications at the following public agencies or municipal districts: Central and West Basin Water Replenishment District; Dominguez Water Company; Harbor Regional Park; California Water Service Company - Palos Verdes District; California Regional Water Quality Control Board - Los Angeles Region (RWQCB); West Basin Municipal Water District; and the City of Torrance Water Department.

Hydrogeologic data for PVLF were available from numerous reports done for previous studies. The primary sources of hydrogeologic information at PVLF were reports by the Sanitation Districts (1986a; 1986b; 1986c; 1987; 1989a), Herzog (1991a; 1991b), Kleinfelder (1988), Stone (1975), CDWR (1961), and Poland (1959). Reports by the Sanitation Districts (1986a; 1986b; 1986c) and Audell (1986) provided information on borings and wells completed at the landfill. Groundwater monitoring wells at the PVLF were also installed by Associated Soils Engineering, Inc., (1984) and Hinkle (1986). Geofon, Inc., (1985; 1986) performed geologic studies related to installation of a subsurface barrier at the landfill.

Systematic groundwater sampling and chemical analysis at the PVLF began in the late 1970s, when monitoring wells MW-1 through MW-6 were placed along the northern boundary of the main site. In 1991, wells MW-1 through MW-6 were abandoned. A total of 58 additional monitoring wells, 11 extraction wells, and two sumps have been installed around the perimeter and at specific downgradient and upgradient locations near the PVLF. Figures 2.1 and 2.2 show the locations of the borings and wells in the study area.

A report completed by the Sanitation Districts (1987) for the RWQCB provides information on the geologic and hydrogeologic setting, surface water hydrology, and off-site water wells in the vicinity of the landfill. This report also proposed additional borings and groundwater monitoring wells which were subsequently completed by Kleinfelder (1988). Hydrogeologic and soil characterization plans completed by the Sanitation Districts (1989a; 1989b) give a comprehensive review of geologic, stratigraphic, and hydrogeologic information, history of the site, and the results of the Kleinfelder (1988) drilling and aquifer testing program. These documents also propose further hydrogeologic site investigations which were later completed by Herzog Associates (1991a; 1991b). The Herzog results include detailed logs for borings and monitoring wells located both upgradient and downgradient of the PVLF, along with geophysical data, aquifer test data, and physical testing results.

Studies of the surface and subsurface geologic conditions near the PVLF are provided in several geotechnical and environmental investigations completed by and for the Sanitation Districts. Surface geologic mapping of a portion of landfill was conducted by Robert Stone & Associates, Inc., (1975; 1976) prior to completion of Parcel 6 as a Class I landfill. Numerous geotechnical reports have been prepared for various construction projects in and around the landfill. A complete listing of previous geotechnical investigations performed for the landfill prior to 1987 is provided in a report completed by the Sanitation Districts (1987).

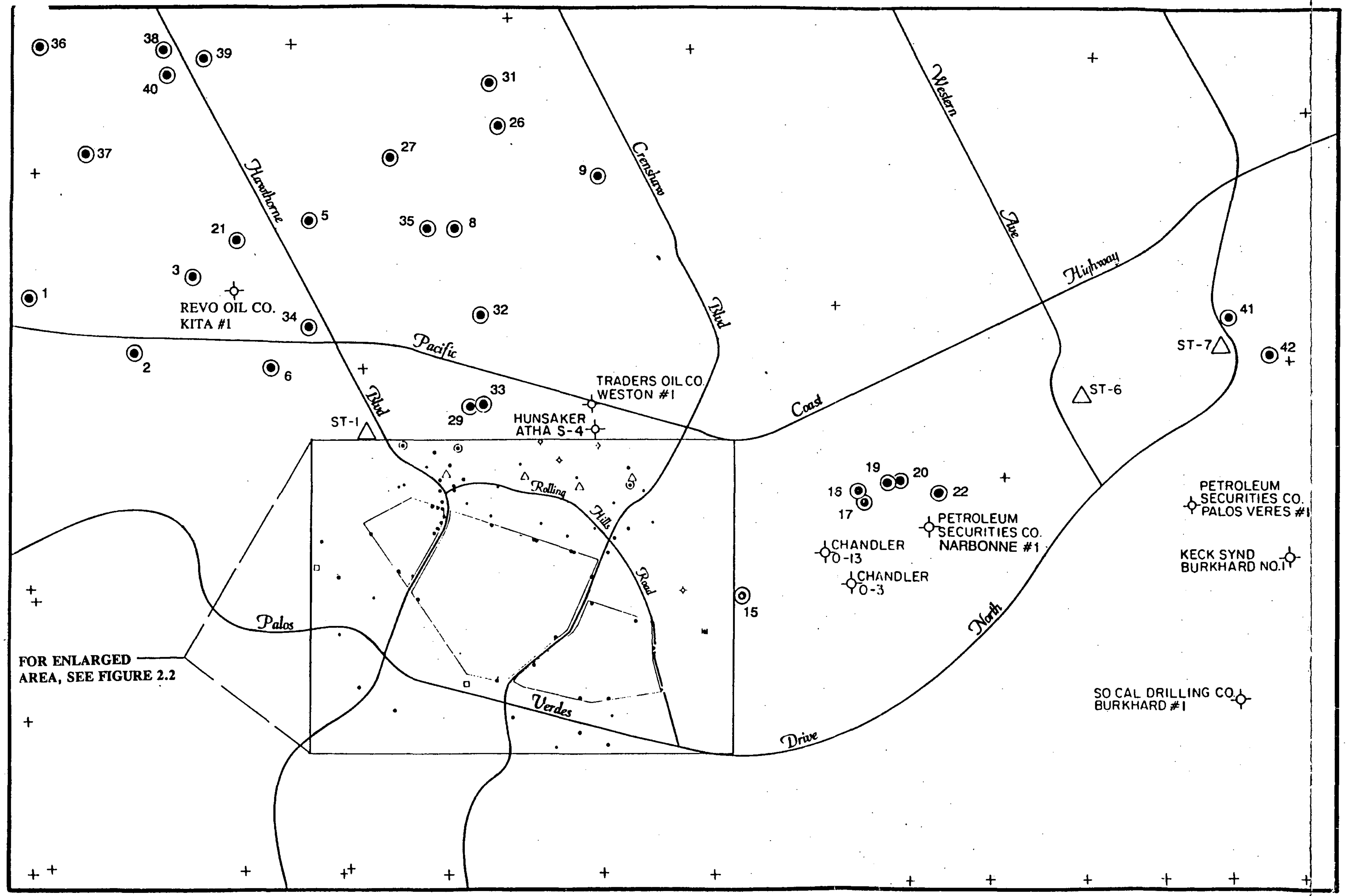

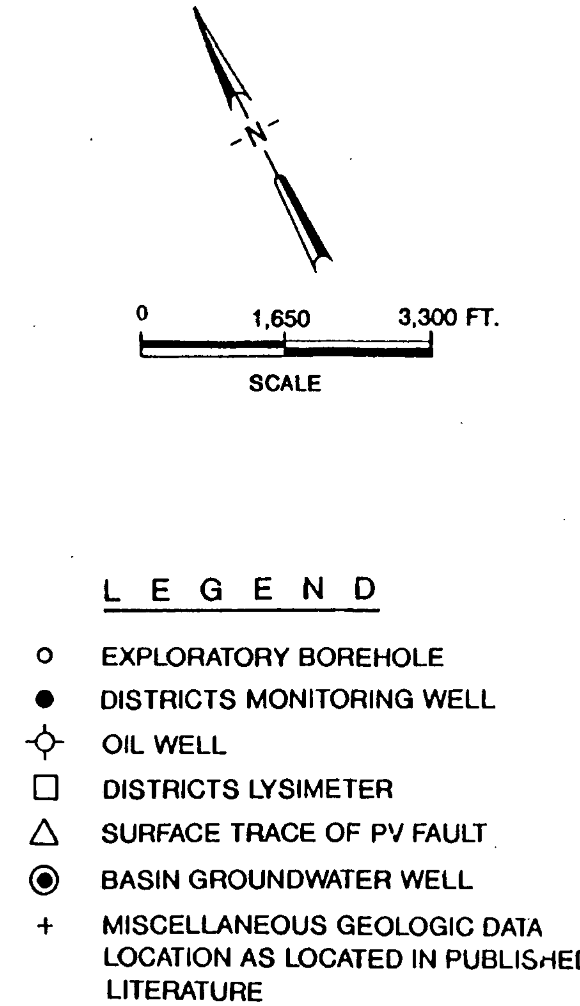

BASE MAP SOURCE: SANITATION DISTRICTS HC REPORT, PHASES II AND III

FIGURE 2.1
Locations of Borings and Wells in Study Area

DAMES & MOORE

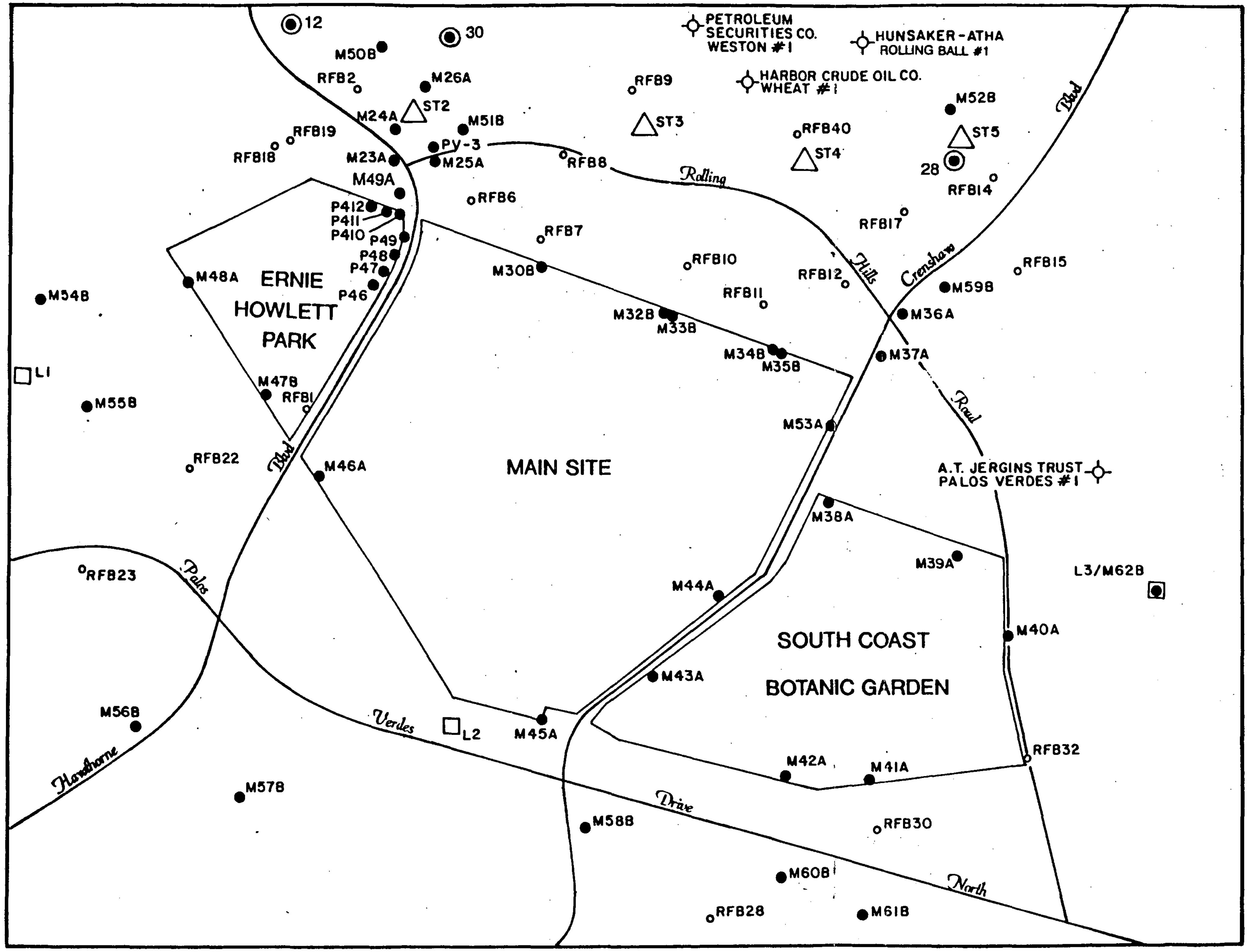

LEGEND

- ○ EXPLORATORY BOREHOLE
- ● DISTRICTS MONITORING WELL
- ⌖ OIL WELL
- □ DISTRICTS LYSIMETER
- △ SURFACE TRACE OF PV FAULT
- ◉ BASIN GROUNDWATER WELL
- \+ MISCELLANEOUS GEOLOGIC DATA LOCATION AS LOCATED IN PUBLISHED LITERATURE

BASE MAP SOURCE: SANITATION DISTRICTS HC REPORT, PHASES II AND III

FIGURE 2.2
Location of Borings and Wells in PVLF Area

DAMES & MOORE

3.0 GEOLOGIC SETTING

Information presented in this section provides a general overview of the geologic conditions within the study area. The following information reflects geologic descriptions provided to Dames & Moore by the Sanitation Districts.

3.1 REGIONAL GEOLOGY

The geologic conditions surrounding the PVLF reflect the regional geologic setting of the Palos Verdes peninsula. A geologic map of the PVLF study area is provided on Figure 3.1 (in pocket). This map portrays the geology of the surface of the study area, with the unconsolidated alluvium and landfill materials removed. Geologic cross-sections are provided in Figures 3.2 through 3.6, with the Legend to the cross sections shown on Figure 3.7. These figures were prepared by the Sanitation Districts for their Hydrogeologic Characterization Report (1992).

Structurally, the Palos Verdes peninsula is a doubly plunging, asymmetrical anticlinorium, created largely by movement along the Palos Verdes fault zone. Potentially several hundred feet wide, this primarily right-lateral strike slip fault zone is also composed of a series of several subparallel, oblique reverse faults separating the southeastern edge of the Los Angeles Basin and West Coast groundwater basin from the Palos Verdes peninsula. The Palos Verdes fault zone forms both a geologic boundary and a hydrologic attenuation zone between the geologic units of the Palos Verdes peninsula to the southwest and those of the Los Angeles Basin to the northeast.

The geologic formations within the study area, from oldest to youngest, consist of (1) the Jurassic age Catalina Schist, (2) the three members of the middle Miocene age Monterey Formation; the Altamira Shale, the Valmonte Diatomite, and the Malaga Mudstone; (3) Pleistocene age rock units, including from oldest to youngest the San Pedro Formation, which includes the Lomita Marl, the Timms Point Silt, and the San Pedro Sand, continental terrace deposits, and the Palos Verdes Sand; and (4) Holocene age materials which include, alluvium, colluvium, and mine tailings.

L E G E N D

Lf	Landfill Deposits	
Qo	Overburden Deposits	
Qus	Undifferentiated Sand Deposits	
Tmm	Malaga Mudstone Member	Monterey Formation
Tmv	Valmonte Diatomite Member	Monterey Formation
Tma	Altamira Shale Member	Monterey Formation
Jc	Catalina Schist	
	Fault Zone	

FIGURE 3.7
Legend to Figures 3.2 - 3.6

DAMES & MOORE

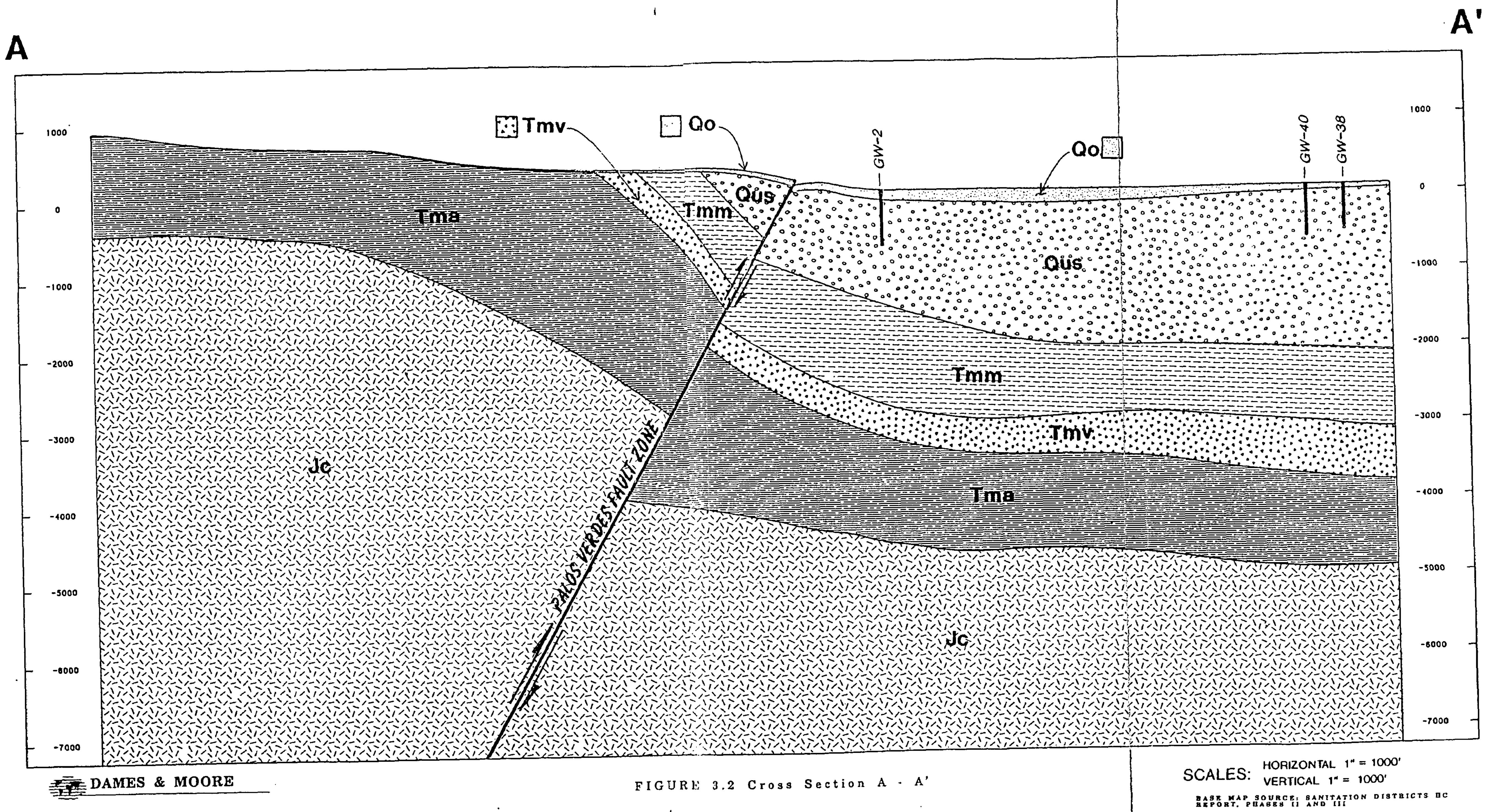

DAMES & MOORE

FIGURE 3.2 Cross Section A - A'

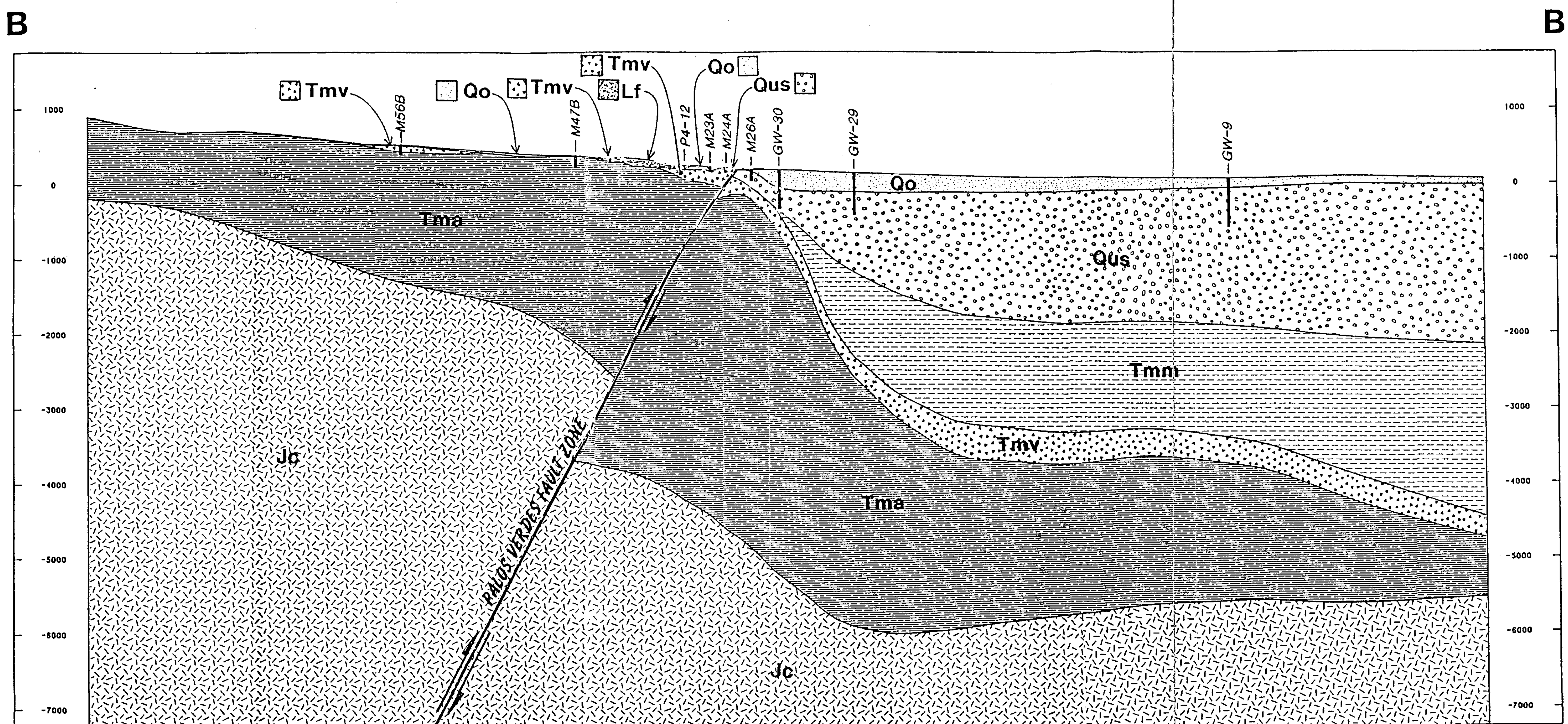

DAMES & MOORE

FIGURE 3.3 Cross Section B - B'

SCALES: HORIZONTAL 1" = 1000'
VERTICAL 1" = 1000'

BASE MAP SOURCE: SANITATION DISTRICTS IIC REPORT, PHASES II AND III

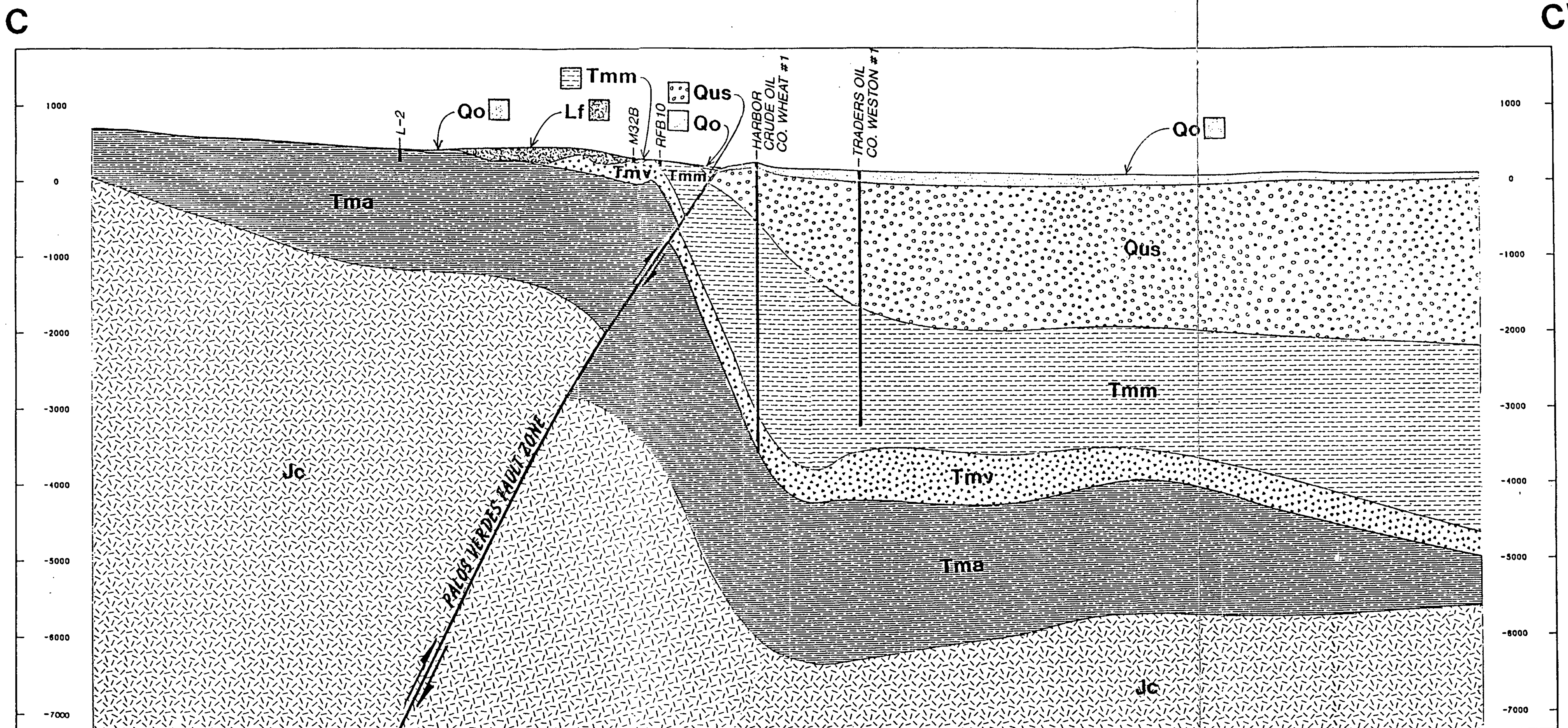

DAMES & MOORE

FIGURE 3.4 Cross Section C - C'

SCALES: HORIZONTAL 1" = 1000'
VERTICAL 1" = 1000'

BASE MAP SOURCE: SANITATION DISTRICTS DC REPORT, PHASES II AND III

D'

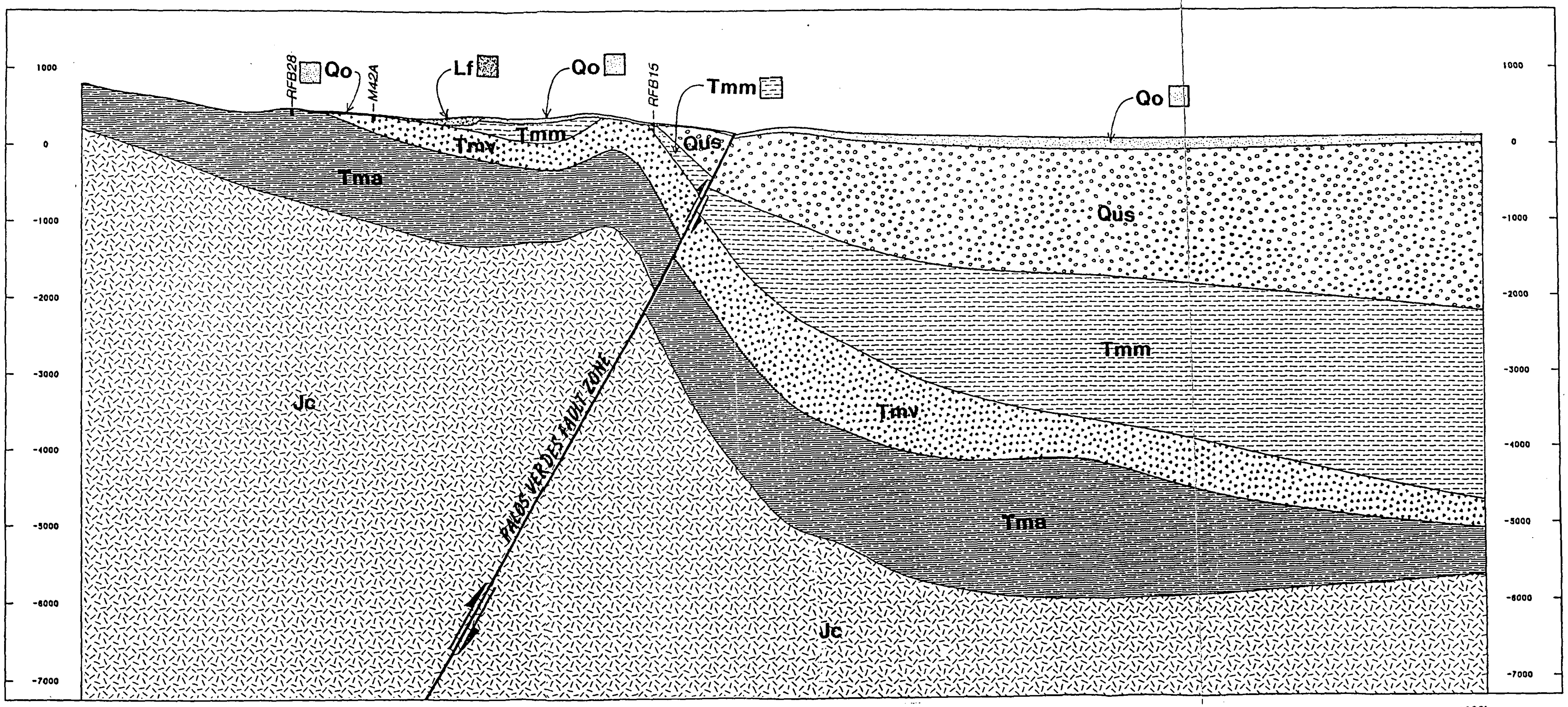

DAMES & MOORE

FIGURE 3.5 Cross Section D - D'

SCALES: HORIZONTAL 1" = 1000'
VERTICAL 1" = 1000'

BASE MAP SOURCE: SANITATION DISTRICTS UC REPORT, PHASES II AND III

E E'

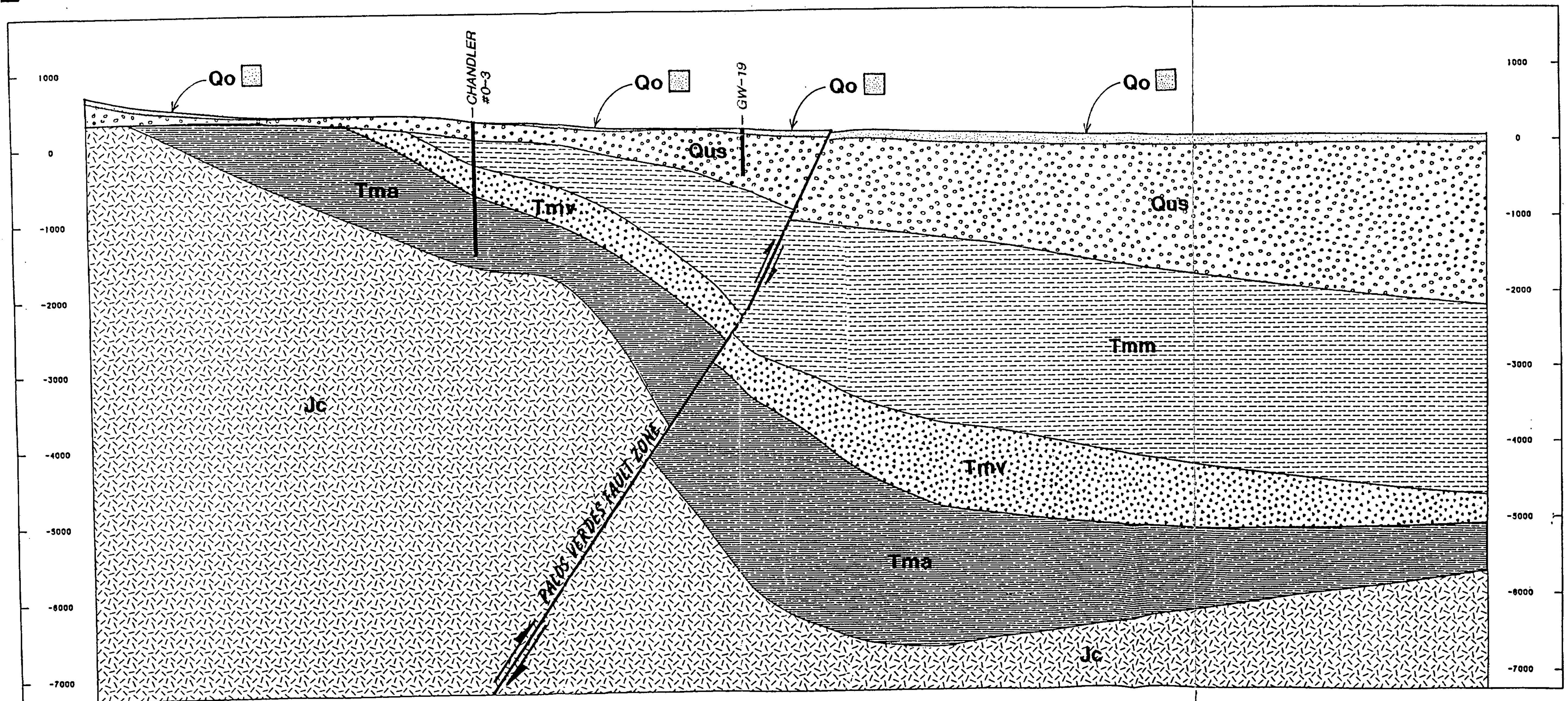

DAMES & MOORE

FIGURE 3.6 Cross Section E - E'

SCALES: HORIZONTAL 1" = 1000'
VERTICAL 1" = 1000'

BASE MAP SOURCE: SANITATION DISTRICTS HC REPORT, PHASES II AND III

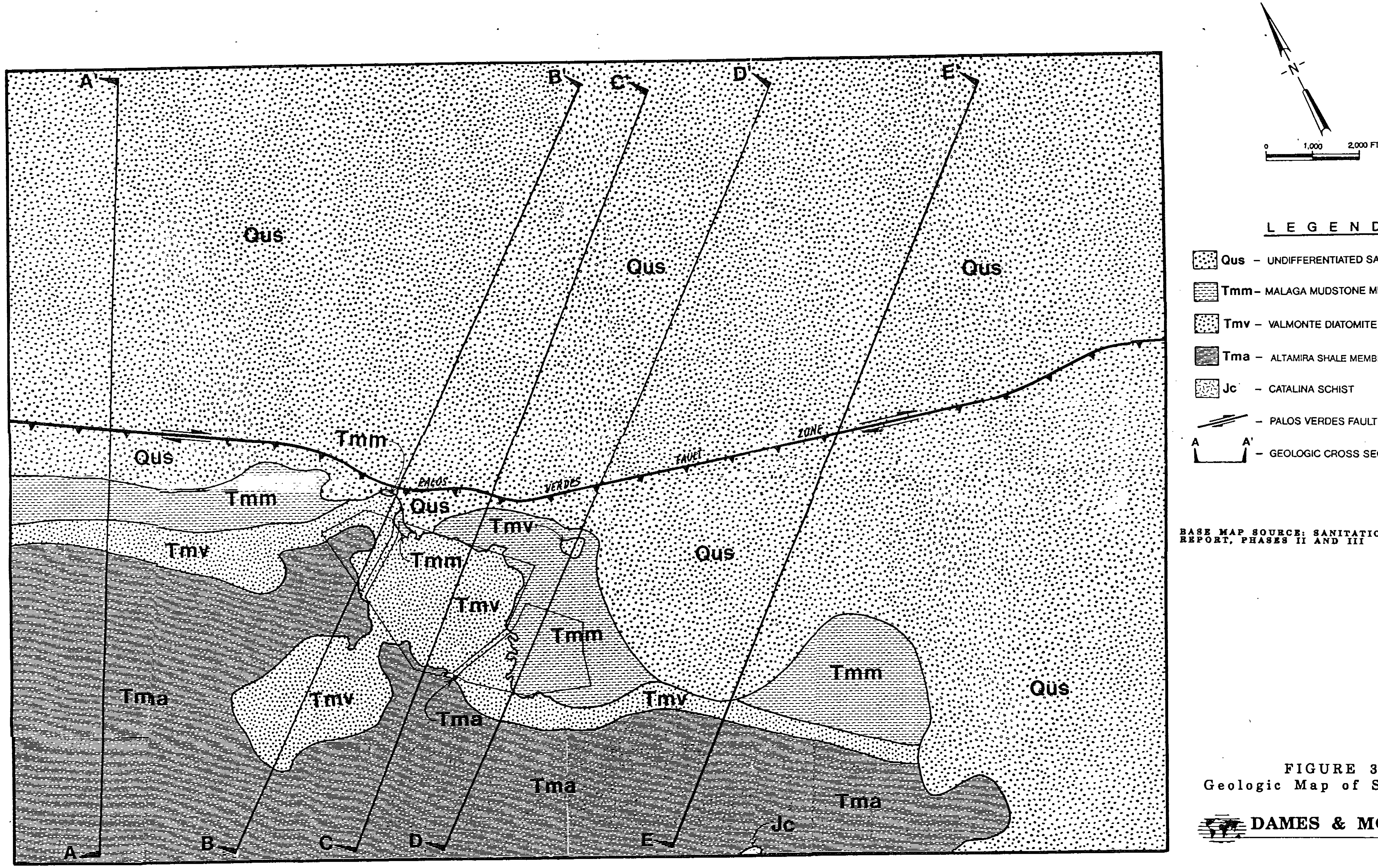

LEGEND

Qus – UNDIFFERENTIATED SAND DEPOSITS

Tmm – MALAGA MUDSTONE MEMBER

Tmv – VALMONTE DIATOMITE MEMBER

Tma – ALTAMIRA SHALE MEMBER

Jc – CATALINA SCHIST

– PALOS VERDES FAULT ZONE

A A' – GEOLOGIC CROSS SECTION LINE

BASE MAP SOURCE: SANITATION DISTRICTS HC REPORT, PHASES II AND III

FIGURE 3.1
Geologic Map of Study Area

DAMES & MOORE

3.2 STRATIGRAPHY

A typical stratigraphic sequence of the study area consists of an unknown thickness of Catalina Schist unconformably overlain by approximately 3,000 feet of undifferentiated Monterey Formation rocks. Interfingering sandstone formations unconformably overlie and onlap the Monterey Formation members. Intermittent alluvium, colluvium, topsoil landfill, and mine tailings form the top of a typical stratigraphic sequence of the Palos Verdes Hills region. The general stratigraphy of the study area is discussed in the following paragraphs.

3.2.1 Catalina Schist (Jc)

The oldest rock unit exposed on the Palos Verdes peninsula is the Catalina Schist, a metamorphic basement complex of possible Jurassic age (208 to 144 million years before present; mybp). Stratigraphically, the Catalina Schist is equivalent to the Franciscan Formation Schist found in the Coast Ranges of California. Lithologically, the Catalina Schist is a quartz-glaucophane and quartz-sericite schist with minor amounts of talc, albite, and other blue schist facies minerals. The schist includes intrusions of basaltic sills and dikes. Under the PVLF, the Catalina Schist is found between 1,000 and 2,000 feet below the surface, dipping steeply to the northeast.

3.2.2 Monterey Formation

The Miocene Monterey Formation unconformably overlies the Catalina Schist on the Palos Verdes peninsula. The Monterey Formation is a sedimentary formation of marine origin which is often petroliferous and contains extensive deposits of biogenic origin such as chert, dolostone, and diatomite. In the Palos Verdes region, all members of the Monterey Formation are weathered and fractured. The Monterey Formation is the primary oil producing source rock in Southern California and many fractures are filled by tar. At PVLF, the Monterey Formation is divided into three distinct, conformable members: The Altamira Shale (Tma), the Valmonte Diatomite (Tmv), and the Malaga Mudstone (Tmm).

3.2.2.1 Altamira Shale (Tma)

The Altamira Shale member of the Monterey Formation is the oldest (16 to 14 mybp) and deepest Miocene rock unit encountered during the Sanitation Districts' prior field investigations at the PVLF. This member has a measured stratigraphic thickness of 1,250 feet (Woodring, 1946). Highly fractured throughout, the Altamira Shale consists generally of interlayered silty and sandy shales with interbedded diatomite, cherty and phosphatic shale, conglomerate, bentonitic ash/tuff, and dolostone. Fractures are frequently tar-filled.

3.2.2.2 Valmonte Diatomite (Tmv)

The Valmonte Diatomite member of the Monterey Formation is the middle member of the Monterey Formation. This unit, deposited 12.5 to 7 mybp, varies in thickness in the Palos Verdes Hills between 300 and 500 feet. The Valmonte Diatomite consists primarily of thinly laminated to thickly bedded deposits of diatomite and diatomaceous shale and mudstone, with minor interbeds of mudstone, phosphatic shale, dolostone, volcanic ash, and chert. In outcrop, the Valmonte Diatomite is characteristically white or off-white. In the subsurface, this formation is typically medium gray to white. The contact between the Valmonte Diatomite and the overlying Malaga Mudstone is gradational. The Valmonte Diatomite member underlies the majority of the Palos Verdes landfill. Prior to landfilling operations, this geologic unit was extensively mined for commercial purposes.

3.2.2.3 Malaga Mudstone (Tmm)

The uppermost and youngest member of the Monterey Formation at the site is the Malaga Mudstone. The Malaga Mudstone was deposited from 7 to 5.3 mybp and varies in thickness between 300 and 500 feet. This unit consists primarily of massive deposits of dark grayish brown to black radiolarian mudstone containing minor interbeds of diatomite, volcanic ash, fossil mollusc fragments, and dolostone. The Malaga Mudstone member is a highly petroliferous unit which yields the majority of the hydrocarbons found in the Monterey Formation.

3.2.3 Repetto Formation (Tr)

The Pliocene age Repetto Formation has an approximate thickness of 4,000 to 5,000 feet within the Los Angeles Basin, thinning southward toward the Palos Verdes Hills where it has a maximum exposed thickness of 150 feet (Woodring, et al, 1946). Within the study area, the closest occurrence of this formation is roughly one mile to the east of the PVLF. Stratigraphically, the Repetto Formation unconformably overlies the Malaga Mudstone member of the Monterey Formation, but it may also occur in fault contact against older members of the

Monterey Formation. The Repetto Formation is typically a dark bluish-gray, fine grained, glauconitic, foraminiferal, clayey siltstone with rare beds of coarser clastics. Like the Malaga Mudstone Member of the Monterey Formation, the Repetto Formation is a major source of petroleum hydrocarbons in the Los Angeles Basin.

3.2.4 Pico Formation (Tp)

The Pliocene age Pico Formation conformably overlies the Repetto Formation. In the Los Angeles Basin the Pico Formation is a substantial rock unit, varying in thickness between several hundred to 3,000 feet (Woodring, et al, 1946). Within the study area, the closest occurrence of this formation is roughly one mile to the east of the PVLF. Like the Repetto Formation, the Pico Formation thins considerably toward the Palos Verdes peninsula. This formation is characterized by light tan to brown layers of sandstone, gravelly sandstone, and conglomerate beds derived from local, continental sources. Interbeds of clayey siltstone, siltstone, and sandy siltstone may occur locally.

3.2.5 San Pedro Formation, Continental Terrace Deposits, Palos Verdes Sand (Qus)

The San Pedro Formation includes the Pleistocene age Lomita Marl and San Pedro Sand. Other deposits include continental terrace deposits and the Palos Verdes Sand. These deposits are all discontinuous, shallow marine, calcareous sandstone deposits which unconformably overlie the eroded tops of the Monterey, Repetto, and Pico Formations. Thickly cross-bedded to massive, these units are composed chiefly of fossiliferous, quartzo-feldspathic sands. Mollusc shell fragments are abundant, especially in the Lomita Marl unit. The undifferentiated Quaternary sediments in the West Coast Basin above the San Pedro Formation are collectively known as the Lakewood Formation. For convenience, all these units discussed in this paragraph are grouped as Undifferentiated Quaternary deposits (Qus) as used later in this report.

3.2.6 Overburden (Qo)

All alluvium, colluvium, mine tailings, and other miscellaneous, non-formational, non-landfill materials, such as topsoil and earthen fill, are grouped into one unit called overburden (Qo). These units represent weathered, reworked, and eroded surficial units (either natural or man-made) derived from previously deposited rock units. Individually, each of these units occupies only a small area, encompassing a volume of material whose boundaries are not well defined.

Because of lithologic and hydrologic similarities, these units are grouped together as a continuous, mappable geologic unit.

3.2.7 Hydrocarbon Deposits

A detailed review of boring logs from the Kleinfelder (1988) and Herzog Associates (1991a; 1991b) investigations was conducted for information regarding the presence, frequency, and character of hydrocarbon deposits in the different stratigraphic members of the Monterey Formation (Tmm, Tmv, and Tma units). A summary of this information is presented on Table 3.1.

Of the three Monterey Formation members, the Malaga Mudstone (Tmm) contains the most significant amounts of naturally occurring hydrocarbons. Approximately three-quarters of the 19 boreholes which penetrated Malaga Mudstone contained evidence of hydrocarbons. The Malaga Mudstone subcrops mainly in the southeast portion of the landfill. Approximately one-third of the borings and wells which penetrated the Valmonte Diatomite (Tmv) contained evidence of hydrocarbons, consisting of sporadic tar-filled fractures. The Altamira Shale (Tma), which subcrops mainly in the northwestern corner and along the western edge of the landfill, also contained tar-filled fractures in about half of the borings in which it was encountered. Fractures were commonly filled and/or stained with iron oxide or magnesium oxide. Gypsum, clay, and tar infilling were also noted. Infilling of fractures by secondary materials would restrict the flow of fluids such as groundwater through the fracture network.

The presence of hydrocarbons in interstitial space of saturated geologic media, either in tarry form or free-phase liquid, tends to decrease the ability of the geologic media to transmit water because of the loss of available pore space. The effect of the hydrocarbons on the groundwater movement has been incorporated into the groundwater flow model (to be discussed later) through the calibrated hydraulic conductivity values for the Monterey Formation bedrock.

3.3 GEOLOGIC STRUCTURE

The Palos Verdes peninsula is a coastline projection controlled by movement along the Palos Verdes fault zone. Tectonic motion related to crustal movement along the San Andreas Fault and similar, subparallel faults such as the Palos Verdes fault zone, have resulted in folding and faulting of the rocks in the area occupied by and surrounding the PVLF site.

TABLE 3.1

OCCURRENCE OF HYDROCARBONS (HCs) IN MONTEREY FORMATION

BORING/WELL	MONTEREY MEMBERS ENCOUNTERED	DEPTH OF HCs ENCOUNTERED (feet bgs)	DEPTH OF FIRST HCs BELOW TOP OF MONTEREY (feet bgs)	TOTAL THICKNESS OF MONTEREY (feet)	REMARKS
M23A	Tmv	–	–	17	No HCs encountered.
M24A	Tmv	–	–	46	No HCs encountered.
M25A	Tmv	–	–	75	No HCs encountered; occasional black Fe-oxide staining; strong "organic" odor noted.
M26A	(No Monterey encountered)	–	–	0	
M36A (including M36A-2) and M36A-3)	Tmm	20-41	0	37	"Slight gasoline oil odor" throughout Monterey.
M37A	Tmv	–	–	18	No HCs encountered.
M38A (including M38A-2)	Tmm	–	–	21	No HCs encountered.
M39A	Tmm	–	–	27	No HCs encountered.
M40A	Tmm	38-48	8	21	HC evidence: black organic stains.
M41A	Tmm	–	–	18	No HCs encountered.
M42A	Tmv	–	–	67	No HCs encountered; "sewer odor" noted.
M43A	Tmv	100-105	35	41	HC evidence: petroliferous odor.
M44A	Tmv	–	–	10	No HCs encountered.
M45-A (including M45A-2)	Tmv	75-80	15	48	Possible dark brown to black petroleum staining on joint faces.
M46A (including M46A-2)	Tmv	–	–	20	No HC evidence.
M48A	Tma	55-63	6	14	Locally asphaltic, strong petroleum or tar odor.
M49A	Tmv	–	–	6	No HCs encountered.
M30B	Tmv	44-72	29	106	Moderate to strong petroleum odor.
M32B	Tmm	–	–	30	No HCs encountered.
M33B	Tmm	–	–	75	No HCs encountered.
M34B	Tmm	–	–	25	No HCs encountered.
M35B	Tmm	–	–	115	No HCs encountered.
M47B	Tma	29-30; 74-149	23	143	Gilsonite; petroliferous siltstone (oil shale); oily odor; and tar along fractures, joints, and bedding from 74 to TD.
RFB-1	Tmv/Tma	45-175	27	157	Tar-filled fractures and tarry shale in both Tmv and Tma.
RFB-2	Tmv	–	–	8	No HCs encountered.
RFB-3/M50B	(WELL COMPLETED IN QUS ONLY)			0	
RFB-4/M51B (including RFB-4A and 4B)	Tmm/Tmv	82-90	0	100	No HCs encountered in RFB-4 or 4B; weak petroleum odor noted in RFB-4A.
RFB-6	Tmm	90-174	5	89	Strong petroliferous odor.
RFB-7	Tmm/Tmv	25-190	12	282	Hydrocarbon odor in Tmm; tar-filled fractures and hydrocarbon odor in Tmv; no hydrocarbons below depth of 190 feet to TD of 295.
RFB-8	Tmm	–	–	14	No HCs encountered.
RFB-9	(No Monterey encountered)	–	–	0	
RFB-10	Tmm	5-75	5	75	Slight to heavy petroleum odor.
RFB-11	Tmm/Tmv	18-27	0	157	Moderate "natural organic odor" noted in Tmm; no HC evidence in Tmv.
RFB-12	Tmm	5-175	5	175	Moderate to strong petroleum odor.
RFB-13/M52B	(No Monterey encountered)	–	–	0	
RFB-14	(No Monterey encountered)	–	–	0	
RFB-15	Tmm	40-100	15	75	Moderate to strong petroleum odor.
RFB-16/16A/M53B	Tmm/Tmv	240-350	179	289	HC evidence in Tmv only: tar-filled fractures; sheen on core; tar sands; oil shows in mud pit.
RFB-17	Tmm	132-146	0	14	Moderate to strong petroleum odor.
RFB-40	(No Monterey encountered)	–	–	0	
RFB-18	Tmv	167-220	160	234	HC evidence: "hydrocarbon odor".
RFB-19	Tmv	135-220	118	234	HC evidence: tar-filled fractures in dolostone; slight hydrocarbon odor in diatomaceous shale.
RFB-20/M54B	Tma	–	–	80	No HC evidence encountered.
RFB-21/M55B	Tma	–	–	39	No HCs encountered.
RFB-21/M55B	Tma	110-111	102	107	Tar-filled fractures in tuffaceous facies of Tma only.
RFB-23	Tma	–	–	92	No HCs encountered.
RFB-24/M56B	Tmv/Tma	127-136	117	150	Slight to strong HC odor and slight HC sheen in siltstone and siliceous shale of Tma.
RFB-25/M57B	Tmv/Tma	–	–	136	No HCs encountered.
RFB-26/M58B	Tma	–	–	60	No HCs encountered.
RFB-27/M59B	Tmm/Tmv	62-75	38	76	"Slight HC odor" in Tmm only.
RFB-28	Tma	–	–	82	No HCs encountered.
RFB-29/M60B	Tma	88-90 192-241	55	301	Tar-filled fractures and vitreous asphalt in fractured chert, dolostone, shale, and siltstone.
RFB-30/30A	Tmv/Tma	15-110	13	201	Tar clasts, tar-filled fractures, and HC odor in Tmv only.
RFB-31/31A/M61B	Tma	–	–	73	No HCs encountered.
RFB-32	Tmm/Tmv	70-72; 218-278	52	335	Tmm: slight HC odor. Tmv: "bituminous (?)", "organic-rich"; tar-filled fractures.
RFB-L1	Tmv/Tma	92-200	90	198	Tar-filled fractures in Tma only.
RFB-L2/L2A	Tma	65-71	63	174	Tar-filled fractures in shale.
RFB-L3/3A/3B/M62B	Tmm	92-270	32	294	Strong HC odor.

NEW3_1.WK3

HCs = Hydrocarbons
TD = Total depth of borehole
Tmm = Malaga Mudstone Memeber, Monterey Formation
Tmv = Valmonte Diatomite Member, Monterey Formation
Tma = Altamira Shale Member, Monterey Formation
– = Not applicable

3.3.1 Folding

Structurally, the geologic character of the Palos Verdes peninsula is dominated by the doubly plunging Palos Verdes anticlinorium. This structure is a complex of several, generally parallel, anticlines and synclines. Typically, the fold axes trend to the northwest at 34° to 40° west of north. Locally, in the vicinity of the PVLF minor fold trends may vary considerably. This folding of the Monterey Formation members is a result of tectonic compressional forces which peaked during the late Pliocene through Pleistocene epochs (5.3 to 0.01 mybp). Several major synclines and anticlines, including the Gaffey syncline, are included in this structure. Interformational and intermember folding is the result of deformation of these rock units during or immediately following deposition. The bedding orientation of the formational rock units depends on locality and formation. In a very general sense, the members of the Monterey Formation strike 20° to 70° west of north and dip 20° to 90° to the northeast within the study area. Digressions from these typical orientations are due to numerous small folds and local reorientation due to landsliding.

3.3.2 Faulting

Although the predominant structural character in the Palos Verdes area is the large complex of folds, the Palos Verdes fault zone is certainly the most significant single structural feature. The Palos Verdes fault zone consists of several subparallel, oblique reverse faults, which form a structural boundary between the Palos Verdes Hills to the southwest and the Los Angeles Basin to the northeast. The Palos Verdes fault zone strikes in a northwesterly direction along the northeastern border of the Palos Verdes Hills and dips steeply at roughly 60° to the southwest. The fault zone has the potential to be several hundred feet wide, as the number of splays related to the fault is unknown.

4.0 GEOLOGIC MODEL

To accurately model the geologic conditions beneath the study area, the Sanitation Districts are currently using a three-dimensional geologic computer model called MCS (Mapping-Contouring System). This model was developed by Scientific Computer Applications of Tulsa, Oklahoma. The first iterations of this software were developed in 1969 when it was originally intended to be a geologic tool useful for modeling the geologic conditions and reservoir capacities of oil fields. Data generated from MCS can be output in various formats compatible with many groundwater flow models. Information on the MCS geologic model is provided in the Sanitation Districts' report on Phase 2 and Phase 3 of the HCP (Sanitation Districts, 1992).

The MCS geologic computer model was used as a database for hydrogeologic modeling and as an interpretative tool to assist in understanding the distribution and structure of geologic units beneath the study area. The information used by the Sanitation Districts to construct the geologic model is presented on Table 4.1. In developing the MCS model, geologic units in the study area were either treated separately or grouped together based on available data coverage and lithologic similarities or differences. The following geologic units were included in the MCS model:

- Quaternary overburden deposits (Qo) including all unconsolidated surficial materials around the PVLF except for the actual landfilled refuse. Landfill or refuse deposits were treated separately.

- Undifferentiated Quaternary deposits (Qus) including all unconsolidated or semi-consolidated deposits of late Pleistocene and Pliocene age. These units include the San Pedro Formation (Qsp), Palos Verdes Sand, continental terrace deposits, and the Pico Formation (Tp).

- The three members of the Monterey Formation: the Malaga Mudstone (Tmm), the Valmonte Diatomite (Tmv), and the Altamira Shale (Tma), were each treated separately in the MCS model. The Repetto Formation was included as part of the Malaga Mudstone because of their similar geologic properties.

- The Jurassic Catalina Schist (Jc) was used as the base rock unit for the geologic model.

TABLE 4.1

SOURCES OF INFORMATION USED IN GEOLOGIC MODEL

DATA SOURCE	TYPE OF DATA	GEOLOGIC FEATURES REPRESENTED BY DATA	AREA COVERED IN MODEL
Kleinfelder (1988)	Detailed boring logs	Qo, Qus, upper 200' of Tm	Palos Verdes Landfill
Herzog Associates (1991b)	Detailed boring logs	Qo, Qus, upper 200' of Tm	Northeast side (downgradient side), Palos Verdes Landfill
Woodring and others (1946)	Geologic map; regional cross-sections C-C' and D-D'; oil well picks	Deep bedrock picks, including Jc; near-surface structure within Tm	Primarily upgradient (southwest) side of Palos Verdes fault
CDWR (1961)	Regional cross-sections E-E' and J-J'	Qo/Qus contact in basin; correlations to other basin well information; water-bearing information or Pico and Repetto Formations in basin	Southeastern and northeastern boundaries of model
LACDPW (various dates)	Generalized well logs; water levels	Qo/Qus picks in basin deposits	Northern quadrant of model, and along upgradient side of Palos Verdes fault
Davis and others (1989)	Regional retrodeformable structural cross-section B-B'	Regional dip and displacement of Palos Verdes fault; deep bedrock (Jc and Tm) picks on both sides of fault	Northwest edge of model
Hauksson (1990)	Earthquake focal mechanism and fault plane solution data	Regional dip of Palos Verdes fault: data gives general trend of seismically active zone beneath Palos Verdes peninsula	Used regional data for whole model
Woodward-Clyde MESA (1983)	Fault map	Surface trace of Palos Verdes fault	Along Palos Verdes fault throughout model area
CDOG oil well logs (various dates)	Generalized borings logs and electrical logs	Deep bedrock and fault picks	Central portion of model just downgradient of landfill; and southeast quadrant of model
Schoelhammer and Woodford (1951)	Structural contour map, cross-section, and oil well picks	Depth of Jc basement rock	Whole model area
Historical Arerial Photos and Grading Plans obtained by the Districts (various dates)	Aerial photos and topographic maps	Topographic base of landfill deposits, and approximate location of former alluvial drainages	Landfill and immediately surrounding area

NEW4_1.WK3

Qo = Quatenary overburden deposits
Qus = Quatenary undifferentiated sand deposits
Tm = Monterey Formation
Jc = *Catalina Schist*
LACDPW = Los Angeles Department of Public Works
CDWR = California Department of Water Resources
MESA = Marine Environmental Science Associates
CDOG = California Division of Oil and Gas

In addition to modeling the stratigraphy of the above units, information on geologic structure was incorporated into the MCS model by the Sanitation Districts using data from Woodring, et al (1946), P. Guptill (written communication, 1991), and oil and gas well logs on file at the CDOG.

5.0 HYDROGEOLOGIC SETTING

An understanding of the regional and local hydrogeology is essential to the development of a groundwater flow model that is representative of the study area. This section provides a basic description of the science of hydrogeology, and describes the hydrogeologic conditions at the PVLF area.

5.1 OVERVIEW

Water beneath the land surface is referred to as underground water. The equivalent term for water on the land surface is surface water. Underground water generally occurs in two different zones. One zone, which occurs immediately below the land surface in most areas, contains both water and air and is referred to as the unsaturated or vadose zone. The vadose zone is almost invariably underlain by a zone in which all interconnected openings or pores are full of water. This zone is referred to as the saturated zone.

Water in the saturated zone is the only underground water that is readily available to supply wells and springs, and is the water to which the term groundwater is usually applied. Recharge of the saturated zone usually occurs by percolation of water from the land surface through the unsaturated zone. The science of hydrogeology involves the study of the occurrence and movement of groundwater, aquifer characteristics, and the subsurface geologic environment.

5.2 REGIONAL HYDROGEOLOGY

The PVLF is situated near the boundary between two groundwater flow systems, the West Coast groundwater basin aquifers (West Coast Basin) and the Palos Verdes Hills flow system. Locally, these systems are separated by the Palos Verdes fault zone. The PVLF directly overlies the Palos Verdes Hills flow system, which is discussed in Section 5.3.

The West Coast Basin is 160 square-miles in area, and is bounded on the north by the Ballona Escarpment, on the east by the Newport-Inglewood Fault, on the south and west by the Pacific Ocean, and on the southwest by the Palos Verdes Hills and the Palos Verdes fault zone (Figure 5.1). Figure 5.2 provides cross-sectional views through the West Coast Basin.

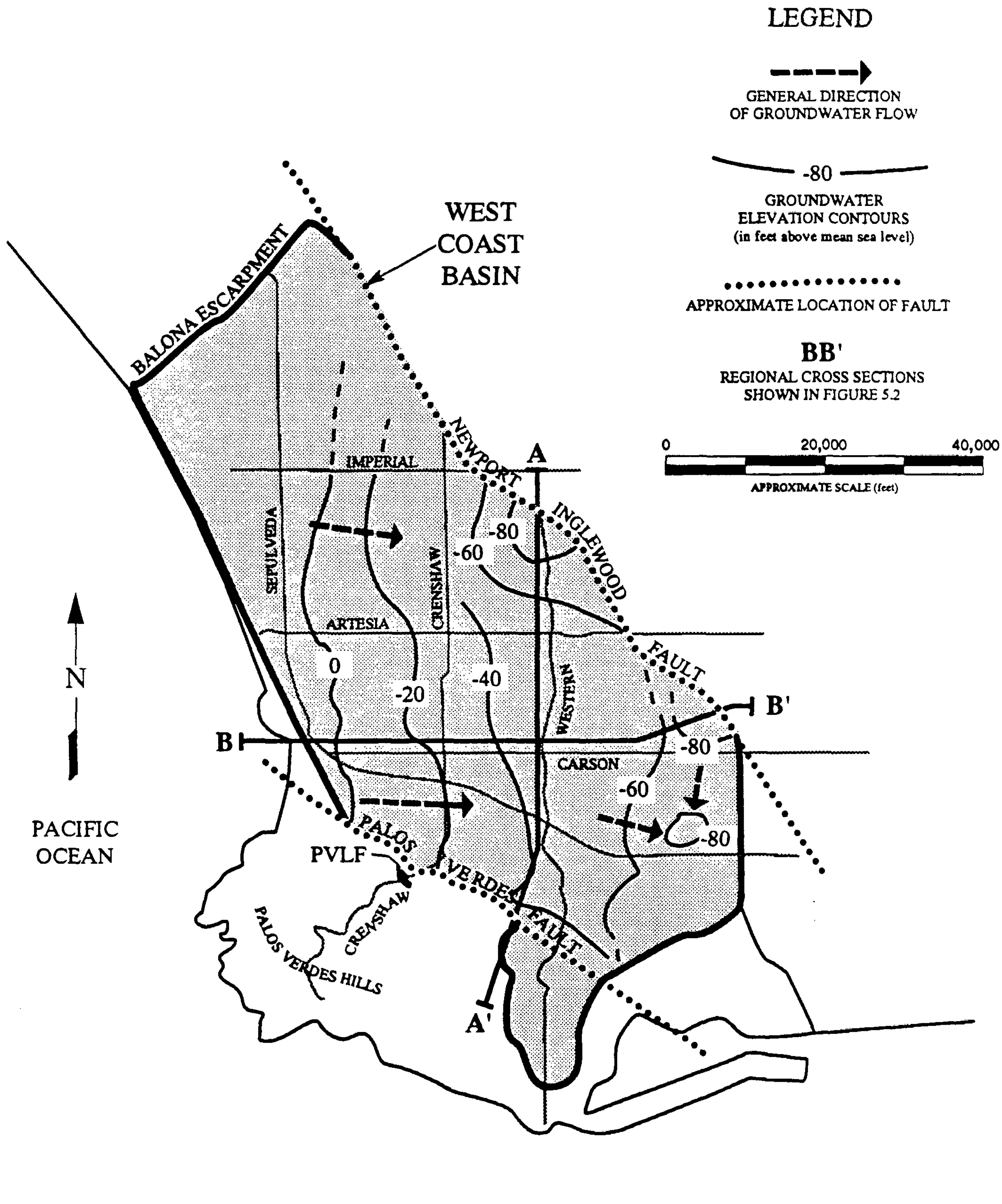

REFERENCES:
Fall 1990, Coastal Plain: Deep Aquifer /Groundwater Contour Map, County of Los Angeles Department of Public Works

Figure 5.1
MAP SHOWING WEST COAST BASIN

Groundwater aquifers of the West Coast Basin occur in relatively permeable zones of primarily Quaternary-aged sedimentary materials. Late Pleistocene alluvial deposits of the Lakewood Formation occur at or near ground surface east of the Palos Verdes fault zone, and reach a thickness of approximately 150 to 200 feet (CDWR, 1961). The basal portion of these deposits constitute the Gardena and Gage aquifers. The underlying San Pedro Formation contains the Lynwood and Silverado Aquifers, which extend to depths of 500 to 800 feet below ground surface (bgs) within the area modeled for this study. The base of the strata that yields fresh water lies within the Pico Formation (Tp) at depths of 900 to 1,100 feet bgs, east of the Palos Verdes fault zone (CDWR, 1961).

Historically, groundwater pumped from the West Coast Basin has been used for municipal, domestic, industrial, and agricultural purposes. However, over the past 20 years, the number of active wells in the basin has continuously declined, primarily because of impaired water quality due to sea-water intrusion. This has resulted in numerous abandoned wells in the West Coast Basin. With the exception of the extraction wells at the PVLF subsurface barrier, no actively pumping groundwater wells have been identified within 1 mile of the landfill. The nearest domestic supply well currently in use is located approximately 3-1/2 miles north-northeast of the PVLF in the City of Torrance (Mr. Chuck Schaich, City of Torrance Water Department, personal communication; CDWR, 1990). The nearest active commercial or industrial supply well is located just over 1 mile east of the PVLF, at the Chandler Palos Verdes Sand and Gravel Company. The Chandler Well has been identified as the only active well in the study area. Extraction wells for remediation purposes, at the Hawthorne Boulevard barrier, were not considered as active wells in this study, as their relatively minor, intermittent pumping rates do not affect the regional flow of groundwater. Tables 5.1 and 5.2 provide well construction information for PVLF area monitoring wells and study area water wells, respectively. The locations of these wells are shown on Figures 2.1 and 2.2.

The majority of the groundwater wells drilled in the West Coast Basin near the landfill (which are now abandoned, except for the Chandler well) are screened across the Gage, Gardena, Silverado, and Lynwood Aquifers. Well logs dating back to the 1920s were reviewed for information on well construction details, water levels, and geologic formations encountered. Generally, depths to groundwater averaged between 75 and 85 feet in wells within 3 miles of the PVLF. Aquifer materials were generally described as "yellow sands" and "blue sands". Prior to 1955, groundwater levels in the West Coast Basin were declining at the rate of approximately 2 feet per year. Since 1955, when extractions began to be controlled by local

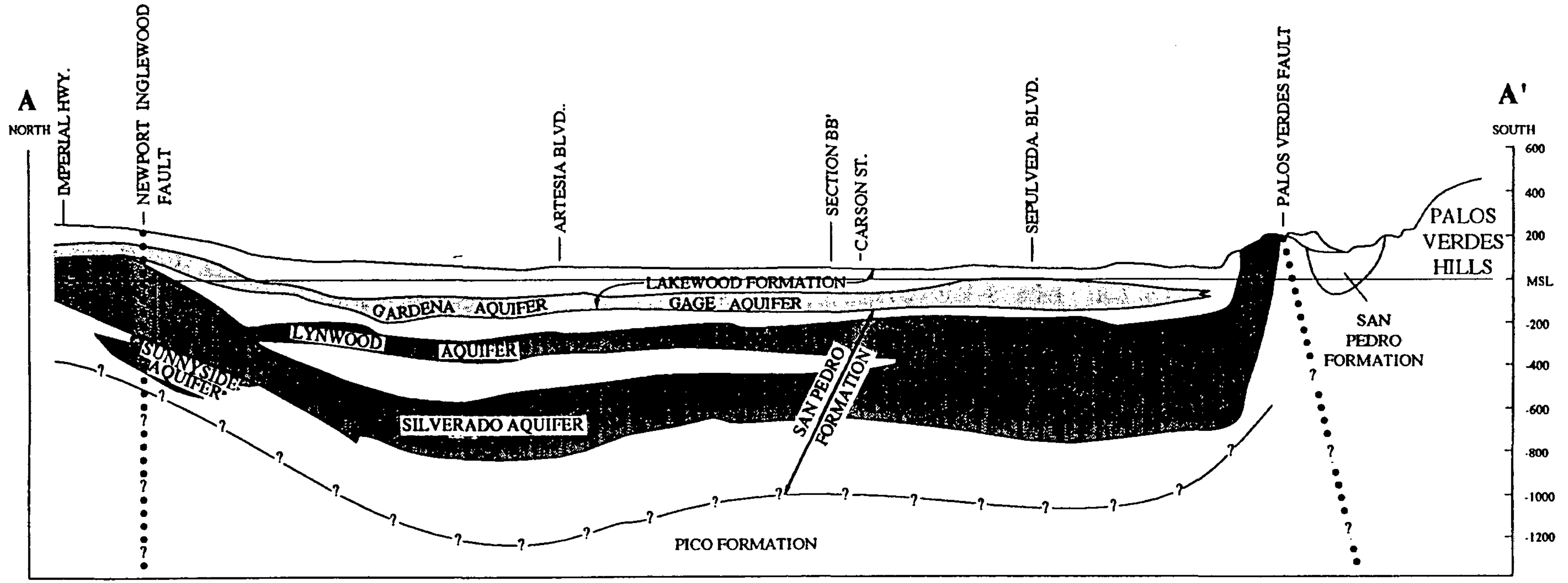

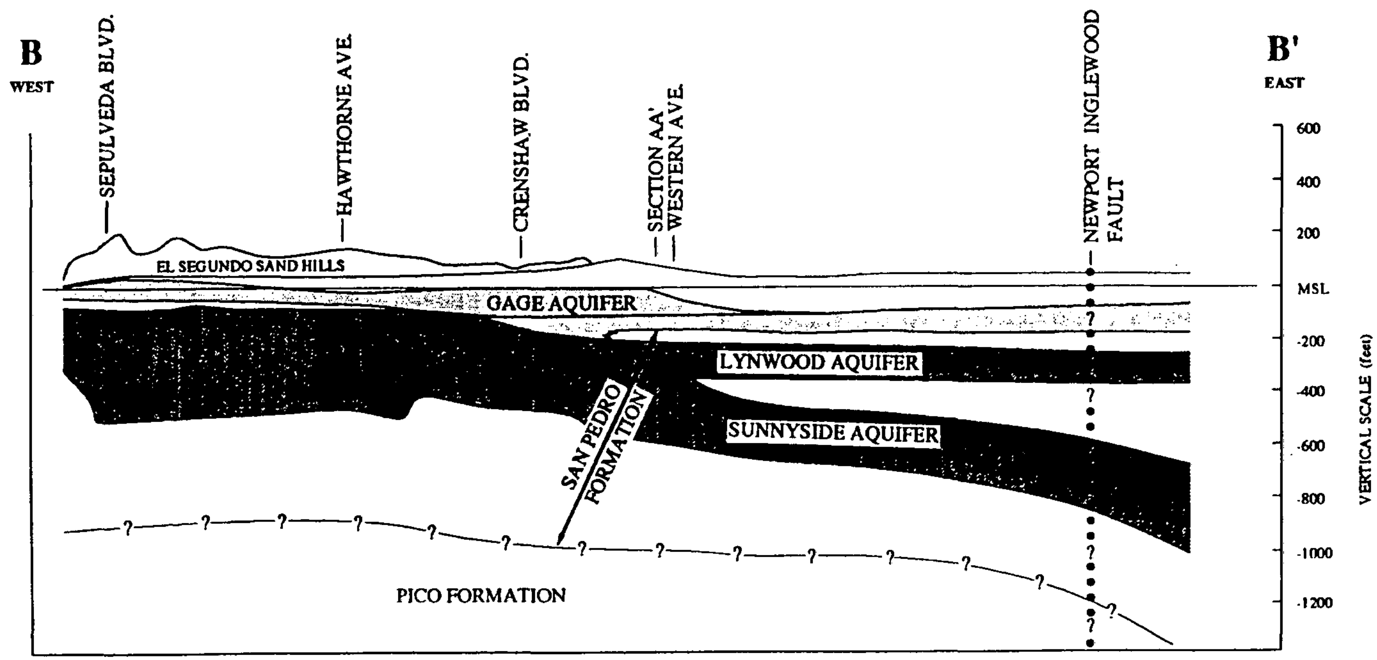

LEGEND

AQUICLUDES AND DEEPER UNDIFFERENTIATED FORMATIONS

AQUIFERS OF THE LAKEWOOD FORMATION

AQUIFERS OF THE SAN PEDRO FORMATION

APPROXIMATE LOCATION OF FAULT

Modified from: 1961, Ground Water Geology of the Coastal Plain of Los Angeles County, State of California Department of Water Ressources

0 6000 12000

APPROXIMATE HORIZONTAL SCALE (feet)

Figure 5.2

CROSS SECTION THROUGH WEST COAST BASIN

DAMES & MOORE

TABLE 5.1

PVLF AREA MONITORING WELLS

WELL NO.	EASTING (Feet)	NORTHING (Feet)	WELL HEAD ELEVATION (Ft. - MSL)	TOTAL DEPTH (Feet)	SCREENED INTERVAL (Feet)	SCREENED FORMATION
M23A	4182145.76	4037722.40	229.93	51.62	31 - 51.62	Qo/Tmv
M24A	4182234.72	4037962.80	221.79	52.00	32 - 52	Tmv
M25A	4182380.63	4037622.59	233.01	82.30	40.8 - 82.3	Qo/Tmv
M26A	4182542.53	4038132.30	195.61	232.10	180.2 - 232.1	Qus
M30B	4182782.18	4036652.43	324.61	121.00	90 - 121	Tmv
M32B	4183423.86	4036005.38	310.47	46.20	25.5 - 46.2	Tmm
M33B	4183434.67	4035995.55	311.73	91.10	70.5 - 91.1	Tmm/Tmv
M34B	4183904.86	4035517.91	332.73	48.00	28 - 48	Tmm
M35B	4183911.74	4035512.51	332.90	121.00	100 - 121	Tmm
M36A	4184804.67	4034968.24	253.99	41.25	20.8 - 41.25	Qo/Tmm
M37A	4184533.10	4035187.28	264.09	31.60	10.8 - 31.6	Qo
M38A	4183785.99	4034447.62	343.28	99.00	59 - 99	Qo/Tmm
M39A	4184400.69	4033756.95	342.74	79.60	59.2 - 79.6	Tmm
M40A	4184435.48	4033113.97	338.00	50.00	30 - 50	Tmm
M41A	4183224.02	4032662.43	356.01	40.00	20 - 40	Qo/Tmm
M42A	4182774.09	4032898.92	411.55	90.00	63 - 90	Tmv
M43A	4182195.27	4033899.20	381.77	100.00	80 - 100	Tmv
M44A	4182865.12	4034188.78	365.24	96.00	65.2 - 96	Qo/Tmv
M45A2	4181405.76	4034038.99	411.19	105.30	74.5 - 150.3	Tmv/Tma
M46A2	4180783.13	4036093.47	371.75	106.70	75.4 - 106.7	Qo/Tmv
M47B	4180678.98	4036694.46	385.81	139.00	87.3 - 139	Tma
M48A	4180540.17	4037606.18	283.47	35.80	15 - 35.8	Qo
M49A	4182098.48	4037500.07	243.74	56.40	35.7 - 56.4	Qo/Tmv
M50B	4182366.67	4038476.50	181.67	201.00	181 - 201	Qus
M51B	4182644.10	4037746.62	223.21	95.00	60 - 95	Qus/Tmm
M52B	4185668.42	4036452.49	182.69	211.00	191 - 211	Qus
M53B	4184012.04	4034893.82	306.28	65.50	40.5 - 65.5	Qo/Tmm
M54B	4179894.99	4037829.37	283.00	67.00	47 - 67	Tma
M55B	4180009.44	4037243.22	306.61	40.50	20.5 - 40.5	Tma
M56B	4178935.44	4035110.02	522.97	140.00	140 - 160	Tma
M57B	4179263.91	4034362.40	505.84	105.00	75 - 105	Tma
M58B	4181352.66	4033194.01	424.84	71.00	51 - 71	Tma
M59B	4185102.70	4035364.66	285.80	61.00	31 - 61	Tmm
M60B	4182410.42	4032291.22	439.84	120.00	100 - 120	Tma
M61B	4182789.68	4031857.96	437.03	130.00	110 - 130	Tma
M62B	4185588.77	4033035.04	389.55	71.00	51 - 71	Qus/Tmm

Qo = Quaternary overburden deposits and landfill materials
Qus = Quaternary undifferentiated sand deposits
Tmm = Malaga Mudstone member of the Tertiary Monterey Formation
Tmv = Valmonte Diatomite member of the Tertiary Monterey Formation
Tma = Altamira Shale Member of the Tertiary Monterey Formation

NEW5_1.WK3

TABLE 5.2
WATER WELLS IN STUDY AREA OUTSIDE OF PVLF

MAP NO.	STATE WELL NO.	LACFCD NO.	WELL OWNER	DATE DRILLED	ORIGINAL USE	SURFACE ELEVATION (FT. -MSL)	TOTAL DEPTH (Feet)	PERFORATED ZONE (Feet)
1	4S/14W-20G2,3,4	738ABC	LACFCD	04/28/58	OBSERVATION CLUSTER	91	878	A - 550-560 B - 317-327 C - 160-170
2	4S/14W-20J2,3,4	739ABC	LACFCD	06/27/68	OBSERVATION CLUSTER	83	743	A - 565-605 B - 300-460 C - 170-230
3	4S/14W-21L2	749D	FRED KITE	2/21/51	IRRIGATION	73	520	336-378 454-470 494-500
*4	4S/14W-21C1	769C						
5	4S/14W-21G1	758D	LACFCD	8/28/55	OBSERVATION	71	239	186-189
6	4S/14W-21N1	749A	PV BEGONIA FARM	3/24/48	IRRIGATION	101	500	306-335
*7	4S/14W-22L2	769C	J. HENDY/ IRON WORKS	1939		78	501	Intermittent 214-360
8	4S/14W-22N1	759C	A.J. ASHKAR/ HUGHES AIRCRAFT	11/1/50	IRRIGATION	79	464	360-380 442-448
9	4S/14W-22Q1	769	UNION OIL CO.	1929	INDUSTRIAL SUPPLY	75	660	188-197 270-300
*10	4S/14W-27B1	769A	DOHENY/WESTON	No Data	IND. IRRIGATION	82	375	209-240 260-265
*11	4S/14W-27G1	260	WESTON RANCH	1920	IRRIGATION	95	408	Intermittent 246-408
12	4S/14W-28G1	240A	ALBERT LEVITT/ ANNA JONES	1/21/51	IND. IRRIGATION	159	326	286-302
*13	4S/14W-28J1	250	WESTON INV.	4/3/26	IRR. & DOMESTIC	185	500	Intermittent 290-500
*14	4S/14W-27N1	250L	TORRANCE SAND & GRAVEL	8/13/59	INDUSTRIAL	203	No Data	No Data
15	4S/14W-34K1	261	L.H. CHANDLER	1917	NONE	280	240	No Data
16	4S/14W-35E6	271N	CHANDLER SAND AND GRAVEL	118/63	INDUSTRIAL	178	600	300-600
17	4S-14W-35E1	271A	CHANDLER SAND AND GRAVEL	1/11/26	INDUSTRIAL	179	585	280-305 450-475 482-502
*18	4S/14W-35E2	271B	LAC WATERWORKS DISTRICT 13	10/29/29	PUBLIC SUPPLY (DOMESTIC)	185	640	No Data
19	4S/14W-35E7	271P	LAC WATERWORKS DISTRICT 13	12/9/70	MUNICIPAL	185	672	368-648
20	4S/14W-35E8	271L	LACFCD	7/3/57	OBSERVATION	167	299	259-299
21	4S/14W-21F1	748H	LAC WATERWORKS DISTRICT 13	7/1/55	OBSERVATION	71	212	191-193
22	4S/14W-35F2	281C	CHANDLER SAND AND GRAVEL	12/10/51	INDUSTRIAL	194	695	265-290 363-410 430-434
*23	4S/14W-10K2	766A	CITY OF TORRANCE	No Data	DOMESTIC	No Data	No Data	No Data
*24	4S-14W-10K3	766B	CITY OF TORRANCE	No Data	DOMESTIC	No Data	No Data	No Data
*25	No Data	No Data	LACSD WELL PV-3	No Data	OBSERVATION	No Data	No Data	No Data
26	4S/14W-22F2	768B	WILLIAM BROTHERS	1925	No Data	72	982	No Data
27	4S/14W-22E1	758C	A.J. ASHKAR	11/7/51	IRRIGATION	74	440	240-255 405-420
28	4S/14W-27M1	No Data	TORRANCE SAND AND GRAVEL	4/20/59	INDUSTRIAL	250	766	Intermittent 352-744
29	4S/14W-28H1	250B	WESTON RANCH	No Data	No Data	147	553	410-425 450-467
30	4S/14W-28J3	250D	WESTON RANCH	JULY 1937	IRRIGATION	185	510	275-305 347-496
31	4S/14W-22F3	768C	J.E. MARBLES	5/17/39	No Data	75	382	214-232 326-332
32	4S/14W-27D1	759	WESTON RANCH	1920	No Data	108	450	303-450
33	4S/14W-28H2	250A	GRAHM BROTHERS	No Data	No Data	148	500	405-423
34	4S/14W-21P2	749B	No Data	No Data	No Data	86	548	No Data
35	4S/14W-22M1	759A	STANDARD OIL CO.	9/23/19	No Data	79	500	247-257 290-397 420-440
36	4S/14W-17H2	737C	CALIF. WATER SERVICE CO.	MARCH 1947	DOMESTIC	92	456	192-454
37	4S/14W-17R1	737FGH	LACFCD	6/19/68	OBSERVATION	77	673	F - 500-590 G - 21-0405 H - 150-180
38	4S/14W-16L4	747G	CITY OF TORRANCE	11/24/52	MUNICIPAL	77	654	257-329 448-545 593-655
39	4S/14W-16Q1	747C	EDISON CO.	No Data	NEVER USED	77	270	No Data
40	4S/14W-16L5	747J,K	LACFCD	6/2/69	OBSERVATION	74	673	J - 410-540 K - 130-260
41	4S/14W-36G2,3,4	301EFG	LACFCD	5/18/60	OBSERVATION	41	1200	E - 530-540 F - 319-329 G - 180-190
42	4S/14W-36H1	301	PV ESTATE WATER CO.	JULY 1923	DOMESTIC	44	610	208-214 332-610
*43	4S/14W-36J1	301C	PV ESTATE WATER CO.	1931	MUNICIPAL	48	500	300-481
*44	4S/14W-21B1	NONE	M. COLOGNE	12/26/50	IRRIGATION	76	548	Intermittent 254-522
*45	4S/14W-21D1	748	KITE BROTHERS	12/15/54	IRRIGATION	75	592	516-586
*46	4S/14W-22-1	769B	J. HENDY CORP.	5/2/28	No Data	78	353	212-336

Map number is shown on Figure 2.1 of text
* indicates that the well data were not used in the model

NEW5_2.WK3

purveyors due to basin adjudication efforts, groundwater levels have either stabilized or steadily increased. Presently, groundwater levels in the West Coast Basin are at their highest elevations in over 60 years. Historic data on PVLF wells are not available to compare against the water level increases in the West Coast Basin. As shown on Figure 5.1, the general direction of groundwater flow in the study area portion of the West Coast Basin is primarily to the east.

Groundwater recharge to the West Coast Basin comes primarily in the form of underflow from the Central Basin to the east, and from injected imported water used to control seawater intrusion (Sanitation Districts, 1987; 1989a). Water imported from the State Water Project and Colorado River is injected at the West Coast Basin and Dominguez Gap Barrier Projects to create fresh groundwater barriers along the north and south coasts adjacent to the Palos Verdes peninsula. Both of these sea-water intrusion barrier projects are outside the study area.

5.3 STUDY AREA HYDROGEOLOGY

The Monterey Formation rocks which largely comprise the Palos Verdes Hills and underlie the PVLF are generally considered incapable of storing and transmitting significant amounts of groundwater (CDWR, 1961). However, relatively minor amount of groundwater is present in the fractures of the Monterey Formation bedrock and in the Qo and Qus deposits overlying these bedrock units. Subsurface flow from the Palos Verdes Hills represents only a small contribution to the total subsurface inflow into the regional West Coast Basin aquifers. This relatively small amount of groundwater flow occurs mainly within ancient depositional drainages, recent alluvium, and weathered/fractured bedrock.

Review of geologic and hydrogeologic data suggests that groundwater in the vicinity of the PVLF generally occurs under unconfined conditions. Water levels in the area wells generally stand at or about the level measured during drilling. Well logs reviewed do not commonly reveal the presence of intervening dry, nonwater bearing zones. This suggests that groundwater within the various geologic formations (Qo, Qus, and bedrock) may be hydraulically interconnected to some degree. Characteristics of groundwater flow in the Palos Verdes area vary according to the unique hydraulic properties of the various geologic formations. Therefore, certain hydrostratigraphic flow zones may be identified based on these unique characteristics. The flow zones identified in this study are correlative with the geologic units described in Section 3.0 and are defined below.

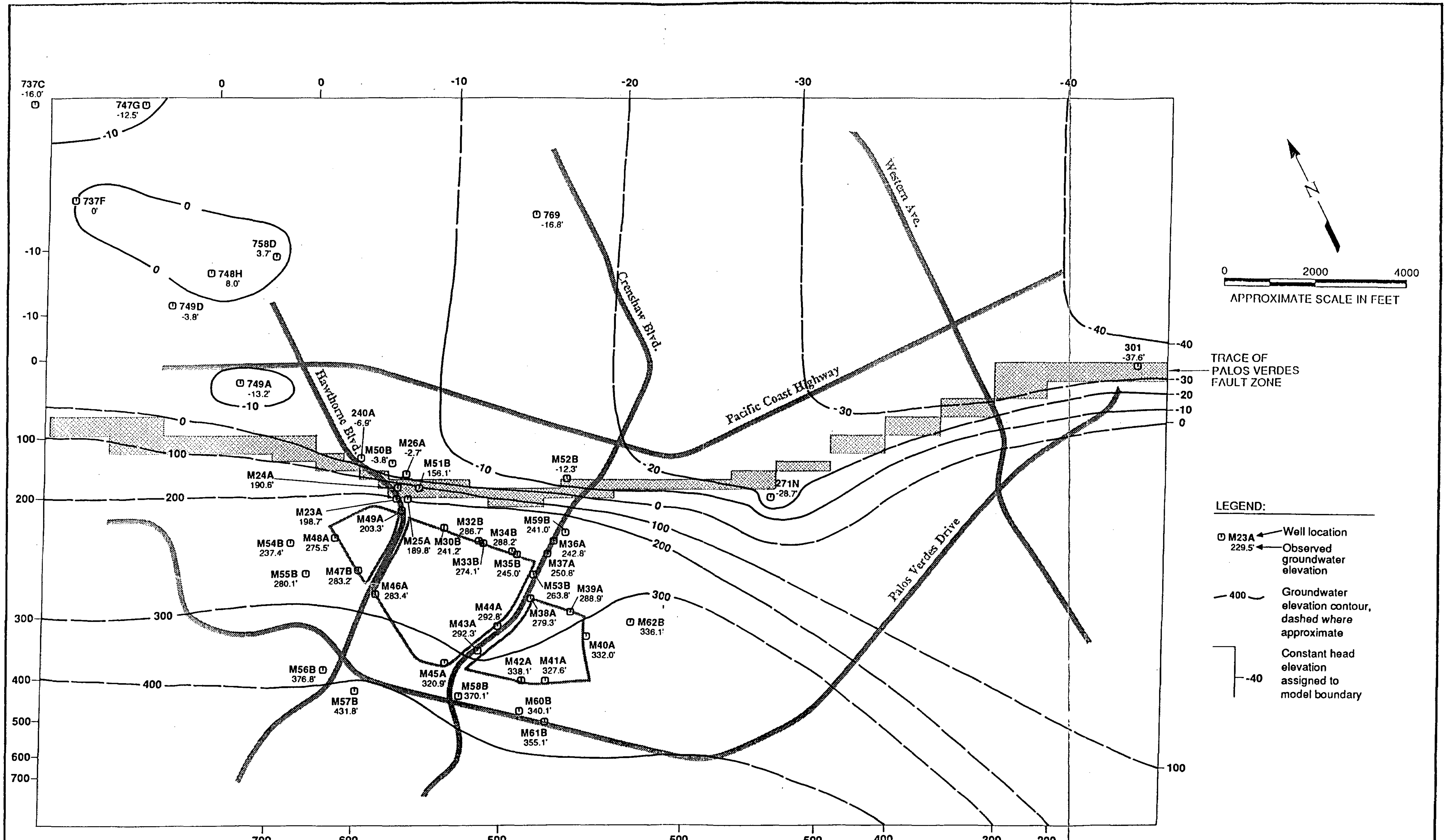

Figure 5.3
MARCH / APRIL 1991 GROUNDWATER ELEVATION CONTOUR MAP OF STUDY AREA

5.3.1 Definition and Characteristics of the Hydrostratigraphic Flow Zones

The primary hydrostratigraphic flow zones and their characteristics are interpreted from geologic and hydrogeologic information presented in previous studies reviewed by Dames & Moore. Groundwater moves through each flow zones at a rate determined by the intrinsic hydraulic conductivity of the aquifer materials and the regional hydraulic gradient. The regional gradient was determined by reviewing groundwater elevation contour maps. Figure 5.3 shows groundwater elevation contours for PVLF based on March/April 1991 data. The hydraulic conductivities are evaluated through field and laboratory tests presented in reports by the Sanitation Districts (1987; 1989a), Herzog (1991a; 1991b), Kleinfelder (1988), and Stone (1975). A summary of all the hydraulic conductivity values listed in these reports and the formations tested, is presented on Table 5.3. A discussion of the different test methodologies used to collect the data is presented in the Sanitation Districts HCP report (1989a). The limitations to methods used to identify the hydraulic conductivity values for these flow zones are discussed in Section 6.2.2.1

The following paragraphs describe the primary hydrostratigraphic flow zones used in the model and provide quantitative discussions of hydraulic conductivity within each flow zone.

5.3.1.1 Catalina Schist (Jc)

The Jurassic-age Catalina Schist serves as the base of the hydrogeologic model, as flow through this metamorphosed unit is considered extremely small compared to the overlying zones. Due to its depth beneath the PVLF and its non-granular nature, borings have not been drilled into the Jc to test its hydraulic conductivity values. Therefore, hydraulic conductivity of this zone was assigned the conservatively high value of 1.0 E-7 (0.0000001) centimeters per second (cm/sec), which is the maximum value for the range of hydraulic conductivities for metamorphic rocks (Freeze and Cherry, 1979).

5.3.1.2 Altamira Shale (Tma)

The hydraulic conductivity values for the Tma flow zone were obtained from Kleinfelder (1988) slug tests and Herzog (1991) packer tests. Reported values range from 2.09 E-7 cm/sec in borehole RFB-22 to 1.30 E-3 cm/sec in borehole M45A2. The high degree of variation is

TABLE 5.3

LIST OF AVAILABLE HYDRAULIC CONDUCTIVITY DATA

(PAGE 1 OF 2)

BORING/ WELL	K (cm/sec)	K (ft/day)	TEST TYPE	ROCK TYPE	DATA SOURCE
P-1	1.00E-05	2.83E-02	Permeameter	PVLF Cover	Woodward-Clyde, 1981
P-2	3.40E-05	9.64E-02	Permeameter	PVLF Cover	Woodward-Clyde, 1981
P-3	1.00E-05	2.83E-02	Permeameter	PVLF Cover	Woodward-Clyde, 1981
C-5	4.00E-08	1.13E-04	Remold	Qo	Stone, 1975
C-5	3.00E-07	8.50E-04	Sieve	Qo	Stone, 1975
LE-1	7.20E-04	2.04E+00	Aquifer	Qo	Sanitation Districts, 1986a
M37A	1.24E-04	3.51E-01	Slug	Qo	Kleinfelder, 1988
M48A	3.70E-05	1.05E-01	Slug	Qo	Kleinfelder, 1988
M36A	1.20E-03	3.40E+00	Slug	Qo/Tmm	Kleinfelder, 1988
M38A	8.50E-05	2.41E-01	Slug	Qo/Tmm	Kleinfelder, 1988
RFB16/M53B	1.40E-05	3.97E-02	Aquifer	Qo/Tmm	Herzog, 1991a
M23A	5.50E-05	1.56E-01	Slug	Qo/Tmv	Kleinfelder, 1988
M25A	4.20E-05	1.19E-01	Slug	Qo/Tmv	Kleinfelder, 1988
M41A	3.34E-04	9.47E-01	Slug	Qo/Tmv	Kleinfelder, 1988
M44A	3.55E-03	1.01E+01	Slug	Qo/Tmv	Kleinfelder, 1988
M46A2	3.80E-05	1.08E-01	Slug	Qo/Tmv	Kleinfelder, 1988
M49A	1.30E-05	3.69E-02	Slug	Qo/Tmv	Kleinfelder, 1988
A-5	1.60E-05	4.54E-02	Permeameter	Qus	Stone, 1975
A-8	3.60E-06	1.02E-02	Permeameter	Qus	Stone, 1975
C-1	6.17E-06	1.75E-02	Remold	Qus	Stone, 1975
C-1	9.00E-06	2.55E-02	Sieve	Qus	Stone, 1975
C-9	2.10E-03	5.95E+00	Remold	Qus	Stone, 1975
M26A	9.90E-06	2.81E-02	Slug	Qus	Kleinfelder, 1988
RFB13/M52B	6.60E-05	1.87E-01	Aquifer	Qus	Herzog, 1991a
RFB13/M52B	6.62E-04	1.88E+00	Lab	Qus	Herzog, 1991a
RFB14	3.60E-04	1.02E+00	Lab	Qus	Herzog, 1991a
RFB17	8.06E-04	2.28E+00	Lab	Qus	Herzog, 1991a
RFB3/M50B	1.75E-03	4.96E+00	Aquifer	Qus	Herzog, 1991a
RFB3/M50B	9.10E-04	2.58E+00	Lab	Qus	Herzog, 1991a
RFB4/M51B	1.20E-04	3.40E-01	Aquifer	Qus	Herzog, 1991a
BC-2	3.00E-06	8.50E-03	Packer	Bedrock	Sanitation Districts, 1986a
BC-2	5.00E-06	1.42E-02	Packer	Bedrock	Sanitation Districts, 1986a
BC-2	2.00E-06	5.67E-03	Packer	Bedrock	Sanitation Districts, 1986a
BC-3	3.00E-06	8.50E-03	Packer	Bedrock	Sanitation Districts, 1986a
BC-3	5.00E-06	1.42E-02	Packer	Bedrock	Sanitation Districts, 1986a
BC-3	4.00E-06	1.13E-02	Packer	Bedrock	Sanitation Districts, 1986a
C-3	2.00E-06	5.67E-03	Sieve	Bedrock	Stone, 1975
Parcel 6	5.00E-07	1.42E-03	Field Perc.	Bedrock	Stone, 1975
A-2	1.60E-06	4.54E-03	Permeameter	Tmm	Stone, 1975
A-3	2.10E-06	5.95E-03	Permeameter	Tmm	Stone, 1975
A-4	2.70E-07	7.65E-04	Permeameter	Tmm	Stone, 1975
A-9	1.30E-05	3.69E-02	Permeameter	Tmm	Stone, 1975
C-1	6.10E-08	1.73E-04	Lab	Tmm	Stone, 1975
C-1	1.70E-08	4.82E-05	Lab	Tmm	Stone, 1975
C-1	2.23E-07	6.32E-04	Remold	Tmm	Stone, 1975
C-3	4.53E-08	1.29E-04	Remold	Tmm	Stone, 1975
C-3	1.10E-08	3.12E-05	Lab	Tmm	Stone, 1975
C-3	2.50E-08	7.09E-05	Lab	Tmm	Stone, 1975
L3/M62B	4.57E-07	1.30E-03	Packer	Tmm	Herzog, 1991a
L3/M62B	6.16E-08	1.75E-04	Packer	Tmm	Herzog, 1991a
L3/M62B	6.47E-08	1.83E-04	Packer	Tmm	Herzog, 1991a
M32B	4.12E-03	1.17E+01	Slug	Tmm	Kleinfelder, 1988
M34B	2.79E-03	7.91E+00	Slug	Tmm	Kleinfelder, 1988
M39A	4.50E-03	1.28E+01	Slug	Tmm	Kleinfelder, 1988
M40A	1.03E-03	2.92E+00	Slug	Tmm	Kleinfelder, 1988
RFB10	1.10E-06	3.12E-03	Lab	Tmm	Herzog, 1991a
RFB12	6.30E-07	1.79E-03	Packer	Tmm	Herzog, 1991a
RFB12	1.54E-06	4.37E-03	Packer	Tmm	Herzog, 1991a
RFB12	2.91E-07	8.25E-04	Packer	Tmm	Herzog, 1991a
RFB12	7.23E-08	2.05E-04	Lab	Tmm	Herzog, 1991a
RFB15	4.40E-08	1.25E-04	Lab	Tmm	Herzog, 1991a
RFB32	8.65E-07	2.45E-03	Packer	Tmm	Herzog, 1991a
RFB6	1.61E-07	4.56E-04	Packer	Tmm	Herzog, 1991a
RFB6	1.05E-07	2.98E-04	Packer	Tmm	Herzog, 1991a
RFB7	2.63E-07	7.46E-04	Packer	Tmm	Herzog, 1991a
RFB7	9.77E-06	2.77E-02	Lab	Tmm	Herzog, 1991a
RFB7	1.21E-07	3.43E-04	Packer	Tmm	Herzog, 1991a
M33B	1.59E-03	4.51E+00	Slug	Tmm/Tmv	Kleinfelder, 1988
M24A	1.30E-04	3.69E-01	Slug	Tmv	Kleinfelder, 1988
M42A	4.38E-04	1.24E+00	Slug	Tmv	Kleinfelder, 1988
M43A	2.28E-03	6.46E+00	Slug	Tmv	Kleinfelder, 1988
RFB11	1.06E-07	3.00E-04	Packer	Tmv	Herzog, 1991a

TABLE 5.3

LIST OF AVAILABLE HYDRAULIC CONDUCTIVITY DATA
(PAGE 2 OF 2)

BORING/ WELL	K (cm/sec)	K (ft/day)	TEST TYPE	ROCK TYPE	DATA SOURCE
RFB11	1.65E-07	4.68E-04	Packer	Tmv	Herzog, 1991a
RFB11	9.14E-07	2.59E-03	Packer	Tmv	Herzog, 1991a
RFB16/M53B	1.49E-07	4.22E-04	Packer	Tmv	Herzog, 1991a
RFB19	1.79E-04	5.07E-01	Packer	Tmv	Herzog, 1991a
RFB19	1.10E-07	3.12E-04	Packer	Tmv	Herzog, 1991a
RFB24/M56B	1.52E-06	4.31E-03	Packer	Tmv	Herzog, 1991a
RFB30A	4.47E-06	1.27E-02	Packer	Tmv	Herzog, 1991a
RFB30A	6.55E-06	1.86E-02	Packer	Tmv	Herzog, 1991a
RFB32	2.33E-07	6.60E-04	Packer	Tmv	Herzog, 1991a
RFB32	5.07E-07	1.44E-03	Packer	Tmv	Herzog, 1991a
RFB7	6.97E-08	1.98E-04	Packer	Tmv	Herzog, 1991a
RFB7	1.97E-07	5.58E-04	Packer	Tmv	Herzog, 1991a
M45A2	1.30E-03	3.69E+00	Slug	Tma	Kleinfelder, 1988
M47B	3.70E-04	1.05E+00	Slug	Tma	Kleinfelder, 1988
RFB1	2.00E-05	5.67E-02	Packer	Tma	Herzog, 1991a
RFB1	9.53E-05	2.70E-01	Packer	Tma	Herzog, 1991a
RFB1	1.24E-04	3.51E-01	Packer	Tma	Herzog, 1991a
RFB22	2.09E-07	5.92E-04	Packer	Tma	Herzog, 1991a
RFB22	3.64E-07	1.03E-03	Packer	Tma	Herzog, 1991a
RFB22	1.08E-06	3.06E-03	Packer	Tma	Herzog, 1991a
RFB24/M56B	1.67E-06	4.73E-03	Packer	Tma	Herzog, 1991a
RFB25/M57B	1.10E-06	3.12E-03	Packer	Tma	Herzog, 1991a
RFB25/M57B	1.45E-05	4.11E-02	Packer	Tma	Herzog, 1991a
RFB25/M57B	4.22E-07	1.20E-03	Packer	Tma	Herzog, 1991a
RFB29/M60B	7.18E-07	2.04E-03	Packer	Tma	Herzog, 1991a
RFB29/M60B	1.43E-04	4.05E-01	Packer	Tma	Herzog, 1991a
RFB29/M60B	2.36E-04	6.69E-01	Packer	Tma	Herzog, 1991a

NEW5_3.WK3

Qo = Quaternary overburden deposits and landfill refuse
Qus = Quaternary undifferentiated sand deposits
Tmm = Malaga Mudstone member of the Tertiary Monterey Formation
Tmv = Valmonte Diatomite member of the Tertiary Monterey Formation
Tma = Altamira Shale member of the Tertiary Monterey Formation
Bedrock = Monterey, Undifferentiated
Remold K Values are an Average of 85%, 90%, and 95% Compactions
cm/sec = centimeters per second
ft/day = feet per day
2.36E-04 is scientific notation for 0.000236
For a discussion of test type methodologies, see Sanitation Districts HC Report, Phases II and III (1992)

attributed to methods of analysis as well as variations in physical characteristics of the Altamira Shale.

5.3.1.3 Valmonte Diatomite (Tmv)

Ranges of values for hydraulic conductivity for the Tmv flow zone were obtained from Kleinfelder (1988) slug tests and Herzog (1991) packer tests. Reported values range from 6.97 E-8 cm/sec in borehole RFB-7 to 2.28 E-3 cm/sec in borehole M43A. The high degree of variation is attributed both to different methods of analysis and to variations in physical characteristics of the Valmonte Diatomite.

5.3.1.4 Malaga Mudstone (Tmm)

Values of hydraulic conductivity for the Tmm flow zone were obtained from Kleinfelder (1988) slug tests, from Stone (1975) remolded, laboratory, and permeameter tests, and from Herzog (1991) laboratory and packer tests. Reported values range from 1.10 E-8 cm/sec in borehole C-3 to 4.50 E-3 cm/sec in borehole M39A. The high degree of variation is attributed to variations in physical characteristics of the Malaga Mudstone, such as random distribution of fracture zones that significantly affect hydraulic conductivity, as well as to the different methods of analysis.

5.3.1.5 Undifferentiated Sand (Qus)

Hydraulic conductivity values for the Qus flow zone were obtained from Kleinfelder (1988) slug test data, from Stone (1975) test data on remolded samples, sieve analysis data, and field permeameter tests, and from Herzog (1991) laboratory and field aquifer tests. Reported values range from 3.60 E-6 cm/sec in borehole A-8 to 2.10 E-3 cm/sec in borehole C-9. The high degree of variation in results is attributed to the different methods of analysis, the locations of the tests, and the variability of soil types.

5.3.1.6 Overburden (Qo)

The overburden flow zone includes all unconsolidated sediments and landfill materials which locally overlie the undifferentiated sand (Qus) flow zone. Hydraulic conductivity values for the Qo were obtained from slug tests (Kleinfelder 1988), laboratory tests on remolded samples and a sieve analysis (Stone 1975), and on field aquifer tests (Sanitation Districts, 1986a, and Herzog, 1991). Reported values range from 4.00 E-8 cm/sec in borehole C-5 to 3.55 E-3 (0.00355) centimeters per second (cm/sec) in borehole M44A. The high degree of variation in test results is attributed to the different methods of analysis as well as the variability of soil types found in the Qo zone.

5.3.2 Hydrogeologic Effects of Geologic Structures

The two structures that have the most significant impact on groundwater flow are the Palos Verdes fault zone and the fracture network in the Monterey Formation. These elements of geologic structure, and their impacts upon the flow of groundwater, are discussed in the following paragraphs.

5.3.2.1 Palos Verdes Fault Zone

The effect of the Palos Verdes fault zone as a partial barrier to groundwater flow is evidenced by nearly a 200 feet drop in groundwater elevations between wells on the upgradient (PVLF) side of the fault (e.g., M24A) and wells on the downgradient (West Coast Basin) side of the fault (e.g., M26A). This effect is especially pronounced near the intersection of Hawthorne Boulevard and the northeastern side of the landfill (Figure 2.7). The near-surface location of the fault is at its closest point to the landfill in this area, and monitoring wells here provide data documenting the relatively abrupt drop in groundwater elevation across the fault.

The hydraulic barrier effect appears to be less pronounced northeast along the Palos Verdes fault zone. However, fewer wells exist in this area to document groundwater elevations, which produce data suggesting a more gradational water level change (due to the lateral distances between wells). This less-pronounced effect may also be partly due to a more widespread occurrence of the San Pedro Formation in this area, both on the upgradient and downgradient sides of the fault. The generally higher hydraulic conductivity of the San Pedro Formation would tend to reduce the hydraulic barrier effect of the faulted portion of this unit.

5.3.2.2 Fracture Network

The Kleinfelder (1988) and Herzog Associates (1991a; 1991b) reports provided information regarding fracture characteristics of the Monterey Formation members, including the occurrence, frequency, fracture separation, and generalized fracture trends.

For the purpose of quantifying the descriptive terms in the boring logs, numerical values were assigned to each borehole representing the degree of fracturing according to fracture spacing and fracture separation criteria outlined in Herzog (1991a; 1991b). These criteria are presented in Table 5.4. However, fracture descriptions in the Kleinfelder and Herzog borings are not mutually consistent, due in part to drilling methods, and in part to different descriptions provided by different on-site geologists. Fracture descriptions were given with each core length in most of the Kleinfelder logs, whereas descriptions were less consistent in the Herzog logs.

The range of numerical values representing the fracture descriptions in each borehole were plotted on a subcrop map (Figure 3.1, in pocket) showing the contacts between Monterey Formation members and the location of the Palos Verdes Fault. No trends in the fracture descriptions were apparent when considering either all of the boreholes together, or considering the Kleinfelder boreholes, alone. Fracturing appeared to be ubiquitous throughout the Monterey Formation, with most descriptions in the range of "moderately fractured" to "intensely fractured," that is, fracture spacings of 3 feet to less than 2 inches. Most fracture spacings were described as "closed" to "very narrow", that is, aperture widths of 0.0 to 0.1 millimeters (mm). Occasionally, "narrow" fracture widths (e.g., 0.1 to 1 mm) were described, and "wide" fracture width (up to 5 mm) was noted in one borehole, Well M47B. The Sanitation Districts found during their HCP investigation that fracture openings in the Malaga Mudstone tend to close up at depths of 100 feet below the ground surface northeast of the PVLF.

5.3.3 Groundwater Occurrence and Movement at PVLF

Groundwater at PVLF occurs both in the Monterey Formation bedrock and the overlying deposits. As previously described, the near surface geologic materials at the PVLF area consist of undifferentiated sands (Qus) and unconsolidated sediments and backfill material composed of reused mine tailings (Qo). Relatively higher in hydraulic conductivity than the bedrock units, these materials act to transmit downwardly percolating waters to the water table, or to former natural drainages and the fracture networks in the bedrock formations below. Prior to landfilling

TABLE 5.4

FRACTURE CLASSIFICATION SYSTEM

FRACTURE DESCRIPTION	SPACING OF FRACTURES	SEPARATION OF FRACTURES (millimeters)	DEFINITION
Intensely Fractured	Less than 2-Inches	-	-
Highly Fractured	2-Inches to 1-Foot	-	-
Moderately Fractured	1-Foot to 3-Feet	-	-
Slightly Fractured	3-Feet to 10-Feet	-	-
Massive	Greater than 10-Feet	-	-
Closed	-	0	-
Very Narrow	-	0.0 to 0.1	-
Narrow	-	0.1 to 1.0	-
Wide	-	1.0 to 5.0	-
Very Wide	-	5.0 to 15.0+	-
Clean	-	-	No Fracture Filling
Stained	-	-	Discoloration of Fracture
Filled	-	-	Fracture Filled with Recognizable Material (such as hydrocarbons)

Classification Data From Herzog Boring Logs (1991a) NEW5_4.WK3 and mining operations, two primary surface water drainages, Agua Negra and Agua Magna Canyons, crossed the present landfill site (Figure 5.4). Aerial photographs taken in the 1930s through the 1950s show the gradual alteration of these drainages by the deposition of mine tailings. Percolating surface waters may preferentially follow these former drainages.

At PVLF, groundwater in the Monterey Formation occurs in a complex network of fractures and bedding planes. Borehole logs and water-level data were studied for evidence of groundwater occurrence and flow characteristics between members of the Monterey Formation and the overlying deposits. In most cases, data suggest that the Monterey Formation is hydraulically connected to the overburden materials. That is, there does not appear to be a confining layer separating the two flow systems. Logs of several boreholes described moisture in the Qo or Qus units, indicating seepage conditions or possibly minor, localized perched zones. Additionally, water was often found at the Qo or Qus and Monterey Formation contact, which is not unexpected due to the lower hydraulic conductivities of the bedrock.

In a general sense, groundwater flow beneath the PVLF follows the local topographic relief, which results in a predominant northeasterly flow (Figure 5.3). Groundwater flow is generally faster in the overburden (Qo) and undifferentiated sand (Qus) flow zones, and slowly percolates into the fractures of the subcropping Monterey Formation members. This infiltration may take place preferentially along areas of increased weathering and/or fracturing. Groundwater is likely recharged from upgradient (southwest) lateral inflow, and through infiltration of precipitation and irrigation waters.

N

SCALE IN FEET

0 600 1200

BOUNDARY OF HISTORICAL LANDFILL PROPERTY

DRAINAGE CHANNELS TRACED FROM AIR PHOTOS (FROM CSDLAC AUGUST 1987)

BASE MAP SOURCE: SANITATION DISTRICTS HC REPORT, PHASES II AND III

FIGURE 5.4
Former Drainage Across Landfill

DAMES & MOORE

6.0 HYDROGEOLOGIC MODEL

The purpose of hydrogeologic modeling (commonly referred to as groundwater modeling) is to develop an analytical tool to help understand and predict the actual groundwater flow conditions in an area of interest. Groundwater modeling has been extensively used since the mid 1960's to help analyze many groundwater related problems, including regional aquifer studies, basin analysis, well field design, and contaminant transport matters. The development of groundwater models generally involved the following two major steps: development of conceptual models; and development of detailed mathematical models (Mercer and Faust, 1981).

6.1 OVERVIEW

A conceptual model is simply the basic understanding of the aquifer system, including a knowledge of important physical characteristics such as head elevations, gradients, hydraulic conductivities, layer thickness, and locations of potential barriers to flow (e.g. faults). The mathematical models translates the ideas of the conceptual model into a set of mathematical equations based on acceptable physical laws. A mathematical model for groundwater flow consists of a set of governing partial differential equations together with appropriate boundary and initial conditions that describe continuous variables (e.g., hydraulic head) over the region of interest. Once the mathematical model is formulated, a solution to the governing mathematical equations may be obtained through one of the two general approaches: analytical approach and numerical approach. The analytical approach is utilized when simplifying assumptions, such as homogeneous hydraulic properties, and simple geometry, are justifiable. For problems where the analytical approach is not applicable, the governing equations may be solved by a numerical technique whereby the governing partial differential equations are approximated by a finite number of algebraic equations. This approach constitutes a numerical model and generally is used to simulate complex hydrogeologic system such as the one at PVLF. Generally, a computed program (code) is written to solve the groundwater flow equations on a digital computer. The hydrogeologic model developed for PVLF is a numerical model based on the MODFLOW computer code developed by the USGS (McDonnall and Harbaugh, 1988).

The general steps required to construct a groundwater flow model are presented below. For a more detailed introduction to modeling, the reader should refer to specific texts on the subject, such as Mercer and Faust (1981).

1. Decide whether a numerical model is necessary: If the groundwater problem is simple and there are very limited data, a numerical model is probably not necessary and not warranted. If there are sufficient data to show the complexity and heterogeneity of the site geology and hydrogeology, then a numerical model may be appropriate.

2. Collect available data: After the boundaries of the area of interest have been identified, all available information on the geologic and hydrogeologic properties must be obtained. Typical information required includes, but is not limited to, elevations of aquifers and aquitards, confined and unconfined water elevations, locations of wells, location of recharge areas and annual amounts of infiltration, hydraulic conductivity and porosity values for all geologic layers within the model area, saturated thicknesses of aquifers, storage coefficient values, location of pumping wells, locations of faults or other potential barriers to flow, aquifer test records, and historical water elevation data.

3. Discretize the model area: After determining the model boundaries, the area is subdivided (discretized) into grids or blocks. A rectangular grid system is used for finite-difference numerical models, and irregular polygonal subdivisions are used for finite-element numerical models (see Huyakorn and Pinder (1983) for details). The grid spacing depends on the amount of detail which is needed or the complexity of the site. Grids are usually spaced closer near areas where greater accuracy is needed, such as around pumping wells, observation wells, potential receptors, or anomalous features in the aquifer system, such as faults or injection wells. If the numerical model is three-dimensional, then the model area is discretized both laterally and vertically. A complex three-dimensional numerical model typically has 5,000 to 10,000 individual grid blocks, or more.

4. Data input: After constructing the grid, the specific aquifer parameters such as hydraulic conductivity, recharge, layer thickness, well locations, fault locations, water elevations, storage coefficients, boundary conditions, and porosity values are entered for each grid block.

5. Model calibration: The numerical model is run on a digital computer using the input data. The results, which usually consist of water elevation values at each

grid block, are compared to actual water elevations measured in the field. If the actual elevations are within statistical limits of the model calculated elevations, then the model is said to be calibrated to real-world conditions. To establish greater confidence in the model, the calibrated parameter values may be validated using a second set of field data (Anderson and Woessner, 1992).

Once the model is validated (and/or calibrated), it may be used for predictive analysis. Sensitivity analysis must also be carried out to quantify potential predictive errors due to parameter uncertainty. The definition of the word "validation" in this study is consistent with that defined in 10 CFR 60 (US Nuclear Regulatory Commission, 1983). In accordance with 10 CFR 60, validation is the process of obtaining assurance that a model as embodied in a computer program is a correct representation of the process or system for which it is intended. Validation is thus carried out by comparison of calculations with field observations and experimental measurements (International Atomic Energy Authority, 1982). In many instances, data sets for model validation are unavailable. For calibrated models which are not validated, careful sensitivity analyses (see Item 6 below) must be conducted and evaluated prior to performing predictive analyses (Anderson and Woessner (1992); the word "verification" used by these authors corresponds to the word "validation" in this report).

6. Sensitivity/uncertainty analysis: To assess how modifications to parameters affect the calibrated model, and to identify areas of data uncertainty, sensitivity and uncertainty analyses are performed. This involves re-running the calibrated model numerous times, each time changing a different parameter value and observing the results. For example, the hydraulic conductivity values could be decreased by an order of magnitude to observe whether any changes occur to the flow system. If there are no significant changes, then the model is not sensitive to decreases in hydraulic conductivity. The results of the analysis indicate which parameters the model is most sensitive to, thereby identifying critical areas which require the most reliable and accurate data.

7. Model application: The calibrated (and validated if possible) model can then be used to predict future aquifer characteristics under steady-state, transient, stressed, and unstressed conditions, as well as provide supporting evidence for the

conceptual understanding of the aquifer flow system. It can be used to simulate groundwater flow conditions, and estimate the velocity and direction of groundwater. In addition, the model can be used to assess the effects of pumping one or more wells screened in different aquifers at different rates for different periods of time and the effects of faults or other barriers on the flow of groundwater. The model can also be used in conjunction with a contaminant transport model to simulate the movement of pollutants through the groundwater. If it is not possible to validate the model using a second set of field data, a sensitivity analysis must be conducted to evaluate the range of uncertainty associated with calibration and prediction. The developed model, with appropriate sensitivity and uncertainty analysis, may be used as a management and predictive tool to assess the effects of different scenarios and parameters on the groundwater flow system.

6.2 HYDROGEOLOGIC FLOW MODEL

Hydrogeologic flow modeling is a widely accepted tool for investigating and evaluating hydrogeologic conditions at sites such as the PVLF. A literature review on technical modeling approaches and modeling projects similar to the PVLF is presented in Appendix B.

6.2.1 Model Selection and Development

Numerous computer codes are available for characterization and simulation of groundwater flow conditions. Although nearly all published codes are suitable for some specific purposes, not all codes are appropriate for each groundwater flow modeling project. The specific needs of the project and the objectives to be realized in groundwater flow modeling must be taken into account in selecting the optimum computer code for each specific project. This section describes the basis for selection of the computer code used in this project for groundwater flow modeling of the study area (model area).

6.2.1.1 Conceptual Model Development

Prior to the development of a numerical flow model, all aspects of the hydrogeologic conditions within the model area must be adequately understood and presented in the form of a conceptual model. For the PVLF, the conceptual model was developed using the Sanitation Districts' MCS based geologic model, hydrogeologic data presented in previous PVLF studies, and data on groundwater elevations in the model area outside of the PVLF. These data promote a three-dimensional understanding of the hydrogeologic conditions within the study area, and are the basis for model calibration and verification.

The developed conceptual model consisted of two interrelated groundwater flow subsystems: (1) the regional flow in the West Coast Basin, and (2) the topographically-driven flow in on the Palos Verdes Hills area. These two subsystems are distinct groundwater flow systems separated by the Palos Verdes fault zone. Hydrogeologic data from monitoring wells near the fault (MW-24A and MW-26A) suggest that the fault may impede and/or redirect the flow of groundwater along its length.

6.2.1.2 Model Selection

The selection process involved identification and definition of appropriate criteria for selection; identification of available computer codes; evaluation of the available codes using the selected criteria; and selection of the code that best fits the project at hand. Identification and definition of criteria are the most important parts of this process.

6.2.1.2.1 Selection Criteria

The complexity of the geologic and hydrogeologic conditions in the vicinity of the PVLF necessitated the use of a three-dimensional groundwater flow model in order to accurately simulate the behavior of fluids in the subsurface materials. There are numerous groundwater flow models available commercially as well as in the public domain and each has its own advantages and disadvantages. Dames & Moore established a set of criteria for the PVLF modeling task to evaluate different codes for the purpose of selecting the most appropriate model to accurately simulate and predict groundwater movement within the model area. These criteria include the following:

- Objective Criteria: The selected flow model should have the ability to simulate with acceptable accuracy the flow and transport of groundwater at the PVLF.

- Technical Criteria: The selected flow model should be capable of handling three-dimensional, geologically heterogeneous aquifers. It should allow for free surface (water table) conditions, infiltration at the water table, an irregular-domain configuration, and optional free-phase liquid capabilities.

- Historical Application Criteria: The selected flow model should have a proven history of success with similar sites for similar purposes.

- Implementation Criteria: The selected flow model should be in the public domain for ease in accessibility, should have adequate support documentation, should have been verified against analytical solutions, and should be validated with actual field data.

6.2.1.2.2 Evaluation of Available Models

Twelve numerical flow models were evaluated to measure their appropriateness for meeting the objectives for the PVLF. The models were evaluated against the criteria and were ranked as either meeting the criteria, not meeting the criteria, or partially meeting the criteria. Table 6.1 provides a list of the evaluated models and their qualifications against the established criteria.

As a result of Dames & Moore's evaluation, the USGS model known as MODFLOW was selected to use as a basis for the development of the groundwater flow model for the PVLF. MODFLOW is a well known and widely used groundwater modeling code which has been validated in numerous applications. It is efficient to use because of the modular nature of various packages in the model, which allow the simulation of groundwater flow, effects of sources and sinks, and the effects of varying precipitation and recharge areas. The advantages to MODFLOW are: it is in the public domain; it can handle phreatic surface (water table) transient and steady-state conditions, and variable layer thicknesses; it utilizes efficient solution techniques; and it can simulate heterogeneity and irregular-flow domains.

TABLE 6.1

MODEL CODES EVALUATED FOR USE AT PVLF

GROUNDWATER FLOW MODEL EVALUATED	OBJECTIVE CRITERIA	TECHNICAL CRITERIA	IMPLEMENTATION CRITERIA	HISTORICAL APPLICATION CRITERIA	PUBLIC DOMAIN	REMARKS
MODFLOW	Yes	Yes	Yes	Yes	Yes	
PTC	Yes	Yes	Yes	Yes	No	
SWIFT	Yes	Yes	Yes	Yes	Yes	1
CFEST	Yes	Yes	Yes	Yes	Yes	2
TARGET	Yes	Yes	Yes	Yes	No	
FLAMINCO	Yes	Yes	Yes	Yes	No	
SATURN	Yes	Yes	Yes	Yes	No	
TRUST	Yes	Yes	Yes	Yes	Yes	3
SEGOL	Yes	Yes	Yes	Yes	Yes	3
PLASM	Yes	Partial	Yes	Yes	Yes	
PORFLOW	Yes	Yes	Yes	Yes	No	
SUTRA	Yes	Partial	Yes	Yes	Yes	

NEW6_1.WK3

NOTES:

1 Cannot handle piezometric head. Requires extensive input for non-uniform layer thickness. Requires extensive memory to run.

2 Unconfined flow is possible only through manual iteration.

3 Computational effort is prohibitive for large three-dimensional problems.

6.2.2 Hydrogeologic Characteristics of Flow Zones

The hydrogeologic characteristics of the identified flow zones were input into MODFLOW. These characteristics included hydraulic conductivity, porosity, layer thickness, and groundwater elevations. These are discussed in the following paragraphs.

6.2.2.1 Hydraulic Conductivity

Numerous field and laboratory hydraulic conductivity tests have been performed at the PVLF. Data on these tests are provided in reports by the Sanitation Districts (1987; 1989a), Herzog (1991a; 1991b), Kleinfelder (1988), and Stone (1975). A discussion of the different test methodologies used to collect the data is presented in a report by the Sanitation Districts (1989a). An analysis of all available hydraulic conductivity values was performed by Dames & Moore to establish whether there were representative values for each zone or whether zone values changed with depth and/or distance across the site.

Initially, all available hydraulic conductivity data (Table 5.3) were plotted and reviewed for anomalous or questionable data. Anomalous data sometimes occurred as a result of test methodologies or data interpretations. The anomalous or questionable data were excluded from the hydraulic conductivity analysis, so that only the geologically reasonable data were addressed. Table 6.2 shows the reduced set of hydraulic conductivity values Dames & Moore considered to be geologically reasonable based on the test methodologies used. The reasons for identifying and deleting anomalous data values are discussed below.

- Remolded laboratory analyses were excluded. The test methodology involves laboratory compaction of a bulk sample collected in the field. The resulting hydraulic conductivity values may not represent actual in-situ characteristics.

- Field permeameter tests were excluded since they may not accurately represent in-situ formational hydraulic conductivity values. The tests were performed only in shallow (usually 1 cubic foot) test holes at the surface or near the surface of the PVLF, where weathering or the physical action of digging the holes might affect the hydraulic conductivity value. This limitation to these results was discussed in Stone (1975, page 13).

TABLE 6.2

REDUCED DATA SET FOR HYDRAULIC CONDUCTIVITY

BORING/ WELL	K (cm/sec)	K (ft/day)	DEPTH BGS (ft)	TEST TYPE	ROCK TYPE	DATA SOURCE
M48A	3.70E-05	1.05E-01	15-35	Slug	Qo	Kleinfelder, 1988
M37A	1.24E-04	3.51E-01	11-33	Slug	Qo	Kleinfelder, 1988
RFB16/M53B	1.40E-05	3.97E-02	41-66	Aquifer	Qo/Tmm	Herzog, 1991a
M38A	8.50E-05	2.41E-01	59-99	Slug	Qo/Tmm	Kleinfelder, 1988
M36A	1.20E-03	3.40E+00	21-41	Slug	Qo/Tmm	Kleinfelder, 1988
M49A	1.30E-05	3.69E-02	36-56	Slug	Qo/Tmv	Kleinfelder, 1988
M46A2	3.80E-05	1.08E-01	75-107	Slug	Qo/Tmv	Kleinfelder, 1988
M25A	4.20E-05	1.19E-01	41-82	Slug	Qo/Tmv	Kleinfelder, 1988
M23A	5.50E-05	1.56E-01	30-50	Slug	Qo/Tmv	Kleinfelder, 1988
M41A	3.34E-04	9.47E-01	20-40	Slug	Qo/Tmv	Kleinfelder, 1988
M44A	3.55E-03	1.01E+01	65-96	Slug	Qo/Tmv	Kleinfelder, 1988
RFB13/M52B	6.60E-05	1.87E-01	191-211	Aquifer	Qus	Herzog, 1991a
RFB4/M51B	1.20E-04	3.40E-01	60-95	Aquifer	Qus	Herzog, 1991a
RFB14	3.60E-04	1.02E+00	115	Lab	Qus	Herzog, 1991a
RFB13/M52B	6.62E-04	1.88E+00	180	Lab	Qus	Herzog, 1991a
RFB17	8.06E-04	2.28E+00	25	Lab	Qus	Herzog, 1991a
RFB3/M50B	9.10E-04	2.58E+00	180	Lab	Qus	Herzog, 1991a
RFB3/M50B	1.75E-03	4.96E+00	181-201	Aquifer	Qus	Herzog, 1991a
RFB15	4.40E-08	1.25E-04	55	Lab	Tmm	Herzog, 1991a
L3/M62B	6.16E-08	1.75E-04	99-109	Packer	Tmm	Herzog, 1991a
L3/M62B	6.47E-08	1.83E-04	114-124	Packer	Tmm	Herzog, 1991a
RFB12	7.23E-08	2.05E-04	20	Lab	Tmm	Herzog, 1991a
RFB6	1.05E-07	2.98E-04	130-140	Packer	Tmm	Herzog, 1991a
RFB7	1.21E-07	3.43E-04	35-45.3	Packer	Tmm	Herzog, 1991a
RFB6	1.61E-07	4.56E-04	139-149	Packer	Tmm	Herzog, 1991a
RFB7	2.63E-07	7.46E-04	50-58.5	Packer	Tmm	Herzog, 1991a
RFB12	2.91E-07	8.25E-04	140-150	Packer	Tmm	Herzog, 1991a
L3/M62B	4.57E-07	1.30E-03	66-76	Packer	Tmm	Herzog, 1991a
RFB12	6.30E-07	1.79E-03	100-110	Packer	Tmm	Herzog, 1991a
RFB32	8.65E-07	2.45E-03	100-110	Packer	Tmm	Herzog, 1991a
RFB10	1.10E-06	3.12E-03	15	Lab	Tmm	Herzog, 1991a
RFB12	1.54E-06	4.37E-03	80-90	Packer	Tmm	Herzog, 1991a
RFB7	9.77E-06	2.77E-02	20	Lab	Tmm	Herzog, 1991a
RFB7	6.97E-08	1.98E-04	113-121.5	Packer	Tmv	Herzog, 1991a
RFB11	1.06E-07	3.00E-04	136.5-145	Packer	Tmv	Herzog, 1991a
RFB19	1.10E-07	3.12E-04	192-200.5	Packer	Tmv	Herzog, 1991a
RFB16/M53B	1.49E-07	4.22E-04	131-141	Packer	Tmv	Herzog, 1991a
RFB11	1.65E-07	4.68E-04	25-33.5	Packer	Tmv	Herzog, 1991a
RFB7	1.97E-07	5.58E-04	100-108.5	Packer	Tmv	Herzog, 1991a
RFB32	2.33E-07	6.60E-04	300-310	Packer	Tmv	Herzog, 1991a
RFB32	5.07E-07	1.44E-03	195-205	Packer	Tmv	Herzog, 1991a
RFB11	9.14E-07	2.59E-03	99-107.5	Packer	Tmv	Herzog, 1991a
RFB24/M56B	1.52E-06	4.31E-03	59-67.5	Packer	Tmv	Herzog, 1991a
RFB30A	4.47E-06	1.27E-02	58-66.5	Packer	Tmv	Herzog, 1991a
RFB30A	6.55E-06	1.86E-02	61-69.5	Packer	Tmv	Herzog, 1991a
RFB19	1.79E-04	5.07E-01	150-158.5	Packer	Tmv	Herzog, 1991a
RFB22	2.09E-07	5.92E-04	100-110	Packer	Tma	Herzog, 1991a
RFB22	3.64E-07	1.03E-03	76-86	Packer	Tma	Herzog, 1991a
RFB25/M57B	4.22E-07	1.20E-03	95-105	Packer	Tma	Herzog, 1991a
RFB29/M60B	7.18E-07	2.04E-03	110-118.5	Packer	Tma	Herzog, 1991a
RFB22	1.08E-06	3.06E-03	54-64	Packer	Tma	Herzog, 1991a
RFB25/M57B	1.10E-06	3.12E-03	128-138	Packer	Tma	Herzog, 1991a
RFB24/M56B	1.67E-06	4.73E-03	90-98.5	Packer	Tma	Herzog, 1991a
RFB25/M57B	1.45E-05	4.11E-02	80-90	Packer	Tma	Herzog, 1991a
RFB1	2.00E-05	5.67E-02	75-85	Packer	Tma	Herzog, 1991a
RFB1	9.53E-05	2.70E-01	132-142	Packer	Tma	Herzog, 1991a
RFB1	1.24E-04	3.51E-01	142-152	Packer	Tma	Herzog, 1991a
RFB29/M60B	1.43E-04	4.05E-01	149-159	Packer	Tma	Herzog, 1991a
RFB29/M60B	2.36E-04	6.69E-01	50-58.5	Packer	Tma	Herzog, 1991a

Qo = Quaternary overburden deposits and landfill refuse NEW6_2.WK3

Qus = Quaternary undifferentiated sand deposits

Tmm = Malaga Mudstone member of the Tertiary Monterey Formation

Tmv = Valmonte Diatomite member of the Tertiary Monterey Formation

Tma = Altamira Shale member of the Tertiary Monterey Formation

cm/sec = centimeters per second

ft/day = feet per day

BGS = below ground surface

2.36E-04 is scientific notation for 0.000236

For a discussion of test type methodologies, see Sanitation Districts HC Report Phases II and III (1992)

- Laboratory sieve analyses were excluded since the resulting hydraulic conductivity values were estimates obtained from disturbed samples for geotechnical purposes. The accuracy of the resulting values as applied to the entire in-situ formational hydraulic conductivities is questionable.

- Kleinfelder slug test data collected in the San Pedro Sand, the Malaga Mudstone, the Valmonte Diatomite, and the Altamira Shale were not used because the hydraulic conductivity values were either anomalously higher or lower by several orders of magnitude than the majority of other tests performed in like formations. This could be attributed to the method of analysis, or the fact that slug tests only analyze the hydraulic properties of materials immediately adjacent to the well. Slug test data from Kleinfelder (1988) were, however, used for the overburden (Qo) flow zone, since no other data on hydraulic conductivity values for these earth materials were available, and these data appeared hydrogeologically reasonable, based on published data (Driscoll, 1986).

After anomalous or questionable data were excluded, the remaining data were analyzed by numerous methods to assess whether there were consistent hydraulic conductivity values within each formation. The data were evaluated separately by each formation. Arithmetic and logarithmic plots were made of hydraulic conductivity versus depth in formation, hydraulic conductivity versus frequency of occurrence, and hydraulic conductivity versus a root mean square value. These plots are included in Appendix E.

Results of the analysis indicated that there was no clear obvious lateral or vertical changes of hydraulic conductivity within formations across the site or across the Palos Verdes fault zone. This is consistent with the idea that hydraulic conductivities at PVLF will be highly variable due to the randomness of the fracture systems present in the Monterey Formation. However, the logarithmic plots suggested that the hydraulic conductivity values may be log-normally distributed, thereby allowing a geometric mean to be applied to each formation. Using this concept, the geometric mean hydraulic conductivity values shown in Table 6.3 were assigned to each formation as a starting input value to the model. These hydraulic conductivity values were modified during the model calibration process as needed to adjust the model to the actual field conditions. Hydraulic conductivity values were not available in the study area east of the Palos Verdes fault zone (in the West Coast Basin). Therefore, the values listed in Table 6.3 were extended throughout the entire study area.

TABLE 6.3

INITIAL HYDRAULIC CONDUCTIVITY VALUES
USED IN MODFLOW

HYDROGEOLOGIC UNIT	HYDRAULIC CONDUCTIVITY (cm/sec)	HYDRAULIC CONDUCTIVITY (ft/day)
Qo	1.18E-04 *	3.34E-01 *
Qus	4.23E-04 *	1.20E-00 *
Tmm	1.70E-07 *	4.82E-04 *
Tmv	6.46E-07 *	1.83E-03 *
Tma	5.60E-06 *	1.59E-02 *
Jc	1.00E-07 **	2.83E-04 **
PV Fault Zone	1.00E-08 **	2.83E-05 **

NEW6_3.WK3

Qo = Quaternary overburden deposits
Qus = Quaternary undifferentiated sand deposits
Tmm = Malaga Mudstone member of the Monterey Formation
Tmv = Valmonte Diatomite member of the Monterey Formation
Tma = Altamira Shale member of the Monterey Formation
Jc = Jurassic Catalina Schist
1.00 E-07 is scientific notation for 0.0000001
* = Geometric mean value
** = Assumed value

6.2.2.2 Thickness and Porosity

Since the geologic information on stratigraphic thicknesses was imported directly from the Sanitation Districts' MCS-based geologic model, the vertical thicknesses of each MODFLOW layer had to be adjusted to best match the MCS interpretation. A horizontal grid system with variable vertical thicknesses was used in MODFLOW to represent the dipping beds of the Tmm, Tmv, and Tma flow zones.

Porosity can exist as primary porosity (void spaces between grain particles) or secondary porosity (void spaces created after rock development, such as by fracturing). At PVLF, void spaces in the Qo and Qus are probably between grain particles, while void spaces in the Monterey and Catalina Schist Formations are probably from fracturing of the rock bodies. Information on site-specific porosity values was obtained from Herzog (1991a, 1991b). Average total porosity values obtained by Herzog and Associates (1991) for the overburden deposits (Qo), undifferentiated sand deposits (Qus), Malaga Mudstone (Tmm), Valmonte Diatomite (Tmv), and Altamira Shale (Tma) are, respectively, 0.45, 0.44, 0.58, 0.53, and 0.45. It should be noted that these values were determined in the laboratory and represent the magnitude of total porosity (total void space including dead-end pores), not effective porosity. In the Monterey Formation, the measured porosities are most likely the primary porosity (porosity of the solid matrix). The Monterey Formation comprises fractures mudstone, diatomite and shale in which the majority of flow and transport occurs in the secondary porosity (porosity which is structurally controlled). Since the secondary porosities of the geologic units within the Monterey Formation are not available, values from similar geologic materials were estimated based on a review of published literature, such as Driscoll (1986). For the Tmm, Tmv, and Tma flow zones, a range of effective porosity values from 0.01 to 0.05 was used. For the (Qus) flow zone, a range in porosity values from 0.25 to 0.4 was used. For the (Qo) flow zone, a range in porosity values from 0.25 to 0.4 was used. These effective porosity values are one order of magnitude smaller than the Herzog values listed and were employed as an initial estimate of the secondary porosity of the Monterey Formation. The values of effective porosity for the sedimentary deposits overlying the Monterey Formation were not known. However, the values of effective porosity in porous media (sedimentary deposits) are normally smaller than those of the total porosity (Bear, 1972). In this study, the values published by Driscoll (1986), which are appropriately smaller than those reported by Herzog and Associates (1991), were adopted.

6.2.2.3 Groundwater Elevation and Gradient

The Sanitation Districts have compiled groundwater elevation data for the PVLF monitoring wells since the mid 1980s. Groundwater elevation data for West Coast Basin wells dating back to the 1920s were available at the LADPW. These records were reviewed to determine an appropriate period of time where an adequate water elevation contour map could be constructed across the model area. The contour map would then be used for model calibration. Hydrographs informally prepared by the Sanitation Districts for PVLF wells were reviewed to assess the variability of water level elevations, and to look for seasonal trends. Based on the review well elevation data for March/April 1991 were selected to best represent groundwater elevations in the study area. Hydrographs of selected wells are presented in Appendix G. Several West Coast Basin wells, whose October through December 1990 elevations were used since no later measurements were available.

6.2.3 Assumptions

For the purposes of developing the groundwater flow model, assumptions were made regarding groundwater flow and flow zone characteristics in the study area, including: (1) Groundwater is present in all three members of the Monterey Formation, with no intermittent dry zones (aquitards); (2) The fracture systems within the Monterey Formation members are interconnected and thus, the system can be treated as a uniform porous media, this assumption is conservative because groundwater flow is allowed to occur within the fractured members of the Monterey Formation; and (3) Groundwater in the Monterey Formation members occurs under unconfined conditions, this assumption is restricted to the outcropped Monterey Formation members where groundwater may be present between the depths of 100 to 300 feet below ground surface. This assumption is consistent with the previous assumptions regarding the interconnection of the fracture network. In addition to the above assumptions, it was also assumed that the hydraulic properties of all the flow zones are isotropic. In the horizontal direction, it has been observed that chemical plumes in both the alluvium and the Monterey Formation move in the direction of hydraulic gradient suggesting that anisotropy in the horizontal direction is absent. For the Qo and Qus, anisotropy in the vertical direction is likely to be weak due to their depositional histories. For the Monterey Formation (in which flow is controlled by interconnected fracture systems), since the horizontal anisotropy has not been observed, it is not unreasonable to assume that anisotropy in the vertical direction is relatively weak. Furthermore, since the predominant groundwater flow direction is essentially horizontal, the vertical anisotropy of geologic materials is not likely to play an important role in the local groundwater flow system.

The above assumptions may not necessarily reflect the actual conditions in some local areas; however, they are considered conservative and consistent with the objectives of the application of the PVLF hydrogeologic model.

6.2.4 Development and Calibration

The detailed hydrogeologic flow model was developed and calibrated using the compiled data described in the preceding sections. The following subsections describe the steps by which the detailed model was developed. As part of the quality assurance efforts, the selected code (MODFLOW) was first verified against a known analytical solution to a groundwater problem. This step was then followed by the construction of the detailed model using the compiled data. Prior to using the developed model for predictive purposes, the model was calibrated using the available groundwater elevation data. Details of these three steps are described in the following subsections.

6.2.4.1 Code Verification

Prior to applying the MODFLOW code to the PVLF site, the code was first verified with a known analytical solution to ensure that the code could be used to solve the flow equation with sufficient accuracy.

The case that was used to verify the MODFLOW code is presented in Figure 6.1, which shows a one-dimensional unconfined flow situation. This case was chosen because of the presence of water-table conditions at the PVLF site. For the case shown in Figure 6.1, it was assumed that material properties are isotropic and homogeneous. In addition, provided that the Dupuit-Forchheimer's assumption (Bear, 1972) is valid (i.e, the water pressure distribution is approximately hydrostatic). The elevation of the water table, h, is given by the following Equation (1).

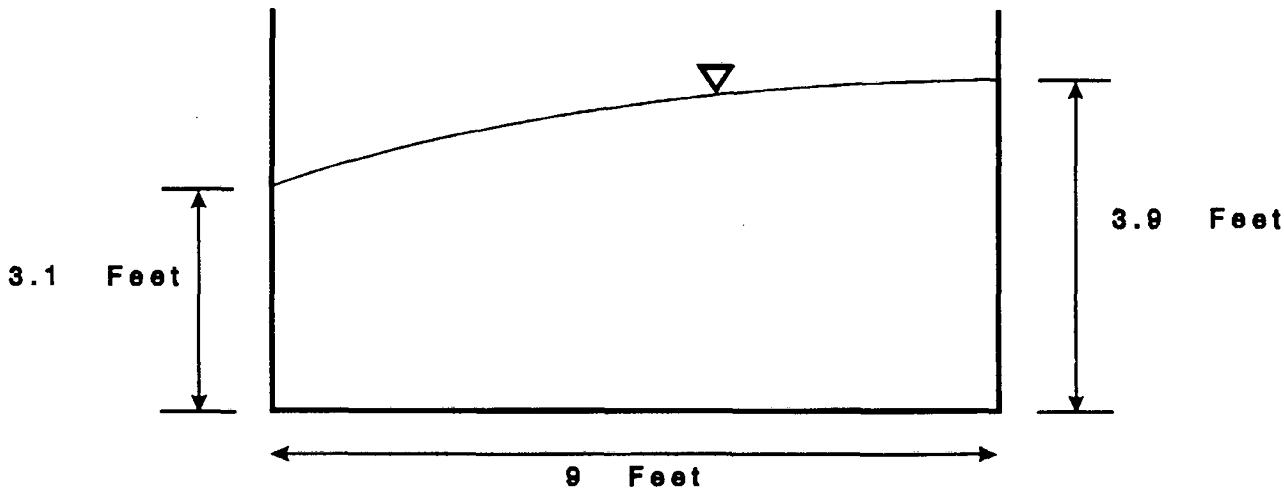

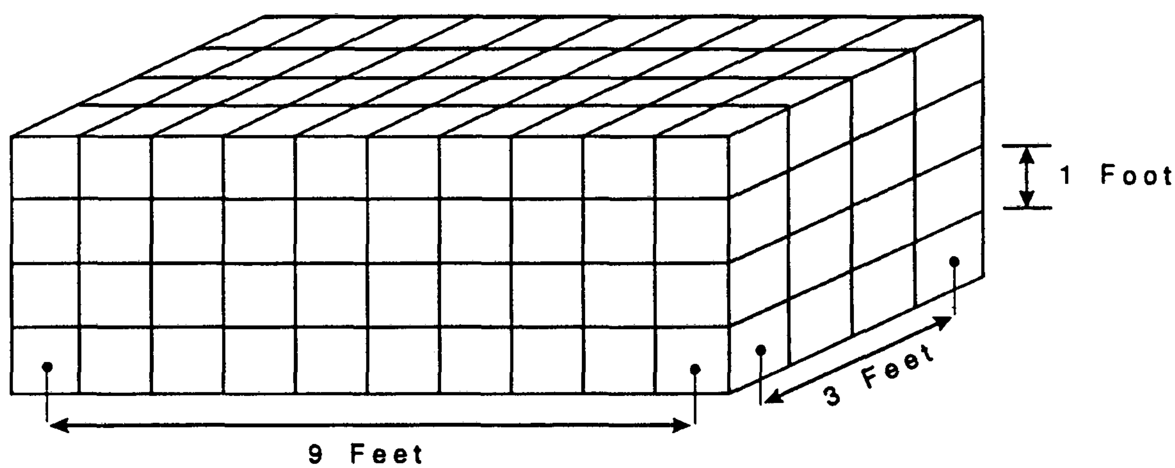

FIGURE 6.1
Problem Definition - Test Case

DAMES & MOORE

$$h = \sqrt{(h_2^2 - h_1^2)\frac{x}{L} + h_1^2}$$

Equation (1)

where h_1 = prescribed head on the left hand side boundary in Figure 6.1,

h_2 = prescribed head on the right-hand-side boundary in Figure 6.1,

L = length between the two extreme boundaries, and

x = distance measure from the left-hand-side boundary.

Equation (1) indicates that, in the absence of infiltration, the location of the water table is independent of the magnitude of hydraulic conductivity of the material. The following values were adopted for analytical-solution verification:

h_1	=	3.1 feet (ft),
h_2	=	3.9 ft,
L	=	9 ft, and
hydraulic conductivity	=	1 foot per day (ft/day).

The flow domain was subdivided (discretized) into ten columns along the flow direction, four rows in the direction normal to the flow direction, and four layers in the vertical direction (see Figure 6.1). The closure criterion (the maximum difference allowed between two successive iterations at convergence) was 0.001 ft and the relaxation factor (factor to accelerate the convergence of the interactive solution schemes used) for the slice-successive over-relaxation-solution technique was 1.2. Results are shown in Table 6.4. As shown in the table, the

TABLE 6.4

COMPARISON BETWEEN MODFLOW AND ANALYTICAL SOLUTION FOR THE TEST CASE

X Feet	h_{TH} Feet	h^{WT}_{MF} Feet	h^{B}_{MF} Feet
0	3.100	3.100	3.100
1	3.198	3.209	3.195
2	3.295	3.304	3.289
3	3.388	3.396	3.381
4	3.478	3.485	3.472
5	3.567	3.572	3.560
6	3.653	3.658	3.647
7	3.737	3.741	3.732
8	3.819	3.822	3.816
9	3.900	3.900	3.900

NEW6_4.WK3

NOTES:

X = Distance from the left-hand-side constant head boundary in figure 6.1.

h_{TH} = Theoretical vertically-averaged piezometric head above the base of aquifer.

h^{WT}_{MF} = MODFLOW - predicted water table elevation above the base of the aquifer.

h^{B}_{MF} = MODFLOW - predicted piezometric head above the base of aquifer.

pressure distribution is almost hydrostatic. The difference between the elevation of the water table at the top and the piezometric head at the base of the aquifer is very small. The difference between the MODFLOW code and the analytical solution is less than 0.012 ft (i.e., 1.5 percent of 0.8 ft, the difference between h_2 and h_1). Based on this analytical-solution verification, the MODFLOW code demonstrated its ability to model a groundwater flow system similar to that at the PVLF area with sufficient accuracy.

6.2.4.2 Model Construction

The areal extent of the hydrogeologic flow model developed for the PVLF is shown on Figure 6.2. The area to be modeled was discretized into 6,125 three-dimensional finite-difference grid blocks (35 rows, 35 columns, and 5 layers) in order to simulate flow in three dimensions. The grid system consists of 5 layers in the vertical direction, each layer comprising 1,225 (35x35) grid blocks. The orientation of the grid was chosen such that one of the principal grid directions is parallel to the trace of the Palos Verdes fault downgradient from the PVLF (Figure 6.2). This gridding arrangement was adopted in order to maximize resolution in the vicinity of the fault immediately down gradient from the PVLF site. A vertical cross section along Slice (column) 14 is presented in Figure 6.3. This figure shows that the upper three layers are assigned to the shallow and intermediate flow systems in the West Coast Basin area. Also, the modeled fault matches the actual fault in the upper 2,000 feet, where the significant portion of flow occurs, but deviates from the actual fault at depth in the Jc unit.

An inspection of Figure 6.3 reveals that some grid blocks may contain more than one stratigraphic unit. For these grid blocks, the following averaging techniques were applied:

<u>Horizontal Direction</u>

$$K_{Heq} = \frac{\Sigma\ d_i K_i}{\Sigma d_i}$$

Equation (2)

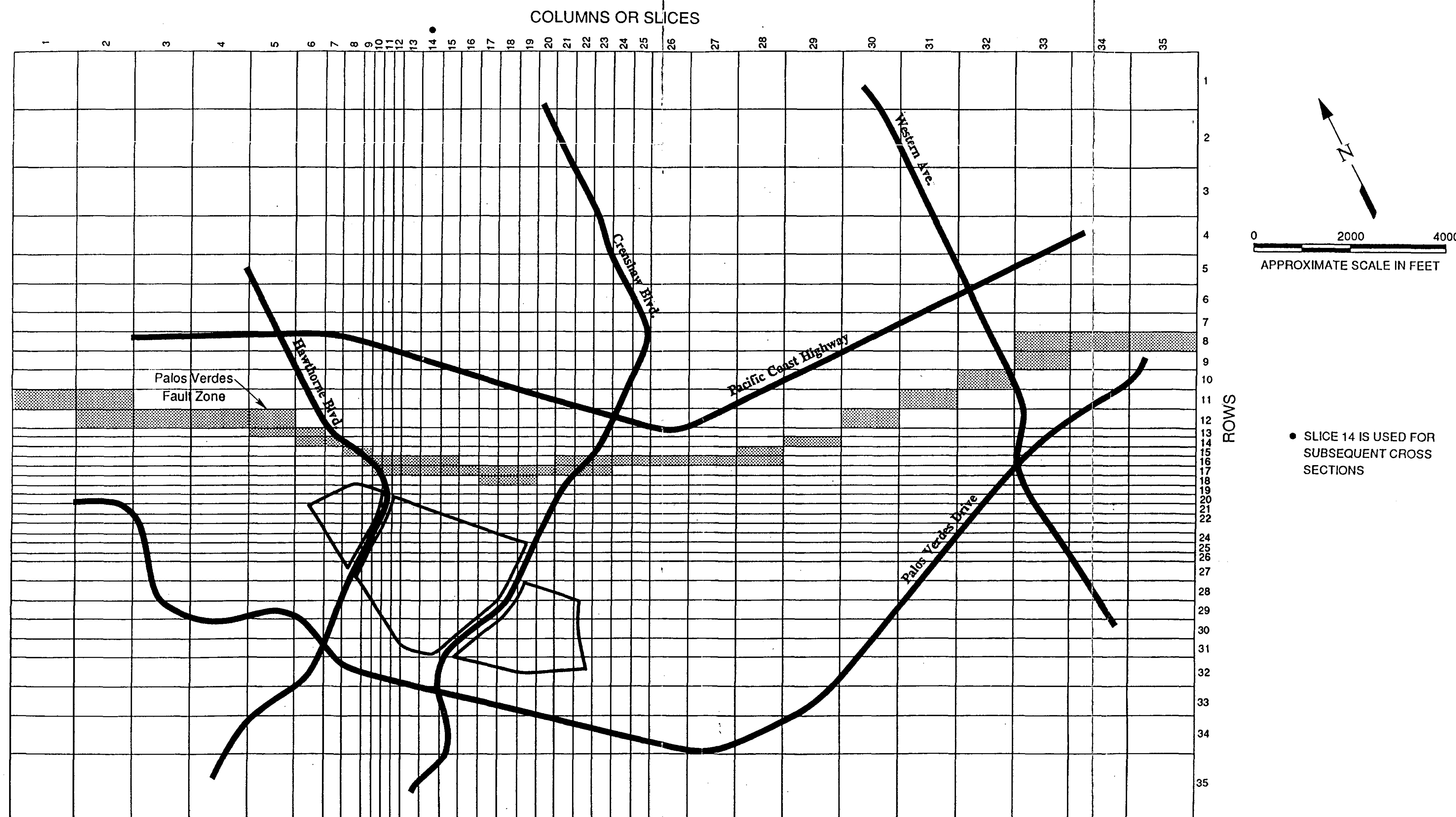

Figure 6.2
PLAN VIEW OF MODEL GRID

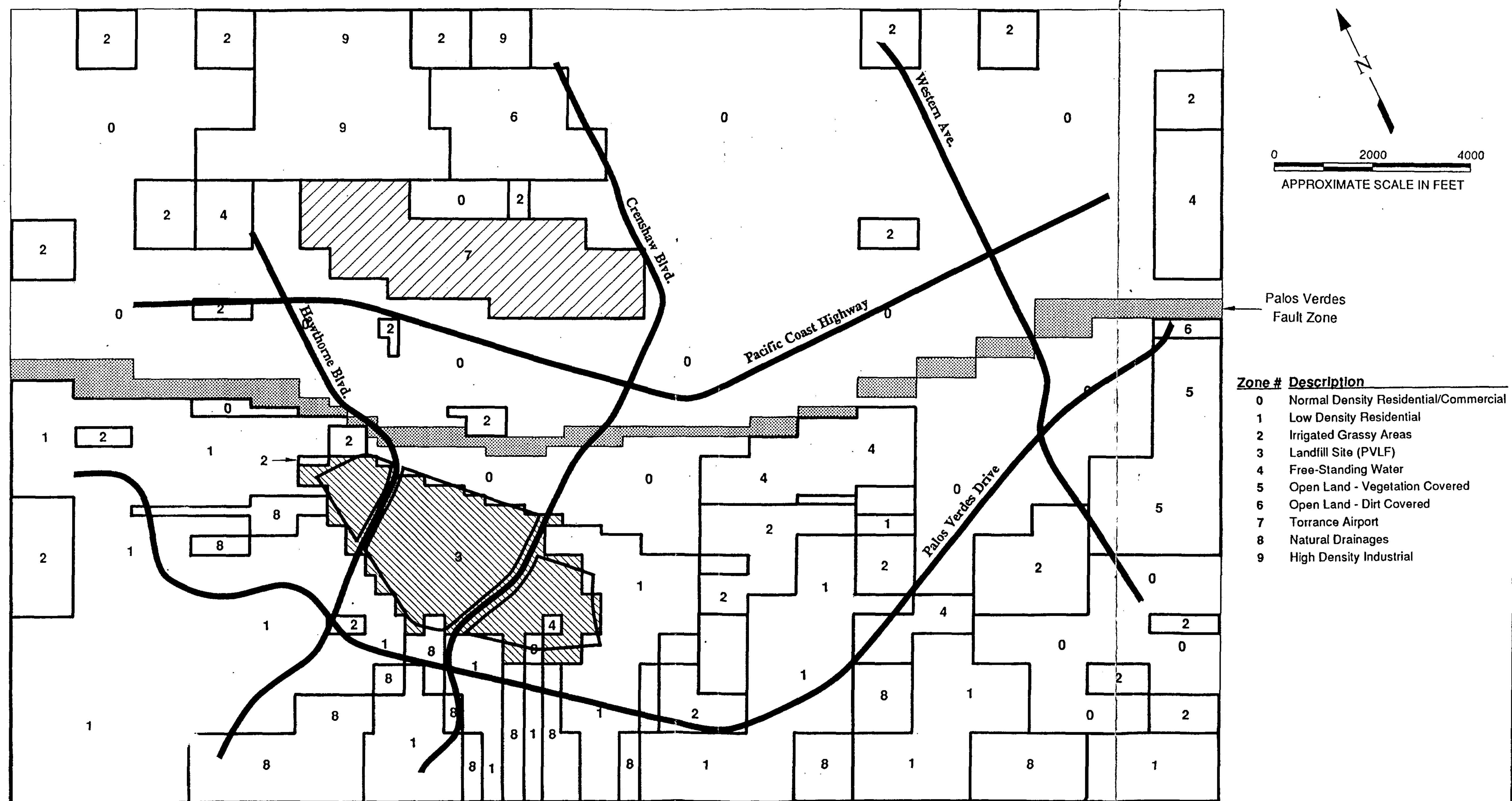

FIGURE 6.4
Model Area Recharge Zones

DAMES & MOORE

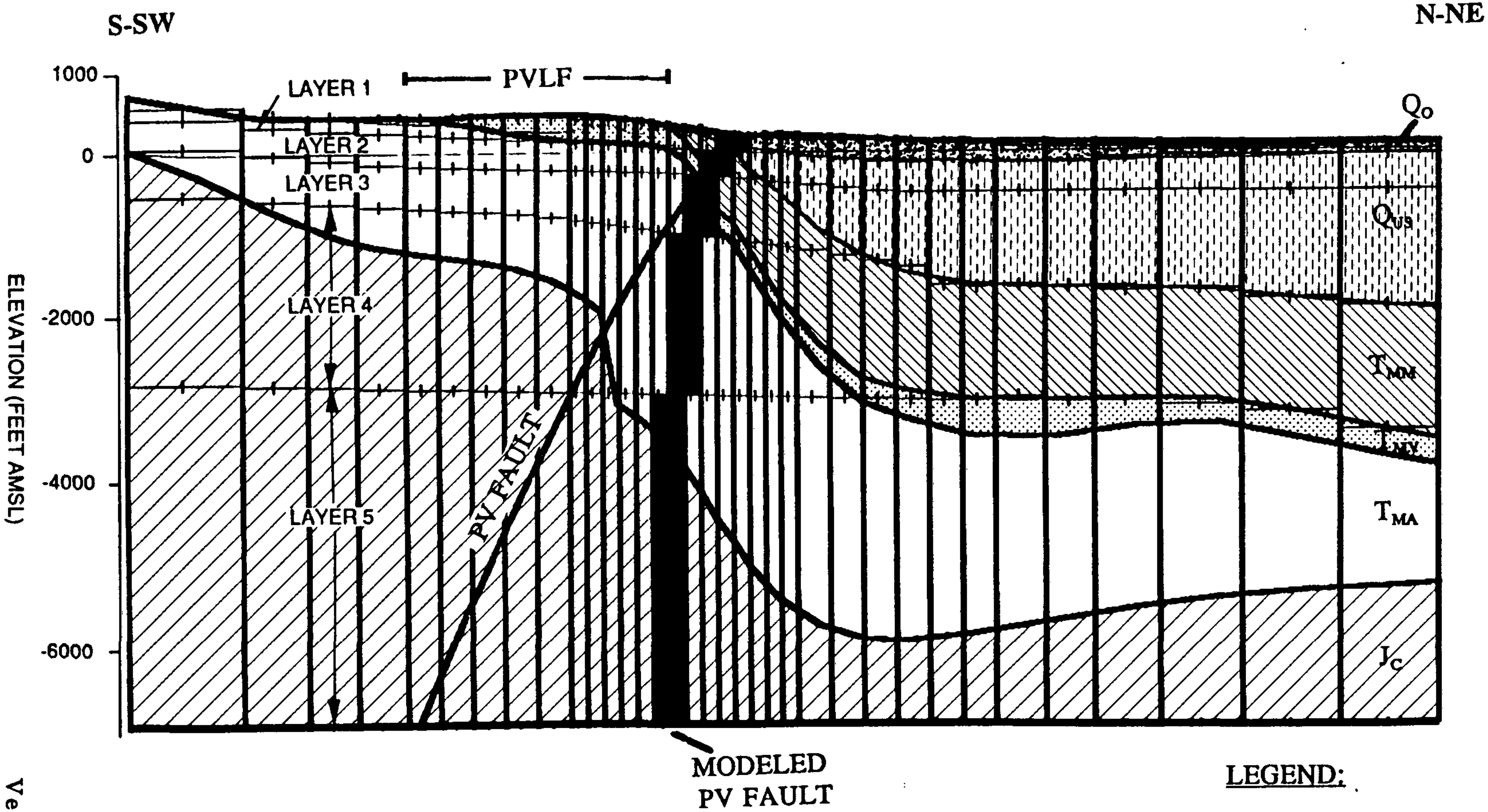

0 2000 4000

APPROXIMATE SCALE IN FEET

VERTICAL MODEL GRID
SLICE 14

LEGEND:

Q_O	Overburden
Q_{US}	Undifferentiated Sand
T_{MM}	Malaga Mudstone
T_{MV}	Valmonte Diatomite
T_{MA}	Altamira Shale
J_C	Caltalina Schist
-+-	Horizontal Model Grid
I	Vertical Model Grid

FIGURE 6.3
Vertical Model Grid

DAMES & MOORE

where K_{Heq} = equivalent hydraulic conductivity in the horizontal direction,

d_i = thickness of stratigraphic unit i within the grid block, and

K_i = hydraulic conductivity of stratigraphic unit i.

For the MODFLOW code, vertical hydraulic conductivity between mid points of two adjacent grid blocks in a vertical grid column is required as part of the input data. The vertical hydraulic conductivity was calculated using the following Equation (3).

Vertical Direction

$$K_{Veq} = \frac{\Sigma l_i}{\Sigma \frac{l_i}{K_i}}$$

Equation (3)

where K_{Veq} = equivalent hydraulic conductivity in the vertical direction,

l_i = thickness of stratigraphic unit i between two mid points of two vertically adjacent grid blocks, and

K_i = hydraulic conductivity of stratigraphic unit i.

Equations (2) and (3) are based on the assumption that all stratigraphic units are predominantly horizontal to slightly dipping. The values for d_i and l_i in these Equations were calculated using stratigraphic information from the geologic model generated by the SIMGEN utility of the MCS code. The values of K_i are shown on Table 6.3. The distributions of hydraulic conductivity in the horizontal direction in the top three layers of the model are shown in Figures H.1 to H.3, Appendix H.

Implicit in equation (2) and (3) is an assumption that the hydraulic conductivities of all the flow units are isotropic. This assumption has been addressed and justified in Section 6.2.3.

The approach of equivalent porous medium was adopted for the fractured rocks of the Tmm, Tmv, and Tma flow zones. The Palos Verdes Fault zone, however, was treated as a distinct feature and not included as part of the material property averaging process. As shown on Figures 6.2 and 6.3, some blocks are used to represent the Palos Verdes fault zone. The groundwater level data in the vicinity of the Palos Verdes fault zone suggests that the fault functions as a partial barrier to the groundwater flow. Since most faults are normally filled with clayey materials, the background hydraulic conductivity of the fault, before calibration, was assumed to be 1.0 E-8 cm/sec. Additionally, the subsurface landfill barrier was incorporated into the model along Hawthorne Boulevard and assigned a hydraulic conductivity of 1.0 E-7 cm/sec.

Specified groundwater level conditions were imposed along the boundary of the modeled area. These specified heads (constant heads) are shown along the model area boundary in Figure 5.3. Information relating to the groundwater elevation at the boundary was extrapolated from existing groundwater wells in the basin north of the Palos Verdes Fault zone and from the relationship between the topography and the water depths in the vicinity of the PVLF site west of the Palos Verdes Fault zone. It should be noted that there are two types of boundary conditions that may be assigned by the model boundaries: specified head; and specified flux (flow rate). Only one type of boundary condition is required as a given finite difference all along the model boundary.

The uppermost groundwater flow system receives recharge from percolation of precipitation and/or irrigation. In the modeled area, ten (10) different zones of general land uses and terrains were identified, necessitating the assignment of appropriately different recharge rates. Since the recharge rates are not exactly known, reasonable and/or conservative assumptions must be made. The different recharge zones are discussed below, and are shown on Figure 6.4.

0) Normal density commercial/residential: This zone covers the majority of the model area. It comprises the commercial and residential units on level ground, typical of an urbanized area such as Torrance. A recharge rate of 2 percent of the mean annual precipitation of 12 inches was assigned to this zone.

1) Low density residential: This zone consists of the large-lot residential units in the Palos Verdes Hills. In this area there is more irrigation of landscaped areas than in Zone 0. A recharge rate of 3.5 percent of the mean annual precipitation was assigned to this zone.

2) Irrigated grassy areas: This zone consists of open-space, irrigated grassy areas identified in the model area, including golf courses, parks, and school yards. Irrigation water in these areas is generally applied efficiently to meet the daily evapotranspiration needs of the grasses. As a result, little or no irrigation water infiltrates below the root depths to provide recharge to groundwater. Thus, recharge in these areas is based on precipitation alone. A recharge rate of 5 percent of the mean annual precipitation was assigned to this zone.

3) Landfill Site (PVLF): This zone consists of the areal boundaries of the PVLF. This area was assumed to receive minimal recharge because of the landfill cover the effective storm water management system, and the absence of irrigated areas. However, some areas may receive more recharge than others because of the current land uses, such as the park and South Coast Botanic Gardens. Water is currently used to maintain the vegetated slopes around the PVLF, but engineered storm runoff control is effective in diverting runoff away from PVLF. A recharge rate of 0.5 percent of the mean annual precipitation was assigned to this zone.

4) Free-standing water: This zone consists of the free bodies of water identified within the model area, including the Walteria Spreading Basin, Harbor Lake, the Palos Verdes reservoir, the lake at the South Coast Botanic Gardens, golf course lakes, and other bodies of water. A recharge rate of 10 percent of the mean annual precipitation was assigned to this zone.

5) Open land - vegetation covered: This zone consists of vacant property covered by grasses, weeds, or other vegetation. It is not manually irrigated. A recharge rate of 5 percent of the mean annual precipitation was assigned to this zone.

6) Open land - dirt covered: This zone consists of vacant property covered only by dirt, such as the Chandler Sand and Gravel Pit, east of the PVLF. A recharge

rate of 8 percent of the mean annual precipitation was assigned to this zone because there is little or no loss due to transportation through vegetative cover.

7) Torrance Airport: The open space within the Torrance Airport was assigned a recharge rate of 1 percent of the mean annual precipitation due to the density of paved surfaces in this area.

8) Natural drainages: Several drainages exist in the canyons of the Palos Verdes Hills which transport water during periods of rainfall. A recharge rate of 20 percent of the mean annual precipitation was assigned to the major drainages and their tributaries.

9) High density industrial: This zone consists of asphalt and concrete covered industrial parks and major businesses, particularly north of the Torrance Airport. Recharge is minimal in this zone. A recharge rate of 1 percent of the mean annual precipitation was assigned to this zone.

The assignment of the above recharge rates was based on information from a recent study by Slade (1985) who investigated the amount of meteoric water available for recharge in the Santa Clarita area. He indicated that the amount of "available water" (water available for runoff [surface water] and groundwater infiltration) ranges from 3 to 8 percent of annual precipitation. In the residence and commercial areas in the vicinity of the PVLF, there are two major sources of recharge: (1) natural precipitation; and (2) landscape-irrigation. In these areas, the land is partially covered or almost totally covered by buildings and paved areas. It is therefore reasonable to assume that the average recharge is not likely to exceed 5 to 6 percent of annual precipitation. Recharge rates due to infiltration from natural drainage channels and/or surface water bodies are likely to be greater than 8 percent of the mean annual precipitation. The recharge rate for the 10 zones, mentioned above, were obtained by trial and error after a number of model simulations. Those rates were found to provide good agreement between the model and field information.

Within the model area, the Chandler Well (Well 271N in Figure 6.5) is the only significant pumping well. The pumping rate at this well is currently unknown. Pumping was simulated by specifying a fixed hydraulic head (observed) value to the cell block corresponding to the Chandler Well. Along the Hawthorne Boulevard, a number of extraction wells were installed in 1986. Pumping at these wells is intermittent and the average rates are extremely small. Since the effects of these wells on the regional flow have not been observed, they were not included in the model.

6.2.4.3 Model Calibration

In most regional groundwater flow situations, groundwater levels change so slowly that, at any given time, the flow is said to be in a pseudo-steady-state condition. In most cases, despite the change in groundwater level, the most important characteristic of the flow, hydraulic gradient (magnitude and direction), remains approximately the same. This observation is especially true when there are minimal anthropogenic activities (pumping, artificial recharge, etc.), and there are no significant water bodies such as rivers located nearby.

At the PVLF site, the groundwater-monitoring program began in the 1980s. Hydrographs from monitoring wells at the site available at the Sanitation Districts' offices suggest that the groundwater levels at the site fluctuate very little, and that the predominant hydraulic gradients remain essentially constant, trending in the north-northeast direction. Selected hydrographs at monitoring wells within the PVLF area are presented in Appendix G. In the West Coast basin, the water levels have not been observed to change dramatically since the major decline ended in the mid 1950s.

To appropriately calibrate the groundwater flow model described in this report, a set of groundwater elevations is required for both the West Coast Basin and the PVLF site. The most complete set of groundwater elevations is available for the period between late 1990 and early 1991. This data set was employed for the calibration of the model. Groundwater elevation data for this time period were used to develop Figures 5.1 and 5.3. In areas where water level data were not available, the existing data were extrapolated based on the existing approximate relationship between the topography and groundwater elevation.

To ensure that the model resembles the true hydrogeologic conditions as much as possible, the following constraints were applied.

- Hydraulic conductivity values: During the calibration process, values of hydraulic conductivity are normally adjusted to enable the model to emulate more closely the local hydraulic gradient (and subsequently groundwater elevations).

Figure 6.5
GROUNDWATER ELEVATIONS FOR THE CALIBRATED MODEL

At the PVLF site, hydraulic conductivity values obtained from field and laboratory tests are available. Because of the scale difference between the size of each model grid block (hundreds or thousands of feet) and the size of area associated with laboratory and field tests (one to a few tens of feet), the hydraulic conductivity values at the model scale may be somewhat different from the test values. Owing to the fact that spatial variability of hydraulic conductivity is often log-normally distributed, the hydraulic conductivity values could differ up to several orders of magnitude (see Table 6.3). For the PVLF site model, the variation of hydraulic conductivity at most of the finite-difference grid blocks was confined to two orders of magnitude on either side of the geometric mean hydraulic conductivity value of each flow zone. The selection of geometric mean hydraulic conductivity values was discussed in Section 6.2.2.1. The distributions of the upper three layers of the model are shown in Figures H.4 to H.6, Appendix H.

- Recharge rate: In southern California, the potential evapotranspiration rate (48 inches per year) (Linsley et al, 1982) exceeds that of the mean annual precipitation rate (12 inches per year). As a result, the amount of water that eventually infiltrates to the groundwater is usually very small. A recent study by Slade (1985) for a number of catchments in the nearby Santa Clarita area indicates that the amount of "available water" (water available for runoff [surface water] and groundwater infiltration) ranges from 3 to 8 percent of the annual precipitation. For the PVLF modeling study it is assumed that the recharge rate (due to infiltration) varies between 0.5 to 8 percent of the mean annual precipitation of 12 inches depending on the type of soil cover. Mean annual precipitation based on rainfall data between 1941-1970 is 11.08 inches in the Palos Verdes Hills area and 12.21 inches in the Torrance area (DWR, 1981).

Starting with the geometric mean value of hydraulic conductivity in each flow zone, the model hydraulic conductivity values of some nodes were gradually adjusted to minimize residual error (difference between the groundwater elevation computed by the model and field observations). In adjusting the model parameters using the trial-and-error approach the following pattern emerged:

- The hydraulic conductivity values in topographically high zones and near the fault were decreased in order to replicate the steep hydraulic gradients in these areas.

- In the middle of the landfill area, where the hydraulic gradient is relatively flat, little parameter adjustment was required.

- Additional recharge was required in the following areas to take into account of anomalously high groundwater elevations.

  - Area in the vicinity of well M59B: This is a high topographical area where recharge activity was reported by Herzog (1991a). This reported water source is a municipal Torrance water reservoir adjacent to M59B which is known to be leaking.

  - Area in the vicinity of M62B: A pond was observed approximately 1,000 feet to the east on areal photographs, and may be a source of increased recharge.

- Recharge was reduced in the following areas to better match field observations.

  - Area beneath the Torrance Airport (Zone 7).

  - Area beneath the high density industrial properties (Zone 9).

  - Several areas of denser home clusters in the Palos Verdes Hills.

  - Area beneath the PVLF.

It was also found that the hydraulic conductivity value for the fault that could most closely replicate the steep gradient near the fault is 1.0 E-8 cm/sec.

Contours of the computed groundwater elevations in the uppermost layer of the model are presented in Figure 6.5. Residuals at all the wells are also presented in Figure 6.5. In comparing these contours of computed groundwater elevation with the contours from field observation shown in Figures 5.1 and 5.3, it is apparent that they are qualitatively similar. The simulated groundwater flow direction beneath the PVLF and Palos Verdes Hills is to the north-northeast. After passing the Palos Verdes Fault zone, the water moves in an easterly direction. In order to quantitatively measure the closeness between the model and field observations, the following parameters were used: 1) maximum absolute residual (maximum difference between actual elevation and model predicted elevation), 2) root mean square of residuals, and 3) correlation coefficient between the model and field observations (Cooley, 1977). A comparison between the pre-calibrated model and the calibrated model is presented below.

Parameter	Pre-calibration	Post-calibration
Max. absolute residual (ft)	175.0	27.9
Root mean square of residuals (ft)	90.4	11.0
Correlation coefficient	0.740	0.994

A total of 43 monitoring wells were used in the calculation. These wells are listed in Table 6.5. Wells 737C, 747G, 737FGH, and 301 were not used for calibration, as they are on the boundaries of the model, where specified head conditions were applied. The correlation coefficient is an indication of the match between the model and field observations. The maximum value is unity which corresponds to the perfect agreement between the model and the data used for calibration.

This case has 41 degrees of freedom. The number of degrees of freedom was obtained by subtracting the number of constraints (2) from the total number of wells (43). A discussion regarding the degree of freedom with specific response to the significance of correlation may be found in Paradive and Rivett (1970). The critical correlation for 41 degrees of freedom at a level of significance of 0.001 is 0.485, which implies that there is a probability of 0.001 that the correlation will exceed 0.485 with uncorrelated data. In other words, the correlation between the model and the field observations is significant when the correlation coefficient exceeds 0.485. As shown above, the pre-calibrated correlation coefficient of 0.740 is well above 0.485. Thus, this correlation is significant. This is due to the fact that the flow characteristics were already reasonably reflected by the precalibrated model. The calibration process improved the model-observation correlation, increasing the correlation coefficient to a value of 0.994, which is near the ideal value of unity (value of 1.0). Thus, the calibrated model closely represents actual physical conditions found at the site.

TABLE 6.5

Comparison Between MODFLOW and Field Observation

Root mean square of residuals	11.0 FT
Absolute maximum residual	27.94 FT
Correlation -model vs. observed	0.994

WELL	H(observed) (ft)	H(model) (ft)	RESIDUAL (ft)	PERCENTAGE OF MAX HEAD DIFFERENCE
M23A	198.70	204.25	5.55	1.182
M24A	190.60	179.08	-11.52	-2.454
M25A	189.80	217.74	27.94	5.952
M26A	-2.70	3.88	6.58	1.402
M30B	241.20	258.13	16.93	3.607
M32B	286.70	266.07	-20.63	-4.395
M33B	274.10	265.52	-8.58	-1.828
M34B	288.20	267.21	-20.99	-4.472
M35B	245.00	267.60	22.60	4.815
M36A	242.80	239.00	-3.80	-0.810
M37A	250.80	259.19	8.39	1.787
M38A	279.30	281.56	2.26	0.481
M39A	288.90	297.52	8.62	1.836
M40A	332.00	321.83	-10.17	-2.167
M41A	327.60	334.56	6.96	1.483
M42A	338.10	338.13	0.03	0.006
M43A	292.30	292.42	0.12	0.026
M44A	292.80	284.67	-8.13	-1.732
M45A	320.90	311.49	-9.41	-2.005
M46A	283.40	287.00	3.60	0.767
M47B	283.20	278.67	-4.53	-0.965
M48A	275.50	268.81	-6.69	-1.425
M49A	203.30	213.97	10.67	2.273
M50B	-3.80	6.02	9.82	2.092
M51B	156.10	169.46	13.36	2.846
M52B	-12.30	-11.02	1.28	0.273
M53B	263.80	271.66	7.86	1.674
M54B	237.40	242.95	5.55	1.182
M55B	280.10	269.12	-10.98	-2.339
M56B	376.80	380.83	4.03	0.859
M57B	431.80	415.01	-16.79	-3.577
M58B	370.10	369.31	-0.79	-0.168
M59B	241.00	235.60	-5.40	-1.150
M60B	340.10	348.86	8.76	1.866
M61B	355.10	361.17	6.07	1.293
M62B	336.10	332.71	-3.39	-0.722
749D	-3.80	-0.27	3.53	0.752
748H	8.00	-1.60	-9.60	-2.045
758D	3.70	-2.12	-5.82	-1.240
749A	-13.20	4.65	17.85	3.803
769	-16.80	-14.36	2.44	0.520
240A	-6.90	13.42	20.32	4.329
271N	-28.70	-28.70	0.00	0.000

NEW6_5.WK3

Note: Residual is the difference between H Observed and H Model
Percentage of Maximum Head Difference is equivalent to the Residual divided by the maximum head difference over the entire model area. This max. head difference = 469.4, the difference between the head at MW-57B (431.8) and Basin Well 301 (-37.6). Basin Well 301 is not shown on the table, as it was not used for model calibration.

A further comparison may be seen in Table 6.5. All wells have residuals smaller than 27.94 ft., an absolute value of which is 5.95 percent of 469.4 ft., the difference between the maximum groundwater elevation (431.8 ft at M57B) and the minimum groundwater elevation (-37.6 ft at well 301N).

As shown in Figure 6.5, positive residuals are present in the mid western portion of the West Coast Basin within the modeled area. These residuals are associated with Wells 749A, 240A and M50B. The residuals associated with these wells were thought to be associated with uncertainty of the fault zone location. The residual at Well 749A was thought to be associated with the uncertainty of water level measurement. The water level at this well, measured in May 1991, suggests that pumping may be taking place at that time. However, an inquiry with the well operator revealed that no pumping was performed in or just before May 1991. However, positive residuals in this vicinity cause the simulated hydraulic gradient to be stronger than the observed gradient. This is considered conservative for the chemical transport simulation because the steeper the hydraulic gradient, the more rapid the groundwater velocity and the more rapid chemicals are transported in the West Coast Basin.

As stated earlier, the objective of the model is to provide a hydrogeologic framework for contaminant transport model (Dames & Moore, 1993), which in turn, provides technical information for risk assessment of potential receptors downgradient from the PVLF. As such, the model was designed to be a reasonably accurate and conservative simulator of the groundwater flow path. The degree of accuracy of the flow path in the horizontal direction has been indirectly demonstrated by the favorable agreement between the observed and simulated hydraulic heads and by the existing chemical data (Dames & More, 1993). In the PVLF area, steep downward gradient was observed to occur at the following well pairs: M23A-M25A, M32B-M33B, and M34B-M35B. The steeper the downward gradient, the longer the path of groundwater before reaching the potential receptors. In addition, the organic-carbon-rich Monterey formation would significantly attenuate the organic chemicals through adsorption. In order to make the flow model conservative, this hydrogeologic feature (steep downward gradient) was not included in the model.

A comparison was made between the actual hydraulic conductivity values obtained from field tests (Table 6.2) and the values assigned to grid blocks after model calibration. Table 6.6 presents a summary of this comparison.

TABLE 6.6
COMPARISON OF FIELD-OBTAINED HYDRAULIC CONDUCTIVITY VALUES VS. CALIBRATED MODEL VALUES

Location	Well/Borehole[1]	Formation Tested	Hydraulic Conductivity (ft/day) Obtained in the Field[2]	Hydraulic conductivity (ft/day) Assigned to the Grid Block[3]
Upgradient of PVLF	M56B	Tmv	0.00431	0.0318
	M57B	Tma	0.0411	0.0149
	M60B	Tma	0.405	0.277
	RFB22	Tmm	0.00306	0.00794
	RFB30A	Tmv	0.0186	0.689
On PVLF	M44A	Qo/Tmv	10.1	0.112
	M46A	Qo/Tmv	0.108	0.0788
	M48A	Qo	0.105	0.0689
	M53B	Qo/Tmm	0.0397	0.0152
	RFB32	Tmv	0.00144	0.0155
Downgradient of PVLF	M23A	Qo/Tmv	0.156	0.0955
	M50B[4]	Qus	2.58	0.207
	RFB7	Tmm	0.0277	0.0632
	RFB12	Tmm	0.00437	0.00584
	RFB14	Qus	1.02	0.947

Notes:
1. Well and borehole locations are shown on Figure 2.2
2. Selected values taken from Table 6.2
3. Layer 1 hydraulic conductivity values for the grid block which the well/borehole occupies.
4. Well is located across the Palos Verdes fault zone from the PVLF.

A:128\tab-6.6

Generally, the hydraulic conductivity values of the calibrated model are nearly equal to, or higher than, the field values in the wells/boreholes upgradient of the PVLF, and nearly equal to, or lower than, the field values in the wells/boreholes both at PVLF and downgradient. The reasons for these general patterns are believed to be as follows: 1) The amount of recharge entering the flow system upgradient of PVLF was probably overestimated, resulting in a need to increase hydraulic conductivity values in this area during model calibration. An overestimation of recharge is a conservative assumption, as it leads to an overestimation of the hydraulic conductivity value and there will be a greater modeled hydraulic driving force than is actually present; 2) the majority of the hydraulic conductivity values at the PVLF and downgradient wells/boreholes was field tested in the Qo and Qus units, whereas most of the flow in these areas on the landfill side of the Palos Verdes fault zone is in the bedrock units. Therefore, the average hydraulic conductivity values for model Layer 1, which reflects the fact that groundwater occurs mainly in the Monterey Formation layers, would be lower than reported values for just the Qo of Qus layers; 3) downgradient Well M50B, which is the only well located on the West Coast Basin side of the Palos Verdes fault zone used in the analysis (Table 6.6), has a field-obtained hydraulic conductivity value of an order of magnitude higher than the modeled value at this location. During calibration of the model, most grid block adjacent to and on both sides of the Palos Verdes fault zone (including M50B) had to be modified so that modeled heads would closely match observed heads. These modifications decreased further away from the fault zone. Figures H.5 and H.6, Appendix H, shows that the calibrated model hydraulic conductivity values in Layer 2 in the West Coast Basin area range from 1 to 10 feet per day, which is the range expected in this area.

The correspondence between the model and the field-observed data in the vicinity of Palos Verdes fault zone is demonstrated by Figure 1.1, Appendix I. In this figure, data from Wells M23A, M24A, M26A, M50B, and M51B are shown. As can be seen from the figure, the steep hydraulic gradient across the fault zone is closely simulated by the model.

6.2.5 Predictive Analysis

To assess the spatial extent of the potential migration of fluids from the landfill, the calibrated model was utilized to assess the following:

- pathlines of groundwater flowing through the landfill area;

- distribution of direction and magnitude of groundwater velocity in the modeled area; and

- distribution of piezometric head of groundwater.

The horizontal distribution of groundwater velocities is shown on Figure 6.6. The horizontal groundwater elevation contours and horizontal velocities are from the topmost of the five layers modeled, where the groundwater table exists. In Figure 6.6, it can be seen that the flow direction is approximately normal to the fault, suggesting that the fault, by virtue of its low hydraulic conductivity, functions as a partial barrier, and that maximum velocity in the top layer is in the order of 0.1 ft/day.

Five hypothetical fluid particles were modeled as being released from various locations surrounding the landfill area. The starting locations and horizontal pathways of these fluid particles are displayed in Figure 6.7. These locations were placed along the perimeter of the PVLF. Each fluid particle was allowed 2,000 years to travel downgradient from the landfill area. The distributions of effective porosity in the top three layers of the model are presents in Figures H.7 to H.9, Appendix H. The porosity values presented in these figures are arithmetic averages of the effective porosity values of the flow zones discussed in Section 6.2.2.2. It was interesting to note that none of the particles penetrated the fault zone. Particle 1 reached the fault at 2,000 years. Particles 2 and 3 reached the fault zone between less than 400 and 1200 years, but did not penetrate the fault. Particles 4 and 5 did not leave the landfill boundary.

6.2.6 Sensitivity/Uncertainty Analysis

Sensitivity/uncertainty analysis is the process of modifying hydrogeologic parameters to assess the resulting affect on model output. It was performed by changing parameters of the calibrated model such as hydraulic conductivity values, functions of the Palos Verdes Fault zone, recharge, and flow conditions due to human interference (pumping). The following paragraphs describe the scenarios for each sensitivity analysis, presents the results of those analyses, and discusses the zone of particle pathways established based on the model runs.

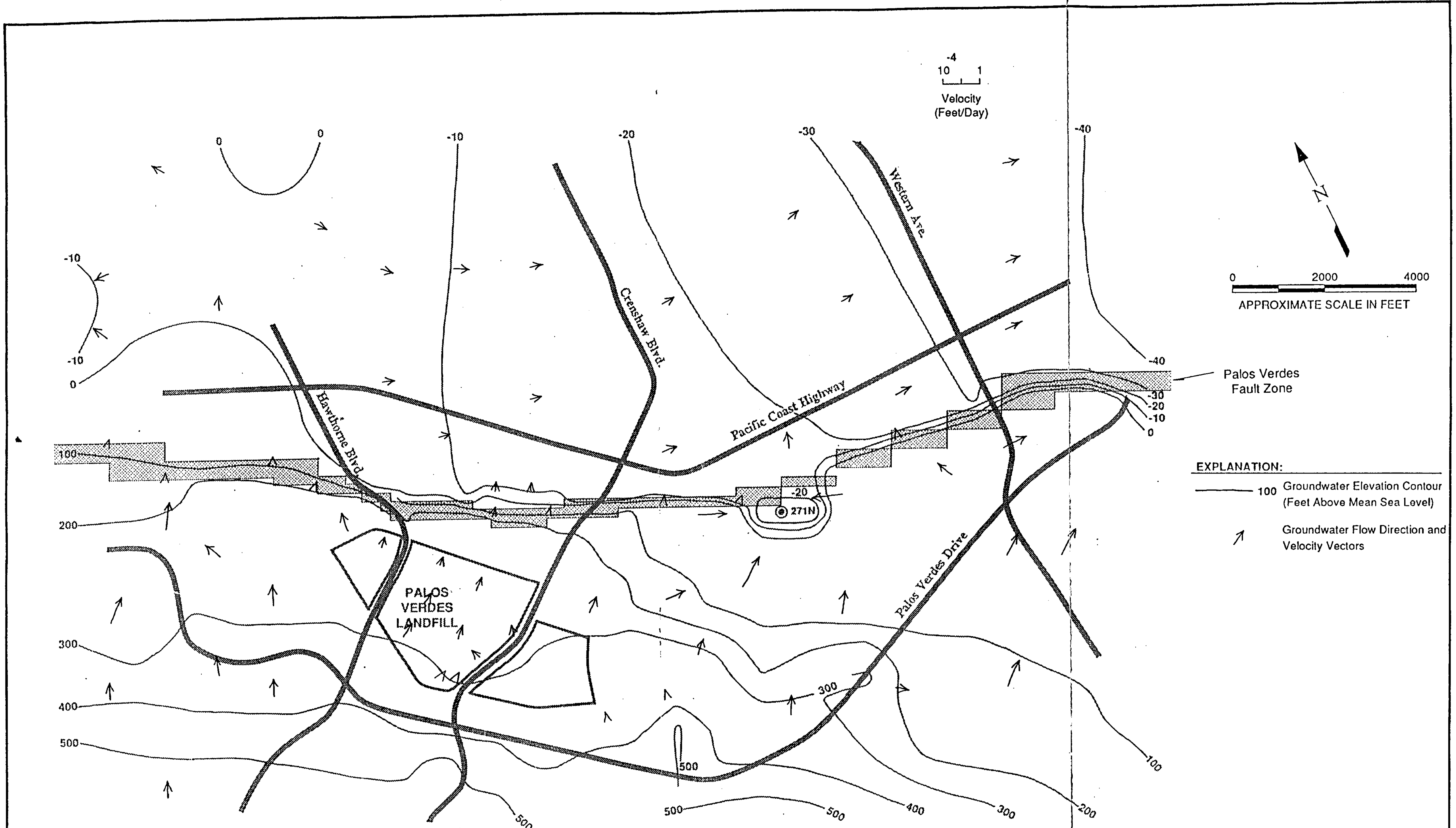

FIGURE 6.6
Distribution of Horizontal Velocities and Contours of Groundwater Elevations, Top Layer, Calibrated Model

DAMES & MOORE

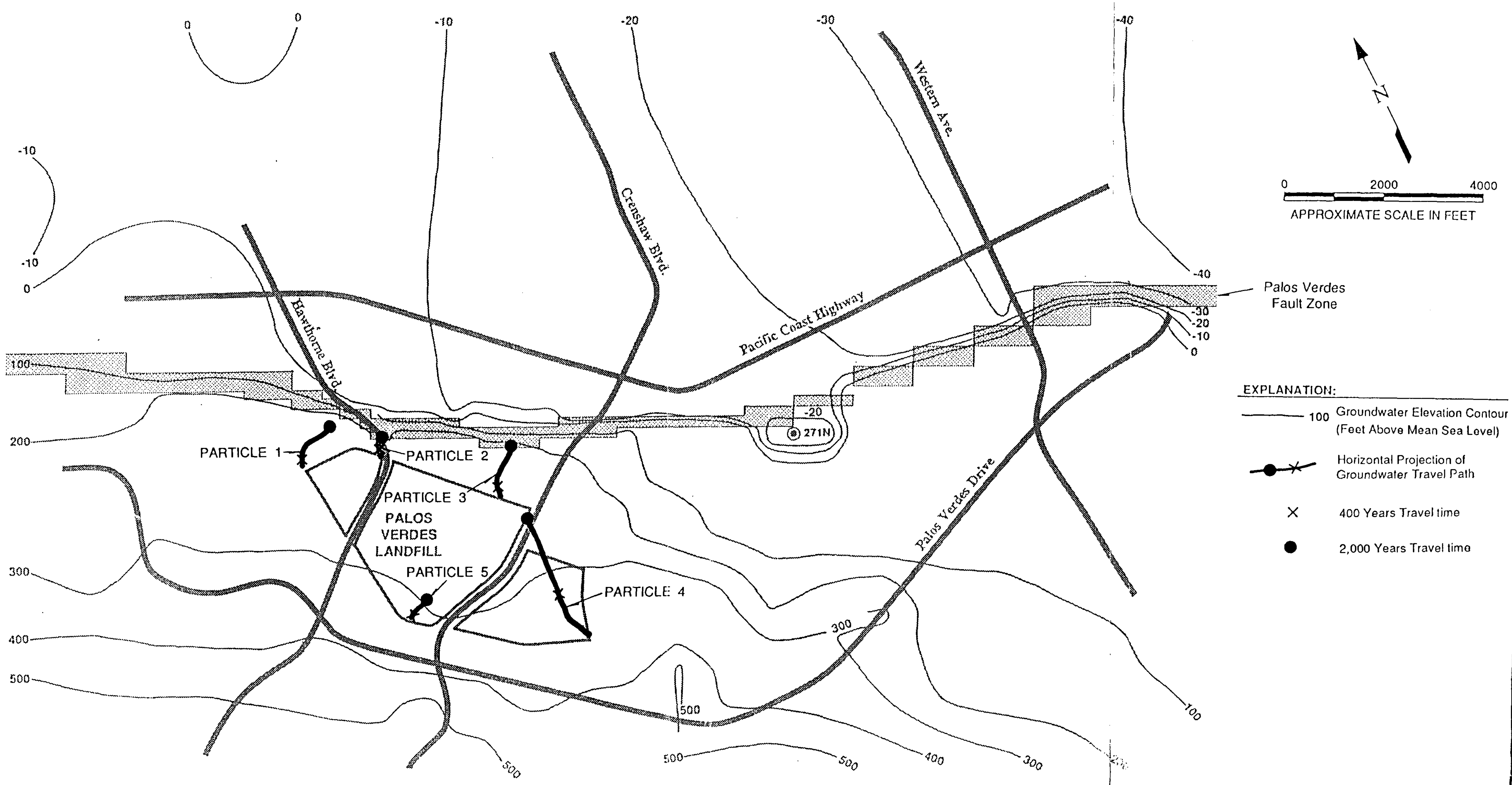

Figure 6.7
GROUNDWATER ELEVATIONS AND PARTICLE PATHWAYS FOR THE CALIBRATED MODEL - 2,000 YEARS TRAVEL TIME

6.2.6.1 Scenarios for Sensitivity/Uncertainty Analysis

To assess the impact that parameter variation may have on the calibrated model, the 28 sensitivity cases (not including Case 0 - the Base Case) were run, each case involving the modification of a parameter used to construct the calibrated model. The following describes each sensitivity case modification.

0. Calibrated Model - Base Case. No parameters were modified in this scenario.

1. Hydraulic conductivity of the non-landfill fill materials (part of Qo) was increased by one order of magnitude (e.g. a ten-fold increase).

2. Hydraulic conductivity of alluvium (part of overburden materials in Qo) was increased by one order of magnitude.

3. Hydraulic conductivity of the Quaternary undifferentiated sand deposits (Qus) was increased by one order of magnitude.

4. Hydraulic conductivity of the Malaga Mudstone (Tmm) was increased by one order of magnitude.

5. Hydraulic conductivity of the Valmonte Diatomite (Tmv) was increased by one order of magnitude.

6. Hydraulic conductivity of the Altamira Shale (Tma) was increased by one order of magnitude.

7. Hydraulic conductivity of the Catalina Schist (Jc) was increased by one order of magnitude.

8. Hydraulic conductivity values representing the Palos Verdes Fault zone at five locations along the fault, were increased 1,000 fold (three orders of magnitude) so that the hydraulic conductivity values at these locations are comparable to those of Qo and Qus. This created several breaks, or "holes" in the fault zone.

9. The global recharge rate was decreased by 75 percent.

10. The global recharge rate was increased by 75 percent.

11. Hydraulic heads were fixed to the observed values at Wells 749A and 240A (see Table 6.5), simulating drawdown due to pumping of these wells, in order to study the effects due to altering the parameters in the flow field in the West Coast Basin. Although these two wells are currently known to be inactive, groundwater elevations at these wells are somewhat low, suggesting that minor pumping may be taking place at these wells.

12. Heads fixed at Wells 749A and 240A, as in Case 11, above, plus the removal of pumping at Well 271N in the Chandler sand pit area.

13. Hydraulic conductivity values on grid blocks immediately adjacent to the fault zone on the PVLF side were assigned a minimum value of 8.0 E-6 cm/sec, a value that is almost two orders of magnitude greater than the assigned fault-zone hydraulic conductivity value of 1.0 E-8 cm/sec. This case was designed to study the effect of the fault in inhibiting the local flow of groundwater.

14. Recharge near Well M59B was removed.

15. Pumping at Well 271N was removed.

16. All grid blocks representing the Palos Verdes Fault zone were assigned a minimum value of 1.0 E-5 cm/sec, thereby eliminating the effect of the fault.

17. The hydraulic conductivity values of the formations in the Palos Verdes Hills, exclusive of the PVLF, are not known. Therefore, the assumed values were increased by a one order of magnitude in these areas.

18. The hydraulic conductivity values of the formations in the West Coast Basin are not known. Therefore, the assumed values were increased by a one order of magnitude.

19. The recharge rate of Zone 1 (hillside residential) was increased by a factor of 2.

20. The recharge rate of Zone 2 (irrigated grasslands) was increased by a factor of 2.

21. The recharge rate of Zone 3 (PVLF) was increased by a factor of 2.

22. The recharge rate of Zone 4 (free-standing water) was increased by a factor of 2.

23. The recharge rate of Zone 5 (vacant land - vegetation covered) was increased by a factor of 2.

24. The recharge rate of Zone 6 (vacant land - dirt covered) was increased by a factor of 2.

25. The recharge rate of Zone 7 (Torrance Airport) was increased by a factor of 2.

26. The recharge rate of Zone 8 (natural drainages) was increased by a factor of 2.

27. The recharge rate of Zone 9 (high density industrial) was increased by a factor of 2.

28. The recharge rate of Zone 0 (normal density commercial/residential) was increased by a factor of 2.

Additional sensitivity analyses relating to uncertainties associated with specified head boundaries and vertical gradient are discussed in the Chemical Model Report (Dames & Moore, 1993).

6.2.6.2 Scenario Analyses and Results

Individual sensitivity/uncertainty analyses were conducted based on the 28 cases (not included in the base case) previously described. Five hypothetical fluid particles, similar to those used in the base case, were released and allowed to travel in each respective flow field for 2,000 years. Diagrams showing groundwater elevation contours and fluid particle paths of each respective scenario analysis are provided in Appendix C (Figures C.0 through C.28).

Summary statistics for each case were calculated. Statistical details for all the cases are provided in Appendix D. Results indicate that correlation coefficients for all cases are above 0.9, suggesting that the model's characteristics are not lost through parameter changes within the range of modifications. Other parameters (absolute maximum residual, and root mean square of residuals), however, vary considerably. The maximum absolute residual value was 151 feet (cases 12 and 15) and the maximum root mean square value was 46 (case 16). The variation of these two parameters is diagrammatically summarized on Figure 6.8.

To facilitate the discussion of the sensitivity analysis results, the 28 scenarios are combined into four appropriate groups. These groups are divided based on categories of parameters considered significant to the model and which may be associated with uncertainties. These parameters include hydraulic properties of the flow zones on both sides of the fault, hydraulic properties within the Palos Verdes Fault zone, and along the fault rims which could dictate the hydrogeologic functions of the fault, recharge rates in various recharge zones, and various pumping scenarios. Each group is collectively discussed below.

1. Increase in Hydraulic Conductivity: Cases 1 through 7, 17, and 18 belong to this group. Because an increase in hydraulic conductivity would accelerate the transport of particles from the site, only the effects due to increases in hydraulic conductivity values were studied. In terms of the change in groundwater elevations, the model is most sensitive to the increase in hydraulic conductivity of the alluvial portion of Qo (case 2), followed by the unit Qus. The model is also somewhat sensitive to the change in hydraulic conductivity value of Tmv and Jc. In terms of particle pathways, the general directions do not change considerably; however, as expected, the distance travelled could increase up to ten fold (Appendix C). When the hydraulic conductivities in the Qo and Jc zones are increased, particles reach pumping well 271N.

2. Hydrogeologic Functions of Fault: Cases 8, 13, and 16 belong to this group. The change in the hydraulic properties of the fault and area immediately adjacent to the fault resulted in an increase of residual and root mean square of residuals (see Figure 6.8). In case 8, hypothetical leakage areas (increases in hydraulic

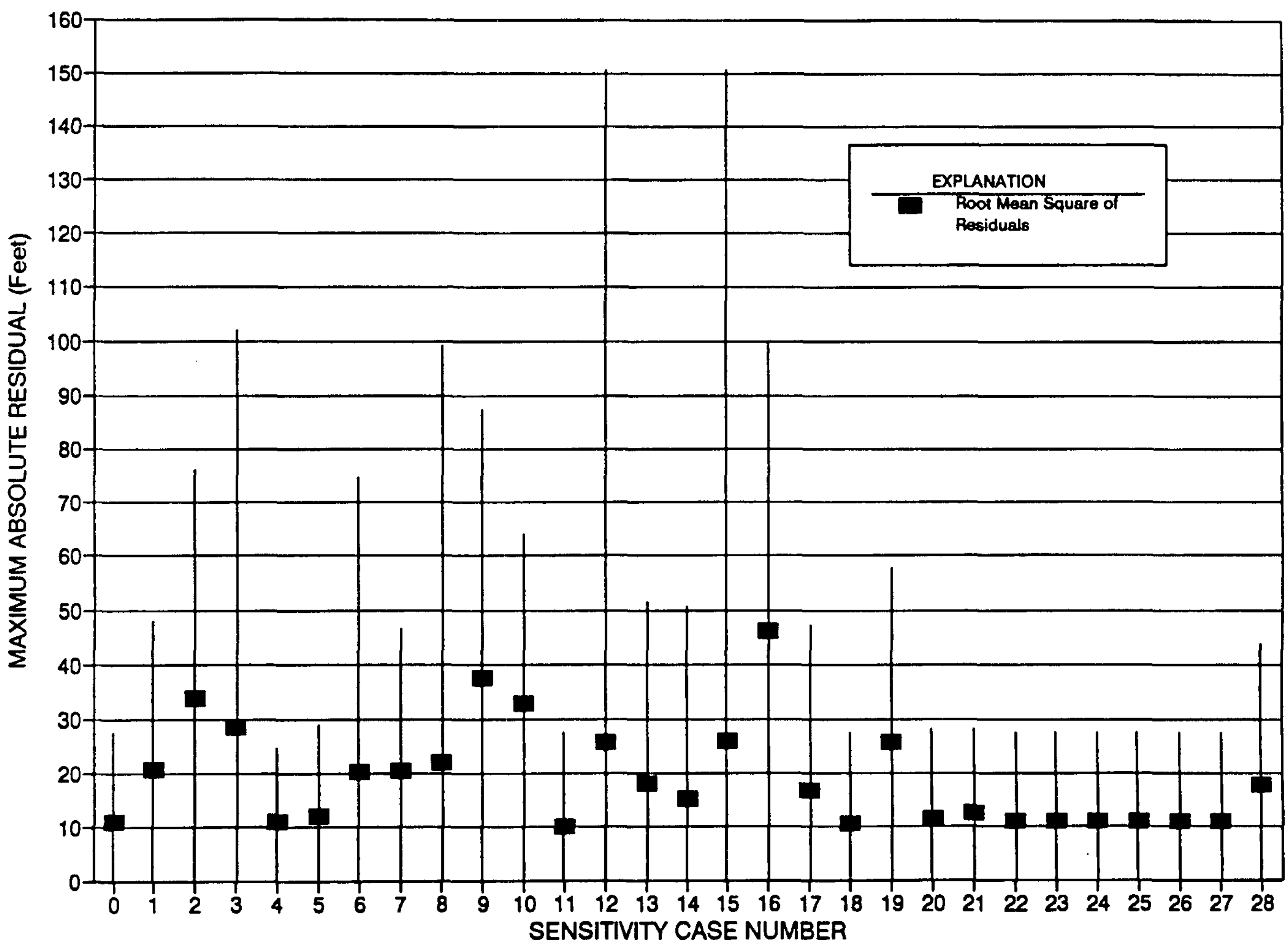

FIGURE 6.8
Summary Statistics from
Sensitivity/Uncertainty Analysis

DAMES & MOORE

conductivity) were imposed at five segments along the fault, one each east and west of PVLF, and one each downgradient of particle 1, particle 2, and particle 3. In this case, it was observed that the percentage of maximum head difference at wells near the fault (MW-23A, MW-24A, MW-25A, MW-49A, MW-51A, and especially MW-26A) increased significantly (see Table D.9), while residuals at other monitoring wells remained essentially constant. As expected, fluid particle 2, which is nearest to the fault, escaped through the hypothetically leaking fault, but particles 1, 3, 4, and 5 did not escape through the fault.

In Case 13, it was observed that water elevations at several monitoring wells located on the fault or close to the fault were affected, and residuals at these wells increased. Because of the change in hydraulic gradient in areas near the fault, flow paths and flow speeds were different, but not appreciably different, from the base case (see Figures C.1 and C.14). Major characteristics of the particle flow paths remained unchanged. The possible hydrogeologic function of the fault as a flow deflector (e.g. the flow is diverted to the direction along the fault rim) was not apparent. This is partially due to the fact that flow from the topographically high areas is approximately normal to the fault. An increase in hydraulic conductivity along the fault rim would not appreciably alter the major flow direction near the fault.

Case 16 involved removing the fault entirely. As expected, two particles, 1 and 2, located near the fault easily flowed into the West Coast Basin. This case, however, should not be considered as a realistic scenario since the fault was completely removed. This case and its particle paths is not represented in subsequent figures or analysis of findings.

3. Variation of Recharge Rates: Cases 9, 10, 14, and 19 through 28 belong to this group. In case 9, the recharge rate at all nodes was decreased by 75 percent. The opposite was true for Case 10, that is, the recharge was increased by 75 percent. In both cases, the root mean square of residuals and absolute maximum residuals were approximately tripled those of the base case. Areas receiving localized concentrated recharge on the landfill side of the fault, and some areas near the fault, tended to be affected more than others. Inspection of the general groundwater elevation contours did not reveal a significant change in the general

flow pattern (see Figures C.1, C.10, and C.11). In addition, the particle flow paths were not observed to be appreciably sensitive to the variation of the recharge rate except for particle 4, which flowed into pumping well 271N in case 9. In Case 14, localized recharge near Well M59B was removed. The removal of this localized recharge caused the local flow pattern to alter, thus allowing Particle 4 to flow toward the fault, then change direction parallel to the fault until subsequently reach the pumping well 271N. Cases 19 through 28 involved increasing the recharge rate in each recharge zone by a factor of two. The most sensitive of these cases proved to be number 19, where the root mean square of residual and absolute maximum residuals increased from 11.0 and 27.9 for the base case, to 25.7 and 58.1, respectively. Particle flow paths in these cases did not change significantly.

4. Pumping Scenarios: Cases 11, 12, and 15 belong to this group. Various combinations of pumping and removal of pumping were studied. Particle paths and groundwater elevation contours are shown in Figures C.12, C.13, and C.16. The imposition of minor pumping at 749A and 240A had very little effect on the regional flow and local particle paths.

The scatter of particle flow paths within 400-year and 2,000-year time frames in all the sensitivity cases is presented on Figures 6.9 and 6.10, respectively. Case 16 elimination of the Palos Verdes Fault zone, is excluded from these figures, as it is an unrealistic case. From these figures, it is apparent that most particle paths are similar in their general directions for all of the sensitivity cases and only one case, Case 8, is shown penetrating the fault. Thus, the calibrated model is not unduly sensitive to variations in individual parameters, with respect to flow paths.

6.2.6.3 Zone of Particle Pathways

To study the movement of fluid particles originating from the PVLF, five hypothetical fluid particles from various locations along the landfill perimeter were allowed to move with the groundwater velocity so as to define an approximate spatial extent of the zone of particle pathways. The particles were tracked until they left the flow domain. The period of 4,000,000 years was chosen to ensure that a complete flow path was obtained for each scenario. However, caution should be used when interpreting model results for extremely long periods of time.

An example of particle paths between the PVLF and model boundaries from the base cases is presented in Figure 6.11. An envelope was established for the particle paths based on the current knowledge of the flow system and potential human-related activities. The envelope is a zone into which streamlines emanating from the landfill area enter. The sensitivity/uncertainty cases used to create a flow-path envelope included the steady-state base case and cases 1 through 8, 11, 13, 15, 16, 18, and 28. These cases were chosen based on the diversity of the particle paths of 2,000 years. The envelope of the pathways is summarized in Figure 6.12 in which the zone is shaded. All of the scattered particle pathways shown in Figures 6.9 and 6.10 approximately fall into this envelope.

A typical distribution of the particle pathways in the vertical direction is shown in Figure 6.13. As shown in this figure, the pathways tend to be confined within the shallow flow zone. Once the fluid particles enter the West Coast Basin, the pathways are bounded by the Qus flow zone below the overburden.

The envelope of particle pathways, shown shaded on Figure 6.12, represents the area within, and downgradient of the PVLF through which particles of water from the PVLF may migrate over a very long period of time. This will be the area of interest for future contaminant transport modeling and risk assessment studies.

6.2.6.4 Summary

The sensitivity analysis results indicate a relatively consistent directions of the five fluid particles. In other words, the direction of groundwater flow in the vicinity of the PVLF is not sensitive to parameter uncertainty. Because of the consistency of the flow direction, the effects due to parameter uncertainty were quantified by analyzing the variation of horizontal hydraulic gradient across the PVLF. The well pair M38A-M41A was chosen to provide a representative hydraulic gradient across the PVLF.

Results are summarized in Table 6.7. In the table, one can see that the simulated gradient is very close to the observed gradient. The deviation is within 10 percent of the observed gradient. An inspection of Table 6.7 reveals that the deviation of gradient about the base case is within a factor of 2.5. Other well pairs, such as M49A-M46A, may also be used for this analysis. A limited analysis of the M49A-M46A well pair, based on the key sensitivity analysis cases (Case 1 - minimum gradient, and Case 19 - maximum gradient) indicates a similar conclusion.

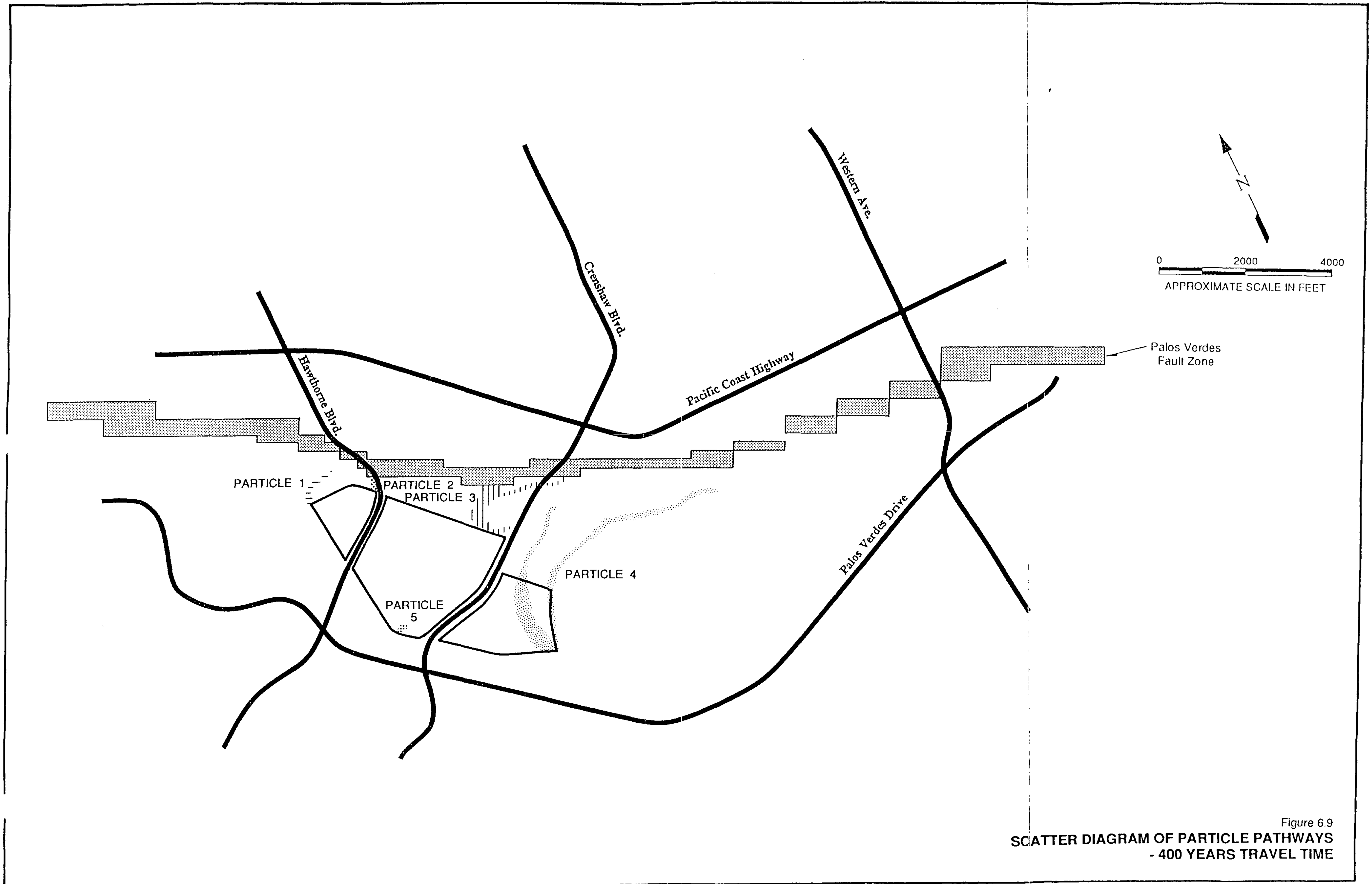

Figure 6.9
SCATTER DIAGRAM OF PARTICLE PATHWAYS - 400 YEARS TRAVEL TIME

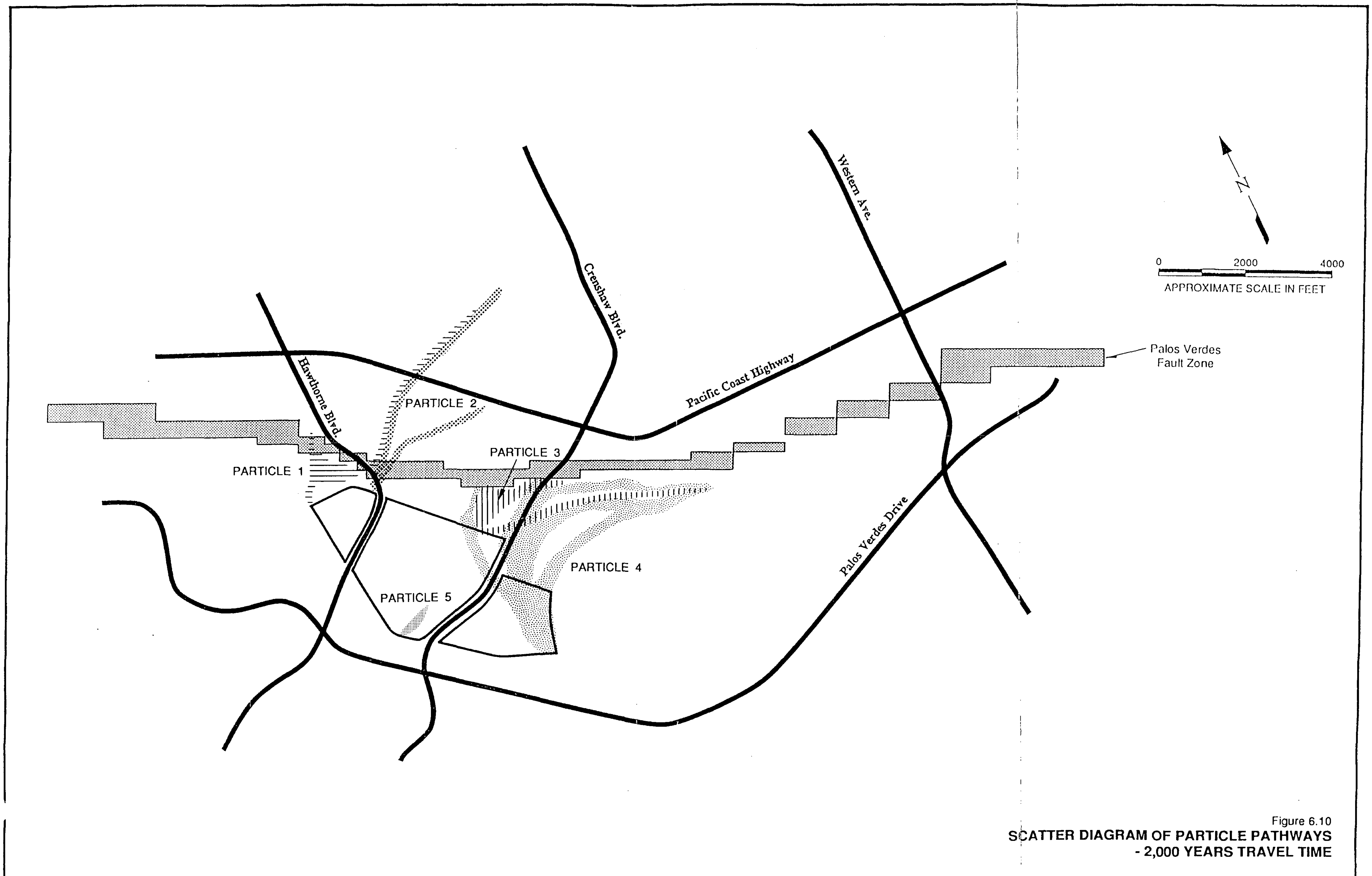

Figure 6.10
SCATTER DIAGRAM OF PARTICLE PATHWAYS - 2,000 YEARS TRAVEL TIME

TABLE 6.7
HYDRAULIC GRADIENT ACROSS THE PALOS VERDES LANDFILL BETWEEN M41A AND M38A
(Page 1 of 1)

Case	Hydraulic Head at M41A (ft above MSL)	Hydraulic Head at M38A (ft above MSL)	Hydraulic Gradient*
Observed	327.6	279.30	.025
0	334.56	281.56	0.0275
1	293.92	272.11	0.0113
2	276.69	326.16	0.0210
3	313.67	260.4	0.0277
4	326.01	276.57	0.0257
5	322.27	273.35	0.0254
6	319.79	283.63	0.0188
7	366.86	294.48	0.0376
8	334.29	280.93	0.0277
9	274.73	243.03	0.0165
10	388.57	316.14	0.0376
11	334.56	218.55	0.0275
12	340.92	288.17	0.0274
13	323.82	266.33	0.0298
14	329.08	274.09	0.0286
15	340.92	288.18	0.0274
16	299.77	231.78	0.0353
17	320.39	273.05	0.0246
18	332.03	278.15	0.0280
19	374.19	300.10	0.0385
20	338.90	285.36	0.0278

A:128\t6.7

TABLE 6.7
HYDRAULIC GRADIENT ACROSS THE PALOS VERDES LANDFILL
BETWEEN M41A AND M38A
(Page 1 of 2)

Case	Hydraulic Head at M41A (ft above MSL)	Hydraulic Head at M38A (ft above MSL)	Hydraulic Gradient*
21	348.82	288.48	0.0313
22	335.85	282.29	0.0278
23	335.22	281.89	0.0277
24	334.88	281.92	0.0277
25	334.56	281.56	0.0275
26	334.61	281.57	0.0275
27	334.56	281.56	0.0275
28	348.06	298.57	0.0257

Note:
(*) Based on the horizontal distance of 1926 feet between Wells M41A and M38A.

A:128\t6.7

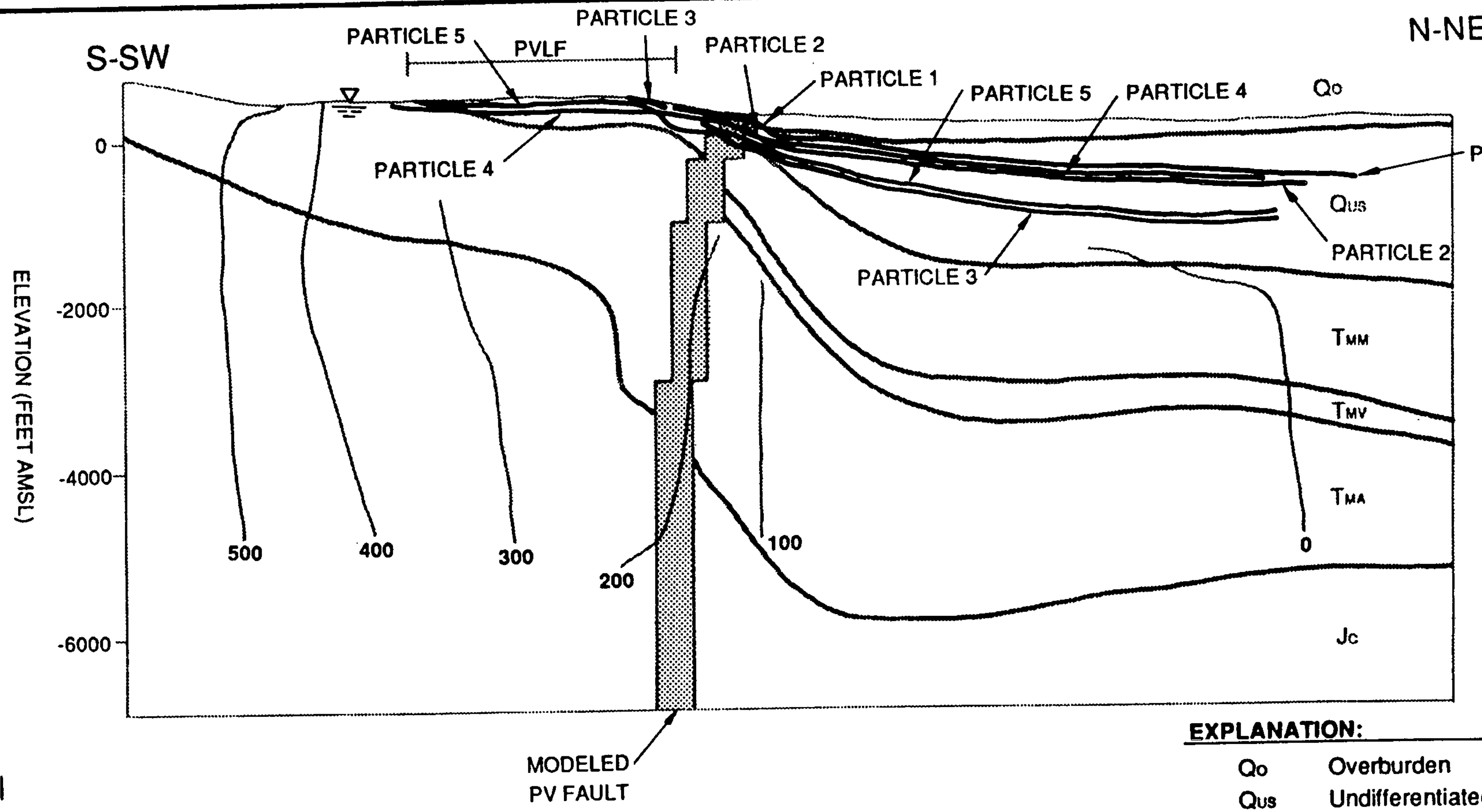

EXPLANATION:

Qo	Overburden
Qus	Undifferentiated Sand
TMM	Malaga Mudstone
TMV	Valmonte Diatomite
TMA	Altamira Shale
Jc	Catalina Achist
——100	Contours Of Hydraulic Head Of Groundwater (Feet Above Mean Sea Level)
——	Projection Of Particle Path

0 2000 4000

APPROXIMATE SCALE IN FEET

Figure 6.13

PARTICLE PATHWAYS BETWEEN THE PVLF AND MODEL BOUNDARY AND CONTOURS OF GROUNDWATER HEADS, SLICE 14, CALIBRATED MODEL

DAMES & MOORE

The variation of hydraulic gradient is an indicator of potential variation of groundwater velocity for a given distribution of hydraulic conductivity and porosity. The variation of groundwater velocity was not analyzed herein because the model has not been calibrated against the existing chemical data. The actual velocity with which chemicals are transported in the groundwater is dependent on adsorptive properties of the geologic media. The effects of velocity uncertainty on chemical transport are reported in the chemical transport modeling document (Dames & Moore, 1993).

Figure 6.11
GROUNDWATER ELEVATIONS AND PARTICLE PATHS BETWEEN THE PALOS VERDES LANDFILL AND THE MODEL BOUNDARY CALIBRATED MODEL

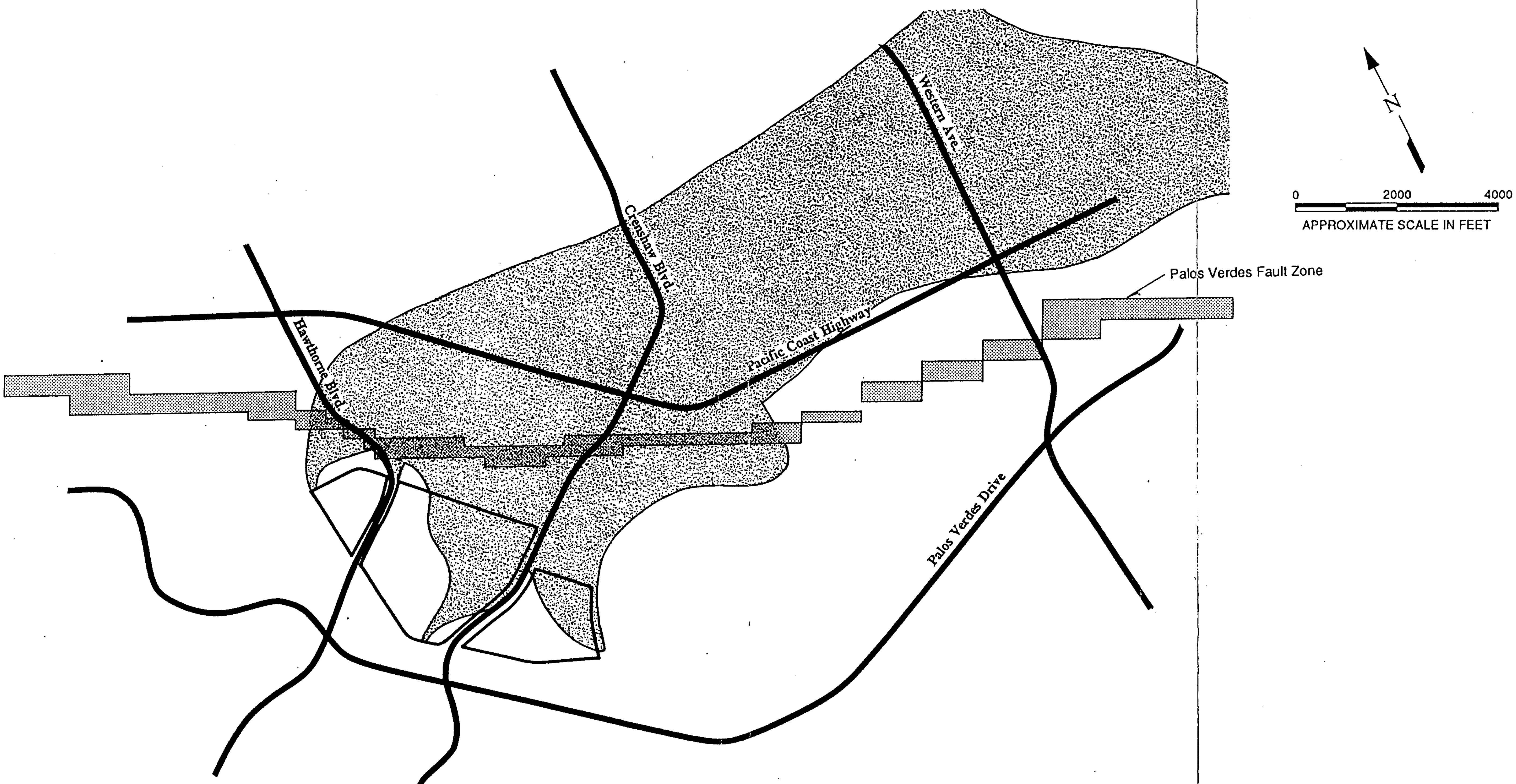

Figure 6.12
ENVELOPE OF PARTICLE PATHS BETWEEN THE PALOS VERDES LANDFILL AND THE MODEL BOUNDARY

7.0 FINDINGS AND CONCLUSIONS

The primary objective of this study was to develop a computer groundwater flow model representative of the hydrogeologic conditions in the vicinity of the PVLF, and capable of simulating the flow of groundwater in this area. The study involved an evaluation of hydrogeologic data, selection of an appropriate groundwater flow model code, and application of the hydrogeologic data to develop a representative groundwater flow model. This section presents the pertinent findings identified during completion of the study, followed by a list of significant conclusions resulting from the evaluation of hydrogeologic data and development of the groundwater flow model.

7.1 FINDINGS

Listed below are the pertinent findings identified during the study.

1. The PVLF area is located topographically on the north-facing foothills of the Palos Verdes peninsula in the south-portion of Los Angeles County. It is structurally separated from the southern fringe of the West Coast Basin by the Palos Verdes Fault zone.

2. The West Coast Basin is a 160-square mile groundwater basin which is bound on the north by the Ballona Escarpment, on the west by the Pacific Ocean, on the east by the Newport-Inglewood Fault, and on the south by the Palos Verdes Fault zone.

3. Aquifers within the West Coast Basin occur in the permeable zones of thick Quaternary and Tertiary-aged basin deposits.

4. The general flow direction of groundwater in the West Coast Basin is to the east/southeast, approximately parallel to the Palos Verdes Fault zone in the vicinity of the PVLF.

5. The Palos Verdes Fault zone acts as a semi-permeable barrier (or partial barrier) to the groundwater flow from the PVLF area into the West Coast Basin.

6. Groundwater flow in the Palos Verdes Hills in the vicinity of the PVLF follows the local topographic relief, generally flowing northeast until reaching the Palos Verdes Fault zone.

7. There is a substantial drop in groundwater elevation between the wells on the upgradient side of the Palos Verdes Fault zone and the wells on the downgradient side of this zone.

8. There are six primary hydrostratigraphic flow zones common to the PVLF area and the adjoining portion of the West Coast Basin. These flow zones and their hydraulic properties are listed below:

   - Overburden (Qo), which includes all saturated, unconsolidated sediments and landfill materials which overlie the undifferentiated sand (Qus) flow zone (see below), with hydraulic conductivity values ranging from 4.00 E-8 cm/sec centimeters per second (cm/sec) to 3.55 E-3 cm/sec;

   - Undifferentiated Sand (Qus), which includes Pleistocene sands, marl, and terrace deposits, with hydraulic conductivity values ranging from 3.60 E-6 cm/sec to 2.10 E-3 cm/sec;

   - Monterey Formation - Malaga Mudstone Member (Tmm), with hydraulic conductivity values ranging from 1.10 E-8 cm/sec to 4.50 E-3 cm/sec;

   - Monterey Formation - Valmonte Diatomite Member (Tmv), with values for hydraulic conductivity ranging from 6.97 E-8 cm/sec to 2.28 E-3 cm/sec;

   - Monterey Formation - Altamira Shale Member (Tma), with hydraulic conductivity values ranging from 2.09 E-7 cm/sec to 1.30 E-3 cm/sec; and

   - Jurassic Catalina Schist (Jc). Flow through this unit is expected to be minimal as compared to the overlying units because of its greater depth, age, and metamorphic nature. Data were not available for hydraulic conductivity values in this zone. Therefore, a conservatively high value of 1.0 E-7 cm/sec was used, which is the maximum value for the published range of hydraulic conductivities for metamorphic rocks.

9. The groundwater flow model was developed utilizing structural data from the MCS geologic model, provided by the Sanitation Districts. Elevations of the tops of the hydrostratigraphic zones were obtained from the Sanitation District's MCS based geologic model, and these data were incorporated into the selected groundwater flow model (MODFLOW), along with appropriate initial values of hydraulic conductivity, porosity, recharge rates, and water table elevations.

10. Groundwater flow beneath the PVLF occurs in the primary pore spaces of the Qo and Qus zones, and in the secondary pore spaces (fractured porosity) of the Monterey Formation rocks.

11. The intensely fractured Monterey Formation allows potential hydraulic communication between the void spaces in adjacent rock units, through interconnection of the fractures in the units.

12. The single-porosity approach was found to be the most technically appropriate approach for modeling the hydrogeology at the PVLF site. This approach uses the equivalent-porous-medium concept to represent the fractured rocks in the Monterey Formation.

13. Twelve groundwater flow simulation codes were reviewed for application to this site, and the MODFLOW code was selected for flow modeling based on specific technical and application criteria.

14. The developed conceptual model consisted of two interrelated flow subsystems: (1) the regional flow system in the West Coast Basin; and (2) the topographically-driven flow subsystem on the Palos Verdes Hills.

15. Hydrogeologic data from monitoring wells near the Palos Verdes Fault zone indicated that the fault functions as a partial barrier and/or flow deflector separating the two flow subsystems.

16. Data from numerous observation wells at PVLF and in the West Coast Basin were used for the groundwater flow model. The nearest actively pumping wells identified during the study include the intermittent extraction wells at PVLF, domestic supply wells 3 1/2 miles to the north of PVLF, and an industrial supply well 1 mile to the east of PVLF.

17. The groundwater flow model was calibrated using the existing measurements of hydraulic conductivity, inferred recharge rates due to artificial recharge and precipitation, and known pumping activities in the area.

18. The groundwater flow model was calibrated against the existing groundwater level records for the period between late 1990 and early 1991, using a trial-and-error approach and adjusting parameters within pre-specified constraints to closely match the groundwater elevation data.

19. Sensitivity/uncertainty analyses performed on the calibrated model involved 28 cases of variations in parameters in the model.

20. Results of the sensitivity/uncertainty analyses indicate that groundwater flow paths are governed by the interaction between the local and regional flow subsystems, as well as anthropogenic activities such as pumping and artificial recharge.

21. The simulation results demonstrate that the flow subsystem in the PVLF area is tributary to the regional groundwater flow system in the West Coast Basin, although the amount of flow is expected to be minimal as compared to the total flow in the West Coast Basin.

22. The groundwater flow model demonstrates that the Palos Verdes Fault zone functions as a partial barrier, attenuating groundwater flow from the PVLF subsystem into the West Coast Basin. Particle tracking exercises indicate that water leaving the landfill generally requires more than 2,000 years to penetrate the fault zone and enter the West Coast Basin.

7.2 CONCLUSIONS

Based on the results of the hydrogeologic investigations and development of a groundwater flow model for the PVLF area, a number of significant conclusions were reached. Pertinent conclusions resulting from this study are presented below.

1. The calibrated groundwater flow model has been demonstrated to be a reasonably accurate and conservative simulator of the groundwater flow path in the PVLF area.

2. The model shows that particles of water originating in the vicinity of the PVLF flow towards the north-northeast until reaching the Palos Verdes Fault zone, and eventually cross into the West Coast Basin, where flow is in a general easterly direction. Particle tracking exercises, based on the existing hydrogeologic information, indicate that water leaving the landfill generally requires more than 2,000 years to completely cross through the Palos Verdes fault zone.

3. The Palos Verdes fault zone which separates the PVLF areas from the West Coast Basin acts as a partial hydraulic barrier, allowing relatively small lateral inflow from the Palos Verdes Hills to enter the West Coast Basin. Water particles may take over 2,000 years to go from the PVLF, through the fault, and into the West Coast Basin. Effects due to leakage along the Palos Verdes fault zone were investigated through sensitivity analysis. For these cases, travel times across the fault zone are less than 2,000 years.

4. Results from 28 sensitivity cases indicate that the groundwater flow paths are not unduly sensitive to the variation of model parameters. The variation of hydraulic gradient is expected to be within a factor of 2.5 of the base case.

5. Although some relatively minor changes in groundwater flow direction occur upgradient of the Palos Verdes Fault zone, the groundwater flow model indicates that the fault zone does not function as a flow deflector, but as a partial barrier to flow.

6. The model output demonstrates that there is a zone of limited aerial extent within which all particles of groundwater emanating from areas within the PVLF will flow. The zone is approximately the same width as the PVLF, and follows the general direction of groundwater flow from the Palos Verdes Hills area to the northeast, eventually passing through the Palos Verdes Fault zone, then bending southeast in the West Coast Basin due to the predominant flow direction there.

7. Particles of water entering the groundwater flow system from vertical recharge in the PVLF area move essentially in the shallow flow zones in a horizontal direction, and, in a general sense, do not migrate below the base of the Undifferentiated Sand deposits (Qus) in the West Coast Basin.

8. The groundwater flow model demonstrates that groundwater flow in the PVLF area is unconfined, topographically driven, and eventually tributary to the major regional flow in the West Coast Basin.

9. The groundwater flow model developed as a part of this study provides a suitable and appropriate basis for use in conjunction with contaminant transport modeling for purposes of evaluating and predicting future flow and concentration conditions in the PVLF area as input to future risk assessment studies. The groundwater flow model will be further refined, prior to its application to the chemical transport simulation, using the existing chemical data within the PVLF area and its vicinity.

7.3 DISCUSSION OF FINDINGS AND CONCLUSIONS

The flow system in the PVLF is represented by a combination of spatially distributed recharge/pumping rates, spatially distributed hydraulic conductivities identified through the calibration process, and geometry of the hydrogeologic structure, which allows the model to closely reproduce the observed groundwater levels. The hydrogeologic structure has been identified from a large number of well logs and boring logs and is believed to be reasonably accurate. Given that the hydrogeologic structure is reliable, the accuracy of the values of hydraulic conductivity evaluated through the calibration process is dependent on the density of groundwater level data points and the estimated recharge rates. The reliability of the calibrated values is judged by the closeness between the calibrated values and those determined by field adjustment of hydraulic conductivity values and the estimation of the recharge rate from precipitation. The results indicated that the calibrated hydraulic conductivity values are a reasonably good representation of the actual hydrogeologic conditions, especially in those areas where groundwater elevation data are available. Since there are adequate data on groundwater elevations in the PVLF area, the developed model is, therefore, a reasonably good representation of the actual flow system in the vicinity of the PVLF.

In the West Coast Basin there exist few data points. The depositional history of the area indicates that the spatial variability or heterogeneity of the hydrogeologic properties of the aquifers is not likely to be very strong. In addition, the direction of the regional gradient is relatively well known in the West Coast Basin. Based on this evidence, the model can simulate the major characteristics of the flow in the West Coast Basin in the vicinity of the PVLF with reasonable accuracy. Because of the sparsity of data in the basin, however, caution must be exercised when using the model for extremely long-term predictions such as the 4,000,000 year base case.

From a theoretical viewpoint, the currently available data allow for the uniqueness of the ratio of hydraulic conductivity to recharge/discharge rate. If the recharge rates had been underestimated, the values of hydraulic conductivity would have also been underestimated. Along this line of reasoning, the bounds of hydraulic conductivity would be dependent on the bounds of the recharge/discharge rates. Since reasonable bounds were found to have been placed on the hydraulic conductivity values, as well as on the recharge/discharge rates, it is believed that the calibrated hydraulic conductivity values are reasonably close to the true values within the modeled area.

The impact due to parameter uncertainty was investigated through the use of a detailed sensitivity/uncertainty analysis. Results of this analysis indicate that the flow paths of groundwater particles emanating from the landfill area are sensitive to the variability of parameters in terms of speed but not in terms of general flow direction. A composite zone was developed based on sensitivity analysis results to show the zone into which groundwater particles emanating from the landfill area are likely to flow.

The hydrogeologic data from monitoring wells across the Palos Verdes Fault show that groundwater levels drop from the PVLF side to the West Coast Basin, indicating that the Palos Verdes Fault zone functions as a partial barrier to groundwater flow. For the fault to act as either a major conduit or as a flow deflector, the variation of the groundwater elevation data should indicate the existence of a major discontinuity (e.g. a more significant drop in water levels along the fault rim or along the axis of the fault plane than observed). From the model calibration process, the best match between the model and the groundwater elevation data was obtained when a relatively small hydraulic conductivity value was assigned to the fault zone (1.0 E-8 cm/sec).

To assess whether it would be possible for the fault to function as a flow deflector, a sensitivity analysis was conducted by increasing the hydraulic conductivity value of the zone immediately adjacent to the fault. Results suggested that the flow was dominated by the topographically driven flow from the Palos Verdes Hills area moving northeasterly normal to the fault. Flow through the fault at random locations may be possible. Although the sensitivity analysis results showed that fluid particles would escape through the fault at a greater speed than they would otherwise under these higher hydraulic conductivity conditions, the major flow pattern would not be affected. In summary, based on the modeling results, the fault generally functions as a partial barrier to the flow from the PVLF area into the West Coast Basin.

-oOo-

APPENDIX A

REFERENCES

A:128\apndaled.fnl

APPENDIX A

REFERENCES

Anderson, M.P., and W.W. Woessner, 1992, Applied Groundwater Modeling - simulation of Flow and Advective Transport. Academic Press, 381 p.

Associated Soils Engineering, Inc., October 29, 1984, Drilling of water quality wells and sampling of soils, Palos Verdes Landfill, Hawthorne side - Getty facility; Prepared for County Sanitation Districts of Los Angeles County.

Audell, Harry, January 2, 1986, Geologic Services Performed at the Palos Verdes Landfill, Palos Verdes, California; Submittal of Subsurface Geologic Conditions with Boring logs 1 through 10; Prepared for County Sanitation Districts of Los Angeles County.

Barenblatt, G., Zheltov, I.P., and Kochina, I.N., 1960, Basic Concepts in the Theory of Seepage of Homogeneous Liquids in Fissured Rocks; Sov. Appl. Math. Mech. (English Translation).

Bear, J., 1972, Dynamics of Fluids in Porous Media, American Elsevier, New York, NY.

Bookman-Edmonston Engineering, Inc., February 21, 1991, Annual Survey Report on Ground Water Replenishment - 1991; prepared for the Central and West Basin Water Replenishment District

California Air Pollution Control Officers Association, Technical Review Group, Landfill Gas Subcommittee (CAPCDA), August 1990, Suggested Control Measures for Landfill Gas Emissions.

California Air Resources Board (CARB), August 1991, Identification on Volatile Organic Compound Species Profiles; ARB Speciation Manual, Second Edition, Volume 1 of 2.

_____, August 1990, The Landfill Testing Program: Data Analysis and Evaluation Guidelines.

California Department of Water Resources, 1961, Planned Utilization of Groundwater Basins in the Coastal Plain of Los Angeles County; Appendix A - Groundwater Geology, Bulletin 104.

_____, September 1990, Watermaster Service in the West Coast Basin, Los Angeles County, July 1, 1989 - June 30, 1990.

California Division of Oil and Gas, Miscellaneous Well Summary Reports and History of Oil and Gas Well Reports for Wells within model area.

California Regional Water Quality Control Board - Los Angeles Region, 1991, Personal Communication with Mr. Craig Christmann, October 4, 1991.

California Water Service Company - Palos Verdes District, 1991, Personal Communication with Mr. Tom Coe, October 21, 1991.

Central and West Basin Water Replenishment District, 1991, Personal Communication with Ms.Melinda Gleason, September 23, 1991.

City of Torrance Water Department, 1991, Personal Communication with Mr. Chuck Schaich, September 23, 1991.

Cleveland, G,B, 1976, Geology of the Northeast Part of the Palos Verdes Hills, Los Angeles County, California; Calif. Division. Mines and Geology Map Sheet 27, Scale 1:12,000.

Conrad, C.L. and Ehlig, P.L., 1986, The Monterey Formation of the Palos Verdes Peninsula - an Example of Sedimentation in a Tectonically Active Basin within the California Continental Borderland; in Baldwin, J.E., ed., Geology and landslides of the Palos Verdes Hills, California: Guidebook prepared for National Association Geology Teachers, Far Western Section, p. 73-77.

Conrad, C.L. and Ehlig, P.L., 1987, The Monterey Formation of the Palos Verdes Peninsula, California - an Example of Sedimentation in a Tectonically Active Basin within the California Continental Borderland; in Fischer, P.J. and MESA^2, eds., Geology of the Palos Verdes Peninsula and San Pedro Bay, Part I: Pacific Section, Soc. Econ. Paleontologists and Mineralogists, Los Angeles, Calif., p.17-30.

Cooley, R.L, April, 1977, A Method of Estimating Parameters and Assessing Reliability for Models of Steady State Groundwater Flow--1. Theory and Numerical Properties; American Geophysical Union, V. 13, No. 2, pp. 318-324.

County of Los Angeles, Department of Public Works (LACDPW), Miscellaneous Groundwater Well Logs for the West Coast Basin.

County Sanitation Districts of Los Angeles County (Sanitation Districts), January 1986a, Draft Remedial Action Plan for the Palos Verdes Landfill; Prepared for California Regional Water Quality Control Board and Palos Verdes Task Force Committee.

_____, April 1986b, Supplemental Report to Draft Remedial Action Plan for the Palos Verdes Landfill; Prep. for California Regional Water Quality Control Board and Palos Verdes Task Force Committee.

_____, June 16, 1986c, Information Regarding Exploratory Borings at Ernie Howlett Park (Parcel 4 of Palos Verdes Landfill); Letter transmitted to California Regional Water Quality Control Board.

_____, August 1987, Palos Verdes Landfill Groundwater Detection and Monitoring Well Program Report; Report for the California Regional Water Quality Control Board, Los Angeles Region, 69 p.

_____, November 30, 1989a, Final Hydrogeologic Characterization Plan, Palos Verdes Landfill, 25706 Hawthorne Boulevard, Rolling Hills Estates, Los Angeles, California; Prepared for Calif. Dept. of Health Services, 112 p.

_____, November 30, 1989b, Final Palos Verdes Landfill Soil Characterization Plan; Prepared for California Department of Health Services, Toxic Substances Control Division, 12 p.

_____, January 31, 1990, Final Ambient Air/Landfill Gas Characterization Workplan (WP), Palos Verdes Landfill, 25706 Hawthorne Boulevard, Rolling Hills Estates, Los Angeles, California; Prepared for California Department of Health Services.

_____, February 15, 1991, Monitoring Report for Palos Verdes Landfill, September through December 1990; Prepared for California Department of Health Services, Toxic Substances Control Division, Region 4 (Long Beach).

_____, May 15, 1991, Monitoring Report for Palos Verdes Landfill, First Quarter, 1991, (January, February, March); Prepared for California Department of Health Services, Toxic Substances Control Division, Region 4 (Long Beach).

Dames & Moore, October 1985, Physical and Mathematical Background of Two-Dimensional and Three-Dimensional Variably Saturated, Density Coupled Models.

_____, April 12, 1991, Work Plan Addendum, Groundwater Characterization, Coachella Sanitary Landfill, Coachella Valley, California; Prepared for the County of Riverside Waste Management Department, Job No. 22158-001-128

-----, March 12, 1993, Hydrogeologic Modeling for Remedial Investigation/ Feasibility Study, Chemical Transport Model, Palos Verdes Landfill, Prepared for County Sanitation Districts of Los Angeles County.

Dames & Moore and Marine Environmental Science Associates (MESA^2), September 25, 1983, Final Technical Report, Activity and Earthquake Potential of the Palos Verdes Fault; Prepared for U.S. Geological Survey, Contract No. 14-08-0001-19786.

Davis, T.L., Namson, J., and Yerkes, R.F., 1989, A Cross Section of the Los Angeles Area: Seismically Active Fold and Thrust Belt, the 1987 Whittier Narrows Earthquake and Earthquake Hazard; Journal of Geophysical Research, v. 94, No. B7, p. 9644-9664.

de Marsily, G., 1986, Quantitative Hydrogeology, Groundwater Hydrology for Engineers; Academic Press, Inc., Publishers, Orlando, Florida, 440 p.

Driscoll, F.G., 1986, Groundwater and Wells; Second Edition, Johnson Filtration Systems, Inc., Publishers, St. Paul, MN, 1089 p.

Dominguez Water Company, 1991, Personal Communication with Mr. Oscar Luque, October 25, 1991., Federal Register, August 1988, Proposed RCRA Subtitle D Regulations; 40 CFR Part 258, Criteria for Municipal Solid Waste Landfills, V. 53, No. 168, pp. 33405-33422.

Fischer, P.J., MESA^2, Patterson, R.H., Darrow, A.C., Rudat, J.H., and Simila, G., 1987, The Palos Verdes Fault Zone: Onshore to Offshore; in Fischer, P.J. and MESA^2, eds., Geology of the Palos Verdes Peninsula and San Pedro Bay, Part I: Pacific Sect., Soc. Econ. Paleontologists and Mineralogists, Los Angeles, Calif., p. 91-134.

Fleisher, P,. 1971, Submarine Gravitational Origin of Recumbent Folds in the Altamira Shale, Palos Verdes Hills, California; Association of Engineering Geology v. VIII, no. 2, p. 183-195.

Freeze, R.A., and Cherry, J.A., 1979, Groundwater; Prentice-Hall, Inc., Publishers, Englewood Cliffs, NJ, 604 p.

Greene, H.G., Bailey, K.A., Clark, S.H., Ziony, J.I. and Kennedy, M.P., 1979, Implications of Fault Patterns of the Inner California Continental Borderland Between San Pedro and San Diego; in Abbott, P.L. and Elliot, W.J., eds, Earthquakes and other Perils, San Diego Region: San Diego Assoc. Geologists, San Diego, Calif., p. 21-27.

Geofon, Inc., July 19, 1985, Report of Subsurface Geologic Study, Leachate Barrier at Palos Verdes Landfill, Rolling Hills Estates, California; Prepared for County Sanitation Districts of Los Angeles County.

_____, February 12, 1986, Final Report of Supplemental Geologic Study, Leachate Barrier at Palos Verdes Landfill, Rolling Hills Estates, California; Prepared for County Sanitation Districts of Los Angeles County.

Guptil, P., 1991, written communication to County Sanitation Districts of Los Angeles County.

Guvanasen, V., May 21-23, 1984, Flow Simulation in a Fractured Rock Mass; Proceedings of the International Groundwater Symposium on Groundwater Resources Utilization and Contaminant Hydrogeology, The International Association of Hydrogeologists, Canadian National Chapter, Montreal, pp. 403-412.

Harbor Regional Park, 1991, Personal Communication with Mr. Roger Williams, October 25, 1991.

Hauksson, E., 1990, Earthquakes, Faulting, and Stress in the Los Angeles Basin; Journal of Geophysical Research, v. 95, No. B10, p. 15,365-15,394.

Hensel, B.R., Keefer, D.A., Griffin, R.A., and Berg, R.C., March-April 1991, Numerical Assessment of a Landfill Compliance Limit; Ground Water Journal, V.29, No. 2, pp. 218-224.

Herzog Associates, January 29, 1991a, Report, Palos Verdes Landfill, Hydrogeological Investigation, Phase I, Los Angeles County, California; Prepared for County Sanitation Districts of Los Angeles County, Job No. 15384.1-0-7, 70 p.

_____, January 29, 1991b, Report, Palos Verdes Landfill, Hydrogeological Investigation, Phase II, Los Angeles County, California; Prepared for County Sanitation Districts of Los Angeles County, Job No. 15384.1-0-7, 71 p.

Hinkle, Dale, May 20, 1986, Report of Geologic Investigation and Monitoring Well Installation, Palos Verdes Landfill - Parcel 4; Prepared for County Sanitation Districts of Los Angeles County.

Huyakorn, P.S., and Pinder, G.I, 1983, Computational Methods in Subsurface Flow; Academic Press, Inc., Publishers, New York, NY.

Illinois Pollution Control Board, 1988, Recommendations for a Nonhazardous Waste Disposal Program in Illinois and a Background Report to Accompany Proposed Regulations for Solid Waste Disposal Facilities; R84-17 Docket D, unpublished report, scientific/technical section, PCB, Chicago, Il, 70p.

Jennings, C.W., 1977, Geologic Map of California; California Division of Mines and Geology.

Kanehiro, B.Y., Guvanasen, V., Wilson, C.R., and Witherspoon, P.A., June 1981, Fracture Flow Modeling for Low-Level Nuclear Waste Disposal; In Modeling and Low-Level Waste Management: An Interagency Workshop, Denver, December 1-4, 1980, pp. 187-196.

Kleinfelder, June 1988, Report of Monitoring Well Completion and Hydrogeologic Conditions, Palos Verdes Landfill, Palos Verdes, California; Prepared for County Sanitation Districts of Los Angeles County, 2 vol.

Linsley, R.K., Kohler, M.A., and Paulhus, J.L.H., 1982, Hydrology for Engineers, McGraw-Hill.

Long, J.C.S., Remer, J.S., Wilson, C.R., and Witherspoon, P.A., 1982, Porous Media Equivalents for Networks of Discontinuous Fractures; Water Resources Res., pp. 645-658.

Louis, C., and Parnot, M., 1972, Three-Dimensional Investigation of Flow Conditions and Grand Maison Dam Site; Proc. Sym. Percolation Through Fissured Rocks, Stuttgart, Paper T1-C.

Mercer, J.W. and Faust, C.R., 1981, Ground-Water Modeling, Published by National Water well Association.

Miller, W.J., 1989, Use of Groundwater Modeling to Analyze Contaminant Migration Influenced by Multiple Well Fields; Proceedings of the Fourth International Conference on the Use of Models to Analyze and Find Working Solutions to Groundwater Problems, Solving Groundwater Problems with Models, February 7-9, 1989,

Paradine, C.G., and Rivett, B.H.P., 1960, Statistical Methods for Technologists; The English Universities Press Ltd., Publishers, London, England, 288 p.

Patterson, R.H. and Freeman, S.T., 1990, Characterization of the Palos Verdes fault - Onshore; in Worldport LA/Port of Los Angeles (POLA) 2020, Seismic Workshop - Vol 1.) Hazard Session Draft Papers.

Poland, J.F., 1959, Hydrology of the Long Beach - Santa Ana Area, California; U.S. Geological Survey Water Supply Paper 1471, 257 p.

Pollock, D.W., and Zehner, H.H., June 1981, A Conceptual Analysis of the Groundwater Flow System at the Maxey Flats Radioactive Waste Burial Site, Fleming County, Kentucky; In Modeling and Low-Level Waste Management: An Interagency Workshop, Denver, December 1-4, 1980, pp. 197-213.

Prudic, D.E., June 1981, Computer Simulation of Groundwater Flow at a Commercial Radioactive-Waste Landfill Near West Valley, Cattaraugus County, New York; In Modeling and Low-Level Waste Management: An Interagency Workshop, Denver, December 1-4, 1980, pp. 215-248.

Reeves, M., and Duguid, J.O., 1975, Water Movement Through Saturated-Unsaturated Porous Media--A Finite Element Galerkin Model; Oak Ridge, Tenn., Oak Ridge National Lab, ORNL-4927, 232 p.

Rowell, H.C., May 29, 1981, Diatom Biostratigraphy of the Monterey Formation of the Palos Verdes Hills, California; in Garrison, R.E. and Douglas, R.G., eds., The Monterey Formation and related siliceous Rocks of California: Proc. of Soc. Econ. Paleontologists and Mineralogists Research Symposium, p. 55-70.

Rowell, H.C., 1982, Chronostratigraphy of the Monterey Formation of the Palos Verdes Hills; in Cooper, J.D., ed., Landslides and Landslide Abatement, Palos Verdes Peninsula, southern California: Prepared for 78th Annual Meeting, Cordilleran Section, Geologic Society of America, Anaheim, California, p. 7-13.

Robert Stone & Associates, Inc. January 27, 1975, Geologic and Soils Engineering Study, Proposed Class I Landfill, North Portion of Palos Verdes Landfill, Crenshaw Boulevard, Los Angeles County, California; Prepared for County Sanitation Districts of Los Angeles County, Job No. 1-0-0108077, 17 p.

Robert Stone & Associates, Inc. January 13, 1976, Supplementary Geologic and Soils Engineering Study, Proposed Class I landfill, North Portion of Palos Verdes Landfill, Crenshaw Boulevard, Los Angeles County, California; Prepared for County Sanitation Districts of Los Angeles County.

Schoelhammer, J.E. and Woodford, A.O., 1951, The Floor of the Los Angeles Basin, Los Angeles, Orange, and San Bernardino Counties, California; U.S. Geologic Survey Oil and Gas Investigation Map OM-117.

Slade, R.C., 1986, Hydrogeologic Investigation: Perennial Yield and Artificial Recharge Potential of the Alluvial Sediments in the Santa Clarita River Valley of Los Angeles County, California; Prepared for Upper Santa Clara Water Committee Members: Los Angeles County Water Works, District No. 36 - Val Verde, Newhall County Water District, Santa Clarita Water Company, Valencia Water Company, December, 1986.

South Coast Air Quality Management District (SCAQMD) Rule 1150.2: Control of Gaseous Emissions from Inactive Landfills.

Taylor, M.D., 1989, Use of Contaminant Transport Modeling for the Establishment of Aquifer Protection Zones in Lee County, Florida; Proceedings of the Fourth International Conference on the Use of Models to Analyze and Find Working Solutions to Groundwater Problems, Solving Groundwater Problems with Models, February 7-9, 1989,

Todd, D.K., 1980, Groundwater Hydrology, Second Edition; John Wiley & Sons, Publishers, New York, NY, 535 p.

U.S. Nuclear Regulatory Commission, 1983, Disposal of High-level Radioactive Wastes in Geologic Repositories: Technical Criteria (10 CFR 60), Federal Register 48 FR 28194), Washington, D.C., June 21.

West Basin Municipal Water District, 1991, Personal Communication with Mr. Tom Salvano, September 23, 1991.

Woodring, W.P., Bramlette, M.N., and Kew, W.S.W., 1946, Geology and Paleontology of Palos Verdes Hills, California; U.S. Geological Survey, Professional Paper 207, 145 p.

Woodring, W.P., Bramlette, M.N., and Kleinpell, R.M., 1936, Miocene Stratigraphy and Paleontology of Palos Verdes Hills, California; American Association of Petroleum Geologists, v. 20, no. 2, p. 125-149.

Woodward-Clyde Consultants, 1987, Final Technical Report, Late Quaternary Activity Along the Onshore Portion of the Palos Verdes Fault Zone; Prepared for U.S. Geological Survey, Contract No. 14-08-0001-21304.

Yerkes, R.F., McCullovch, T.H., and others, 1965, Geology of the Los Angeles Basin, California: an Introduction: U.S. Geological Survey Professional Paper 420A, 57 p.

Ziony, J.I., Wentworth, C.M., Buchanan-Banks, J.M., and Wagner, H.C., 1974, Preliminary map Showing Recency of Faulting in Coastal Southern California; U.S. Geological Survey Miscellaneous Field Studies Map MF-585.

APPENDIX B

TECHNICAL REFERENCES ON HYDROGEOLOGIC MODELS

APPENDIX B

TECHNICAL REFERENCES ON HYDROGEOLOGIC MODELS

A hydrogeologic model is an approximation of a real hydrogeologic system. The model simulates and describes those features of the system that are essential to the purpose for which the model was developed, and includes various assumptions and constraints pertinent to the system. Thus, a hydrogeologic model expresses the conceptual representation of the system in causal relationships among various components within the system and between the system and its environment. The following sections provide information on three aspects of hydrogeoloic modeling: modeling approaches; modeling techniques; and the application of models to similar situations.

Modeling Approaches

In geologic environments such as at the PVLF, groundwater occurs in both porous (granular) and fractured media. The theoretical fundamental of groundwater flow in porous media is well established and may be found in classical references and groundwater textbooks such as Bear (1972), Freeze and Cherry (1979), Todd (1980), and de Marsily (1986). The flow equation for porous media is based on Darcy's law and the principle of continuity, and may be tensorially expressed as:

$$\frac{\partial}{\partial x_i} K_{ij} \frac{\partial h}{\partial x_j} = S_s \frac{\partial h}{\partial t} + Q$$

where	K_{ij}	=	hydraulic conductivity tensor,
	x_i	=	cartesian coordinates,
	h	=	piezometric head,
	S_s	=	storativity,
	t	=	time, and
	Q	=	injection/extraction per unit volume.

Repeated subscripts denote repetition of the terms. This Equation is also based on the assumption that the groundwater density remains approximately constant, which is the condition expected at the PVLF. Equation (1) provides the flow field for the transport equation.

The mathematical expression for contaminant transport is also well established in the literature (Bear, 1972). The transport equation may be tensorially expressed as:

$$(\theta+(1-\theta)\rho_s K_d)\frac{\partial C_I}{\partial t}+\frac{\partial \theta u_i C_I}{\partial x_i}=\frac{\partial}{\partial x_i}\theta D_{ij}\frac{\partial C_I}{\partial x_j}-\lambda\theta C_I$$

where	u_i	=	fluid velocity in the x_i direction,
	D_{ij}	=	dispersion coefficient tensor,
	t	=	time,
	C_I	=	concentration of contaminant I,
	λ	=	decay constant of C_I, and
	θ	=	effective porosity,
	ρ_s	=	solid density of matrix solid,
	K_d	=	partitioning coefficient for contaminant I.

Fractured rock formations exist in a wide range of geologic circumstances, due to both natural and man-made causes. Great significance is often attributed to the existence of fractures in considering responses to a variety of hydrogeologic phenomena. Among these are fluid movement, contaminant and heat transport, and multi-phase flow. The subject of fluid flow and transport in fractured media has received a great deal of scientific attention over the past three decades. In general, the modeling of flow in fractured media may be divided into two major approaches: the single-porosity approach, and the double-porosity approach. Each of these approaches is further discussed below.

Single-Porosity Approach

Generally, flow through fractured media based on the single-porosity approach may be described mathematically in one of the following three ways (Kanehiro et al., 1981, Guvanasen, 1984):

- o by considering each fracture as a discrete hydraulic conduit;
- o by assuming a hydraulically equivalent porous medium and using an appropriate porous medium model; or

- by a combination of the first two options.

The first option is extremely difficult to apply to regional groundwater flow regimes due to the amount of data required, the computational effort, and the difficulty in obtaining accurate data for many actual problems. One way of circumventing this problem is to represent a fractured system using an equivalent porous medium or fluid-transmitting continuum which, under specific hydrological and geometrical conditions, behaves in a manner similar to the fractured rock. The flow and transport equations for porous media are applicable to equivalent porous media. Extensive work in this area has been carried out by several researchers including Louis and Parnot (1972), and Long et. al. (1982).

In many instances, a rock mass may be considered to consist of a background system of relatively small-scale fractures with some major fracture zones such as lineaments and faults. In this case, the major fracture zone should not be included in determining the background equivalent porous medium properties; otherwise, the dominance of the major system may render the small-scale fracture system not accurately represented by the equivalent porous medium. This situation is similar to that in the vicinity of the PVLF where the area of interest is traversed by the Palos Verdes Fault zone.

Double-Porosity Approach

The concept of double porosity was first introduced by Barrenblatt et. al. (1960) to help quantify flow in fractured rocks. According to this concept, the fractured rock mass is assumed to consist of two interacting, overlapping continual: (1) a continuum of low permeability, or primary-porosity blocks; and (2) a continuum of high permeability, or secondary-porosity fissures. This approach is not applicable to the PVLF case due to the necessary time frame of simulation (tens to hundreds of years).

Modeling Techniques

In order to accommodate the spatial variability of material properties, it is necessary to employ numerical modeling techniques such as finite difference and finite element techniques. Details of these techniques may be found in references such as Huyakorn and Pinder (1983), and de Marsily (1986).

Several computer codes have been developed to solve the problem of groundwater flow and contaminant transport. They are based on either the finite difference technique or the finite-element technique, or the hybrid of the two. A discussion of the codes evaluated for use at PVLF is presented in Section 6.0. These codes have different advantages and disadvantages. In order to select the most appropriate code for the PVLF project, a set of criteria were utilized. These criteria and their use in model selection are also discussed in Section 6.0.

Applications of Models

Numerical groundwater flow and contaminant-transport models have been utilized in situations similar to the PVLF site. Examples presented herein are drawn from technical journals, conference proceedings, and technical reports. In general, models have been used to synthesize and interpret site specific data into a coherent representation of the site and to predict future contaminant and groundwater flow conditions. Such predictions are normally required for the performance of baseline risk assessments and to assess the efficiency of potential remedial alternatives. The following paragraphs provide examples of groundwater flow and contaminant-transport model applications.

To assess the efficacy of the proposed regulatory compliance distances for landfill siting in the state of Illinois, numerical hydrogeologic modeling was performed using the PLASM and RANDOMWALK codes (Hensel, et. al., 1991) to assess 16 generalized geological sequences representative of hydrogeologic conditions over an estimate of 90 to 95 percent throughout the entire state. A compliance distance, which delineates the areal boundaries of a zone of attenuation around a waste disposal site, is a regulatory measure that is intended to provide a buffer area between the waste cell and the points where applicable groundwater standards are to be enforced (Illinois Pollution Control Board, 1988; Federal Register, 1988). The zone of attenuation is three dimensional, bounded at the top by the ground surface, below by the base of the uppermost aquifer, and on each side by the compliance distance. Attenuation within this zone must be sufficient to prevent contaminants from reaching the compliance distance within a 100-year period. The work carried out by Hensel et. al. (1991) suggests that 50 percent of the state would be hydrogeologically suitable for non-hazardous waste disposal if the compliance distance were 100 feet, and 55 percent suitable with the compliance distance of 500 feet. This work demonstrates the utility of hydrogeologic simulations in the development of regulations governing landfill siting.

The Riverside County Waste Management Department conducted modeling for the landfills at Blythe, Coachella Valley, and Mecca, in the County of Riverside, California. Numerical hydrogeologic modeling was conducted to help delineate the potential for migration of low concentration dissolved leachate from the landfills in order to assist in the formulation of site characterization strategies, and in the assessment of subsequent remedial alternatives, if necessary (Dames & Moore, 1991). For these sites, the TARGET code (Dames & Moore, 1985) was utilized.

Groundwater modeling was performed to evaluate contaminant pathways in the vicinity of the Delaware Sand and Gravel Landfill in New Castle, Delaware, and for subsequent use in evaluating selected remediation alternatives (Miller, 1989). The modeling approach included the use of a regional two dimensional groundwater flow model and more detailed and localized three dimensional flow and transport models. This telescopic modeling approach highlighted specific local hydrogeologic complexities in the vicinity of the landfill. The USGS2D model (precursor of USGS3D and MODFLOW) was used for the two dimensional flow modeling, while SWIFT was used for local three dimensional flow and transport modeling.

At the Maxey Flats radioactive waste burial site in Fleming County, Kentucky, the groundwater flow system is complex, with the flow occurring mainly through fractures in hydraulically "tight" shales and sandstones. Two dimensional, vertical, cross-sectional groundwater models were developed to investigate and study the local groundwater flow systems at the site (Pollock and Zehner, 1981). The equivalent porous medium approach was used to represent the fracture systems. At a commercial, low level radioactive waste burial site near West Valley, New York, vertical cross-sectional models were also developed to simulate groundwater flow and radionuclide transport in fractured till and to study the principal factors that control the subsurface movement of radioisotopes in the vicinity of the burial trenches (Prudic, 1981). The models were based on the code developed by Reeve and Duguid (1978). Again the equivalent porous medium approach was adopted.

To address issues of well head protection, groundwater flow and contaminant-transport models were developed for Lee County, Florida, to assist in the formulation of strategies for well-field protection against contamination due to land-use-related activities in upper aquifers and short circuiting of wells in deeper aquifers (Taylor, 1989). The telescopic modeling approach was applied, using a regional model for the county wide flow system and a local model for each well field. The developed models were based on the DYNFLOW/DYNTRACK code.

APPENDIX C

PLOTS OF SENSITIVITY/UNCERTAINTY ANALYSIS CASES

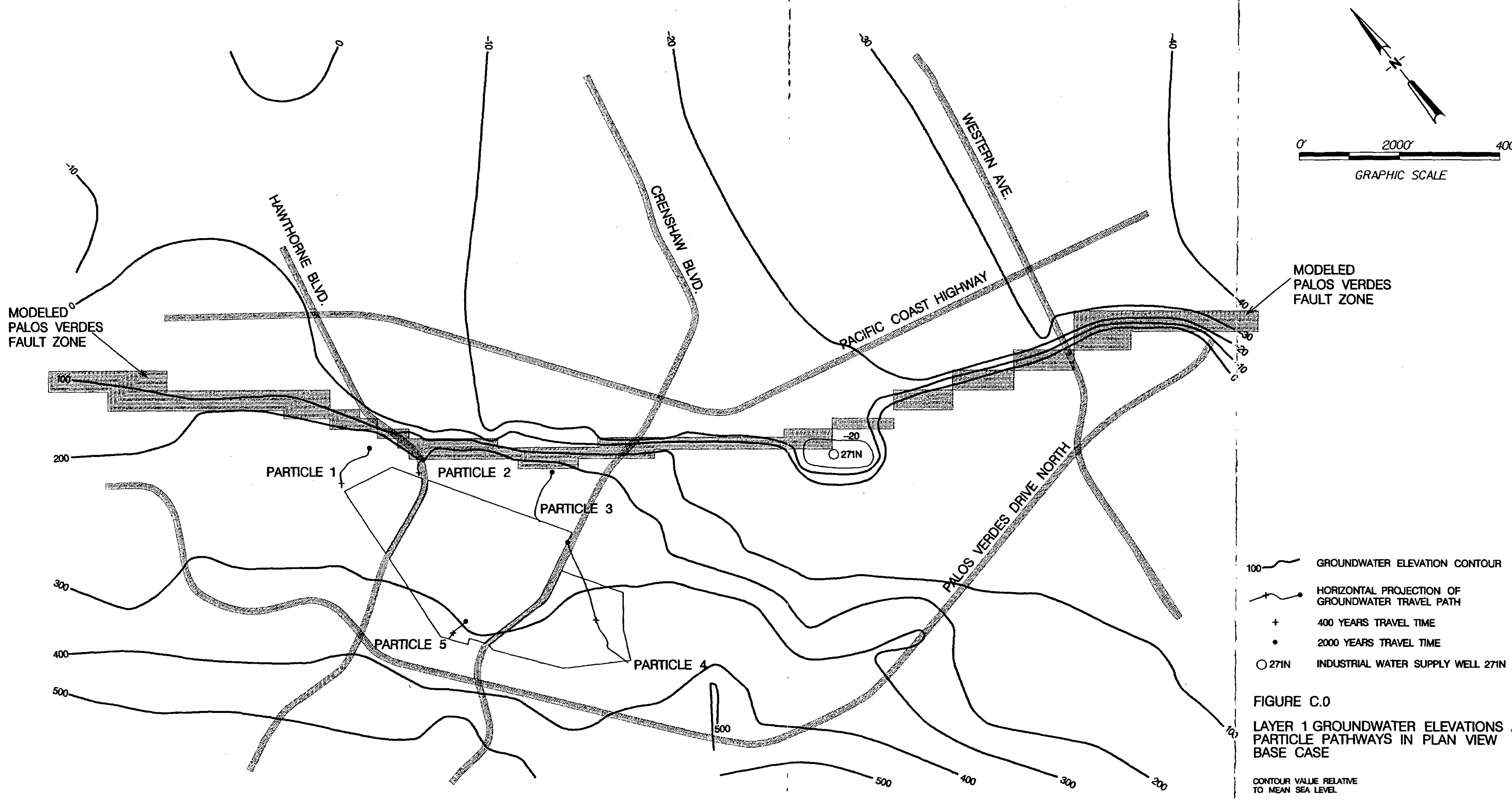

FIGURE C.0

LAYER 1 GROUNDWATER ELEVATIONS AND PARTICLE PATHWAYS IN PLAN VIEW BASE CASE

CONTOUR VALUE RELATIVE TO MEAN SEA LEVEL

PALOS VERDES LANDFILL

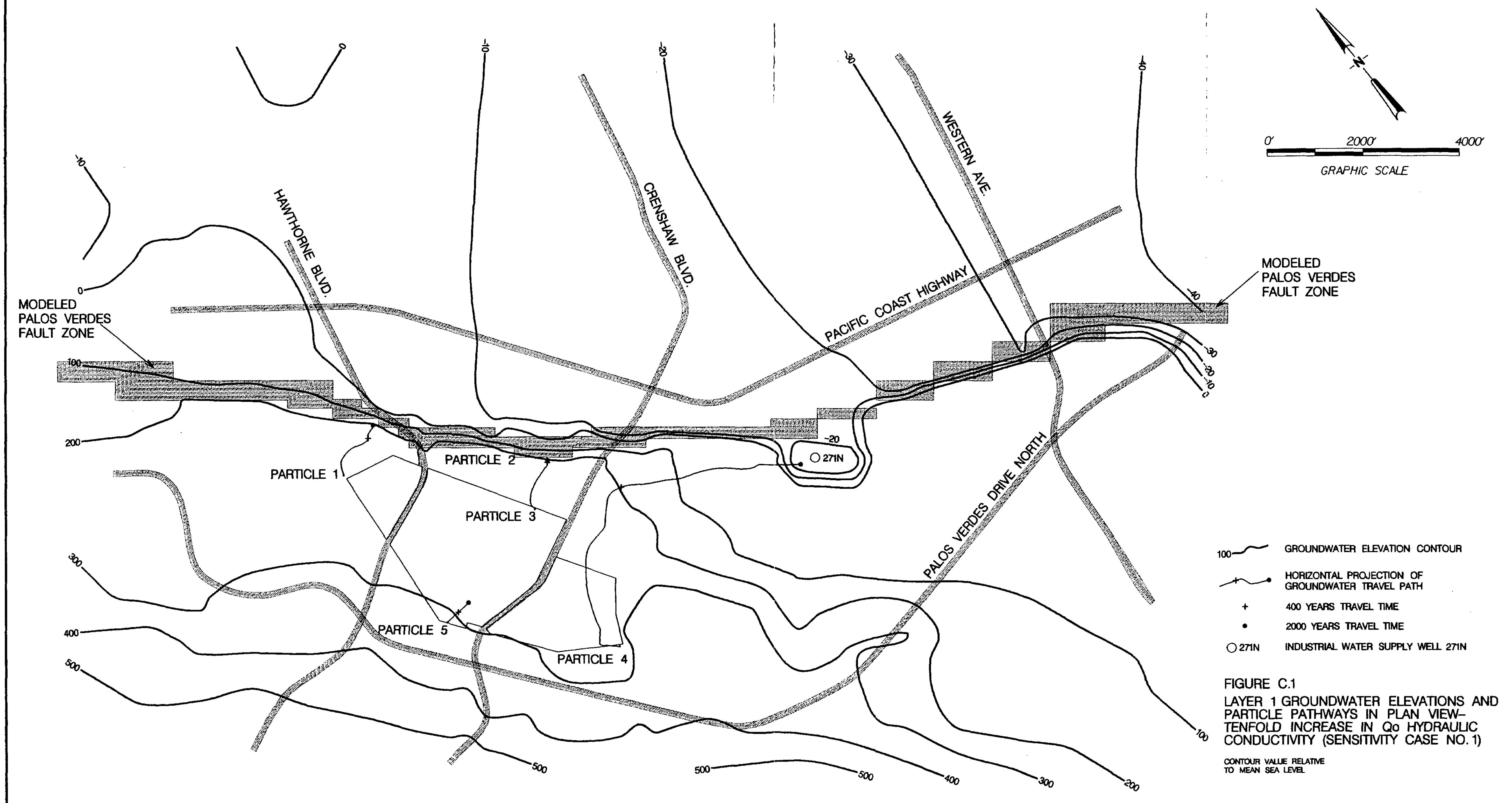

FIGURE C.1
LAYER 1 GROUNDWATER ELEVATIONS AND PARTICLE PATHWAYS IN PLAN VIEW– TENFOLD INCREASE IN Qo HYDRAULIC CONDUCTIVITY (SENSITIVITY CASE NO. 1)

CONTOUR VALUE RELATIVE TO MEAN SEA LEVEL

PALOS VERDES LANDFILL

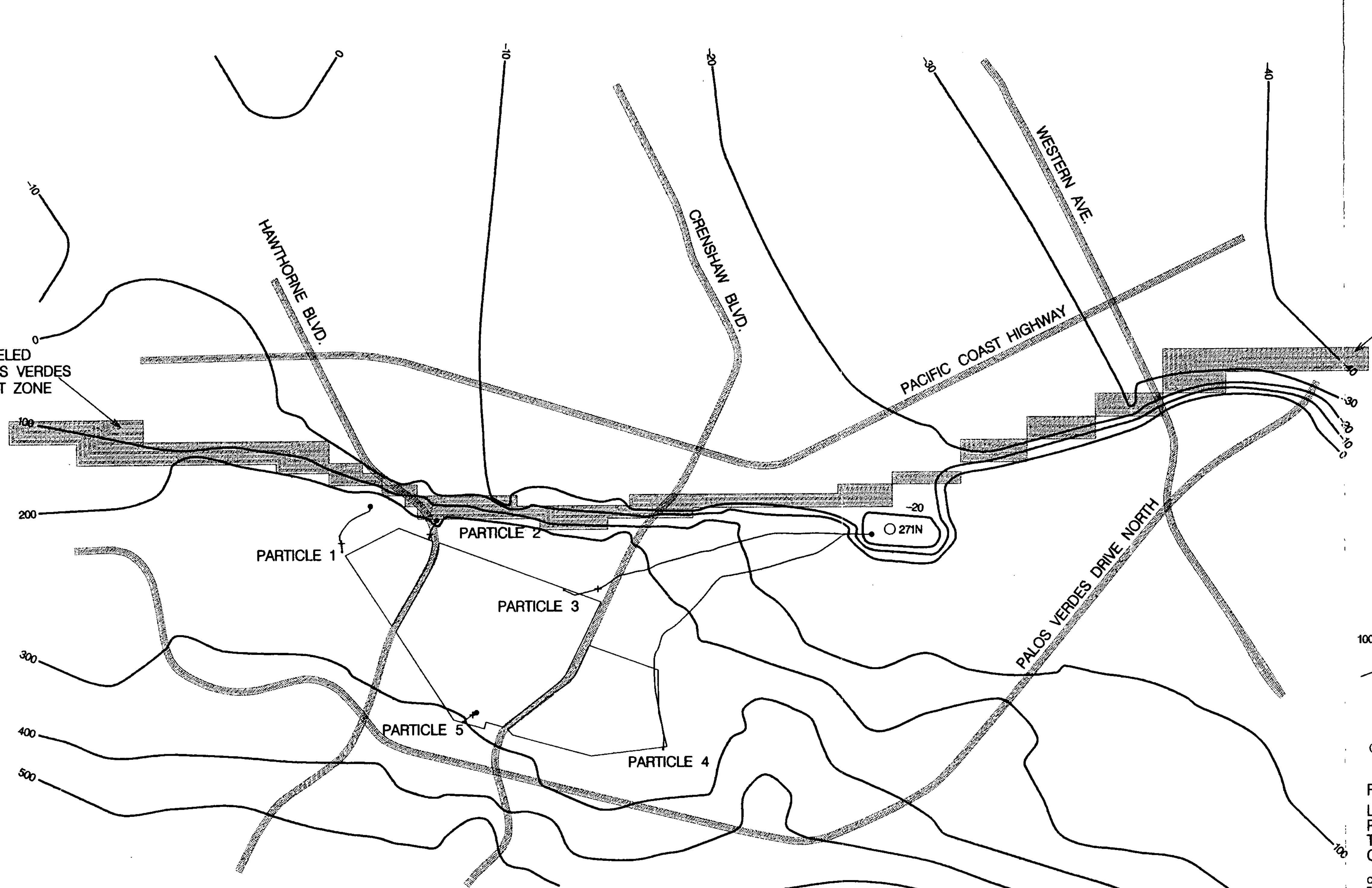

100 GROUNDWATER ELEVATION CONTOUR

HORIZONTAL PROJECTION OF GROUNDWATER TRAVEL PATH

\+ 400 YEARS TRAVEL TIME

• 2000 YEARS TRAVEL TIME

○ 271N INDUSTRIAL WATER SUPPLY WELL 271N

FIGURE C.2

LAYER 1 GROUNDWATER ELEVATIONS AND PARTICLE PATHWAYS IN PLAN VIEW– TENFOLD INCREASE IN ALLUVIUM CONDUCTIVITY (SENSITIVITY CASE NO. 2)

CONTOUR VALUE RELATIVE TO MEAN SEA LEVEL

PALOS VERDES LANDFILL

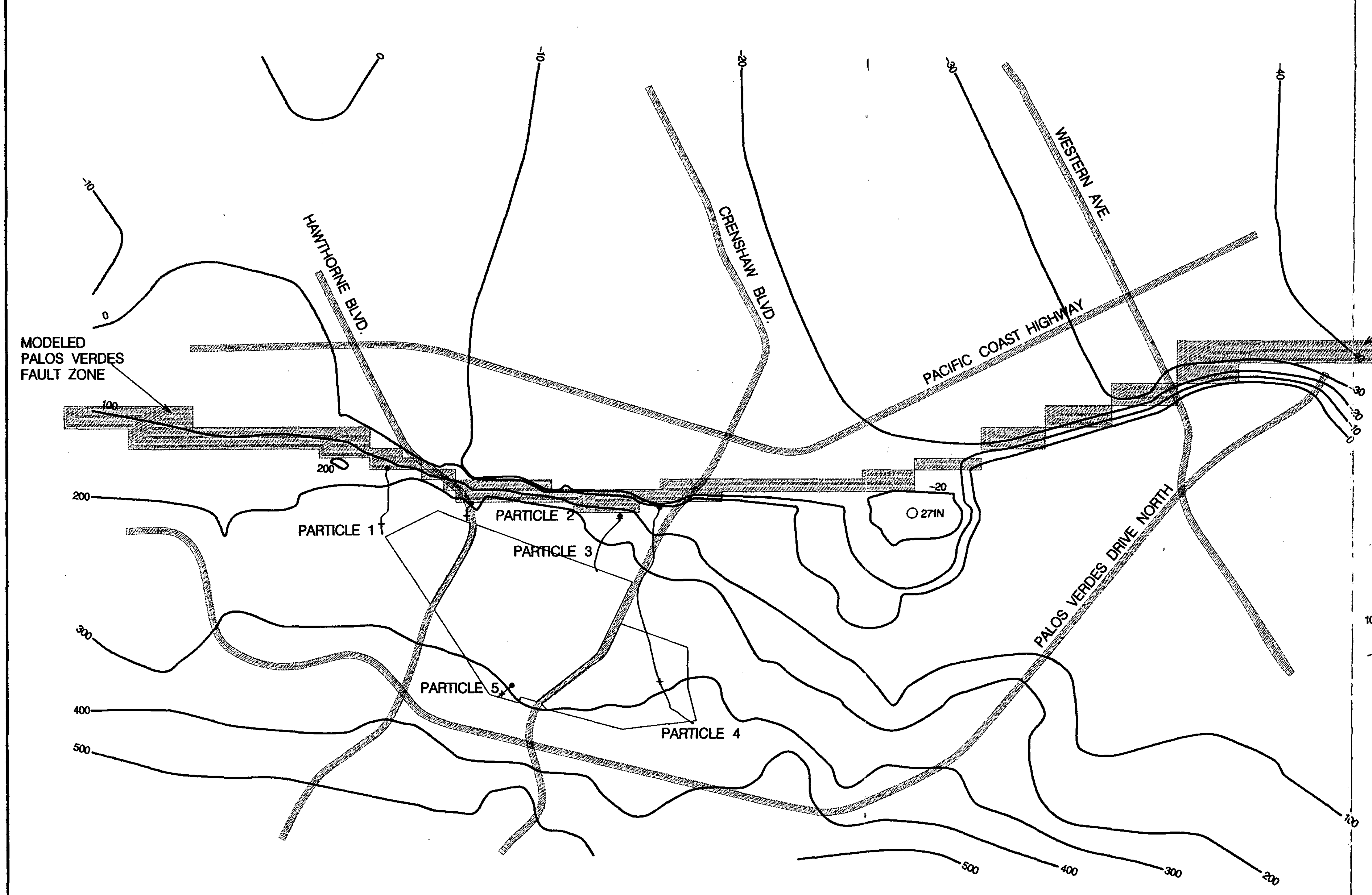

FIGURE C.3

LAYER 1 GROUNDWATER ELEVATIONS AND PARTICLE PATHWAYS IN PLAN VIEW– TENFOLD INCREASE IN Qus HYDRAULIC CONDUCTIVITY (SENSITIVITY CASE NO. 3)

CONTOUR VALUE RELATIVE TO MEAN SEA LEVEL

PALOS VERDES LANDFILL

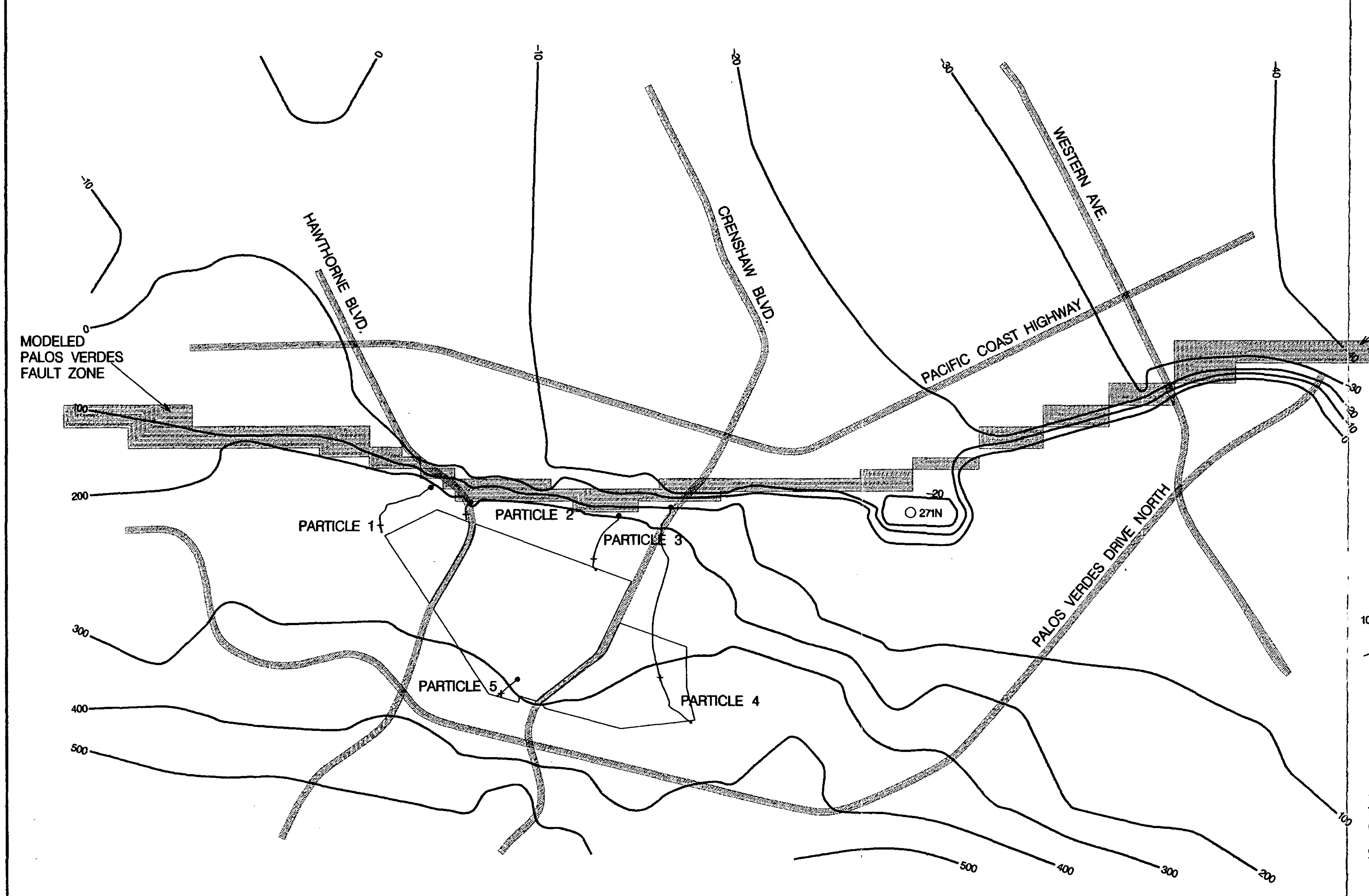

100 GROUNDWATER ELEVATION CONTOUR

HORIZONTAL PROJECTION OF GROUNDWATER TRAVEL PATH

\+ 400 YEARS TRAVEL TIME

• 2000 YEARS TRAVEL TIME

○ 271N INDUSTRIAL WATER SUPPLY WELL 271N

FIGURE C.4

LAYER 1 GROUNDWATER ELEVATIONS AND PARTICLE PATHWAYS IN PLAN VIEW– TENFOLD INCREASE IN Tmm HYDRAULIC CONDUCTIVITY (SENSITIVITY CASE NO. 4)

CONTOUR VALUE RELATIVE TO MEAN SEA LEVEL

PALOS VERDES LANDFILL

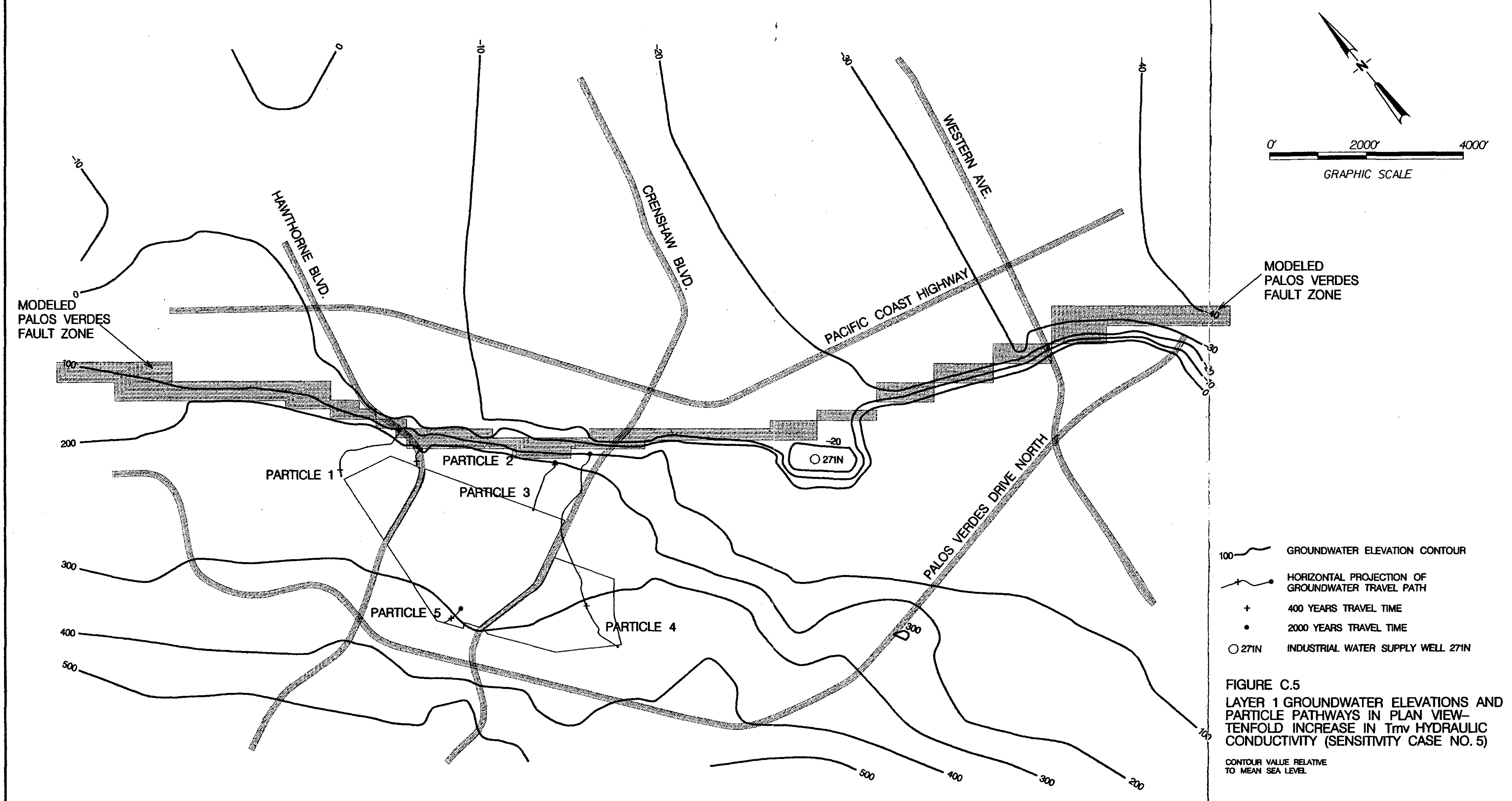

FIGURE C.5

LAYER 1 GROUNDWATER ELEVATIONS AND PARTICLE PATHWAYS IN PLAN VIEW–TENFOLD INCREASE IN Tmv HYDRAULIC CONDUCTIVITY (SENSITIVITY CASE NO. 5)

CONTOUR VALUE RELATIVE TO MEAN SEA LEVEL

PALOS VERDES LANDFILL

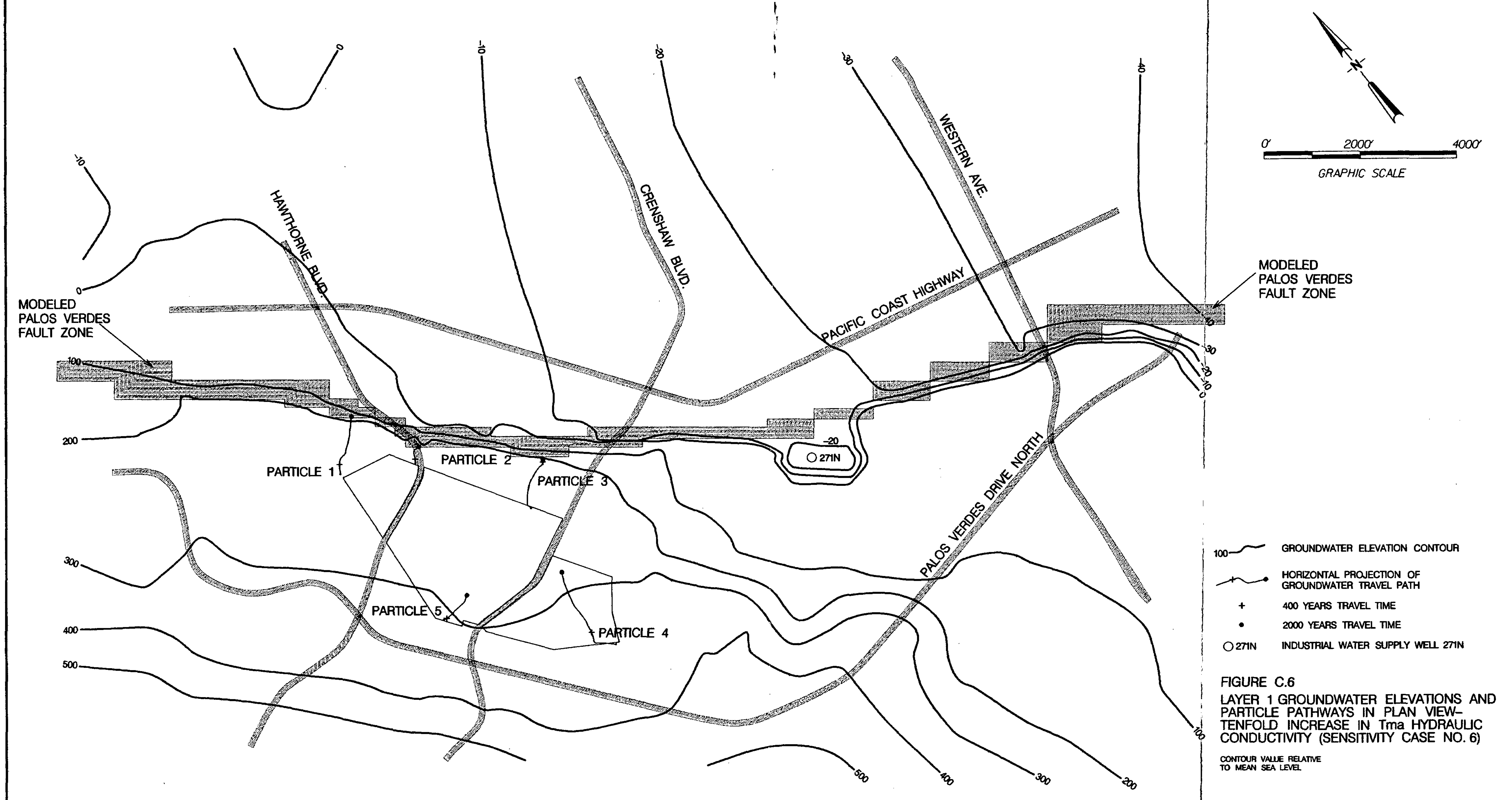

FIGURE C.6

LAYER 1 GROUNDWATER ELEVATIONS AND PARTICLE PATHWAYS IN PLAN VIEW– TENFOLD INCREASE IN Tma HYDRAULIC CONDUCTIVITY (SENSITIVITY CASE NO. 6)

CONTOUR VALUE RELATIVE TO MEAN SEA LEVEL

PALOS VERDES LANDFILL

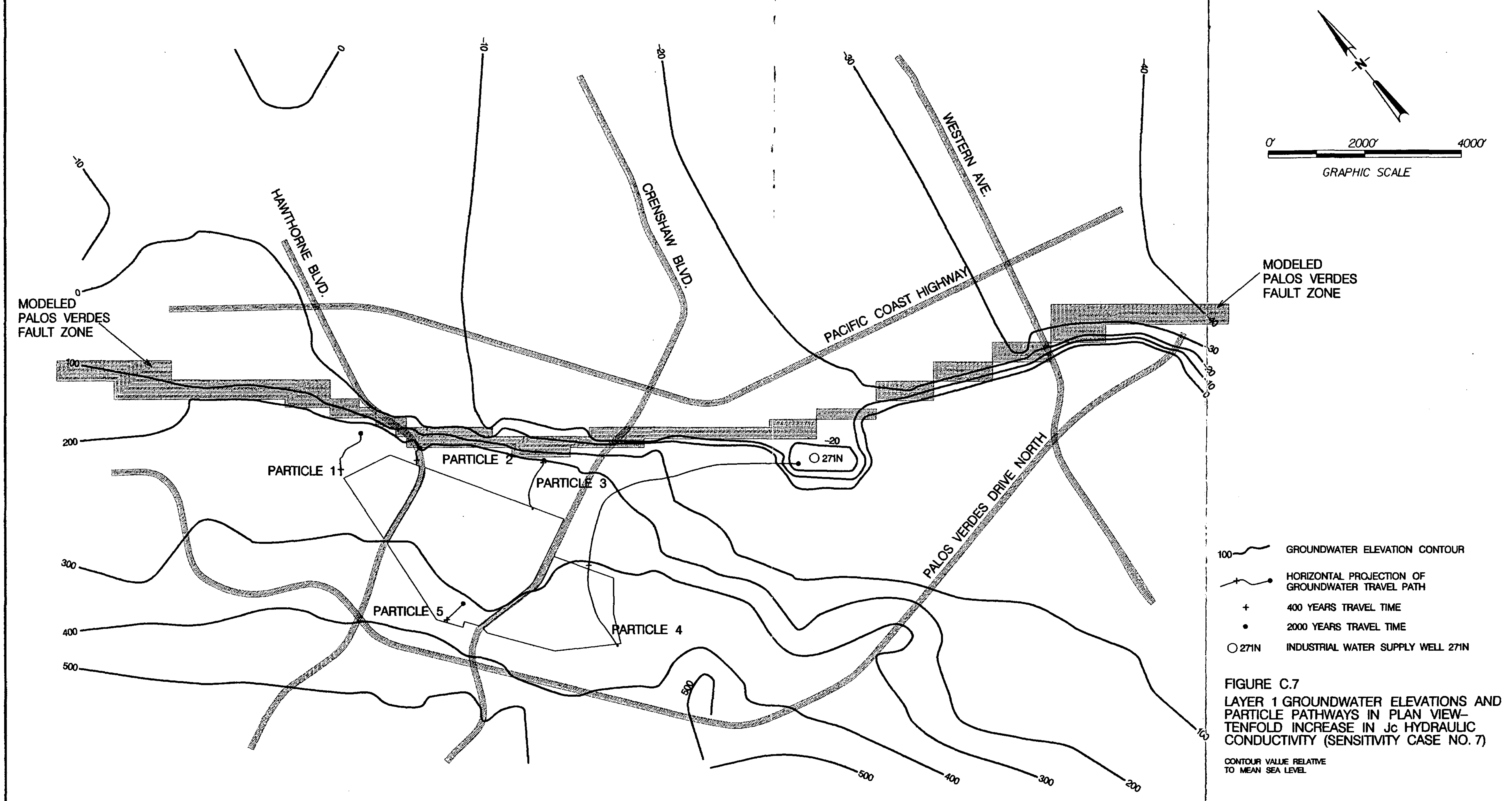

FIGURE C.7
LAYER 1 GROUNDWATER ELEVATIONS AND PARTICLE PATHWAYS IN PLAN VIEW–TENFOLD INCREASE IN Jc HYDRAULIC CONDUCTIVITY (SENSITIVITY CASE NO. 7)

CONTOUR VALUE RELATIVE TO MEAN SEA LEVEL

PALOS VERDES LANDFILL

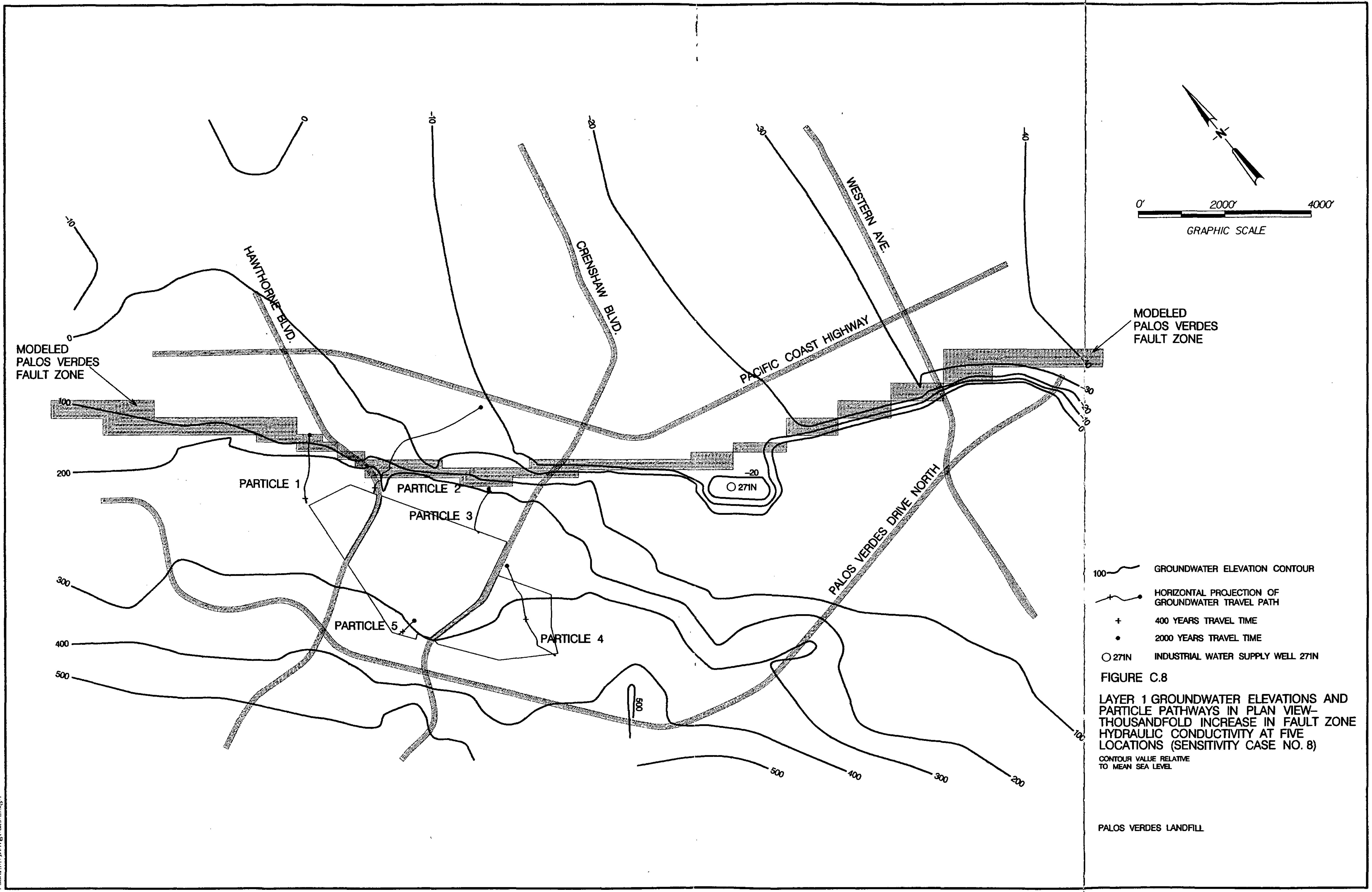

FIGURE C.8

LAYER 1 GROUNDWATER ELEVATIONS AND PARTICLE PATHWAYS IN PLAN VIEW–THOUSANDFOLD INCREASE IN FAULT ZONE HYDRAULIC CONDUCTIVITY AT FIVE LOCATIONS (SENSITIVITY CASE NO. 8)

CONTOUR VALUE RELATIVE TO MEAN SEA LEVEL

PALOS VERDES LANDFILL

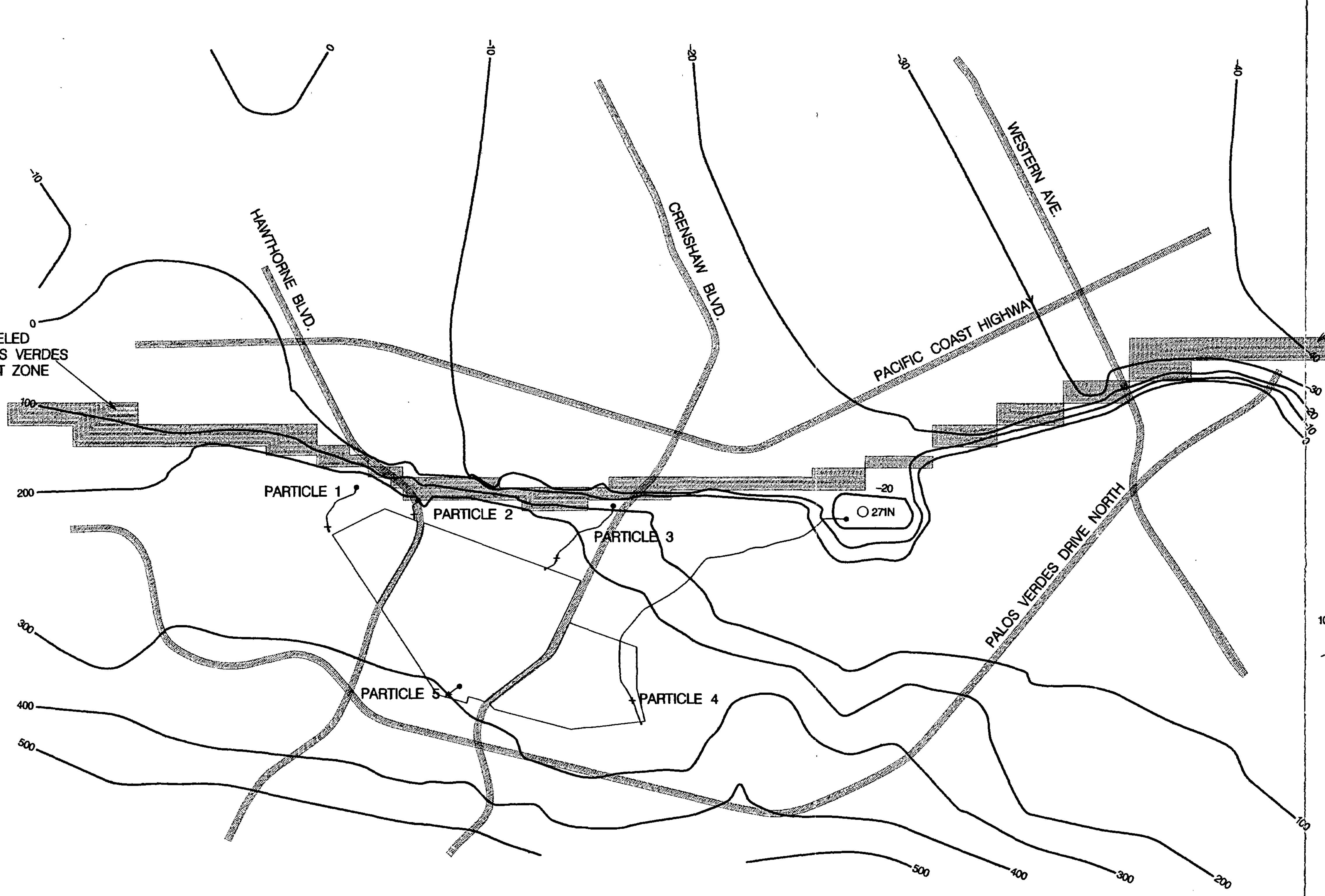

100	GROUNDWATER ELEVATION CONTOUR
	HORIZONTAL PROJECTION OF GROUNDWATER TRAVEL PATH
+	400 YEARS TRAVEL TIME
•	2000 YEARS TRAVEL TIME
○ 271N	INDUSTRIAL WATER SUPPLY WELL 271N

FIGURE C.9

LAYER 1 GROUNDWATER ELEVATIONS AND PARTICLE PATHWAYS IN PLAN VIEW– 75% DECREASE IN GLOBAL RECHARGE RATE (SENSITIVITY CASE NO. 9)

CONTOUR VALUE RELATIVE TO MEAN SEA LEVEL

PALOS VERDES LANDFILL

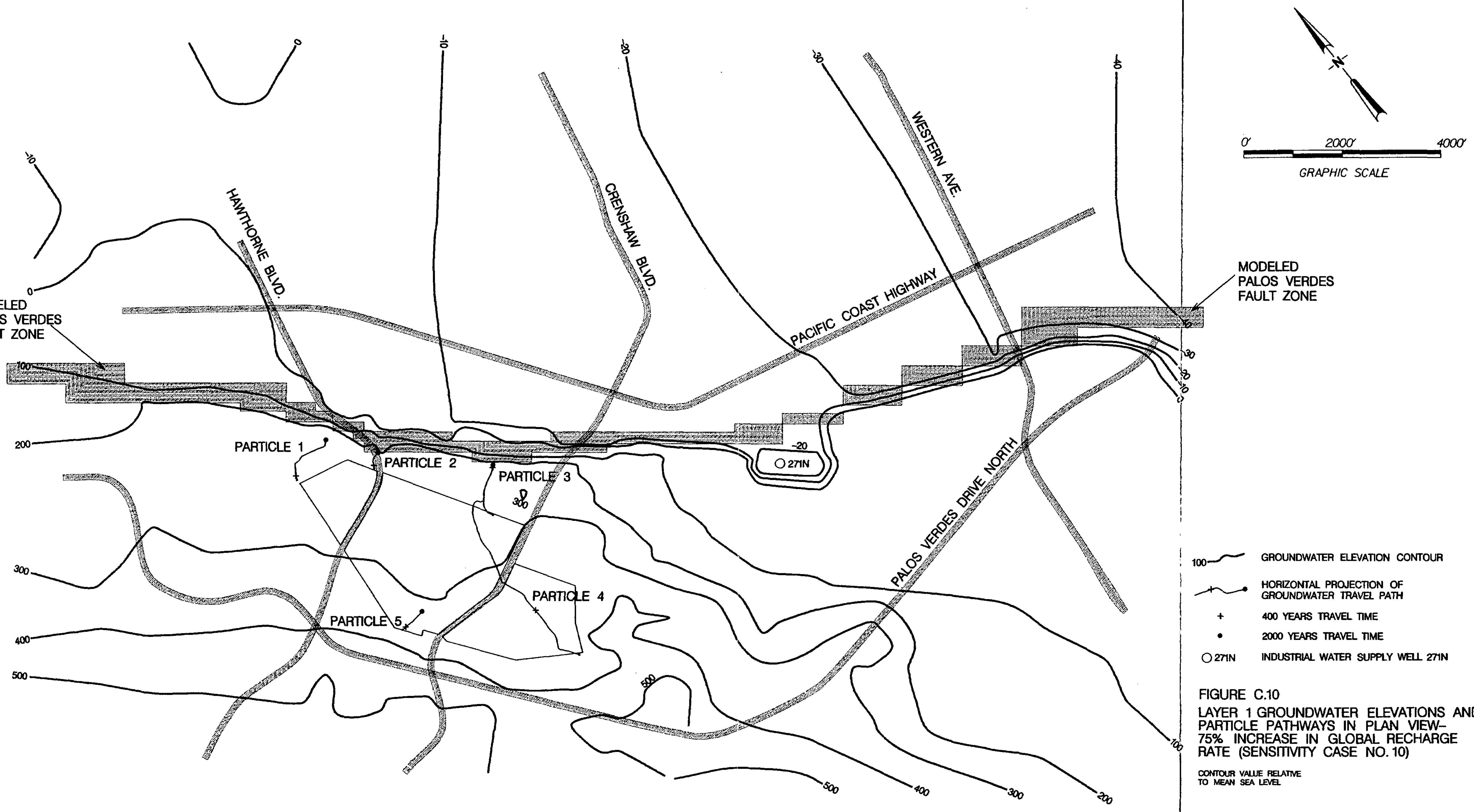

100 GROUNDWATER ELEVATION CONTOUR

HORIZONTAL PROJECTION OF GROUNDWATER TRAVEL PATH

\+ 400 YEARS TRAVEL TIME

• 2000 YEARS TRAVEL TIME

○ 271N INDUSTRIAL WATER SUPPLY WELL 271N

FIGURE C.10

LAYER 1 GROUNDWATER ELEVATIONS AND PARTICLE PATHWAYS IN PLAN VIEW– 75% INCREASE IN GLOBAL RECHARGE RATE (SENSITIVITY CASE NO. 10)

CONTOUR VALUE RELATIVE TO MEAN SEA LEVEL

PALOS VERDES LANDFILL

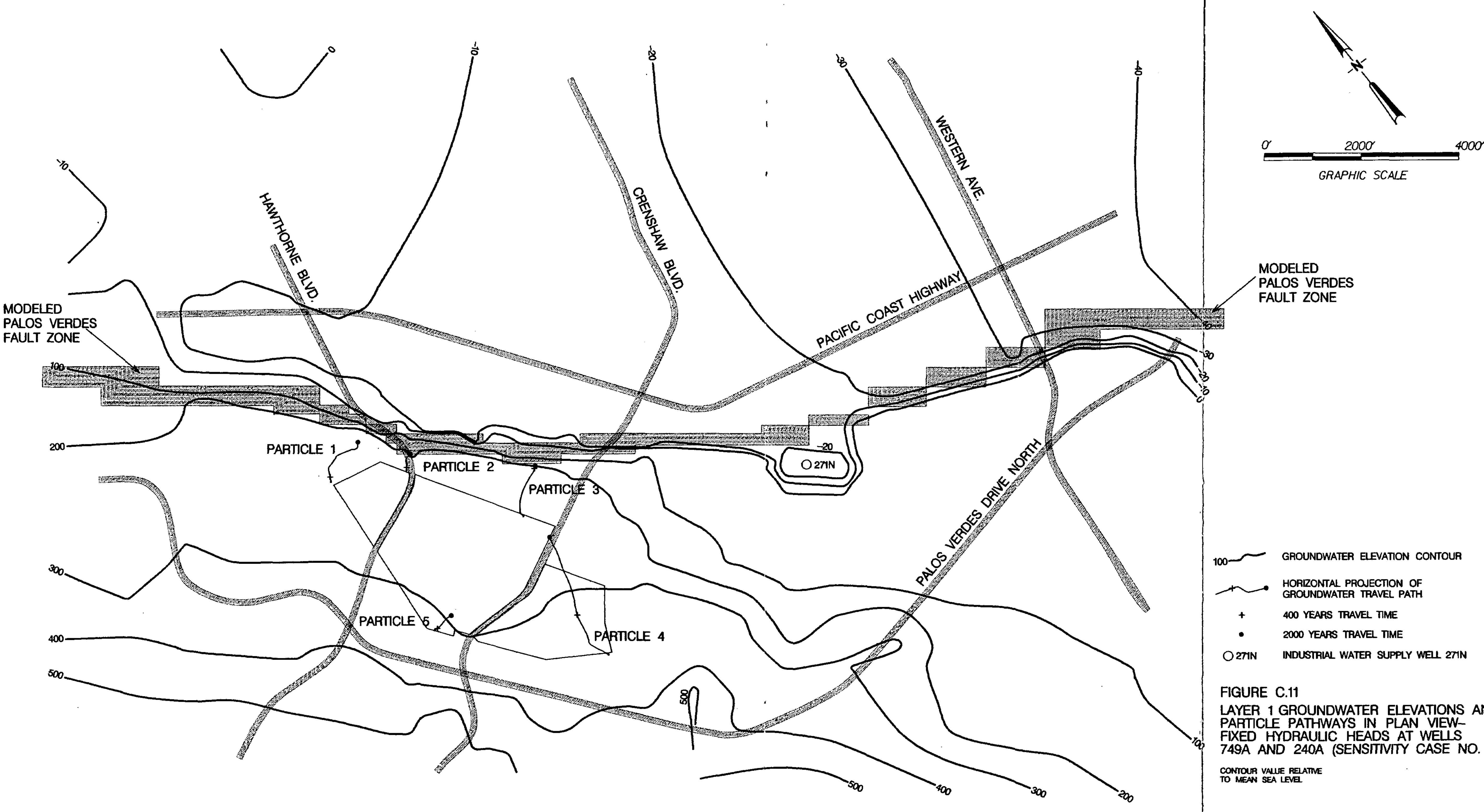

FIGURE C.11

LAYER 1 GROUNDWATER ELEVATIONS AND PARTICLE PATHWAYS IN PLAN VIEW–FIXED HYDRAULIC HEADS AT WELLS 749A AND 240A (SENSITIVITY CASE NO. 11)

CONTOUR VALUE RELATIVE TO MEAN SEA LEVEL

PALOS VERDES LANDFILL

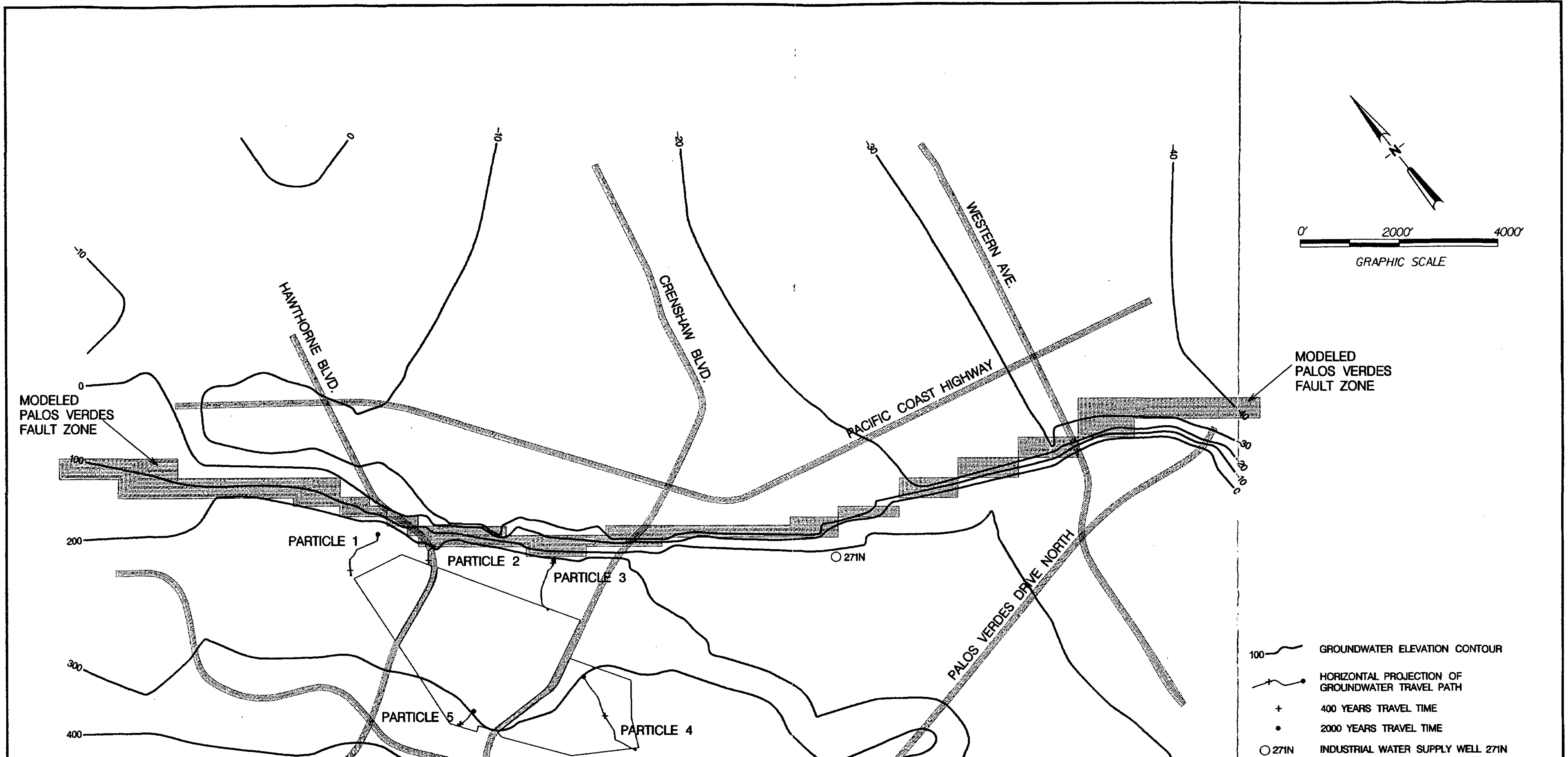

FIGURE C.12

LAYER 1 GROUNDWATER ELEVATIONS AND PARTICLE PATHWAYS IN PLAN VIEW–FIXED HYDRAULIC HEADS AT WELLS 749A AND 240A AND NO PUMPING AT WELL 271N (SENSITIVITY CASE NO. 12)

CONTOUR VALUE RELATIVE TO MEAN SEA LEVEL

PALOS VERDES LANDFILL

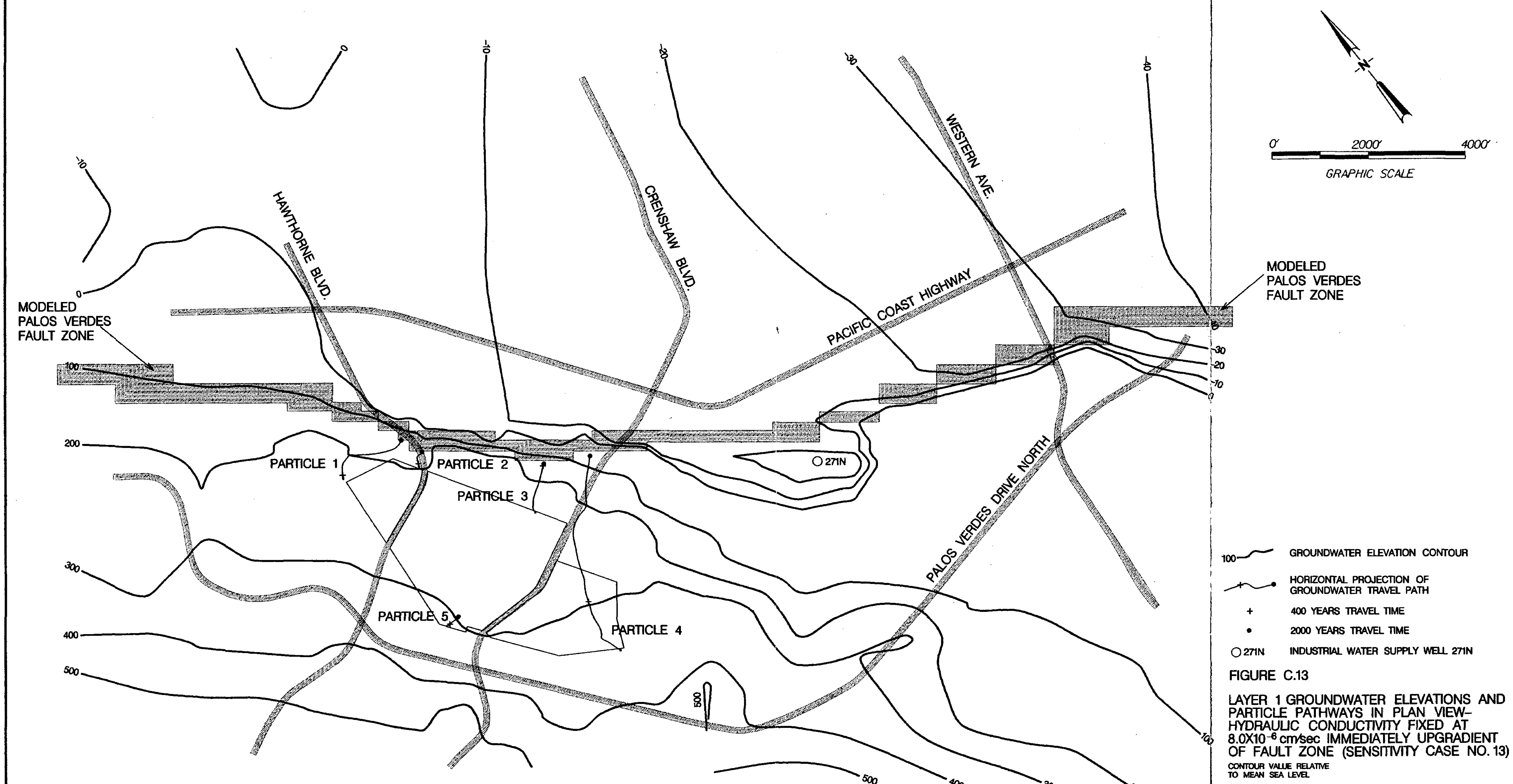

FIGURE C.13

LAYER 1 GROUNDWATER ELEVATIONS AND PARTICLE PATHWAYS IN PLAN VIEW– HYDRAULIC CONDUCTIVITY FIXED AT 8.0×10^{-6} cm/sec IMMEDIATELY UPGRADIENT OF FAULT ZONE (SENSITIVITY CASE NO. 13)

CONTOUR VALUE RELATIVE TO MEAN SEA LEVEL

PALOS VERDES LANDFILL

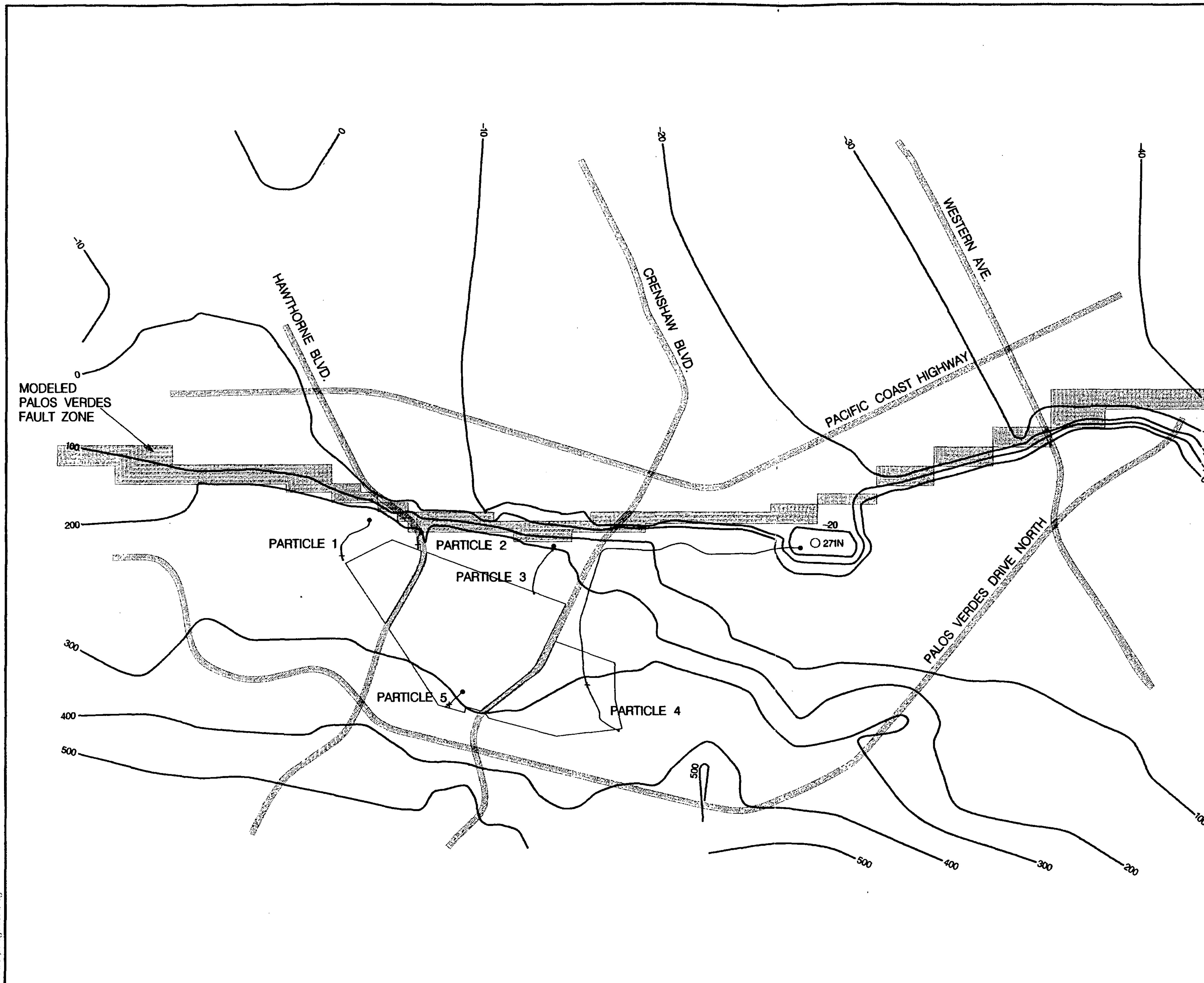

FIGURE C.14
LAYER 1 GROUNDWATER ELEVATIONS AND PARTICLE PATHWAYS IN PLAN VIEW– NO RECHARGE NEAR WELL M59B (SENSITIVITY CASE NO. 14)

CONTOUR VALUE RELATIVE TO MEAN SEA LEVEL

PALOS VERDES LANDFILL

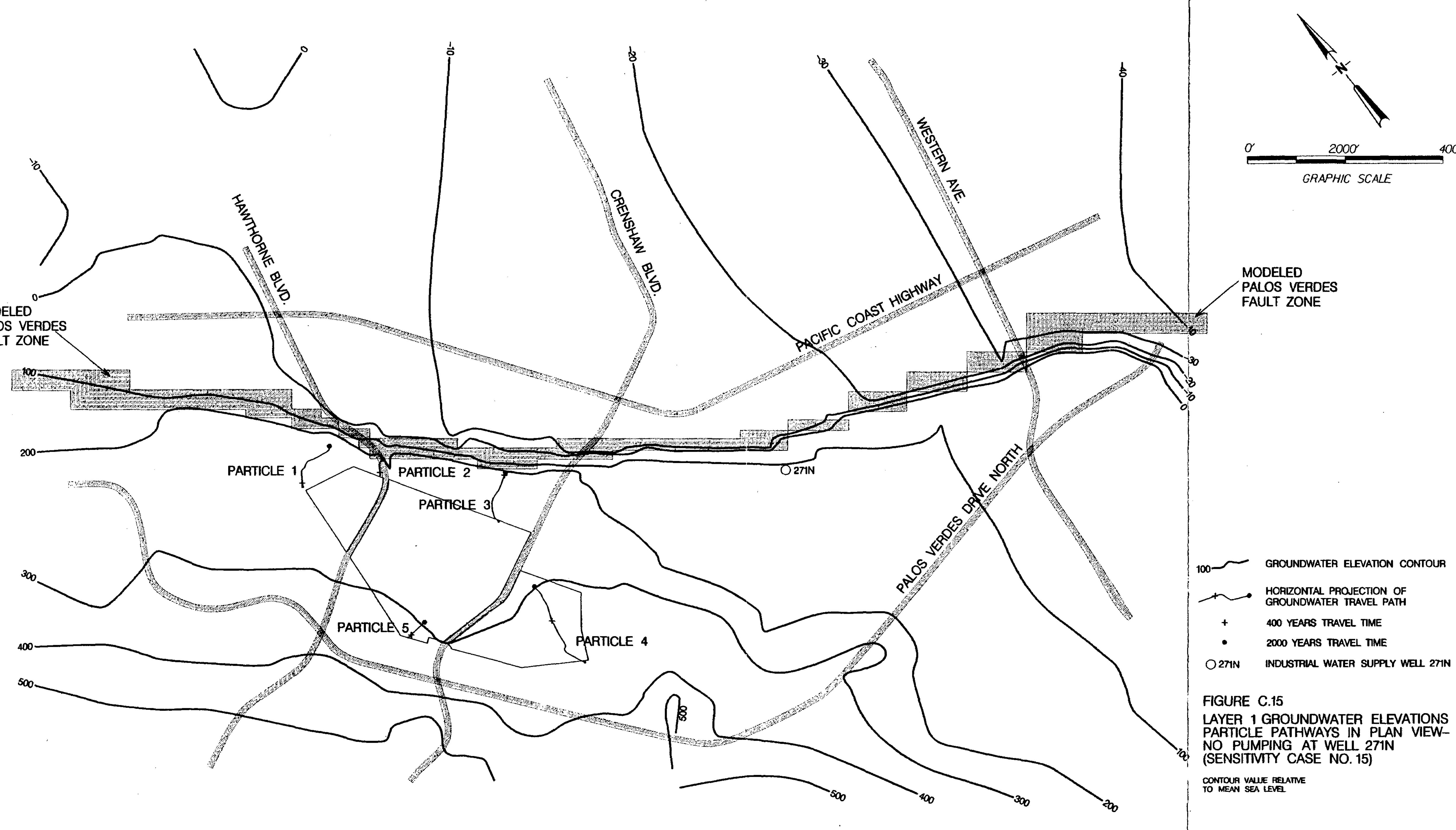

FIGURE C.15

LAYER 1 GROUNDWATER ELEVATIONS AND PARTICLE PATHWAYS IN PLAN VIEW– NO PUMPING AT WELL 271N (SENSITIVITY CASE NO. 15)

CONTOUR VALUE RELATIVE TO MEAN SEA LEVEL

PALOS VERDES LANDFILL

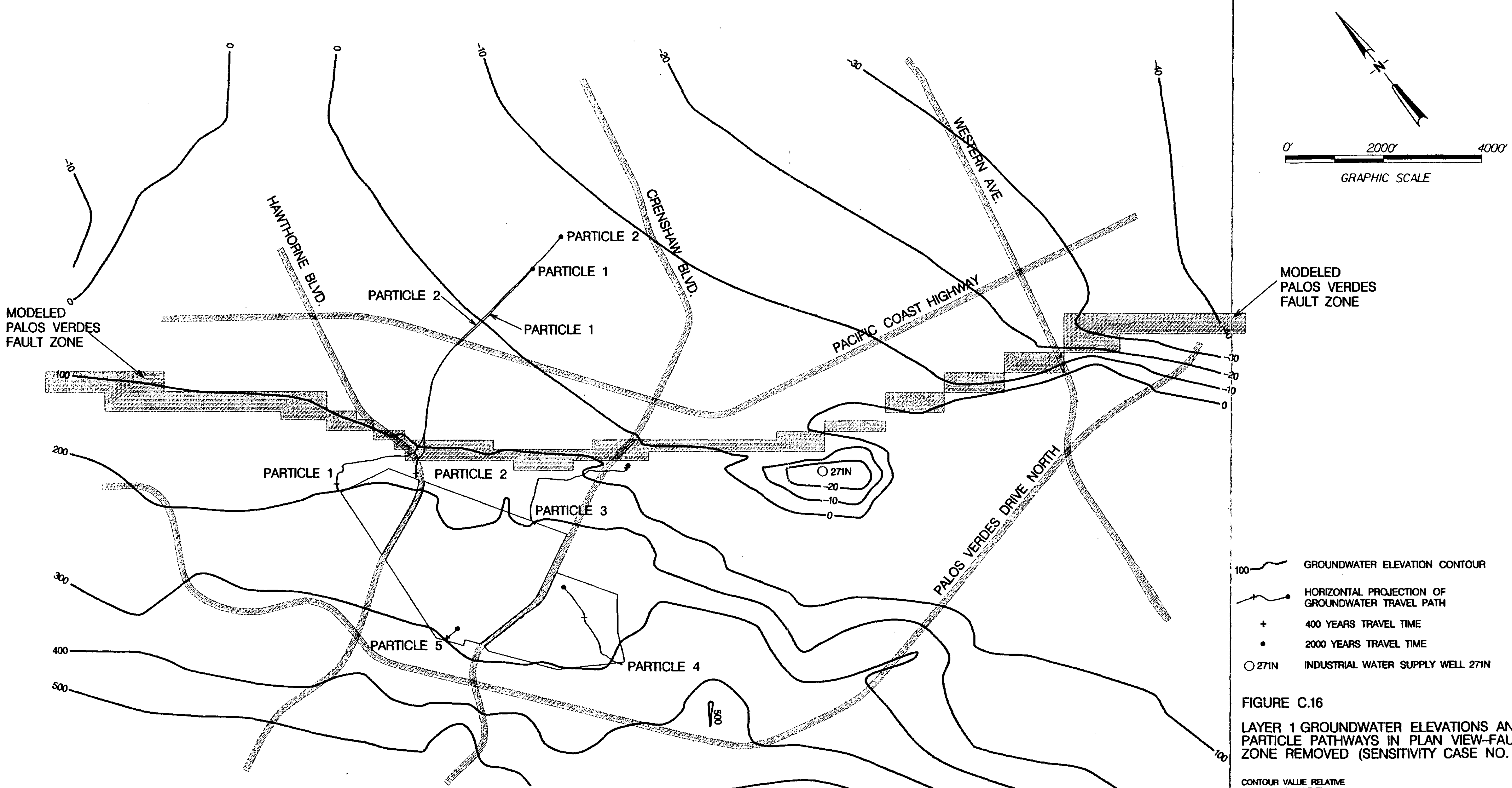

FIGURE C.16

LAYER 1 GROUNDWATER ELEVATIONS AND PARTICLE PATHWAYS IN PLAN VIEW–FAULT ZONE REMOVED (SENSITIVITY CASE NO. 16)

CONTOUR VALUE RELATIVE TO MEAN SEA LEVEL

PALOS VERDES LANDFILL

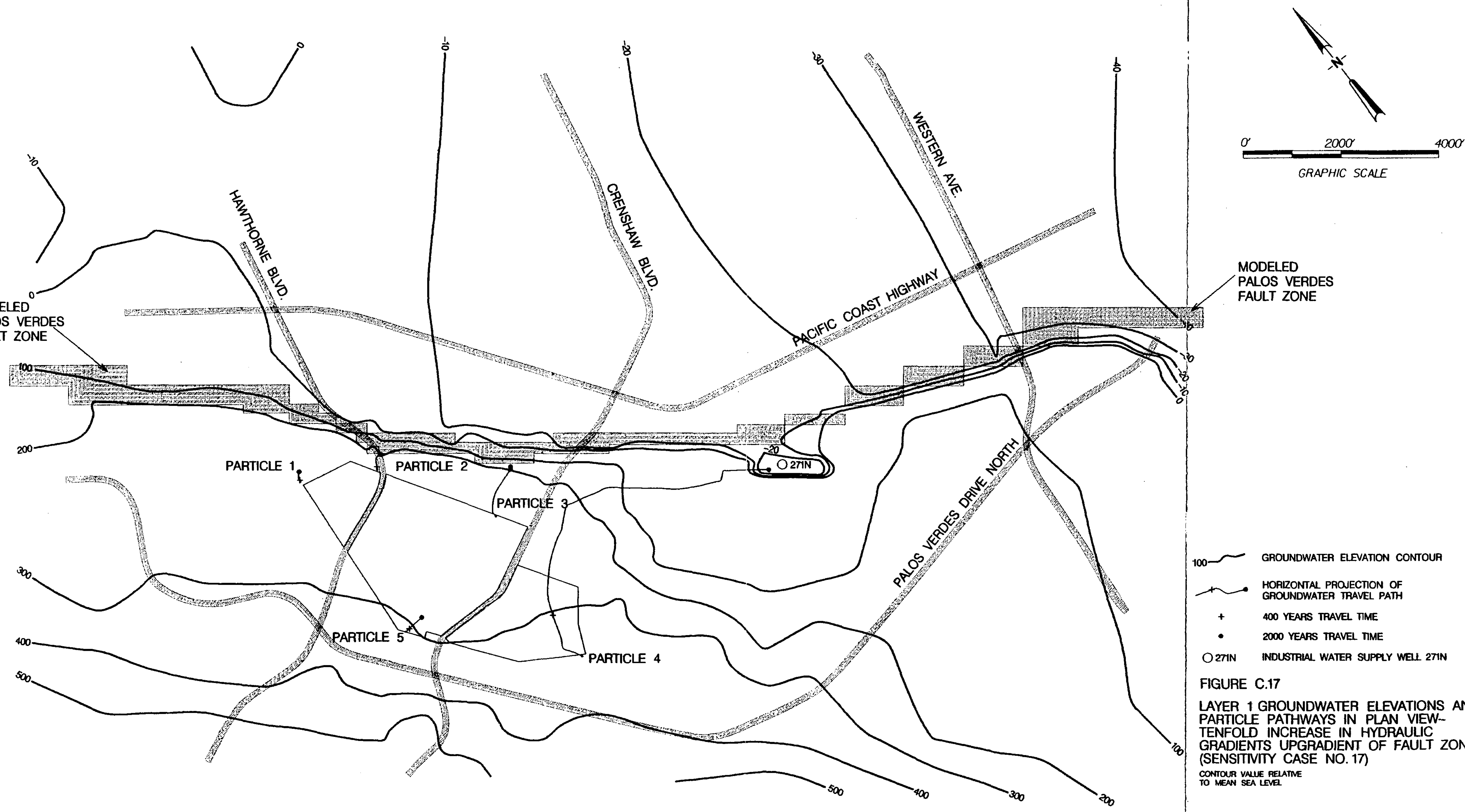

100 GROUNDWATER ELEVATION CONTOUR

HORIZONTAL PROJECTION OF GROUNDWATER TRAVEL PATH

+ 400 YEARS TRAVEL TIME

• 2000 YEARS TRAVEL TIME

○ 271N INDUSTRIAL WATER SUPPLY WELL 271N

FIGURE C.17

LAYER 1 GROUNDWATER ELEVATIONS AND PARTICLE PATHWAYS IN PLAN VIEW– TENFOLD INCREASE IN HYDRAULIC GRADIENTS UPGRADIENT OF FAULT ZONE (SENSITIVITY CASE NO. 17)

CONTOUR VALUE RELATIVE TO MEAN SEA LEVEL

PALOS VERDES LANDFILL

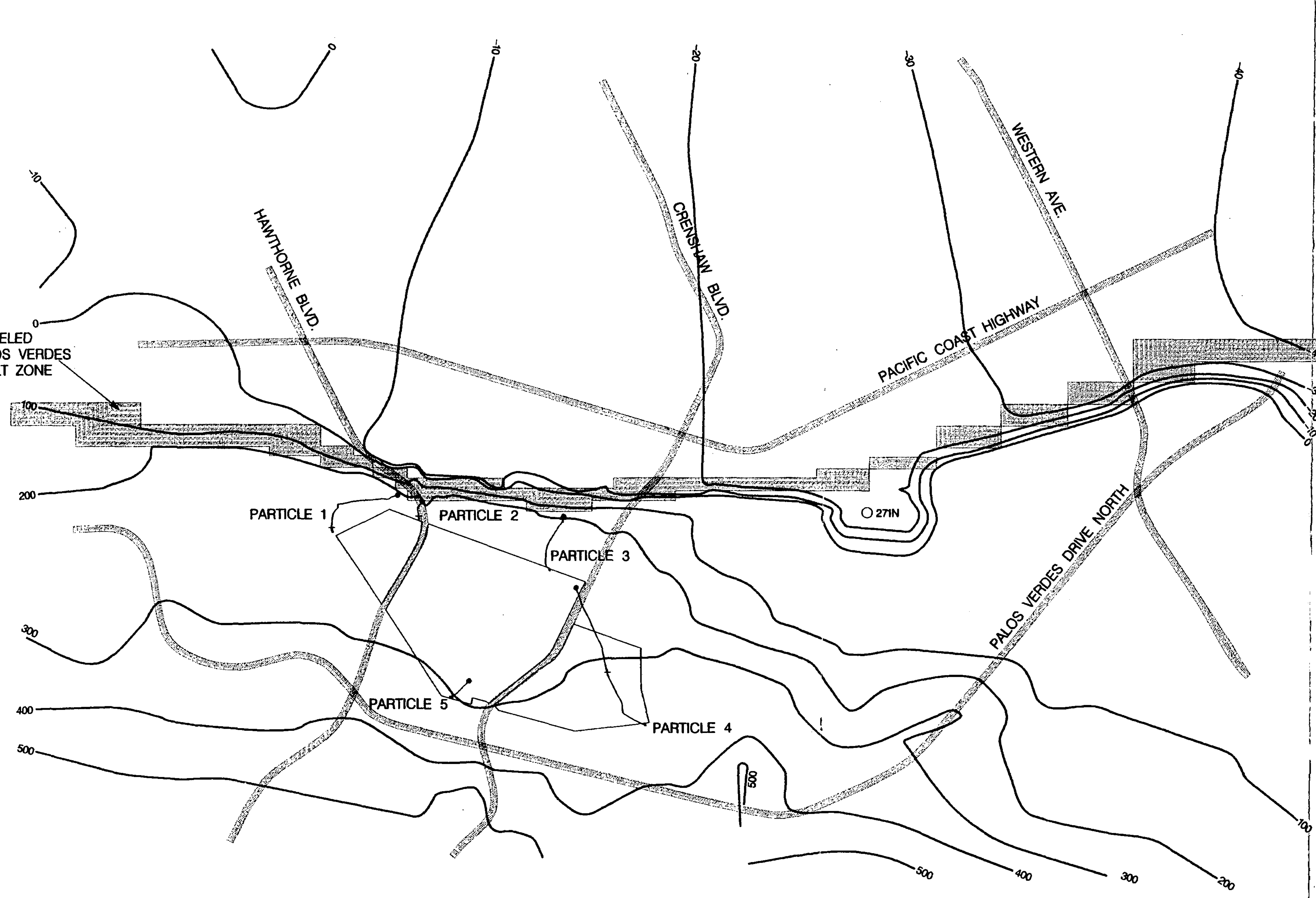

100 GROUNDWATER ELEVATION CONTOUR

HORIZONTAL PROJECTION OF GROUNDWATER TRAVEL PATH

\+ 400 YEARS TRAVEL TIME

• 2000 YEARS TRAVEL TIME

○ 271N INDUSTRIAL WATER SUPPLY WELL 271N

FIGURE C.18

LAYER 1 GROUNDWATER ELEVATIONS AND PARTICLE PATHWAYS IN PLAN VIEW– TENFOLD INCREASE IN HYDRAULIC GRADIENTS DOWNGRADIENT OF FAULT ZONE (SENSITIVITY CASE NO. 18)

CONTOUR VALUE RELATIVE TO MEAN SEA LEVEL

PALOS VERDES LANDFILL

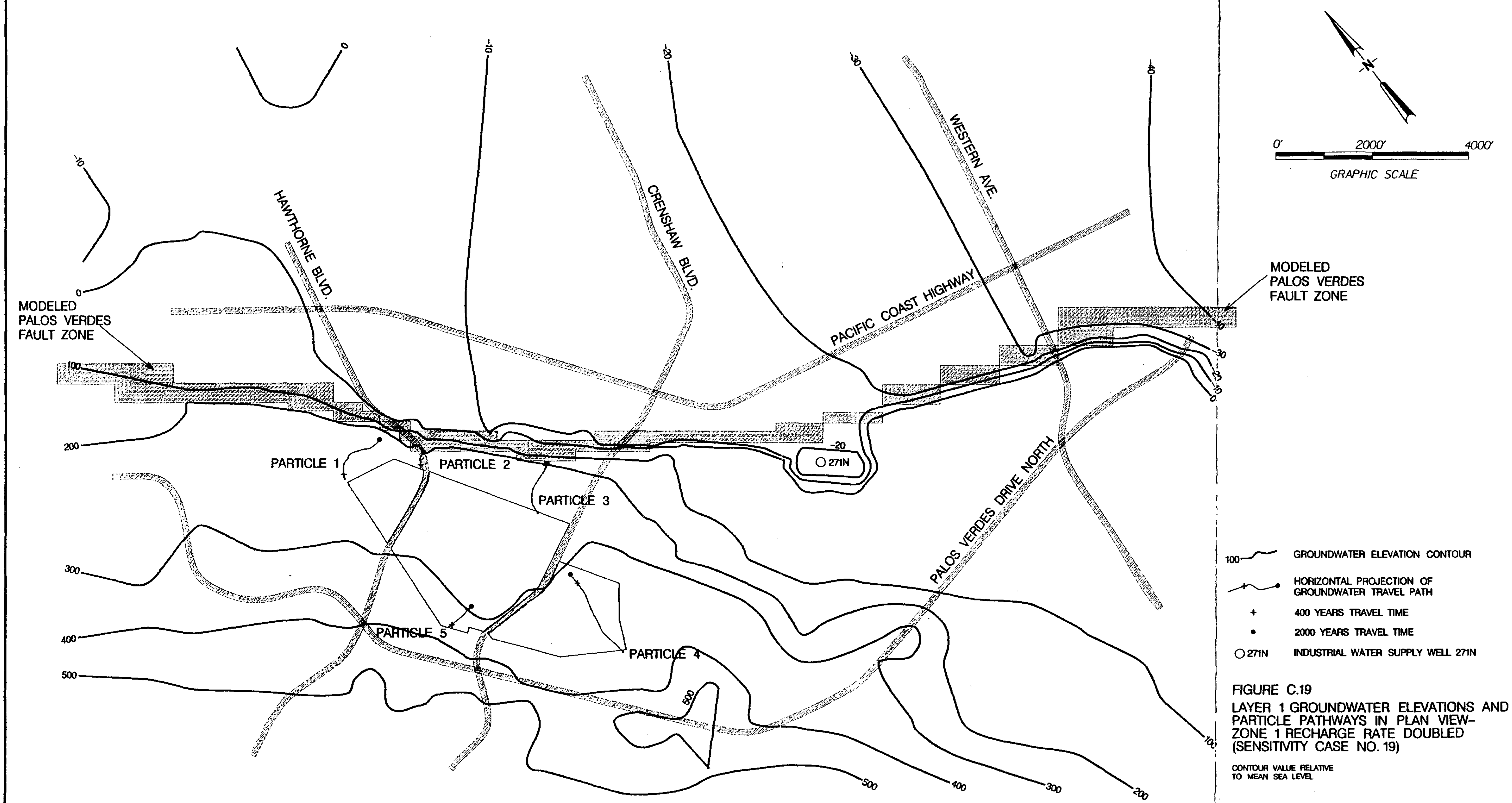

FIGURE C.19
LAYER 1 GROUNDWATER ELEVATIONS AND PARTICLE PATHWAYS IN PLAN VIEW–ZONE 1 RECHARGE RATE DOUBLED (SENSITIVITY CASE NO. 19)

CONTOUR VALUE RELATIVE TO MEAN SEA LEVEL

PALOS VERDES LANDFILL

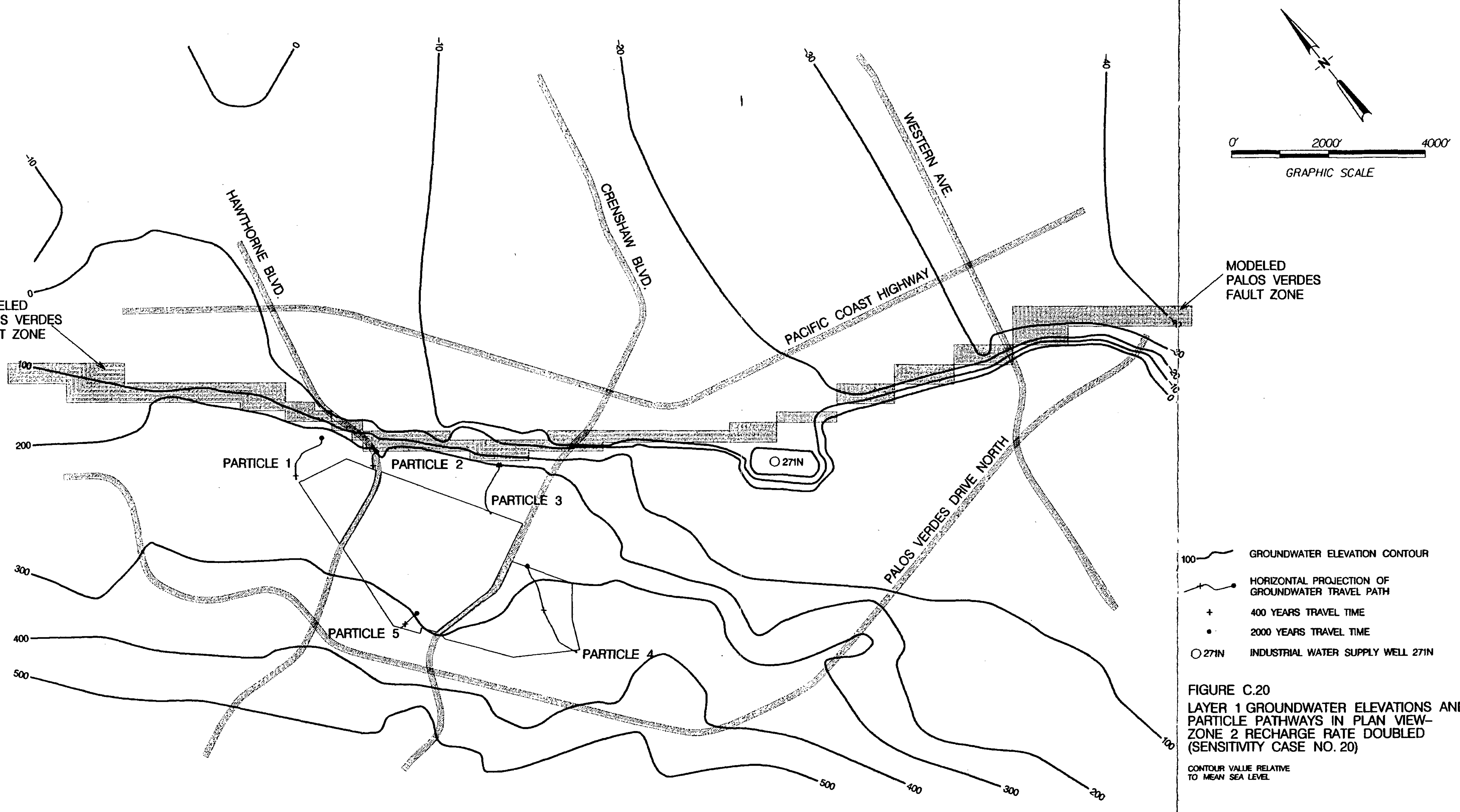

100 GROUNDWATER ELEVATION CONTOUR

HORIZONTAL PROJECTION OF GROUNDWATER TRAVEL PATH

+ 400 YEARS TRAVEL TIME

• 2000 YEARS TRAVEL TIME

○ 271N INDUSTRIAL WATER SUPPLY WELL 271N

FIGURE C.20

LAYER 1 GROUNDWATER ELEVATIONS AND PARTICLE PATHWAYS IN PLAN VIEW– ZONE 2 RECHARGE RATE DOUBLED (SENSITIVITY CASE NO. 20)

CONTOUR VALUE RELATIVE TO MEAN SEA LEVEL

PALOS VERDES LANDFILL

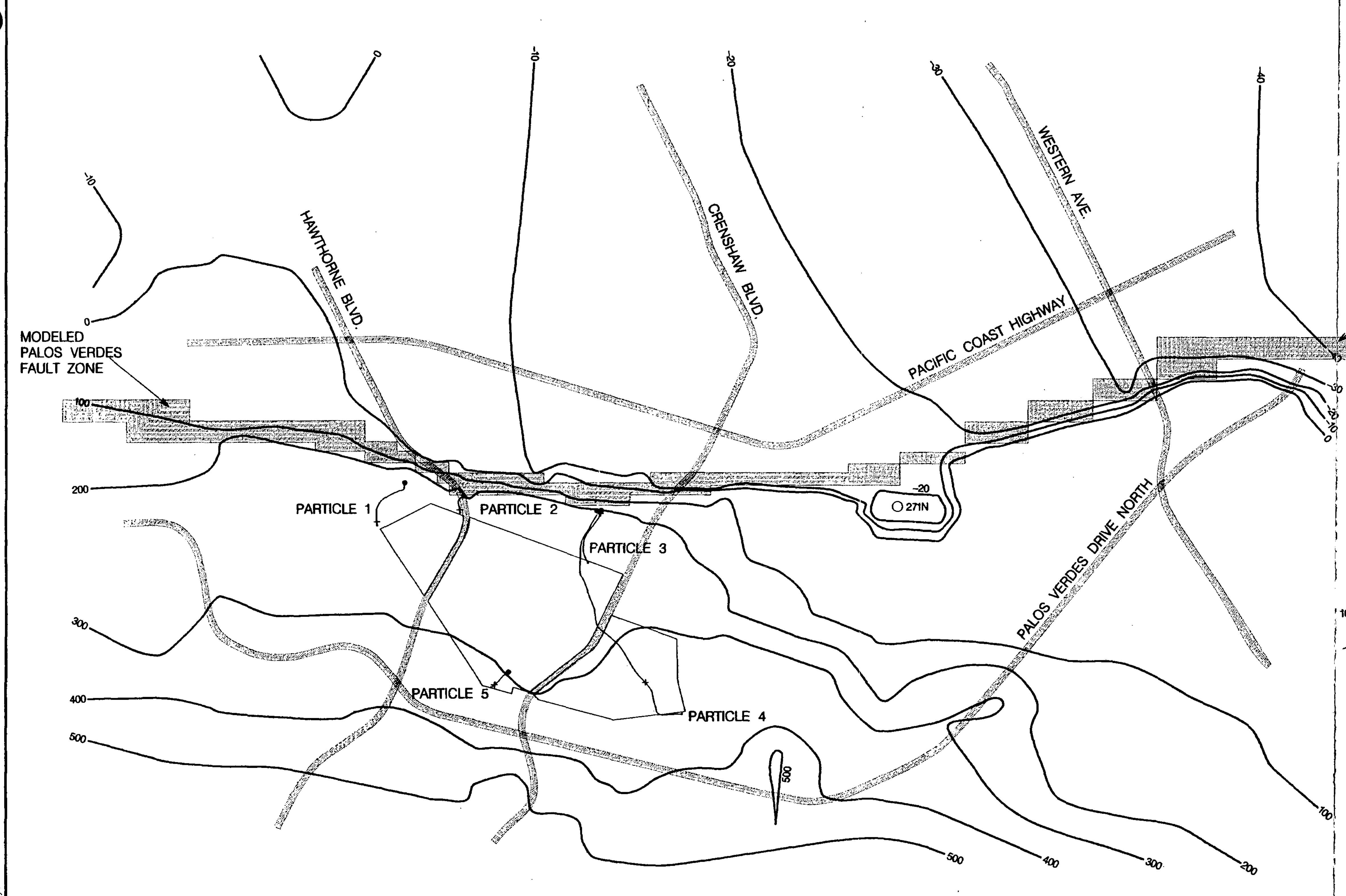

100 GROUNDWATER ELEVATION CONTOUR

HORIZONTAL PROJECTION OF GROUNDWATER TRAVEL PATH

+ 400 YEARS TRAVEL TIME

• 2000 YEARS TRAVEL TIME

○ 271N INDUSTRIAL WATER SUPPLY WELL 271N

FIGURE C.21
LAYER 1 GROUNDWATER ELEVATIONS AND PARTICLE PATHWAYS IN PLAN VIEW–ZONE 3 RECHARGE RATE DOUBLED (SENSITIVITY CASE NO. 21)

CONTOUR VALUE RELATIVE TO MEAN SEA LEVEL

PALOS VERDES LANDFILL

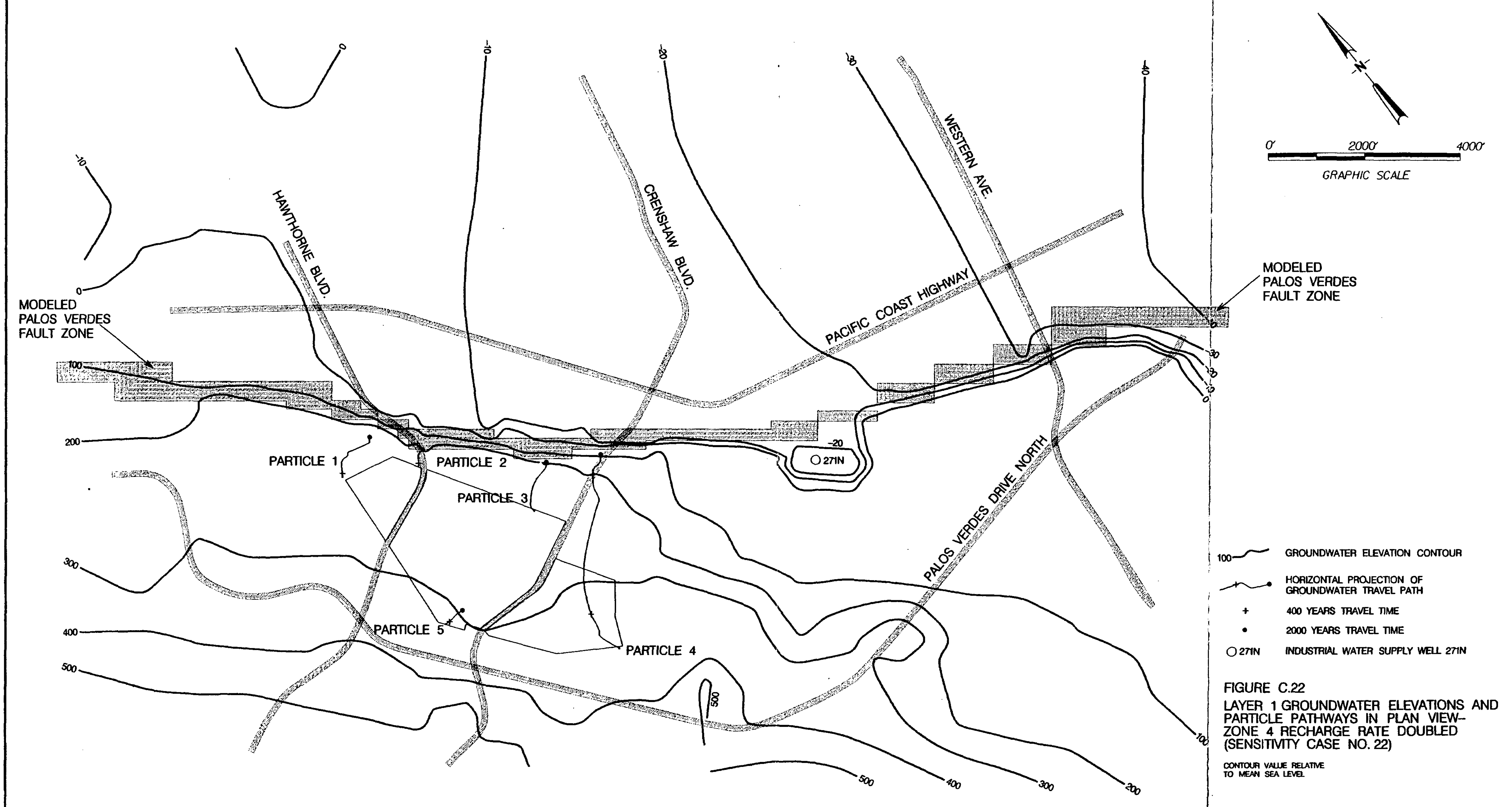

FIGURE C.22

LAYER 1 GROUNDWATER ELEVATIONS AND PARTICLE PATHWAYS IN PLAN VIEW– ZONE 4 RECHARGE RATE DOUBLED (SENSITIVITY CASE NO. 22)

CONTOUR VALUE RELATIVE TO MEAN SEA LEVEL

PALOS VERDES LANDFILL

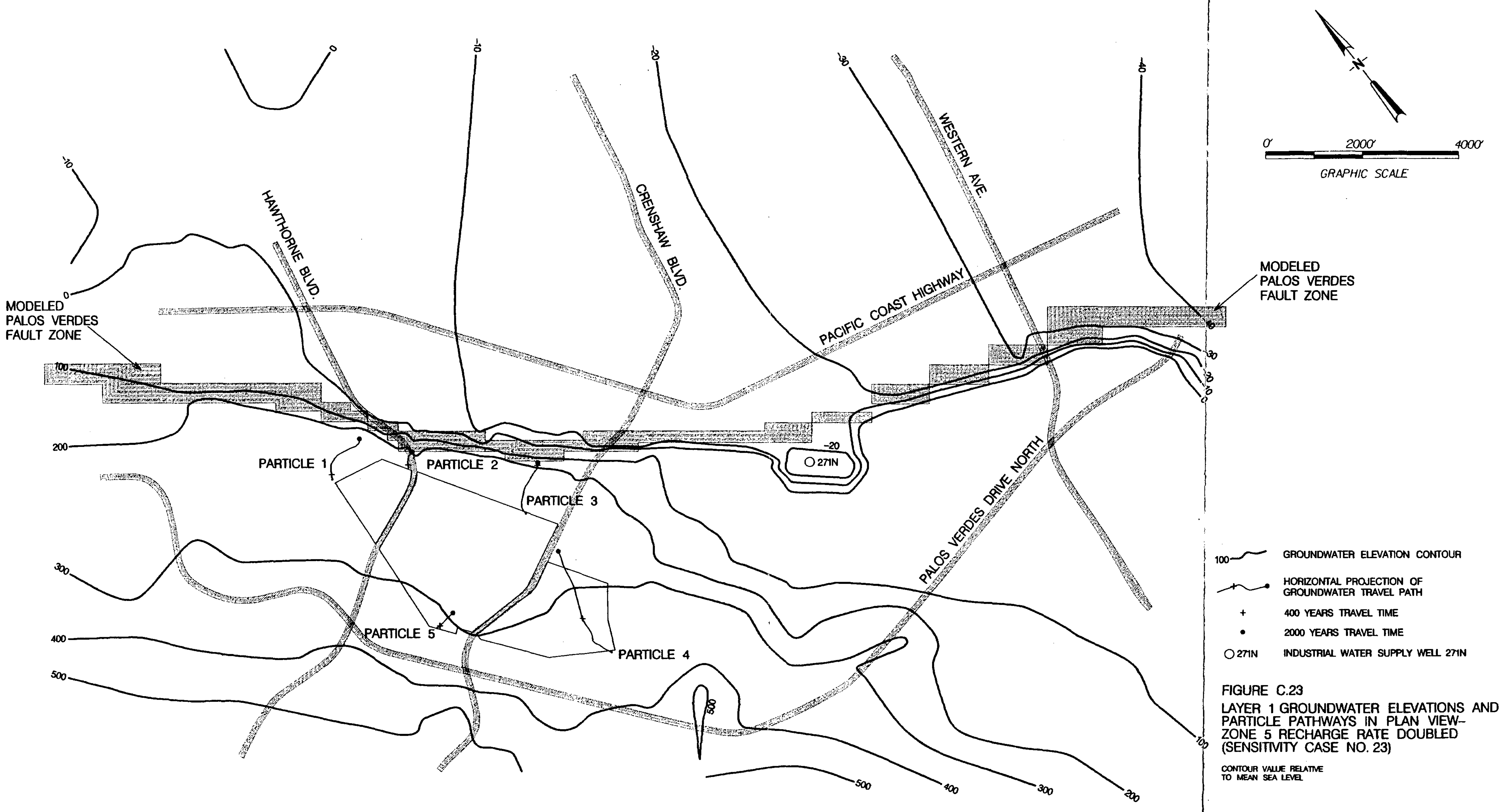

FIGURE C.23
LAYER 1 GROUNDWATER ELEVATIONS AND PARTICLE PATHWAYS IN PLAN VIEW–ZONE 5 RECHARGE RATE DOUBLED (SENSITIVITY CASE NO. 23)

CONTOUR VALUE RELATIVE TO MEAN SEA LEVEL

PALOS VERDES LANDFILL

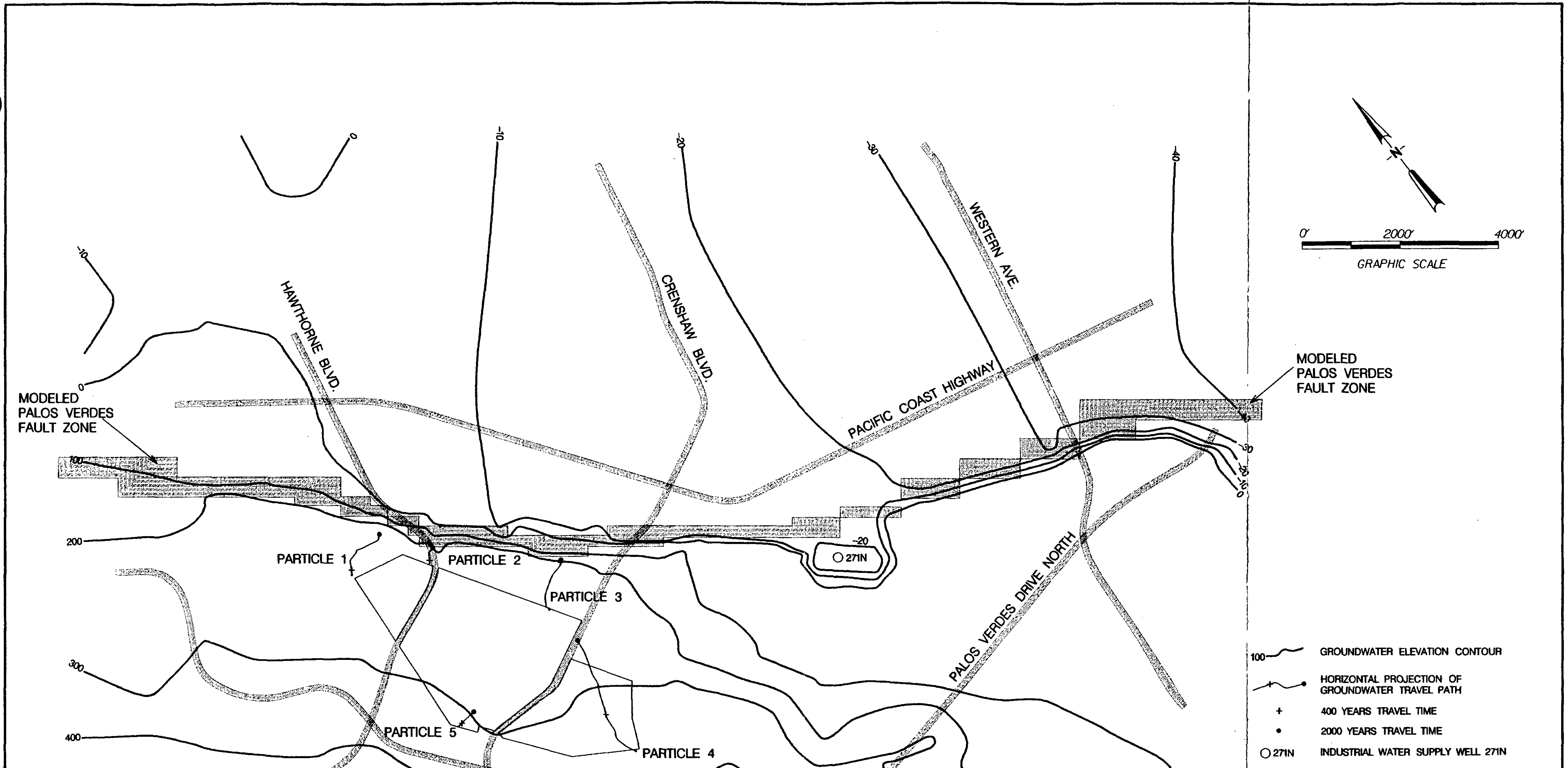

FIGURE C.24

LAYER 1 GROUNDWATER ELEVATIONS AND PARTICLE PATHWAYS IN PLAN VIEW–ZONE 6 RECHARGE RATE DOUBLED (SENSITIVITY CASE NO. 24)

CONTOUR VALUE RELATIVE TO MEAN SEA LEVEL

PALOS VERDES LANDFILL

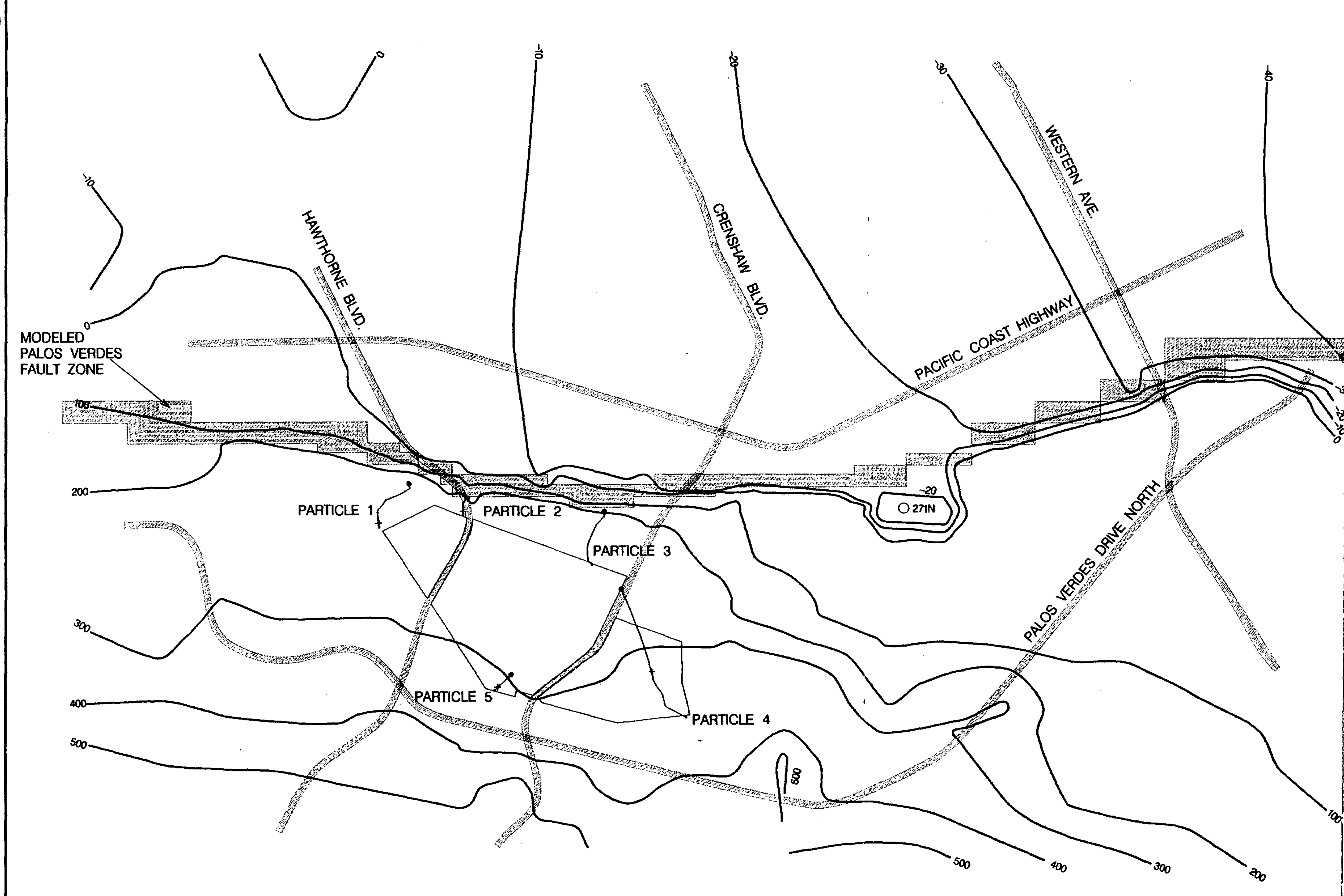

100 GROUNDWATER ELEVATION CONTOUR

HORIZONTAL PROJECTION OF GROUNDWATER TRAVEL PATH

+ 400 YEARS TRAVEL TIME

• 2000 YEARS TRAVEL TIME

○ 271N INDUSTRIAL WATER SUPPLY WELL 271N

FIGURE C.25
LAYER 1 GROUNDWATER ELEVATIONS AND PARTICLE PATHWAYS IN PLAN VIEW– ZONE 7 RECHARGE RATE DOUBLED (SENSITIVITY CASE NO. 25)

CONTOUR VALUE RELATIVE TO MEAN SEA LEVEL

PALOS VERDES LANDFILL

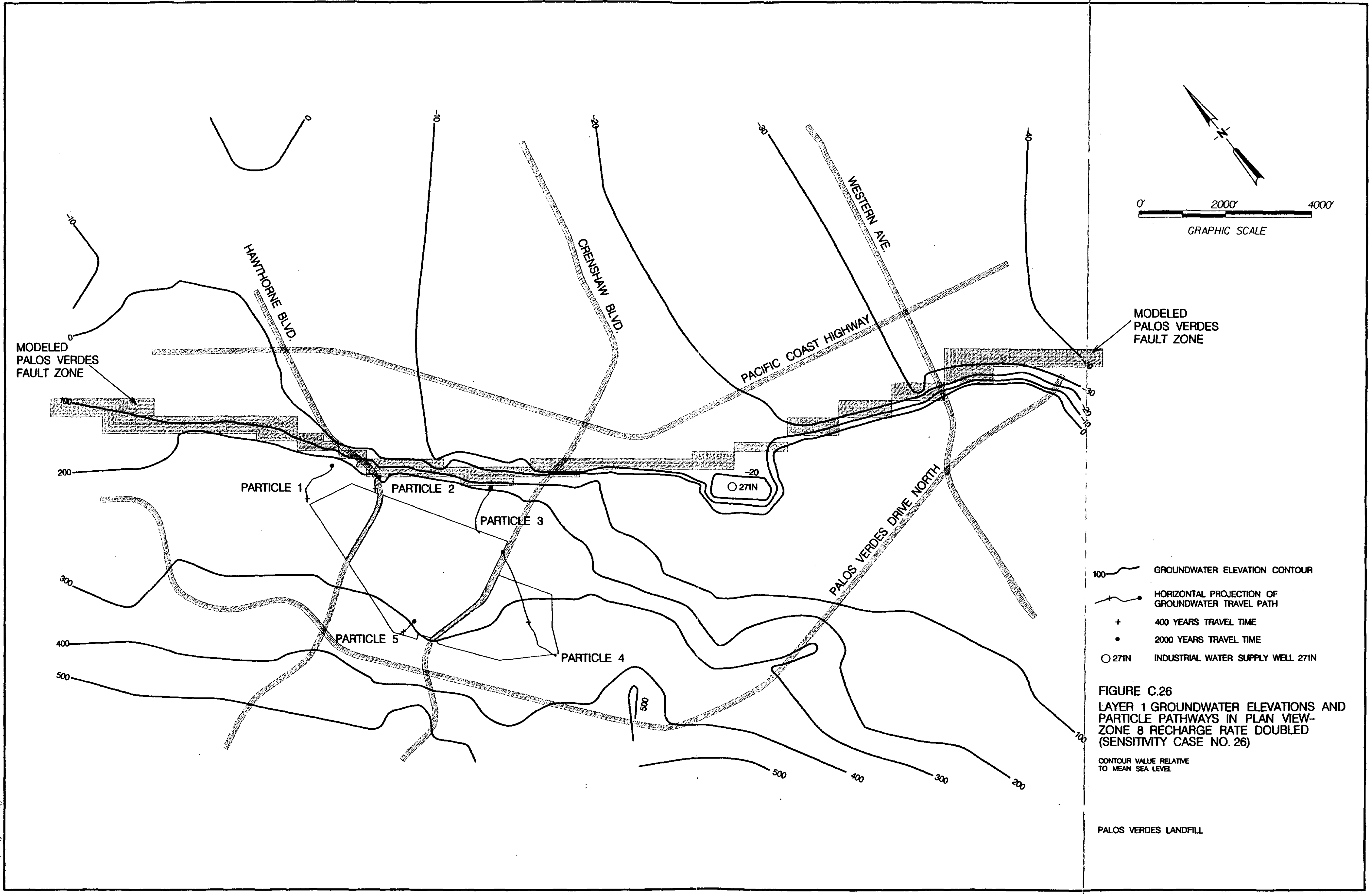

FIGURE C.26

LAYER 1 GROUNDWATER ELEVATIONS AND PARTICLE PATHWAYS IN PLAN VIEW– ZONE 8 RECHARGE RATE DOUBLED (SENSITIVITY CASE NO. 26)

CONTOUR VALUE RELATIVE TO MEAN SEA LEVEL

PALOS VERDES LANDFILL

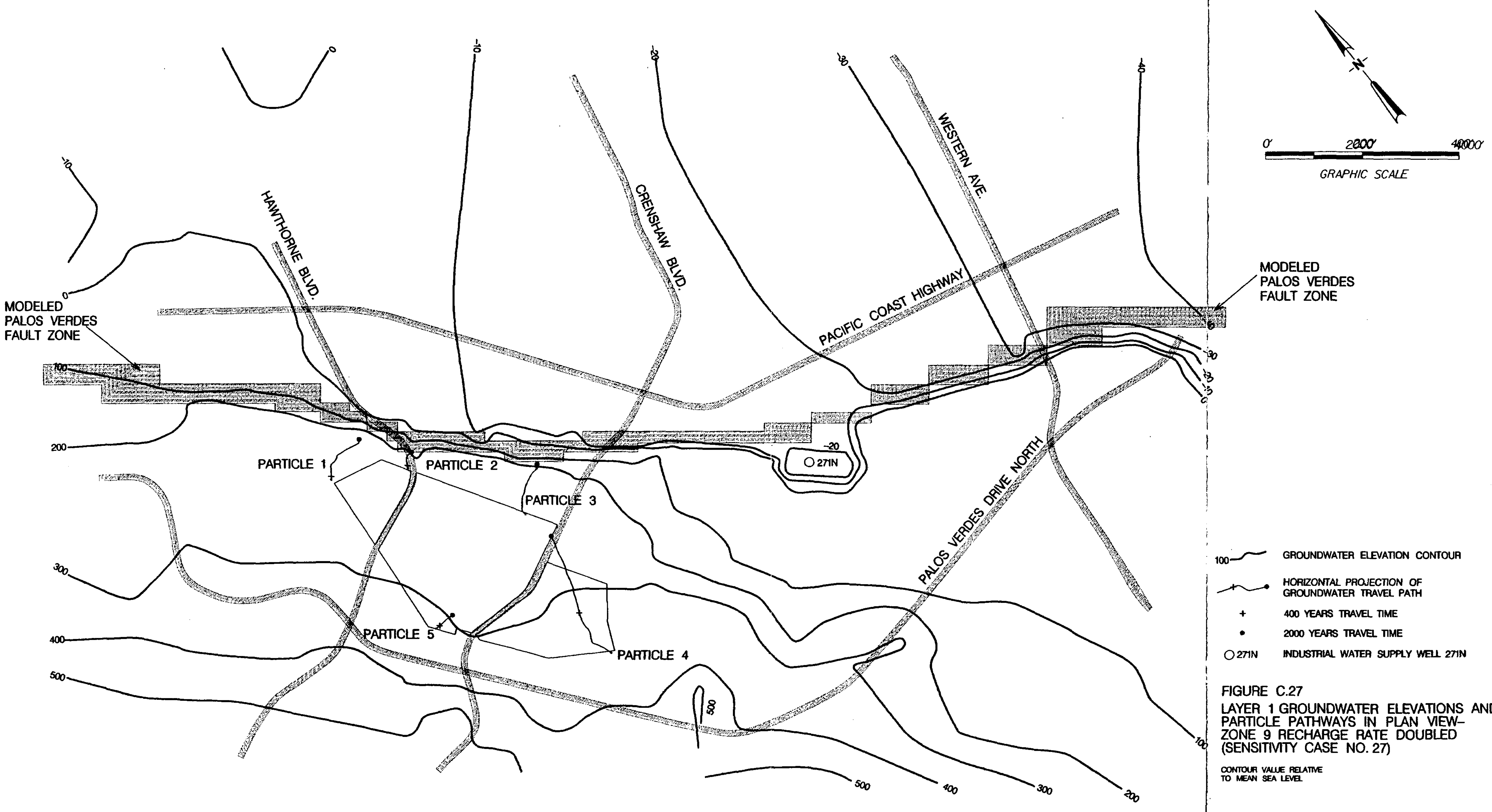

FIGURE C.27

LAYER 1 GROUNDWATER ELEVATIONS AND PARTICLE PATHWAYS IN PLAN VIEW–ZONE 9 RECHARGE RATE DOUBLED (SENSITIVITY CASE NO. 27)

CONTOUR VALUE RELATIVE TO MEAN SEA LEVEL

PALOS VERDES LANDFILL

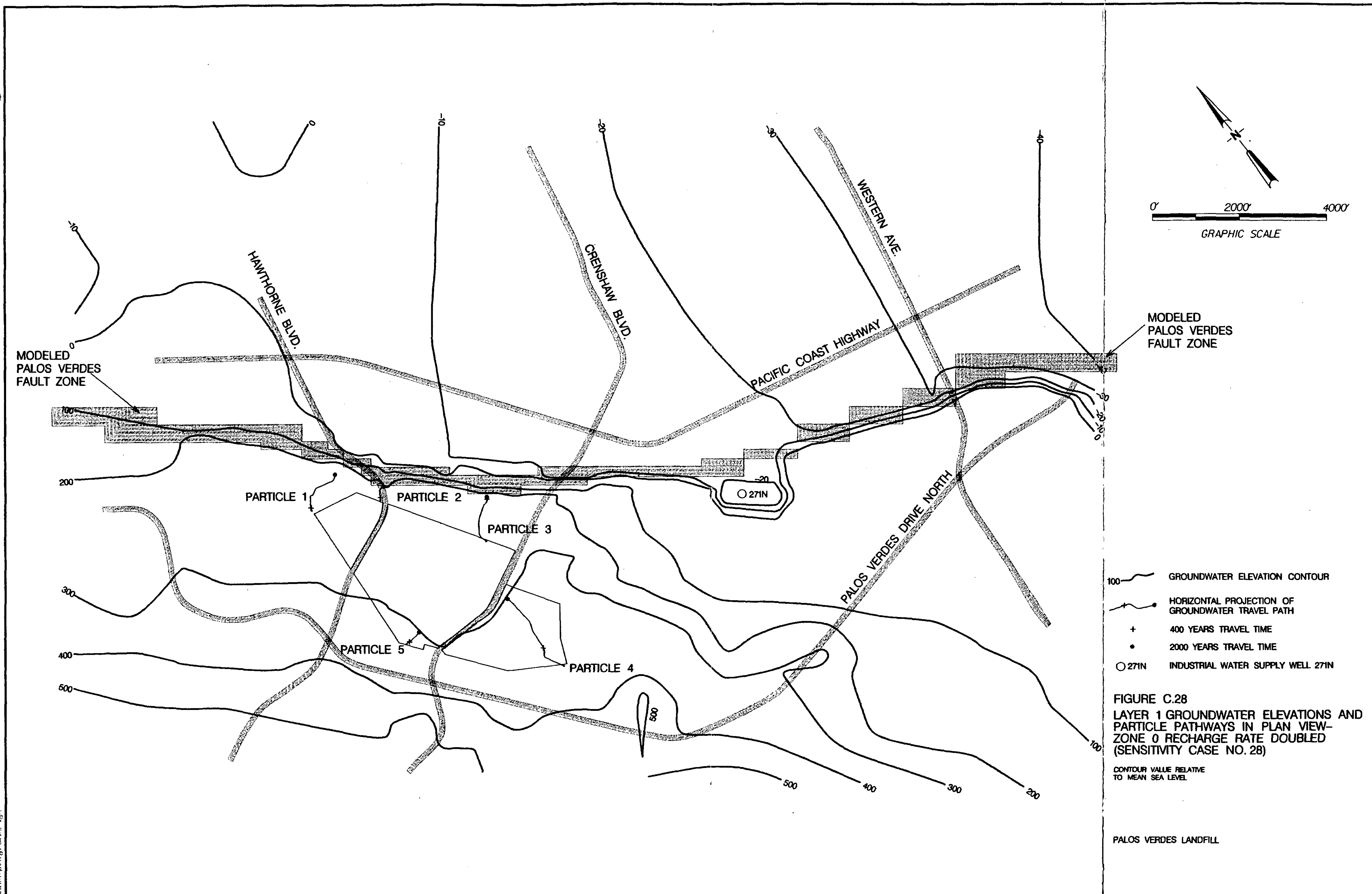

FIGURE C.28

LAYER 1 GROUNDWATER ELEVATIONS AND PARTICLE PATHWAYS IN PLAN VIEW– ZONE 0 RECHARGE RATE DOUBLED (SENSITIVITY CASE NO. 28)

CONTOUR VALUE RELATIVE TO MEAN SEA LEVEL

PALOS VERDES LANDFILL

APPENDIX D

STATISTICS OF SENSITIVITY/UNCERTAINTY ANALYSES

PVLF STEADY-STATE BASE CASE FOR THE CALIBRATED MODEL

Root mean square of residuals	11.0	ft
Absolute maximum residual	27.9	ft
Correlation -model vs. obs	0.994	

WELL	H(obs.) (ft)	H(model) (ft)	RESIDUAL (ft)	PERCENTAGE OF MAX HEAD DIFFERENCE
M23A	198.70	204.25	5.55	1.194
M24A	190.60	179.08	-11.52	-2.480
M25A	189.80	217.74	27.94	6.014
M26A	-2.70	3.88	6.58	1.416
M30B	241.20	258.13	16.93	3.644
M32B	286.70	266.07	-20.63	-4.442
M33B	274.10	265.52	-8.58	-1.847
M34B	288.20	267.21	-20.99	-4.520
M35B	245.00	267.60	22.60	4.866
M36A	242.80	239.00	-3.80	-0.818
M37A	250.80	259.19	8.39	1.806
M38A	279.30	281.56	2.26	0.486
M39A	288.90	297.52	8.62	1.856
M40A	332.00	321.83	-10.17	-2.189
M41A	327.60	334.56	6.96	1.499
M42A	338.10	338.13	0.03	0.007
M43A	292.30	292.42	0.12	0.026
M44A	292.80	284.67	-8.13	-1.751
M45A	320.90	311.49	-9.41	-2.025
M46A	283.40	287.00	3.60	0.775
M47B	283.20	278.67	-4.53	-0.975
M48A	275.50	268.81	-6.69	-1.439
M49A	203.30	213.97	10.67	2.298
M50B	-3.80	6.02	9.82	2.114
M51B	156.10	169.46	13.36	2.877
M52B	-12.30	-11.02	1.28	0.277
M53B	263.80	271.66	7.86	1.693
M54B	237.40	242.95	5.55	1.195
M55B	280.10	269.12	-10.98	-2.363
M56B	376.80	380.83	4.03	0.868
M57B	431.80	415.01	-16.79	-3.614
M58B	370.10	369.31	-0.79	-0.169
M59B	241.00	235.60	-5.40	-1.162
M60B	340.10	348.86	8.76	1.886
M61B	355.10	361.17	6.07	1.306
M62B	336.10	332.71	-3.39	-0.730
749D	-3.80	-0.27	3.53	0.760
748H	8.00	-1.60	-9.60	-2.068
758D	3.70	-2.12	-5.82	-1.253
749A	-13.20	4.65	17.85	3.844
769	-16.80	-14.36	2.44	0.524
240A	-6.90	13.42	20.32	4.374

271N	-28.70	-28.70	0.00	0.000

Note: Head > 1.e+20 denotes dry well

PVLF-SENSITIVITY CASE # 1   K - QO FILL (NON-LANDFILL MATERIALS) * 10

Root mean square of residuals	20.9	ft
Absolute maximum residual	47.7	ft
Correlation -model vs. obs	0.984	

WELL	H(obs.) (ft)	H(model) (ft)	RESIDUAL (ft)	PERCENTAGE OF MAX HEAD DIFFERENCE
M23A	198.70	204.16	5.46	1.176
M24A	190.60	184.67	-5.93	-1.276
M25A	189.80	224.13	34.33	7.391
M26A	-2.70	10.52	13.22	2.846
M30B	241.20	264.52	23.32	5.021
M32B	286.70	268.15	-18.55	-3.994
M33B	274.10	267.76	-6.34	-1.364
M34B	288.20	268.30	-19.90	-4.284
M35B	245.00	268.43	23.43	5.045
M36A	242.80	223.26	-19.54	-4.206
M37A	250.80	249.36	-1.44	-0.310
M38A	279.30	272.11	-7.19	-1.548
M39A	288.90	280.72	-8.18	-1.761
M40A	332.00	288.77	-43.23	-9.307
M41A	327.60	293.92	-33.68	-7.250
M42A	338.10	296.72	-41.38	-8.909
M43A	292.30	278.08	-14.22	-3.062
M44A	292.80	273.77	-19.03	-4.098
M45A	320.90	299.27	-21.63	-4.657
M46A	283.40	277.65	-5.75	-1.238
M47B	283.20	271.93	-11.27	-2.427
M48A	275.50	263.65	-11.85	-2.552
M49A	203.30	211.24	7.94	1.709
M50B	-3.80	11.15	14.95	3.217
M51B	156.10	180.40	24.30	5.232
M52B	-12.30	-2.28	10.02	2.158
M53B	263.80	266.64	2.84	0.611
M54B	237.40	236.81	-0.59	-0.127
M55B	280.10	260.34	-19.76	-4.254
M56B	376.80	368.04	-8.76	-1.887
M57B	431.80	404.31	-27.49	-5.918
M58B	370.10	347.42	-22.68	-4.882
M59B	241.00	219.33	-21.67	-4.666
M60B	340.10	304.16	-35.94	-7.736
M61B	355.10	307.35	-47.75	-10.279
M62B	336.10	307.74	-28.36	-6.105
749D	-3.80	-0.21	3.59	0.774
748H	8.00	-1.53	-9.53	-2.051
758D	3.70	-2.05	-5.75	-1.238
749A	-13.20	4.50	17.70	3.810
769	-16.80	-14.24	2.56	0.552
240A	-6.90	23.75	30.65	6.598
271N	-28.70	-28.70	0.00	0.000

Note: Head > 1.e+20 denotes dry well

PVLF-SENSITIVITY CASE # 2 K-QO ALLUVIUM * 10

Root mean square of residuals	33.8	ft
Absolute maximum residual	75.8	ft
Correlation -model vs. obs	0.976	

WELL	H(obs.) (ft)	H(model) (ft)	RESIDUAL (ft)	PERCENTAGE OF MAX HEAD DIFFERENCE
M23A	198.70	200.90	2.20	0.474
M24A	190.60	174.48	-16.12	-3.471
M25A	189.80	205.94	16.14	3.475
M26A	-2.70	2.26	4.96	1.068
M30B	241.20	240.00	-1.20	-0.257
M32B	286.70	242.91	-43.79	-9.427
M33B	274.10	242.36	-31.74	-6.834
M34B	288.20	236.93	-51.27	-11.037
M35B	245.00	236.54	-8.46	-1.820
M36A	242.80	210.41	-32.39	-6.972
M37A	250.80	219.76	-31.04	-6.684
M38A	279.30	236.16	-43.14	-9.287
M39A	288.90	230.73	-58.17	-12.524
M40A	332.00	256.23	-75.77	-16.311
M41A	327.60	276.69	-50.91	-10.961
M42A	338.10	283.83	-54.27	-11.683
M43A	292.30	254.84	-37.46	-8.065
M44A	292.80	244.35	-48.45	-10.431
M45A	320.90	282.92	-37.98	-8.176
M46A	283.40	280.41	-2.99	-0.645
M47B	283.20	277.67	-5.53	-1.191
M48A	275.50	263.96	-11.54	-2.484
M49A	203.30	209.16	5.86	1.261
M50B	-3.80	5.55	9.35	2.014
M51B	156.10	156.15	0.05	0.011
M52B	-12.30	-11.80	0.50	0.107
M53B	263.80	228.74	-35.06	-7.549
M54B	237.40	240.76	3.36	0.723
M55B	280.10	260.84	-19.26	-4.146
M56B	376.80	354.38	-22.42	-4.826
M57B	431.80	391.06	-40.74	-8.771
M58B	370.10	327.32	-42.78	-9.210
M59B	241.00	207.23	-33.77	-7.270
M60B	340.10	290.56	-49.54	-10.665
M61B	355.10	296.86	-58.24	-12.539
M62B	336.10	274.99	-61.11	-13.156
749D	-3.80	-0.92	2.88	0.620
748H	8.00	-2.14	-10.14	-2.183
758D	3.70	-2.71	-6.41	-1.381
749A	-13.20	2.47	15.67	3.375
769	-16.80	-14.43	2.37	0.510

Note: Head > 1.e+20 denotes dry well

PVLF-SENSITIVITY CASE # 3 K-QUS * 10

Root mean square of residuals	28.8	ft
Absolute maximum residual	102.	ft
Correlation -model vs. obs	0.966	

WELL	H(obs.) (ft)	H(model) (ft)	RESIDUAL (ft)	PERCENTAGE OF MAX HEAD DIFFERENCE
M23A	198.70	198.06	-0.64	-0.137
M24A	190.60	162.19	-28.41	-6.116
M25A	189.80	204.70	14.90	3.207
M26A	-2.70	-1.35	1.35	0.290
M30B	241.20	242.01	0.81	0.175
M32B	286.70	247.64	-39.06	-8.410
M33B	274.10	246.45	-27.65	-5.953
M34B	288.20	245.40	-42.80	-9.215
M35B	245.00	245.77	0.77	0.166
M36A	242.80	171.26	-71.54	-15.402
M37A	250.80	219.33	-31.47	-6.776
M38A	279.30	260.40	-18.90	-4.069
M39A	288.90	277.35	-11.55	-2.488
M40A	332.00	298.53	-33.47	-7.207
M41A	327.60	313.67	-13.93	-2.998
M42A	338.10	317.91	-20.19	-4.347
M43A	292.30	275.59	-16.71	-3.598
M44A	292.80	265.76	-27.04	-5.822
M45A	320.90	299.00	-21.90	-4.716
M46A	283.40	280.84	-2.56	-0.551
M47B	283.20	273.30	-9.90	-2.131
M48A	275.50	264.17	-11.33	-2.438
M49A	203.30	208.01	4.71	1.014
M50B	-3.80	-1.64	2.16	0.465
M51B	156.10	155.19	-0.91	-0.195
M52B	-12.30	-15.27	-2.97	-0.639
M53B	263.80	247.93	-15.87	-3.416
M54B	237.40	239.60	2.20	0.474
M55B	280.10	265.57	-14.53	-3.127
M56B	376.80	376.88	0.08	0.018
M57B	431.80	410.06	-21.74	-4.681
M58B	370.10	356.65	-13.45	-2.895
M59B	241.00	160.18	-80.82	-17.400
M60B	340.10	329.47	-10.63	-2.289
M61B	355.10	342.70	-12.40	-2.669
M62B	336.10	234.09	-102.01	-21.961
749D	-3.80	-0.60	3.20	0.688
748H	8.00	-2.05	-10.05	-2.164
758D	3.70	-2.65	-6.35	-1.368
749A	-13.20	4.20	17.40	3.745
769	-16.80	-14.98	1.82	0.392

Note: Head > 1.e+20 denotes dry well

PVLF-SENSITIVITY CASE # 4 K-TMM * 10

Root mean square of residuals	11.1	ft
Absolute maximum residual	24.9	ft
Correlation -model vs. obs	0.993	

WELL	H(obs.) (ft)	H(model) (ft)	RESIDUAL (ft)	PERCENTAGE OF MAX HEAD DIFFERENCE
M23A	198.70	202.05	3.35	0.721
M24A	190.60	176.87	-13.73	-2.957
M25A	189.80	214.71	24.91	5.363
M26A	-2.70	4.03	6.73	1.448
M30B	241.20	254.84	13.64	2.936
M32B	286.70	263.89	-22.81	-4.911
M33B	274.10	263.34	-10.76	-2.316
M34B	288.20	263.95	-24.25	-5.222
M35B	245.00	264.24	19.24	4.141
M36A	242.80	238.55	-4.25	-0.916
M37A	250.80	256.24	5.44	1.172
M38A	279.30	276.57	-2.73	-0.588
M39A	288.90	290.66	1.76	0.379
M40A	332.00	312.21	-19.79	-4.261
M41A	327.60	326.01	-1.59	-0.341
M42A	338.10	329.97	-8.13	-1.749
M43A	292.30	287.92	-4.38	-0.943
M44A	292.80	280.09	-12.71	-2.737
M45A	320.90	308.17	-12.73	-2.740
M46A	283.40	285.68	2.28	0.490
M47B	283.20	277.58	-5.62	-1.210
M48A	275.50	267.63	-7.87	-1.694
M49A	203.30	212.19	8.89	1.913
M50B	-3.80	3.96	7.76	1.671
M51B	156.10	165.64	9.54	2.055
M52B	-12.30	-10.14	2.16	0.465
M53B	263.80	267.54	3.74	0.804
M54B	237.40	241.33	3.93	0.845
M55B	280.10	267.65	-12.45	-2.681
M56B	376.80	379.42	2.62	0.565
M57B	431.80	413.33	-18.47	-3.976
M58B	370.10	364.59	-5.51	-1.187
M59B	241.00	235.57	-5.43	-1.170
M60B	340.10	340.86	0.76	0.163
M61B	355.10	353.51	-1.59	-0.342
M62B	336.10	322.77	-13.33	-2.869
749D	-3.80	-0.17	3.63	0.782
748H	8.00	-1.50	-9.50	-2.046
758D	3.70	-1.98	-5.68	-1.224
749A	-13.20	4.91	18.11	3.900
769	-16.80	-14.18	2.62	0.564

Note: Head > 1.e+20 denotes dry well

PVLF-SENSITIVITY CASE # 5 K-Tmv * 10

Root mean square of residuals	12.2	ft
Absolute maximum residual	29.1	ft
Correlation -model vs. obs	0.993	

WELL	H(obs.) (ft)	H(model) (ft)	RESIDUAL (ft)	PERCENTAGE OF MAX HEAD DIFFERENCE
M23A	198.70	200.89	2.19	0.472
M24A	190.60	175.95	-14.65	-3.153
M25A	189.80	215.57	25.77	5.547
M26A	-2.70	6.85	9.55	2.057
M30B	241.20	254.77	13.57	2.922
M32B	286.70	261.05	-25.65	-5.522
M33B	274.10	260.59	-13.51	-2.909
M34B	288.20	259.13	-29.07	-6.258
M35B	245.00	259.18	14.18	3.053
M36A	242.80	238.88	-3.92	-0.843
M37A	250.80	253.16	2.36	0.508
M38A	279.30	273.35	-5.95	-1.281
M39A	288.90	287.89	-1.01	-0.217
M40A	332.00	309.80	-22.20	-4.780
M41A	327.60	322.27	-5.33	-1.148
M42A	338.10	325.30	-12.80	-2.755
M43A	292.30	285.39	-6.91	-1.487
M44A	292.80	277.90	-14.90	-3.207
M45A	320.90	305.91	-14.99	-3.226
M46A	283.40	283.75	0.35	0.075
M47B	283.20	275.80	-7.40	-1.594
M48A	275.50	265.74	-9.76	-2.101
M49A	203.30	211.44	8.14	1.752
M50B	-3.80	1.28	5.08	1.094
M51B	156.10	168.09	11.99	2.580
M52B	-12.30	-10.81	1.49	0.321
M53B	263.80	263.41	-0.39	-0.084
M54B	237.40	238.99	1.59	0.343
M55B	280.10	265.06	-15.04	-3.237
M56B	376.80	377.02	0.22	0.048
M57B	431.80	411.01	-20.79	-4.476
M58B	370.10	361.65	-8.45	-1.819
M59B	241.00	234.66	-6.34	-1.365
M60B	340.10	336.91	-3.19	-0.687
M61B	355.10	349.92	-5.18	-1.115
M62B	336.10	322.74	-13.36	-2.876
749D	-3.80	-0.24	3.56	0.766
748H	8.00	-1.57	-9.57	-2.060
758D	3.70	-2.07	-5.77	-1.242
749A	-13.20	4.80	18.00	3.874
769	-16.80	-14.32	2.48	0.534

Note: Head > 1.e+20 denotes dry well

PVLF-SENSITIVITY CASE # 6 K-Tma * 10

Root mean square of residuals	20.4	ft
Absolute maximum residual	74.6	ft
Correlation -model vs. obs	0.978	

WELL	H(obs.) (ft)	H(model) (ft)	RESIDUAL (ft)	PERCENTAGE OF MAX HEAD DIFFERENCE
M23A	198.70	217.38	18.68	4.022
M24A	190.60	190.05	-0.55	-0.118
M25A	189.80	228.64	38.84	8.362
M26A	-2.70	9.66	12.36	2.662
M30B	241.20	269.07	27.87	5.999
M32B	286.70	272.76	-13.94	-3.002
M33B	274.10	272.20	-1.90	-0.410
M34B	288.20	273.09	-15.11	-3.253
M35B	245.00	273.40	28.40	6.115
M36A	242.80	243.18	0.38	0.083
M37A	250.80	263.38	12.58	2.709
M38A	279.30	283.63	4.33	0.932
M39A	288.90	294.32	5.42	1.168
M40A	332.00	315.13	-16.87	-3.632
M41A	327.60	319.79	-7.81	-1.681
M42A	338.10	320.13	-17.97	-3.868
M43A	292.30	291.86	-0.44	-0.094
M44A	292.80	286.37	-6.43	-1.384
M45A	320.90	301.08	-19.82	-4.268
M46A	283.40	280.18	-3.22	-0.692
M47B	283.20	272.31	-10.89	-2.345
M48A	275.50	263.70	-11.80	-2.541
M49A	203.30	226.28	22.98	4.947
M50B	-3.80	29.20	33.00	7.104
M51B	156.10	177.42	21.32	4.589
M52B	-12.30	-9.03	3.27	0.704
M53B	263.80	275.52	11.72	2.523
M54B	237.40	246.58	9.18	1.977
M55B	280.10	264.88	-15.22	-3.277
M56B	376.80	345.31	-31.49	-6.779
M57B	431.80	357.24	-74.56	-16.051
M58B	370.10	334.11	-35.99	-7.749
M59B	241.00	239.59	-1.41	-0.304
M60B	340.10	326.55	-13.55	-2.916
M61B	355.10	335.23	-19.87	-4.278
M62B	336.10	333.99	-2.11	-0.455
749D	-3.80	-0.04	3.76	0.810
748H	8.00	-1.27	-9.27	-1.995
758D	3.70	-1.53	-5.23	-1.126
749A	-13.20	5.55	18.75	4.036
769	-16.80	-13.67	3.13	0.674

Note: Head > 1.e+20 denotes dry well

PVLF-SENSITIVITY CASE # 7 K-JC * 10

Root mean square of residuals	20.6	ft
Absolute maximum residual	46.7	ft
Correlation -model vs. obs	0.990	

WELL	H(obs.) (ft)	H(model) (ft)	RESIDUAL (ft)	PERCENTAGE OF MAX HEAD DIFFERENCE
M23A	198.70	208.69	9.99	2.151
M24A	190.60	182.80	-7.80	-1.680
M25A	189.80	221.77	31.97	6.884
M26A	-2.70	4.11	6.81	1.467
M30B	241.20	263.78	22.58	4.862
M32B	286.70	271.51	-15.19	-3.271
M33B	274.10	270.98	-3.12	-0.672
M34B	288.20	274.19	-14.01	-3.016
M35B	245.00	274.74	29.74	6.403
M36A	242.80	243.14	0.34	0.074
M37A	250.80	266.40	15.60	3.359
M38A	279.30	294.48	15.18	3.268
M39A	288.90	313.79	24.89	5.359
M40A	332.00	343.79	11.79	2.539
M41A	327.60	366.86	39.26	8.452
M42A	338.10	373.58	35.48	7.638
M43A	292.30	312.19	19.89	4.283
M44A	292.80	299.26	6.46	1.390
M45A	320.90	337.09	16.19	3.485
M46A	283.40	305.16	21.76	4.685
M47B	283.20	295.05	11.85	2.552
M48A	275.50	283.55	8.05	1.732
M49A	203.30	219.55	16.25	3.499
M50B	-3.80	6.75	10.55	2.272
M51B	156.10	171.98	15.88	3.419
M52B	-12.30	-11.06	1.24	0.267
M53B	263.80	280.91	17.11	3.683
M54B	237.40	254.29	16.89	3.637
M55B	280.10	285.61	5.51	1.187
M56B	376.80	413.50	36.70	7.901
M57B	431.80	449.94	18.14	3.906
M58B	370.10	408.39	38.29	8.244
M59B	241.00	238.88	-2.12	-0.456
M60B	340.10	386.78	46.68	10.049
M61B	355.10	396.47	41.37	8.907
M62B	336.10	347.35	11.25	2.423
749D	-3.80	-0.26	3.54	0.762
748H	8.00	-1.59	-9.59	-2.065
758D	3.70	-2.11	-5.81	-1.250
749A	-13.20	4.68	17.88	3.850
769	-16.80	-14.38	2.42	0.522

Note: Head > 1.e+20 denotes dry well

PVLF-SENSITIVITY CASE # 8, 5-BREAKS THROUGH FAULT ZONE

Root mean square of residuals	22.0	ft
Absolute maximum residual	99.6	ft
Correlation -model vs. obs	0.978	

WELL	H(obs.) (ft)	H(model) (ft)	RESIDUAL (ft)	PERCENTAGE OF MAX HEAD DIFFERENCE
M23A	198.70	226.29	27.59	5.940
M24A	190.60	219.80	29.20	6.287
M25A	189.80	214.79	24.99	5.380
M26A	-2.70	96.93	99.63	21.448
M30B	241.20	258.27	17.07	3.674
M32B	286.70	265.18	-21.52	-4.633
M33B	274.10	264.57	-9.53	-2.052
M34B	288.20	266.22	-21.98	-4.732
M35B	245.00	266.64	21.64	4.659
M36A	242.80	238.02	-4.78	-1.030
M37A	250.80	258.37	7.57	1.629
M38A	279.30	280.93	1.63	0.352
M39A	288.90	297.06	8.16	1.756
M40A	332.00	321.43	-10.57	-2.276
M41A	327.60	334.20	6.60	1.422
M42A	338.10	337.80	-0.30	-0.065
M43A	292.30	292.09	-0.21	-0.045
M44A	292.80	284.16	-8.64	-1.860
M45A	320.90	311.43	-9.47	-2.040
M46A	283.40	287.45	4.05	0.871
M47B	283.20	279.23	-3.97	-0.855
M48A	275.50	269.76	-5.74	-1.235
M49A	203.30	232.08	28.78	6.196
M50B	-3.80	18.49	22.29	4.799
M51B	156.10	177.13	21.03	4.528
M52B	-12.30	-6.48	5.82	1.253
M53B	263.80	270.90	7.10	1.528
M54B	237.40	244.15	6.75	1.452
M55B	280.10	269.83	-10.27	-2.212
M56B	376.80	381.01	4.21	0.906
M57B	431.80	415.15	-16.65	-3.584
M58B	370.10	369.21	-0.89	-0.191
M59B	241.00	234.66	-6.34	-1.366
M60B	340.10	348.56	8.46	1.822
M61B	355.10	360.88	5.78	1.244
M62B	336.10	332.45	-3.65	-0.785
749D	-3.80	0.08	3.88	0.835
748H	8.00	-1.15	-9.15	-1.969
758D	3.70	-1.39	-5.09	-1.095
749A	-13.20	6.32	19.52	4.202
769	-16.80	-13.70	3.10	0.667
240A	-6.90	50.82	57.72	12.427
271N	-28.70	-28.70	0.00	0.000

Note: Head > 1.e+20 denotes dry well

PVLF-SENSITIVITY CASE # 9, GLOBAL RECH. * .25

Root mean square of residuals	37.7	ft
Absolute maximum residual	87.0	ft
Correlation -model vs. obs	0.968	

WELL	H(obs.) (ft)	H(model) (ft)	RESIDUAL (ft)	PERCENTAGE OF MAX HEAD DIFFERENCE
M23A	198.70	202.25	3.55	0.765
M24A	190.60	177.24	-13.36	-2.875
M25A	189.80	214.33	24.53	5.282
M26A	-2.70	2.94	5.64	1.214
M30B	241.20	250.62	9.42	2.029
M32B	286.70	251.34	-35.36	-7.613
M33B	274.10	250.36	-23.74	-5.111
M34B	288.20	245.69	-42.51	-9.153
M35B	245.00	245.58	0.58	0.125
M36A	242.80	176.69	-66.11	-14.232
M37A	250.80	210.67	-40.13	-8.640
M38A	279.30	243.03	-36.27	-7.807
M39A	288.90	237.88	-51.02	-10.984
M40A	332.00	256.79	-75.21	-16.192
M41A	327.60	274.73	-52.87	-11.382
M42A	338.10	280.18	-57.92	-12.469
M43A	292.30	261.79	-30.51	-6.568
M44A	292.80	252.35	-40.45	-8.708
M45A	320.90	282.36	-38.54	-8.297
M46A	283.40	273.02	-10.38	-2.235
M47B	283.20	268.29	-14.91	-3.210
M48A	275.50	259.35	-16.15	-3.478
M49A	203.30	210.92	7.62	1.641
M50B	-3.80	5.20	9.00	1.937
M51B	156.10	166.43	10.33	2.225
M52B	-12.30	-12.65	-0.35	-0.075
M53B	263.80	236.31	-27.49	-5.917
M54B	237.40	236.52	-0.88	-0.189
M55B	280.10	258.32	-21.78	-4.689
M56B	376.80	344.21	-32.59	-7.017
M57B	431.80	359.28	-72.52	-15.612
M58B	370.10	316.62	-53.48	-11.513
M59B	241.00	166.96	-74.04	-15.940
M60B	340.10	289.15	-50.95	-10.969
M61B	355.10	299.19	-55.91	-12.037
M62B	336.10	249.08	-87.02	-18.735
749D	-3.80	-0.47	3.33	0.717
748H	8.00	-1.88	-9.88	-2.127
758D	3.70	-2.42	-6.12	-1.318
749A	-13.20	4.21	17.41	3.749
769	-16.80	-14.59	2.21	0.475
240A	-6.90	12.64	19.54	4.207
271N	-28.70	-28.70	0.00	0.000

Note: Head > 1.e+20 denotes dry well

PVLF-SENSITIVITY CASE # 10 GLOBAL RECH. * 1.75

Root mean square of residuals	32.9	ft
Absolute maximum residual	64.1	ft
Correlation -model vs. obs	0.984	

WELL	H(obs.) (ft)	H(model) (ft)	RESIDUAL (ft)	PERCENTAGE OF MAX HEAD DIFFERENCE
M23A	198.70	206.63	7.93	1.706
M24A	190.60	181.18	-9.42	-2.027
M25A	189.80	221.02	31.22	6.722
M26A	-2.70	4.75	7.45	1.604
M30B	241.20	264.65	23.45	5.049
M32B	286.70	278.67	-8.04	-1.730
M33B	274.10	278.52	4.42	0.952
M34B	288.20	286.12	-2.08	-0.448
M35B	245.00	286.98	41.98	9.038
M36A	242.80	290.55	47.75	10.281
M37A	250.80	301.29	50.49	10.869
M38A	279.30	316.14	36.84	7.930
M39A	288.90	350.49	61.59	13.259
M40A	332.00	379.49	47.49	10.224
M41A	327.60	388.58	60.98	13.129
M42A	338.10	390.81	52.71	11.347
M43A	292.30	320.48	28.18	6.067
M44A	292.80	313.75	20.95	4.509
M45A	320.90	338.50	17.60	3.789
M46A	283.40	300.00	16.60	3.574
M47B	283.20	288.21	5.01	1.078
M48A	275.50	277.63	2.13	0.458
M49A	203.30	217.28	13.98	3.010
M50B	-3.80	6.73	10.53	2.268
M51B	156.10	172.11	16.01	3.447
M52B	-12.30	-9.58	2.72	0.585
M53B	263.80	303.20	39.40	8.482
M54B	237.40	249.38	11.98	2.579
M55B	280.10	279.54	-0.56	-0.120
M56B	376.80	414.54	37.74	8.125
M57B	431.80	464.91	33.11	7.128
M58B	370.10	417.41	47.31	10.186
M59B	241.00	291.01	50.01	10.766
M60B	340.10	403.26	63.16	13.598
M61B	355.10	417.56	62.46	13.446
M62B	336.10	400.17	64.07	13.794
749D	-3.80	-0.07	3.73	0.803
748H	8.00	-1.33	-9.33	-2.009
758D	3.70	-1.83	-5.53	-1.191
749A	-13.20	5.09	18.29	3.937
769	-16.80	-14.17	2.63	0.567
240A	-6.90	14.11	21.01	4.523
271N	-28.70	-28.70	0.00	0.000

Note: Head > 1.e+20 denotes dry well

PVLF-SENSITIVITY CASE # 11 FIXED HEADS @ 749A AND 240A

Root mean square of residuals	10.2	ft
Absolute maximum residual	27.8	ft
Correlation -model vs. obs	0.994	

WELL	H(obs.) (ft)	H(model) (ft)	RESIDUAL (ft)	PERCENTAGE OF MAX HEAD DIFFERENCE
M23A	198.70	204.05	5.35	1.152
M24A	190.60	178.81	-11.79	-2.539
M25A	189.80	217.58	27.78	5.981
M26A	-2.70	1.63	4.33	0.931
M30B	241.20	258.11	16.91	3.639
M32B	286.70	266.06	-20.64	-4.444
M33B	274.10	265.51	-8.59	-1.849
M34B	288.20	267.20	-21.00	-4.521
M35B	245.00	267.60	22.60	4.865
M36A	242.80	239.00	-3.80	-0.819
M37A	250.80	259.19	8.39	1.805
M38A	279.30	281.55	2.25	0.485
M39A	288.90	297.52	8.62	1.855
M40A	332.00	321.83	-10.17	-2.190
M41A	327.60	334.56	6.96	1.498
M42A	338.10	338.13	0.03	0.006
M43A	292.30	292.41	0.11	0.024
M44A	292.80	284.66	-8.14	-1.753
M45A	320.90	311.48	-9.42	-2.027
M46A	283.40	286.99	3.59	0.773
M47B	283.20	278.66	-4.54	-0.977
M48A	275.50	268.79	-6.71	-1.444
M49A	203.30	213.82	10.52	2.264
M50B	-3.80	-0.60	3.20	0.689
M51B	156.10	168.81	12.71	2.736
M52B	-12.30	-11.90	0.40	0.087
M53B	263.80	271.66	7.86	1.691
M54B	237.40	242.90	5.50	1.185
M55B	280.10	269.09	-11.01	-2.369
M56B	376.80	380.82	4.02	0.865
M57B	431.80	415.01	-16.79	-3.616
M58B	370.10	369.31	-0.79	-0.171
M59B	241.00	235.60	-5.40	-1.163
M60B	340.10	348.86	8.76	1.885
M61B	355.10	361.16	6.06	1.305
M62B	336.10	332.71	-3.39	-0.730
749D	-3.80	-6.16	-2.36	-0.507
748H	8.00	-6.16	-14.16	-3.047
758D	3.70	-5.72	-9.42	-2.027
749A	-13.20	-13.20	0.00	0.000
769	-16.80	-14.86	1.94	0.418
240A	-6.90	-6.90	0.00	0.000
271N	-28.70	-28.70	0.00	0.000

Note: Head > 1.e+20 denotes dry well

PVLF-SENSITIVITY CASE # 12 FIXED HEADS @ 749A AND 240A, STOP PUMPING 271

Root mean square of residuals	25.8	ft
Absolute maximum residual	151.	ft
Correlation -model vs. obs	0.965	

WELL	H(obs.) (ft)	H(model) (ft)	RESIDUAL (ft)	PERCENTAGE OF MAX HEAD DIFFERENCE
M23A	198.70	203.15	4.45	0.958
M24A	190.60	178.09	-12.51	-2.692
M25A	189.80	217.06	27.26	5.869
M26A	-2.70	1.70	4.40	0.948
M30B	241.20	258.53	17.33	3.731
M32B	286.70	268.23	-18.47	-3.977
M33B	274.10	267.90	-6.20	-1.335
M34B	288.20	271.01	-17.19	-3.701
M35B	245.00	271.47	26.47	5.699
M36A	242.80	258.42	15.62	3.363
M37A	250.80	271.70	20.90	4.500
M38A	279.30	288.17	8.87	1.910
M39A	288.90	307.72	18.82	4.052
M40A	332.00	330.02	-1.98	-0.426
M41A	327.60	340.92	13.32	2.867
M42A	338.10	343.97	5.87	1.263
M43A	292.30	296.10	3.80	0.818
M44A	292.80	289.23	-3.57	-0.768
M45A	320.90	313.66	-7.24	-1.558
M46A	283.40	287.35	3.95	0.850
M47B	283.20	278.88	-4.32	-0.930
M48A	275.50	268.78	-6.72	-1.446
M49A	203.30	213.01	9.71	2.091
M50B	-3.80	-0.47	3.33	0.718
M51B	156.10	168.71	12.61	2.714
M52B	-12.30	-11.36	0.94	0.201
M53B	263.80	278.70	14.90	3.209
M54B	237.40	242.37	4.97	1.071
M55B	280.10	268.87	-11.23	-2.417
M56B	376.80	381.11	4.31	0.927
M57B	431.80	415.65	-16.15	-3.477
M58B	370.10	372.40	2.30	0.495
M59B	241.00	256.94	15.94	3.432
M60B	340.10	354.45	14.35	3.089
M61B	355.10	366.52	11.42	2.458
M62B	336.10	344.33	8.23	1.772
749D	-3.80	-6.15	-2.35	-0.506
748H	8.00	-6.15	-14.15	-3.046
758D	3.70	-5.70	-9.40	-2.024
749A	-13.20	-13.20	0.00	0.000
769	-16.80	-14.77	2.03	0.437
240A	-6.90	-6.90	0.00	0.000
271N	-28.70	121.95	150.65	32.433

Note: Head > 1.e+20 denotes dry well

PVLF-SENSITIVITY CASE # 13 INCREASE K * 100 AT FAULT RIM

Root mean square of residuals	18.1	ft
Absolute maximum residual	51.3	ft
Correlation -model vs. obs	0.987	

WELL	H(obs.) (ft)	H(model) (ft)	RESIDUAL (ft)	PERCENTAGE OF MAX HEAD DIFFERENCE
M23A	198.70	185.85	-12.85	-2.766
M24A	190.60	164.65	-25.95	-5.586
M25A	189.80	201.94	12.14	2.613
M26A	-2.70	4.41	7.11	1.530
M30B	241.20	243.11	1.91	0.410
M32B	286.70	252.25	-34.45	-7.417
M33B	274.10	251.00	-23.10	-4.972
M34B	288.20	250.89	-37.31	-8.032
M35B	245.00	251.38	6.38	1.373
M36A	242.80	196.20	-46.60	-10.032
M37A	250.80	232.35	-18.45	-3.972
M38A	279.30	266.33	-12.97	-2.793
M39A	288.90	283.03	-5.87	-1.263
M40A	332.00	309.87	-22.13	-4.764
M41A	327.60	323.82	-3.78	-0.814
M42A	338.10	327.84	-10.26	-2.210
M43A	292.30	281.03	-11.27	-2.425
M44A	292.80	271.63	-21.17	-4.558
M45A	320.90	303.01	-17.89	-3.851
M46A	283.40	283.07	-0.33	-0.072
M47B	283.20	275.50	-7.70	-1.657
M48A	275.50	265.44	-10.06	-2.165
M49A	203.30	196.54	-6.76	-1.455
M50B	-3.80	10.80	14.60	3.142
M51B	156.10	162.85	6.75	1.453
M52B	-12.30	-4.56	7.74	1.666
M53B	263.80	254.26	-9.54	-2.055
M54B	237.40	238.56	1.16	0.250
M55B	280.10	265.85	-14.25	-3.068
M56B	376.80	378.40	1.60	0.345
M57B	431.80	412.09	-19.71	-4.243
M58B	370.10	362.37	-7.73	-1.664
M59B	241.00	189.70	-51.30	-11.044
M60B	340.10	339.24	-0.86	-0.185
M61B	355.10	352.07	-3.03	-0.652
M62B	336.10	324.24	-11.86	-2.554
749D	-3.80	-0.09	3.71	0.798
748H	8.00	-1.44	-9.44	-2.032
758D	3.70	-1.92	-5.62	-1.209
749A	-13.20	5.22	18.42	3.965
769	-16.80	-13.92	2.88	0.621
240A	-6.90	27.32	34.22	7.367
271N	-28.70	-28.70	0.00	0.000

Note: Head > 1.e+20 denotes dry well

PVLF-SENSITIVITY CASE #14 - REMOVE RECHARGE NEAR M59B

Root mean square of residuals	15.2	ft
Absolute maximum residual	51.0	ft
Correlation -model vs. obs	0.988	

WELL	H(obs.) (ft)	H(model) (ft)	RESIDUAL (ft)	PERCENTAGE OF MAX HEAD DIFFERENCE
M23A	198.70	204.20	5.50	1.183
M24A	190.60	179.00	-11.60	-2.497
M25A	189.80	217.18	27.38	5.895
M26A	-2.70	3.86	6.56	1.412
M30B	241.20	256.51	15.31	3.296
M32B	286.70	262.53	-24.17	-5.204
M33B	274.10	261.76	-12.34	-2.657
M34B	288.20	261.60	-26.60	-5.726
M35B	245.00	261.90	16.90	3.638
M36A	242.80	202.13	-40.67	-8.755
M37A	250.80	239.21	-11.59	-2.495
M38A	279.30	274.09	-5.21	-1.122
M39A	288.90	288.52	-0.38	-0.081
M40A	332.00	315.30	-16.70	-3.596
M41A	327.60	329.08	1.48	0.318
M42A	338.10	333.05	-5.05	-1.087
M43A	292.30	288.24	-4.06	-0.875
M44A	292.80	279.43	-13.37	-2.879
M45A	320.90	308.86	-12.04	-2.591
M46A	283.40	286.34	2.94	0.633
M47B	283.20	278.22	-4.98	-1.071
M48A	275.50	268.50	-7.00	-1.507
M49A	203.30	213.87	10.57	2.276
M50B	-3.80	6.01	9.81	2.112
M51B	156.10	168.80	12.70	2.734
M52B	-12.30	-11.25	1.05	0.226
M53B	263.80	262.64	-1.16	-0.250
M54B	237.40	242.83	5.43	1.170
M55B	280.10	268.89	-11.21	-2.414
M56B	376.80	380.33	3.53	0.761
M57B	431.80	414.23	-17.57	-3.783
M58B	370.10	366.44	-3.66	-0.789
M59B	241.00	190.03	-50.97	-10.973
M60B	340.10	344.13	4.03	0.867
M61B	355.10	356.66	1.56	0.337
M62B	336.10	328.56	-7.54	-1.624
749D	-3.80	-0.27	3.53	0.760
748H	8.00	-1.60	-9.60	-2.068
758D	3.70	-2.12	-5.82	-1.253
749A	-13.20	4.65	17.85	3.844
769	-16.80	-14.36	2.44	0.524
240A	-6.90	13.41	20.31	4.372
271N	-28.70	-28.70	0.00	0.000

Note: Head > 1.e+20 denotes dry well

PVLF-SENSITIVITY CASE #15 - REMOVE PUMPING AT 271N

Root mean square of residuals	26.1	ft
Absolute maximum residual	151.	ft
Correlation -model vs. obs	0.966	

WELL	H(obs.) (ft)	H(model) (ft)	RESIDUAL (ft)	PERCENTAGE OF MAX HEAD DIFFERENCE
M23A	198.70	203.33	4.63	0.998
M24A	190.60	178.36	-12.24	-2.635
M25A	189.80	217.21	27.41	5.901
M26A	-2.70	3.93	6.63	1.427
M30B	241.20	258.55	17.35	3.735
M32B	286.70	268.23	-18.47	-3.976
M33B	274.10	267.90	-6.20	-1.334
M34B	288.20	271.01	-17.19	-3.700
M35B	245.00	271.48	26.48	5.701
M36A	242.80	258.42	15.62	3.363
M37A	250.80	271.71	20.91	4.501
M38A	279.30	288.18	8.88	1.911
M39A	288.90	307.72	18.82	4.053
M40A	332.00	330.02	-1.98	-0.426
M41A	327.60	340.92	13.32	2.868
M42A	338.10	343.97	5.87	1.264
M43A	292.30	296.11	3.81	0.820
M44A	292.80	289.24	-3.56	-0.767
M45A	320.90	313.67	-7.23	-1.556
M46A	283.40	287.36	3.96	0.852
M47B	283.20	278.89	-4.31	-0.927
M48A	275.50	268.80	-6.70	-1.442
M49A	203.30	213.16	9.86	2.123
M50B	-3.80	6.14	9.94	2.140
M51B	156.10	169.35	13.25	2.851
M52B	-12.30	-10.52	1.78	0.384
M53B	263.80	278.71	14.91	3.210
M54B	237.40	242.41	5.01	1.080
M55B	280.10	268.90	-11.20	-2.412
M56B	376.80	381.11	4.31	0.929
M57B	431.80	415.66	-16.14	-3.476
M58B	370.10	372.40	2.30	0.496
M59B	241.00	256.95	15.95	3.433
M60B	340.10	354.45	14.35	3.090
M61B	355.10	366.52	11.42	2.459
M62B	336.10	344.33	8.23	1.773
749D	-3.80	-0.27	3.53	0.760
748H	8.00	-1.60	-9.60	-2.067
758D	3.70	-2.11	-5.81	-1.251
749A	-13.20	4.66	17.86	3.845
769	-16.80	-14.29	2.51	0.540
240A	-6.90	13.49	20.39	4.389
271N	-28.70	121.95	150.65	32.433

Note: Head > 1.e+20 denotes dry well

PVLF-SENSITIVITY CASE #16 - REMOVE FAULT (* 1000)

Root mean square of residuals	46.1	ft
Absolute maximum residual	100.	ft
Correlation -model vs. obs	0.944	

WELL	H(obs.) (ft)	H(model) (ft)	RESIDUAL (ft)	PERCENTAGE OF MAX HEAD DIFFERENCE
M23A	198.70	144.26	-54.44	-11.719
M24A	190.60	134.79	-55.81	-12.015
M25A	189.80	155.86	-33.94	-7.307
M26A	-2.70	52.24	54.94	11.827
M30B	241.20	178.19	-63.01	-13.565
M32B	286.70	201.33	-85.37	-18.379
M33B	274.10	200.29	-73.81	-15.889
M34B	288.20	204.69	-83.51	-17.979
M35B	245.00	205.59	-39.41	-8.484
M36A	242.80	182.15	-60.65	-13.058
M37A	250.80	205.59	-45.21	-9.734
M38A	279.30	231.78	-47.52	-10.231
M39A	288.90	261.68	-27.22	-5.859
M40A	332.00	287.22	-44.78	-9.640
M41A	327.60	299.77	-27.83	-5.991
M42A	338.10	303.29	-34.81	-7.493
M43A	292.30	244.80	-47.50	-10.226
M44A	292.80	235.45	-57.35	-12.348
M45A	320.90	269.11	-51.79	-11.150
M46A	283.40	251.74	-31.66	-6.816
M47B	283.20	244.54	-38.66	-8.323
M48A	275.50	235.20	-40.30	-8.675
M49A	203.30	155.59	-47.71	-10.272
M50B	-3.80	40.44	44.24	9.523
M51B	156.10	131.81	-24.29	-5.230
M52B	-12.30	22.88	35.18	7.575
M53B	263.80	218.06	-45.74	-9.847
M54B	237.40	208.83	-28.57	-6.150
M55B	280.10	237.20	-42.90	-9.237
M56B	376.80	359.17	-17.63	-3.796
M57B	431.80	393.47	-38.33	-8.251
M58B	370.10	338.96	-31.14	-6.705
M59B	241.00	180.06	-60.94	-13.119
M60B	340.10	316.04	-24.06	-5.181
M61B	355.10	330.54	-24.56	-5.288
M62B	336.10	311.82	-24.28	-5.226
749D	-3.80	9.08	12.88	2.772
748H	8.00	5.35	-2.65	-0.570
758D	3.70	3.99	0.29	0.063
749A	-13.20	25.37	38.57	8.303
769	-16.80	-10.56	6.24	1.344
240A	-6.90	93.12	100.02	21.532
271N	-28.70	-28.70	0.00	0.000

Note: Head > 1.e+20 denotes dry well

PVLF-SENSITIVITY CASE #17 - K * 10 E&W OF PVLF, S OF FAULT

Root mean square of residuals	16.9	ft
Absolute maximum residual	47.3	ft
Correlation -model vs. obs	0.989	

WELL	H(obs.) (ft)	H(model) (ft)	RESIDUAL (ft)	PERCENTAGE OF MAX HEAD DIFFERENCE
M23A	198.70	208.32	9.62	2.072
M24A	190.60	182.55	-8.05	-1.734
M25A	189.80	218.96	29.16	6.278
M26A	-2.70	4.26	6.96	1.499
M30B	241.20	255.35	14.15	3.045
M32B	286.70	262.99	-23.71	-5.103
M33B	274.10	262.39	-11.71	-2.521
M34B	288.20	262.70	-25.50	-5.489
M35B	245.00	262.98	17.98	3.871
M36A	242.80	232.79	-10.01	-2.155
M37A	250.80	252.20	1.40	0.301
M38A	279.30	273.05	-6.25	-1.346
M39A	288.90	285.20	-3.70	-0.797
M40A	332.00	307.29	-24.71	-5.320
M41A	327.60	320.39	-7.21	-1.553
M42A	338.10	323.87	-14.23	-3.064
M43A	292.30	283.19	-9.11	-1.961
M44A	292.80	276.36	-16.44	-3.540
M45A	320.90	300.39	-20.51	-4.417
M46A	283.40	272.61	-10.79	-2.324
M47B	283.20	263.42	-19.78	-4.258
M48A	275.50	248.83	-26.67	-5.742
M49A	203.30	216.33	13.03	2.804
M50B	-3.80	7.39	11.19	2.409
M51B	156.10	169.29	13.19	2.839
M52B	-12.30	-10.73	1.57	0.337
M53B	263.80	264.72	0.92	0.199
M54B	237.40	232.23	-5.17	-1.114
M55B	280.10	251.49	-28.61	-6.158
M56B	376.80	363.20	-13.60	-2.927
M57B	431.80	397.67	-34.13	-7.347
M58B	370.10	354.88	-15.22	-3.276
M59B	241.00	229.59	-11.41	-2.456
M60B	340.10	334.45	-5.65	-1.216
M61B	355.10	347.51	-7.59	-1.635
M62B	336.10	288.84	-47.26	-10.175
749D	-3.80	-0.25	3.55	0.765
748H	8.00	-1.58	-9.58	-2.062
758D	3.70	-2.08	-5.78	-1.244
749A	-13.20	4.73	17.93	3.860
769	-16.80	-14.26	2.54	0.546
240A	-6.90	15.62	22.52	4.848
271N	-28.70	-28.70	0.00	0.000

Note: Head > 1.e+20 denotes dry well

PVLF-SENSITIVITY CASE #18 - K * 10 IN WEST COAST BASIN

Root mean square of residuals	10.6	ft
Absolute maximum residual	27.3	ft
Correlation -model vs. obs	0.994	

WELL	H(obs.) (ft)	H(model) (ft)	RESIDUAL (ft)	PERCENTAGE OF MAX HEAD DIFFERENCE
M23A	198.70	204.97	6.27	1.350
M24A	190.60	178.46	-12.14	-2.614
M25A	189.80	217.09	27.29	5.874
M26A	-2.70	-0.55	2.15	0.464
M30B	241.20	256.16	14.96	3.220
M32B	286.70	262.02	-24.68	-5.312
M33B	274.10	261.47	-12.63	-2.719
M34B	288.20	263.25	-24.95	-5.371
M35B	245.00	263.66	18.66	4.018
M36A	242.80	234.42	-8.38	-1.803
M37A	250.80	255.15	4.35	0.936
M38A	279.30	278.15	-1.15	-0.247
M39A	288.90	294.62	5.72	1.231
M40A	332.00	319.15	-12.85	-2.767
M41A	327.60	332.03	4.43	0.954
M42A	338.10	335.67	-2.43	-0.523
M43A	292.30	289.65	-2.65	-0.570
M44A	292.80	281.56	-11.24	-2.419
M45A	320.90	309.48	-11.42	-2.458
M46A	283.40	286.18	2.78	0.599
M47B	283.20	277.97	-5.23	-1.126
M48A	275.50	268.89	-6.61	-1.424
M49A	203.30	214.86	11.56	2.488
M50B	-3.80	-9.70	-5.90	-1.271
M51B	156.10	165.51	9.41	2.025
M52B	-12.30	-14.87	-2.57	-0.553
M53B	263.80	267.97	4.17	0.897
M54B	237.40	245.00	7.60	1.637
M55B	280.10	270.15	-9.95	-2.141
M56B	376.80	380.90	4.10	0.883
M57B	431.80	414.72	-17.08	-3.678
M58B	370.10	367.75	-2.35	-0.505
M59B	241.00	230.94	-10.06	-2.167
M60B	340.10	346.57	6.47	1.392
M61B	355.10	358.99	3.89	0.838
M62B	336.10	330.78	-5.32	-1.146
749D	-3.80	-2.71	1.09	0.234
748H	8.00	-3.50	-11.50	-2.477
758D	3.70	-3.79	-7.49	-1.613
749A	-13.20	0.28	13.48	2.902
769	-16.80	-15.64	1.16	0.250
240A	-6.90	-5.77	1.13	0.244
271N	-28.70	-28.70	0.00	0.000

Note: Head > 1.e+20 denotes dry well

PVLF-SENSITIVITY CASE #19 - ZONE 1 (HILLSIDE RES.) RECHARGE * 2

Root mean square of residuals	25.7	ft
Absolute maximum residual	58.1	ft
Correlation -model vs. obs	0.987	

WELL	H(obs.) (ft)	H(model) (ft)	RESIDUAL (ft)	PERCENTAGE OF MAX HEAD DIFFERENCE
M23A	198.70	207.11	8.41	1.810
M24A	190.60	181.48	-9.12	-1.964
M25A	189.80	219.90	30.10	6.479
M26A	-2.70	4.01	6.71	1.444
M30B	241.20	261.13	19.93	4.290
M32B	286.70	270.02	-16.68	-3.591
M33B	274.10	269.59	-4.51	-0.970
M34B	288.20	274.62	-13.58	-2.924
M35B	245.00	275.33	30.33	6.530
M36A	242.80	248.78	5.98	1.286
M37A	250.80	272.86	22.06	4.748
M38A	279.30	300.10	20.80	4.478
M39A	288.90	329.58	40.68	8.759
M40A	332.00	359.65	27.65	5.953
M41A	327.60	374.19	46.59	10.029
M42A	338.10	378.72	40.62	8.745
M43A	292.30	311.30	19.00	4.090
M44A	292.80	301.71	8.91	1.918
M45A	320.90	335.15	14.25	3.067
M46A	283.40	300.76	17.36	3.738
M47B	283.20	288.87	5.67	1.222
M48A	275.50	278.48	2.98	0.641
M49A	203.30	217.47	14.17	3.050
M50B	-3.80	6.07	9.87	2.124
M51B	156.10	170.59	14.49	3.120
M52B	-12.30	-10.94	1.36	0.292
M53B	263.80	286.13	22.33	4.807
M54B	237.40	250.83	13.43	2.892
M55B	280.10	281.64	1.54	0.331
M56B	376.80	421.78	44.98	9.684
M57B	431.80	475.38	43.58	9.383
M58B	370.10	416.64	46.54	10.020
M59B	241.00	244.36	3.36	0.724
M60B	340.10	392.93	52.83	11.374
M61B	355.10	408.81	53.71	11.563
M62B	336.10	394.18	58.08	12.505
749D	-3.80	-0.27	3.53	0.760
748H	8.00	-1.60	-9.60	-2.068
758D	3.70	-2.12	-5.82	-1.253
749A	-13.20	4.66	17.86	3.844
769	-16.80	-14.36	2.44	0.526
240A	-6.90	13.50	20.40	4.391
271N	-28.70	-28.70	0.00	0.000

Note: Head > 1.e+20 denotes dry well

PVLF-SENSITIVITY CASE #20 - ZONE 2 (IRRIGATED GRASSLAND) RECHARGE * 2

Root mean square of residuals	11.6	ft
Absolute maximum residual	28.2	ft
Correlation -model vs. obs	0.993	

WELL	H(obs.) (ft)	H(model) (ft)	RESIDUAL (ft)	PERCENTAGE OF MAX HEAD DIFFERENCE
M23A	198.70	204.35	5.65	1.217
M24A	190.60	179.19	-11.41	-2.456
M25A	189.80	218.00	28.20	6.071
M26A	-2.70	3.97	6.67	1.436
M30B	241.20	258.88	17.68	3.807
M32B	286.70	267.76	-18.94	-4.078
M33B	274.10	267.31	-6.79	-1.461
M34B	288.20	269.81	-18.39	-3.959
M35B	245.00	270.25	25.25	5.437
M36A	242.80	251.16	8.36	1.799
M37A	250.80	266.65	15.85	3.413
M38A	279.30	285.36	6.06	1.304
M39A	288.90	302.57	13.67	2.942
M40A	332.00	326.43	-5.57	-1.199
M41A	327.60	338.90	11.30	2.432
M42A	338.10	342.31	4.21	0.907
M43A	292.30	294.99	2.69	0.580
M44A	292.80	287.59	-5.21	-1.122
M45A	320.90	313.48	-7.42	-1.597
M46A	283.40	287.78	4.38	0.942
M47B	283.20	279.19	-4.01	-0.863
M48A	275.50	269.20	-6.30	-1.356
M49A	203.30	214.12	10.82	2.330
M50B	-3.80	6.12	9.92	2.135
M51B	156.10	169.76	13.66	2.942
M52B	-12.30	-10.81	1.49	0.321
M53B	263.80	275.74	11.94	2.571
M54B	237.40	243.10	5.70	1.227
M55B	280.10	269.44	-10.66	-2.294
M56B	376.80	382.25	5.45	1.174
M57B	431.80	416.91	-14.89	-3.207
M58B	370.10	372.03	1.93	0.416
M59B	241.00	250.04	9.04	1.946
M60B	340.10	353.00	12.90	2.776
M61B	355.10	365.26	10.16	2.187
M62B	336.10	338.39	2.29	0.492
749D	-3.80	-0.21	3.59	0.773
748H	8.00	-1.53	-9.53	-2.052
758D	3.70	-2.08	-5.78	-1.244
749A	-13.20	4.75	17.95	3.863
769	-16.80	-14.34	2.46	0.530
240A	-6.90	13.50	20.40	4.391
271N	-28.70	-28.70	0.00	0.000

Note: Head > 1.e+20 denotes dry well

PVLF-SENSITIVITY CASE #21 - ZONE 3 (PVLF) RECHARGE * 2

Root mean square of residuals	12.6	ft
Absolute maximum residual	28.3	ft
Correlation -model vs. obs	0.992	

WELL	H(obs.) (ft)	H(model) (ft)	RESIDUAL (ft)	PERCENTAGE OF MAX HEAD DIFFERENCE
M23A	198.70	204.37	5.67	1.220
M24A	190.60	179.19	-11.41	-2.457
M25A	189.80	218.07	28.27	6.085
M26A	-2.70	3.89	6.59	1.418
M30B	241.20	258.87	17.67	3.805
M32B	286.70	267.29	-19.41	-4.179
M33B	274.10	266.78	-7.32	-1.576
M34B	288.20	269.64	-18.56	-3.996
M35B	245.00	270.15	25.15	5.414
M36A	242.80	241.48	-1.32	-0.283
M37A	250.80	263.08	12.28	2.644
M38A	279.30	288.48	9.18	1.976
M39A	288.90	309.62	20.72	4.460
M40A	332.00	340.11	8.11	1.745
M41A	327.60	348.82	21.22	4.569
M42A	338.10	350.73	12.63	2.718
M43A	292.30	298.10	5.80	1.249
M44A	292.80	290.99	-1.81	-0.390
M45A	320.90	315.09	-5.81	-1.252
M46A	283.40	288.13	4.73	1.019
M47B	283.20	279.56	-3.64	-0.784
M48A	275.50	269.75	-5.75	-1.238
M49A	203.30	214.50	11.20	2.412
M50B	-3.80	6.02	9.82	2.114
M51B	156.10	169.72	13.62	2.933
M52B	-12.30	-11.00	1.30	0.279
M53B	263.80	276.23	12.43	2.676
M54B	237.40	243.23	5.83	1.255
M55B	280.10	269.61	-10.49	-2.259
M56B	376.80	381.83	5.03	1.083
M57B	431.80	416.67	-15.13	-3.256
M58B	370.10	375.84	5.74	1.236
M59B	241.00	237.70	-3.30	-0.710
M60B	340.10	361.03	20.93	4.505
M61B	355.10	372.85	17.75	3.822
M62B	336.10	340.63	4.53	0.975
749D	-3.80	-0.27	3.53	0.760
748H	8.00	-1.60	-9.60	-2.068
758D	3.70	-2.12	-5.82	-1.253
749A	-13.20	4.65	17.85	3.844
769	-16.80	-14.36	2.44	0.524
240A	-6.90	13.42	20.32	4.374
271N	-28.70	-28.70	0.00	0.000

Note: Head > 1.e+20 denotes dry well

PVLF-SENSITIVITY CASE #22 - ZONE 4 (WATER BODY) RECHARGE * 2

Root mean square of residuals	11.0	ft
Absolute maximum residual	27.8	ft
Correlation -model vs. obs	0.994	

WELL	H(obs.) (ft)	H(model) (ft)	RESIDUAL (ft)	PERCENTAGE OF MAX HEAD DIFFERENCE
M23A	198.70	204.10	5.40	1.163
M24A	190.60	178.97	-11.63	-2.505
M25A	189.80	217.65	27.85	5.995
M26A	-2.70	3.90	6.60	1.422
M30B	241.20	258.16	16.96	3.652
M32B	286.70	266.26	-20.44	-4.401
M33B	274.10	265.71	-8.39	-1.806
M34B	288.20	267.52	-20.68	-4.453
M35B	245.00	267.92	22.92	4.935
M36A	242.80	239.40	-3.40	-0.733
M37A	250.80	259.68	8.88	1.912
M38A	279.30	282.29	2.99	0.643
M39A	288.90	298.72	9.82	2.115
M40A	332.00	323.13	-8.87	-1.909
M41A	327.60	335.85	8.25	1.776
M42A	338.10	339.26	1.16	0.249
M43A	292.30	293.01	0.71	0.152
M44A	292.80	285.39	-7.41	-1.595
M45A	320.90	311.83	-9.07	-1.953
M46A	283.40	287.07	3.67	0.789
M47B	283.20	278.72	-4.48	-0.964
M48A	275.50	268.82	-6.68	-1.437
M49A	203.30	213.85	10.55	2.270
M50B	-3.80	6.06	9.86	2.123
M51B	156.10	169.44	13.34	2.872
M52B	-12.30	-10.98	1.32	0.284
M53B	263.80	272.19	8.39	1.806
M54B	237.40	242.87	5.47	1.177
M55B	280.10	269.09	-11.01	-2.369
M56B	376.80	380.89	4.09	0.881
M57B	431.80	415.14	-16.66	-3.587
M58B	370.10	369.87	-0.23	-0.049
M59B	241.00	235.97	-5.03	-1.083
M60B	340.10	349.90	9.80	2.111
M61B	355.10	362.17	7.07	1.521
M62B	336.10	333.48	-2.62	-0.564
749D	-3.80	-0.21	3.59	0.772
748H	8.00	-1.48	-9.48	-2.040
758D	3.70	-2.00	-5.70	-1.226
749A	-13.20	4.74	17.94	3.862
769	-16.80	-14.35	2.45	0.527
240A	-6.90	13.46	20.36	4.384
271N	-28.70	-28.70	0.00	0.000

Note: Head > 1.e+20 denotes dry well

PVLF-SENSITIVITY CASE #23 - ZONE 5 (VACANT GRASSLAND) RECHARGE * 2

Root mean square of residuals	11.0	ft
Absolute maximum residual	27.8	ft
Correlation -model vs. obs	0.994	

WELL	H(obs.) (ft)	H(model) (ft)	RESIDUAL (ft)	PERCENTAGE OF MAX HEAD DIFFERENCE
M23A	198.70	204.10	5.40	1.163
M24A	190.60	178.96	-11.64	-2.505
M25A	189.80	217.63	27.83	5.992
M26A	-2.70	3.88	6.58	1.416
M30B	241.20	258.13	16.93	3.645
M32B	286.70	266.19	-20.51	-4.415
M33B	274.10	265.65	-8.45	-1.819
M34B	288.20	267.38	-20.82	-4.481
M35B	245.00	267.79	22.79	4.906
M36A	242.80	239.26	-3.54	-0.763
M37A	250.80	259.46	8.66	1.865
M38A	279.30	281.89	2.59	0.558
M39A	288.90	298.04	9.14	1.968
M40A	332.00	322.55	-9.45	-2.035
M41A	327.60	335.22	7.62	1.641
M42A	338.10	338.77	0.67	0.145
M43A	292.30	292.71	0.41	0.087
M44A	292.80	284.97	-7.83	-1.687
M45A	320.90	311.68	-9.22	-1.985
M46A	283.40	287.04	3.64	0.783
M47B	283.20	278.70	-4.50	-0.969
M48A	275.50	268.81	-6.69	-1.441
M49A	203.30	213.84	10.54	2.270
M50B	-3.80	6.03	9.83	2.117
M51B	156.10	169.42	13.32	2.868
M52B	-12.30	-11.00	1.30	0.281
M53B	263.80	271.93	8.13	1.750
M54B	237.40	242.86	5.46	1.176
M55B	280.10	269.08	-11.02	-2.372
M56B	376.80	380.86	4.06	0.874
M57B	431.80	415.09	-16.71	-3.598
M58B	370.10	369.65	-0.45	-0.096
M59B	241.00	235.85	-5.15	-1.108
M60B	340.10	349.50	9.40	2.025
M61B	355.10	361.79	6.69	1.440
M62B	336.10	334.11	-1.99	-0.427
749D	-3.80	-0.27	3.53	0.760
748H	8.00	-1.60	-9.60	-2.068
758D	3.70	-2.12	-5.82	-1.253
749A	-13.20	4.65	17.85	3.844
769	-16.80	-14.36	2.44	0.525
240A	-6.90	13.42	20.32	4.376
271N	-28.70	-28.70	0.00	0.000

Note: Head > 1.e+20 denotes dry well

PVLF-SENSITIVITY CASE #24 - ZONE 6 (VACANT LAND - DIRT COVERED) RECHARG

Root mean square of residuals	11.0	ft
Absolute maximum residual	27.8	ft
Correlation -model vs. obs	0.994	

WELL	H(obs.) (ft)	H(model) (ft)	RESIDUAL (ft)	PERCENTAGE OF MAX HEAD DIFFERENCE
M23A	198.70	204.10	5.40	1.163
M24A	190.60	178.96	-11.64	-2.505
M25A	189.80	217.64	27.84	5.994
M26A	-2.70	3.88	6.58	1.417
M30B	241.20	258.15	16.95	3.648
M32B	286.70	266.25	-20.45	-4.402
M33B	274.10	265.72	-8.38	-1.805
M34B	288.20	267.47	-20.73	-4.463
M35B	245.00	267.87	22.87	4.924
M36A	242.80	240.01	-2.79	-0.600
M37A	250.80	259.85	9.05	1.948
M38A	279.30	281.92	2.62	0.564
M39A	288.90	298.00	9.10	1.960
M40A	332.00	322.22	-9.78	-2.104
M41A	327.60	334.88	7.28	1.567
M42A	338.10	338.43	0.33	0.071
M43A	292.30	292.64	0.34	0.072
M44A	292.80	284.93	-7.87	-1.694
M45A	320.90	311.63	-9.27	-1.997
M46A	283.40	287.03	3.63	0.781
M47B	283.20	278.69	-4.51	-0.970
M48A	275.50	268.80	-6.70	-1.442
M49A	203.30	213.84	10.54	2.269
M50B	-3.80	6.03	9.83	2.117
M51B	156.10	169.43	13.33	2.870
M52B	-12.30	-10.98	1.32	0.284
M53B	263.80	272.05	8.25	1.777
M54B	237.40	242.86	5.46	1.175
M55B	280.10	269.08	-11.02	-2.373
M56B	376.80	380.84	4.04	0.869
M57B	431.80	415.04	-16.76	-3.607
M58B	370.10	369.47	-0.63	-0.135
M59B	241.00	236.71	-4.29	-0.924
M60B	340.10	349.14	9.04	1.947
M61B	355.10	361.44	6.34	1.364
M62B	336.10	333.17	-2.93	-0.630
749D	-3.80	-0.27	3.53	0.760
748H	8.00	-1.60	-9.60	-2.068
758D	3.70	-2.12	-5.82	-1.253
749A	-13.20	4.66	17.86	3.844
769	-16.80	-14.36	2.44	0.526
240A	-6.90	13.43	20.33	4.376
271N	-28.70	-28.70	0.00	0.000

Note: Head > 1.e+20 denotes dry well

PVLF-SENSITIVITY CASE #25 - ZONE 7 (TORRANCE AIRPORT) RECHARGE * 2

Root mean square of residuals	11.0	ft
Absolute maximum residual	27.9	ft
Correlation -model vs. obs	0.994	

WELL	H(obs.) (ft)	H(model) (ft)	RESIDUAL (ft)	PERCENTAGE OF MAX HEAD DIFFERENCE
M23A	198.70	204.25	5.55	1.194
M24A	190.60	179.08	-11.52	-2.480
M25A	189.80	217.74	27.94	6.014
M26A	-2.70	3.88	6.58	1.417
M30B	241.20	258.13	16.93	3.644
M32B	286.70	266.07	-20.63	-4.442
M33B	274.10	265.52	-8.58	-1.847
M34B	288.20	267.21	-20.99	-4.520
M35B	245.00	267.60	22.60	4.866
M36A	242.80	239.00	-3.80	-0.818
M37A	250.80	259.19	8.39	1.806
M38A	279.30	281.56	2.26	0.486
M39A	288.90	297.52	8.62	1.856
M40A	332.00	321.83	-10.17	-2.189
M41A	327.60	334.56	6.96	1.499
M42A	338.10	338.13	0.03	0.007
M43A	292.30	292.42	0.12	0.026
M44A	292.80	284.67	-8.13	-1.751
M45A	320.90	311.49	-9.41	-2.025
M46A	283.40	287.00	3.60	0.775
M47B	283.20	278.67	-4.53	-0.975
M48A	275.50	268.81	-6.69	-1.439
M49A	203.30	213.97	10.67	2.298
M50B	-3.80	6.02	9.82	2.115
M51B	156.10	169.47	13.37	2.877
M52B	-12.30	-11.01	1.29	0.278
M53B	263.80	271.66	7.86	1.693
M54B	237.40	242.95	5.55	1.195
M55B	280.10	269.12	-10.98	-2.363
M56B	376.80	380.83	4.03	0.868
M57B	431.80	415.01	-16.79	-3.614
M58B	370.10	369.31	-0.79	-0.169
M59B	241.00	235.60	-5.40	-1.162
M60B	340.10	348.86	8.76	1.886
M61B	355.10	361.17	6.07	1.306
M62B	336.10	332.71	-3.39	-0.730
749D	-3.80	-0.27	3.53	0.760
748H	8.00	-1.60	-9.60	-2.067
758D	3.70	-2.12	-5.82	-1.253
749A	-13.20	4.66	17.86	3.844
769	-16.80	-14.36	2.44	0.525
240A	-6.90	13.42	20.32	4.375
271N	-28.70	-28.70	0.00	0.000

Note: Head > 1.e+20 denotes dry well

PVLF-SENSITIVITY CASE #26 - ZONE 8 (DRAINAGE) RECHARGE * 2

Root mean square of residuals	11.0	ft
Absolute maximum residual	27.9	ft
Correlation -model vs. obs	0.994	

WELL	H(obs.) (ft)	H(model) (ft)	RESIDUAL (ft)	PERCENTAGE OF MAX HEAD DIFFERENCE
M23A	198.70	204.25	5.55	1.195
M24A	190.60	179.08	-11.52	-2.480
M25A	189.80	217.74	27.94	6.014
M26A	-2.70	3.88	6.58	1.416
M30B	241.20	258.13	16.93	3.645
M32B	286.70	266.07	-20.63	-4.442
M33B	274.10	265.52	-8.58	-1.847
M34B	288.20	267.21	-20.99	-4.519
M35B	245.00	267.61	22.61	4.867
M36A	242.80	239.01	-3.79	-0.817
M37A	250.80	259.20	8.40	1.808
M38A	279.30	281.57	2.27	0.489
M39A	288.90	297.54	8.64	1.860
M40A	332.00	321.86	-10.14	-2.183
M41A	327.60	334.61	7.01	1.508
M42A	338.10	338.18	0.08	0.018
M43A	292.30	292.44	0.14	0.031
M44A	292.80	284.68	-8.12	-1.748
M45A	320.90	311.72	-9.18	-1.975
M46A	283.40	287.01	3.61	0.778
M47B	283.20	278.68	-4.52	-0.973
M48A	275.50	268.82	-6.68	-1.438
M49A	203.30	213.98	10.68	2.299
M50B	-3.80	6.02	9.82	2.114
M51B	156.10	169.46	13.36	2.877
M52B	-12.30	-11.02	1.28	0.277
M53B	263.80	271.67	7.87	1.694
M54B	237.40	242.96	5.56	1.196
M55B	280.10	269.13	-10.97	-2.361
M56B	376.80	380.86	4.06	0.874
M57B	431.80	415.07	-16.73	-3.602
M58B	370.10	369.48	-0.62	-0.133
M59B	241.00	235.61	-5.39	-1.161
M60B	340.10	348.92	8.82	1.899
M61B	355.10	361.22	6.12	1.318
M62B	336.10	332.73	-3.37	-0.727
749D	-3.80	-0.27	3.53	0.760
748H	8.00	-1.60	-9.60	-2.068
758D	3.70	-2.12	-5.82	-1.253
749A	-13.20	4.65	17.85	3.844
769	-16.80	-14.36	2.44	0.524
240A	-6.90	13.42	20.32	4.374
271N	-28.70	-28.70	0.00	0.000

Note: Head > 1.e+20 denotes dry well

PVLF-SENSITIVITY CASE #27 - ZONE 9 (HIGH INDUSTRY) RECHARGE * 2

Root mean square of residuals	11.0	ft
Absolute maximum residual	27.9	ft
Correlation -model vs. obs	0.994	

WELL	H(obs.) (ft)	H(model) (ft)	RESIDUAL (ft)	PERCENTAGE OF MAX HEAD DIFFERENCE
M23A	198.70	204.25	5.55	1.195
M24A	190.60	179.08	-11.52	-2.480
M25A	189.80	217.74	27.94	6.014
M26A	-2.70	3.89	6.59	1.418
M30B	241.20	258.13	16.93	3.644
M32B	286.70	266.07	-20.63	-4.442
M33B	274.10	265.52	-8.58	-1.847
M34B	288.20	267.21	-20.99	-4.520
M35B	245.00	267.60	22.60	4.866
M36A	242.80	239.00	-3.80	-0.818
M37A	250.80	259.19	8.39	1.806
M38A	279.30	281.56	2.26	0.486
M39A	288.90	297.52	8.62	1.856
M40A	332.00	321.83	-10.17	-2.189
M41A	327.60	334.56	6.96	1.499
M42A	338.10	338.13	0.03	0.007
M43A	292.30	292.42	0.12	0.026
M44A	292.80	284.67	-8.13	-1.751
M45A	320.90	311.49	-9.41	-2.025
M46A	283.40	287.00	3.60	0.775
M47B	283.20	278.67	-4.53	-0.975
M48A	275.50	268.81	-6.69	-1.439
M49A	203.30	213.98	10.68	2.298
M50B	-3.80	6.03	9.83	2.117
M51B	156.10	169.47	13.37	2.878
M52B	-12.30	-11.01	1.29	0.278
M53B	263.80	271.66	7.86	1.693
M54B	237.40	242.95	5.55	1.195
M55B	280.10	269.12	-10.98	-2.363
M56B	376.80	380.83	4.03	0.868
M57B	431.80	415.01	-16.79	-3.614
M58B	370.10	369.31	-0.79	-0.169
M59B	241.00	235.60	-5.40	-1.162
M60B	340.10	348.86	8.76	1.886
M61B	355.10	361.17	6.07	1.306
M62B	336.10	332.71	-3.39	-0.730
749D	-3.80	-0.26	3.54	0.761
748H	8.00	-1.59	-9.59	-2.065
758D	3.70	-2.10	-5.80	-1.248
749A	-13.20	4.66	17.86	3.846
769	-16.80	-14.36	2.44	0.526
240A	-6.90	13.43	20.33	4.377
271N	-28.70	-28.70	0.00	0.000

Note: Head > 1.e+20 denotes dry well

PVLF-SENSITIVITY CASE #28 - ZONE 0 (BACKGROUND) RECHARGE * 2

Root mean square of residuals	17.9	ft
Absolute maximum residual	44.1	ft
Correlation -model vs. obs	0.988	

WELL	H(obs.) (ft)	H(model) (ft)	RESIDUAL (ft)	PERCENTAGE OF MAX HEAD DIFFERENCE
M23A	198.70	204.33	5.63	1.211
M24A	190.60	179.27	-11.33	-2.440
M25A	189.80	219.40	29.60	6.372
M26A	-2.70	4.78	7.48	1.610
M30B	241.20	262.40	21.20	4.564
M32B	286.70	276.13	-10.57	-2.275
M33B	274.10	275.86	1.76	0.379
M34B	288.20	280.11	-8.09	-1.742
M35B	245.00	280.66	35.66	7.677
M36A	242.80	284.08	41.28	8.887
M37A	250.80	290.89	40.09	8.632
M38A	279.30	298.57	19.27	4.148
M39A	288.90	319.53	30.63	6.594
M40A	332.00	338.35	6.35	1.368
M41A	327.60	348.06	20.46	4.404
M42A	338.10	350.61	12.51	2.692
M43A	292.30	302.54	10.24	2.204
M44A	292.80	297.12	4.32	0.930
M45A	320.90	317.96	-2.94	-0.634
M46A	283.40	288.72	5.32	1.145
M47B	283.20	279.86	-3.34	-0.720
M48A	275.50	269.64	-5.86	-1.262
M49A	203.30	214.22	10.92	2.352
M50B	-3.80	6.79	10.59	2.280
M51B	156.10	171.34	15.24	3.281
M52B	-12.30	-9.41	2.89	0.623
M53B	263.80	290.91	27.11	5.835
M54B	237.40	243.21	5.81	1.250
M55B	280.10	269.70	-10.40	-2.238
M56B	376.80	382.08	5.28	1.137
M57B	431.80	416.99	-14.81	-3.189
M58B	370.10	376.43	6.33	1.362
M59B	241.00	285.11	44.11	9.495
M60B	340.10	360.55	20.45	4.402
M61B	355.10	372.31	17.21	3.705
M62B	336.10	346.75	10.65	2.293
749D	-3.80	-0.13	3.67	0.790
748H	8.00	-1.45	-9.45	-2.035
758D	3.70	-1.92	-5.62	-1.211
749A	-13.20	5.05	18.25	3.928
769	-16.80	-14.15	2.65	0.570
240A	-6.90	14.13	21.03	4.528
271N	-28.70	-28.70	0.00	0.000

Note: Head > 1.e+20 denotes dry well

APPENDIX E

STATISTICS OF HYDRAULIC CONDUCTIVITY ANALYSES

PALOS VERDES LANDFILL - 12482-009-128
STATISTICAL ANALYSIS OF K VALUES
REVISED BY TAJ 9/24/91

FILL - Qo

Test # (n)	Test Freq.	Standard Deviation	Log K (cm/sec)	K (cm/sec)	Test Type	Boring/ Well
1	0.0500	-1.646	-4.89	1.30E-05	S	M49A
2	0.1500	-1.038	-4.43	3.70E-05	S	M48A
3	0.2500	-0.676	-4.42	3.80E-05	S	M46A2
4	0.3500	-0.388	-4.38	4.20E-05	S	M25A
5	0.4500	-0.128	-4.26	5.50E-05	S	M23A
6	0.5500	0.124	-4.07	8.50E-05	S	M38A
7	0.6500	0.384	-3.91	1.24E-04	S	M37A
8	0.7500	0.672	-3.48	3.34E-04	S	M41A
9	0.8500	1.034	-2.92	1.20E-03	S	M36A
10	0.9500	1.642	-2.45	3.55E-03	S	M44A

0	ARITHMETIC MEAN LOG K	-3.920
1	ARITH. MEAN LOG K + 1 ST	-3.202
-1	ARITH. MEAN LOG K - 1 ST	-4.637
	GEOMETRIC MEAN K	1.18E-04
	GEO. MEAN K + 1 STD.	6.28E-04
	GEO MEAN K - 1 STD.	2.31E-05

S = Slug Test

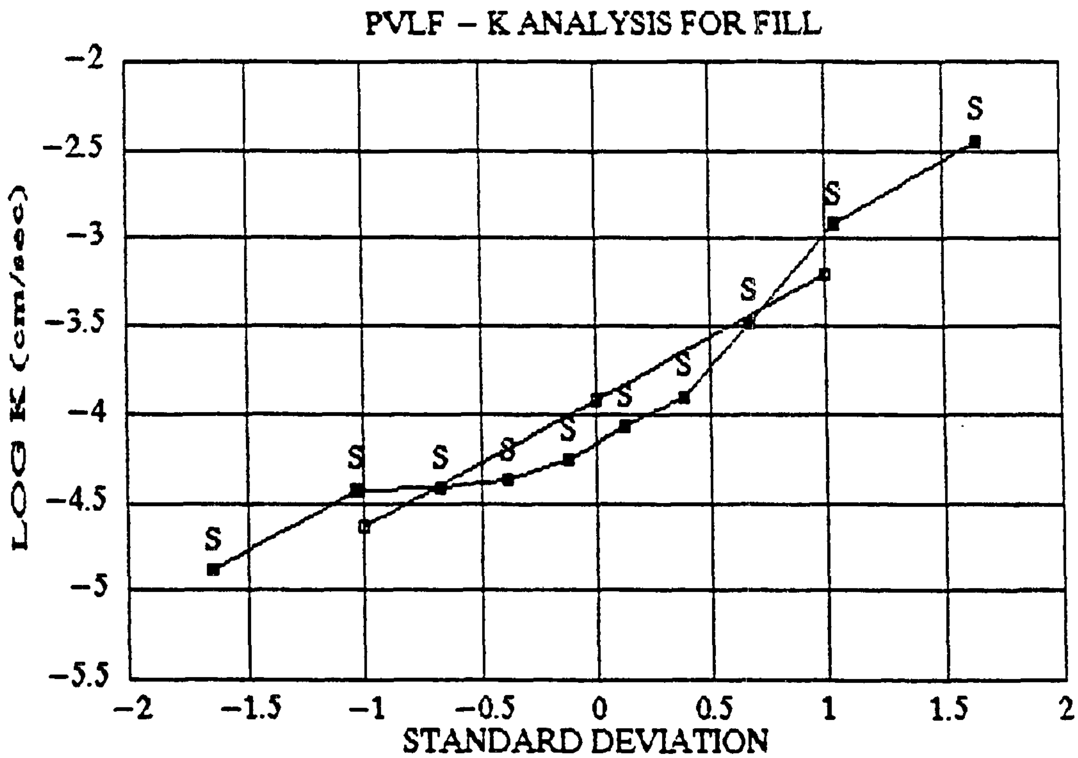

PALOS VERDES LANDFILL - 12482-009-128
STATISTICAL ANALYSIS OF K VALUES
REVISED BY TAJ 9/25/91

SAN PEDRO SAND - Qsp

Test (n)	Test Freq.	Standard Deviation	Log K (cm/sec)	K (cm/sec)	Test Type	Boring/ Well
1	0.0625	-1.536	-5.004	9.90E-06	S	M26A
2	0.1875	-0.89	-4.180	6.60E-05	A	RFB13/M52B
3	0.3125	-0.49	-3.921	1.20E-04	A	RFB4/M51B
4	0.4375	-0.16	-3.444	3.60E-04	L	RFB14
5	0.5625	0.156	-3.179	6.62E-04	L	RFB13/M52B
6	0.6875	0.486	-3.094	8.06E-04	L	RFB17
7	0.8125	0.886	-3.041	9.10E-04	L	RFB3/M50B
8	0.9375	1.532	-2.757	1.75E-03	A	RFB3/M50B

0	ARITHMETIC MEAN LOG K	-3.578
1	AR. MEAN LOG K + 1 STD.	-2.880
-1	AR. MEAN LOG K - 1 STD.	-4.275
	GEOMETRIC MEAN K	2.64E-04
	GEO. MEAN K + 1 STD.	1.32E-03
	GEO. MEAN K - 1 STD.	5.31E-05

A = Aquifer Test
L = Lab Test
S = Slug Test

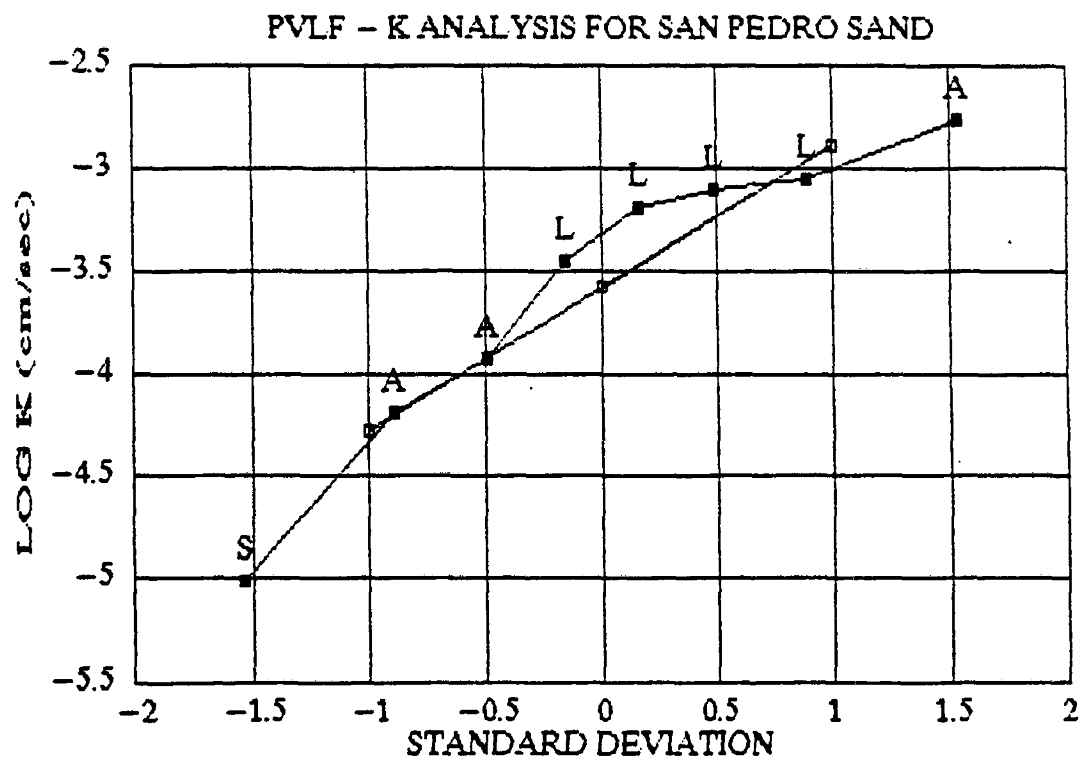

PALOS VERDES LANDFILL - 12482-009-128
STATISTICAL ANALYSIS OF K VALUES
REVISED BY TAJ 9/23/91

MALAGA MUDSTONE - Tm

Test # (n)	Test Freq.	Standard Deviation	Log K (cm/sec)	K (cm/sec)	Test Type	Boring/ Well
1	0.0217	-2.022	-7.96	1.10E-08	L	C-3
2	0.0652	-1.514	-7.77	1.70E-08	L	C-1
3	0.1087	-1.236	-7.60	2.50E-08	L	C-3
4	0.1522	-1.03	-7.36	4.40E-08	L	RFB 15
5	0.1957	-0.86	-7.21	6.10E-08	L	C-1
6	0.2391	-0.712	-7.21	6.16E-08	P	L3/M62B
7	0.2826	-0.578	-7.19	6.47E-08	P	L3/M62B
8	0.3261	-0.452	-7.14	7.23E-08	L	RFB 12
9	0.3696	-0.336	-6.98	1.05E-07	P	RFB 6
10	0.4130	-0.222	-6.92	1.21E-07	P	RFB 7
11	0.4565	-0.112	-6.79	1.61E-07	P	RFB 6
12	0.5000	-0.002	-6.58	2.63E-07	P	RFB 7
13	0.5435	0.108	-6.54	2.91E-07	P	RFB 12
14	0.5870	0.218	-6.34	4.57E-07	P	L3/M62B
15	0.6304	0.332	-6.20	6.30E-07	P	RFB 12
16	0.6739	0.448	-6.06	8.65E-07	P	RFB 32
17	0.7174	0.574	-5.96	1.10E-06	L	RFB 10
18	0.7609	0.708	-5.81	1.54E-06	P	RFB 12
19	0.8043	0.856	-5.01	9.77E-06	L	RFB 7
20	0.8478	1.026	-2.99	1.03E-03	S	M40A
21	0.8913	1.232	-2.55	2.79E-03	S	M34B
22	0.9348	1.51	-2.39	4.12E-03	S	M32B
23	0.9783	2.018	-2.35	4.50E-03	S	M39A

	0	ARITHMETIC MEAN LOG K	-6.039
L = Lab	1	AR. MEAN LOG K + 1 STD.	-4.313
P = Packer	-1	AR. MEAN LOG K - 1 STD.	-7.766
S = Slug		GEOMETRIC MEAN K	9.13E-07
		GEO. MEAN K + 1 STD.	4.87E-05
		GEO. MEAN K - 1 STD.	1.71E-08

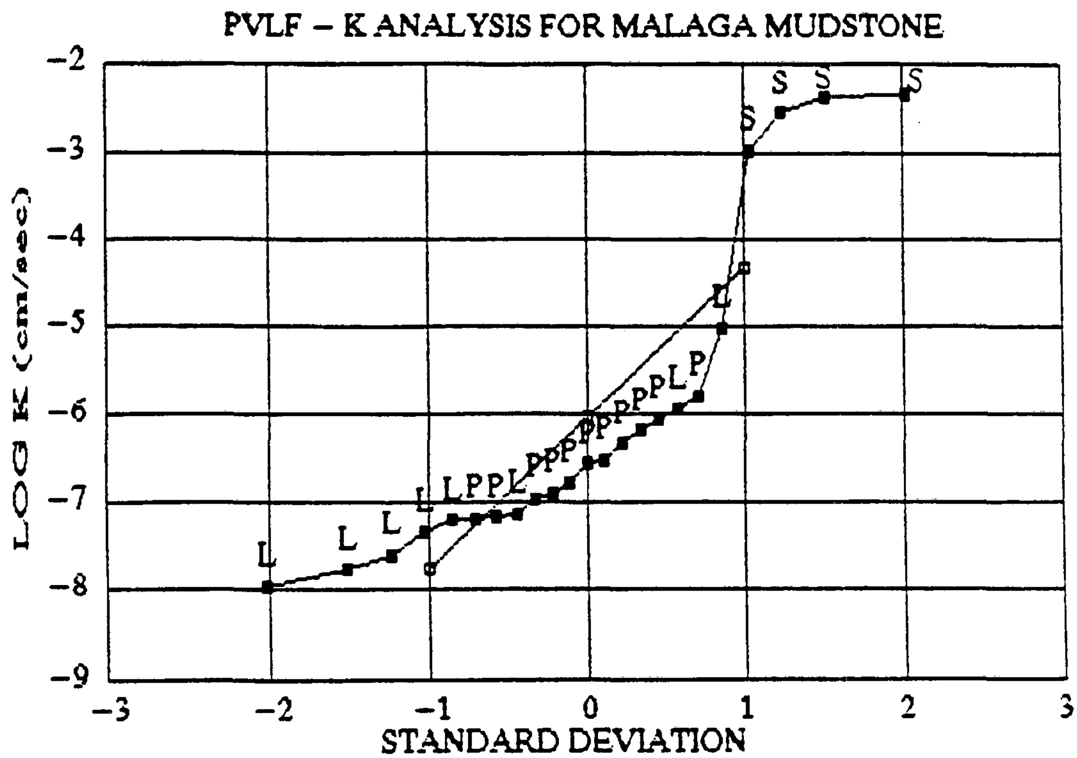
PVLF – K ANALYSIS FOR MALAGA MUDSTONE
LOG K (cm/sec)
STANDARD DEVIATION
−2
−3
−4
−5
−6
−7
−8
−9
−3
−2
−1
0
1
2
3
L
L
L
L
LPPL
PPP
PPPPPPL
P
L
S
S
S
S

PALOS VERDES LANDFILL - 12482-009-128
STATISTICAL ANALYSIS OF K VALUES
REVISED BY TAJ 9/24/91

VALMONTE DIATOMITE - Tv

Test # (n)	Test Freq.	Standard Deviation	Log K (cm/sec)	K (cm/sec)	Test Type	Boring/ Well
1	0.0313	-1.864	-7.157	6.97E-08	P	RFB 7
2	0.0938	-1.32	-6.975	1.06E-07	P	RFB 11
3	0.1563	-1.012	-6.959	1.10E-07	P	RFB 19
4	0.2188	-0.778	-6.827	1.49E-07	P	RFB16/M53B
5	0.2813	-0.582	-6.783	1.65E-07	P	RFB 11
6	0.3438	-0.404	-6.706	1.97E-07	P	RFB 7
7	0.4063	-0.24	-6.633	2.33E-07	P	RFB 32
8	0.4688	-0.08	-6.295	5.07E-07	P	RFB 32
9	0.5313	0.076	-6.039	9.14E-07	P	RFB 11
10	0.5938	0.236	-5.818	1.52E-06	P	RFB24/M56B
11	0.6563	0.4	-5.350	4.47E-06	P	RFB 30A
12	0.7188	0.578	-5.184	6.55E-06	P	RFB 30A
13	0.7813	0.774	-3.886	1.30E-04	S	M24A
14	0.8438	1.008	-3.747	1.79E-04	P	RFB 19
15	0.9063	1.316	-3.359	4.38E-04	S	M42A
16	0.9688	1.86	-2.642	2.28E-03	S	M43A
		0		ARITHMETIC MEAN LOG K		-5.647
		1		AR. MEAN LOG K + 1 STD.		-4.224
		-1		AR. MEAN LOG K - 1 STD.		-7.071
				GEOMETRIC MEAN K		2.12E-06
				GEO. MEAN K + 1 STD.		5.97E-05
				GEO. MEAN K - 1 STD.		8.49E-08

P = Packer Test
S = Slug Test

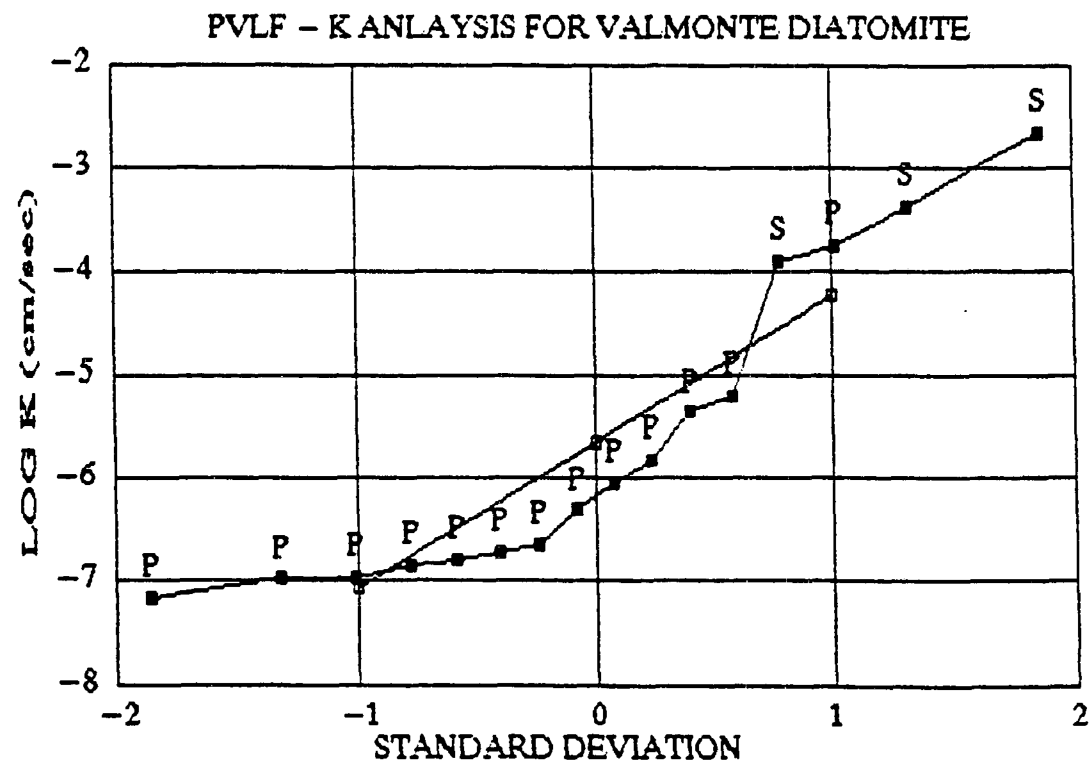

PALOS VERDES LANDFILL - 12482-009-128
STATISTICAL ANALYSIS OF K VALUES
REVISED BY TAJ 9/24/91

ALTAMIRA SHALE

Test # (n)	Test Freq.	Standard Deviation	Log K (cm/sec)	K (cm/sec)	Test Type	Boring/ Well
1	0.0333	-1.836	-6.68	2.09E-07	P	RFB 22
2	0.1000	-1.284	-6.44	3.64E-07	P	RFB 22
3	0.1667	-0.97	-6.37	4.22E-07	P	RFB25/M57B
4	0.2333	-0.73	-6.14	7.18E-07	P	RFB29/M60B
5	0.3000	-0.526	-5.97	1.08E-06	P	RFB 22
6	0.3667	-0.342	-5.96	1.10E-06	P	RFB25/M57B
7	0.4333	-0.17	-5.78	1.67E-06	P	RFB24/M56B
8	0.5000	-0.002	-4.84	1.45E-05	P	RFB25/M57B
9	0.5667	0.166	-4.70	2.00E-05	P	RFB 1
10	0.6333	0.338	-4.02	9.53E-05	P	RFB 1
11	0.7000	0.522	-3.91	1.24E-04	P	RFB 1
12	0.7667	0.726	-3.84	1.43E-04	P	RFB29/M60B
13	0.8333	0.966	-3.63	2.36E-04	P	RFB29/M60B
14	0.9000	1.28	-3.43	3.70E-04	S	M47B
15	0.9667	1.832	-2.89	1.30E-03	S	M45A2

0	ARITHMETIC MEAN LOG K	-4.973
1	AR. MEAN LOG K + 1 STD.	-3.736
-1	AR. MEAN LOG K - 1 STD.	-6.210
	GEOMETRIC MEAN K	1.06E-05
	GEO. MEAN K + 1 STD.	1.84E-04
	GEO. MEAN K - 1 STD.	6.17E-07

S = Slug Test
P = Packer Test

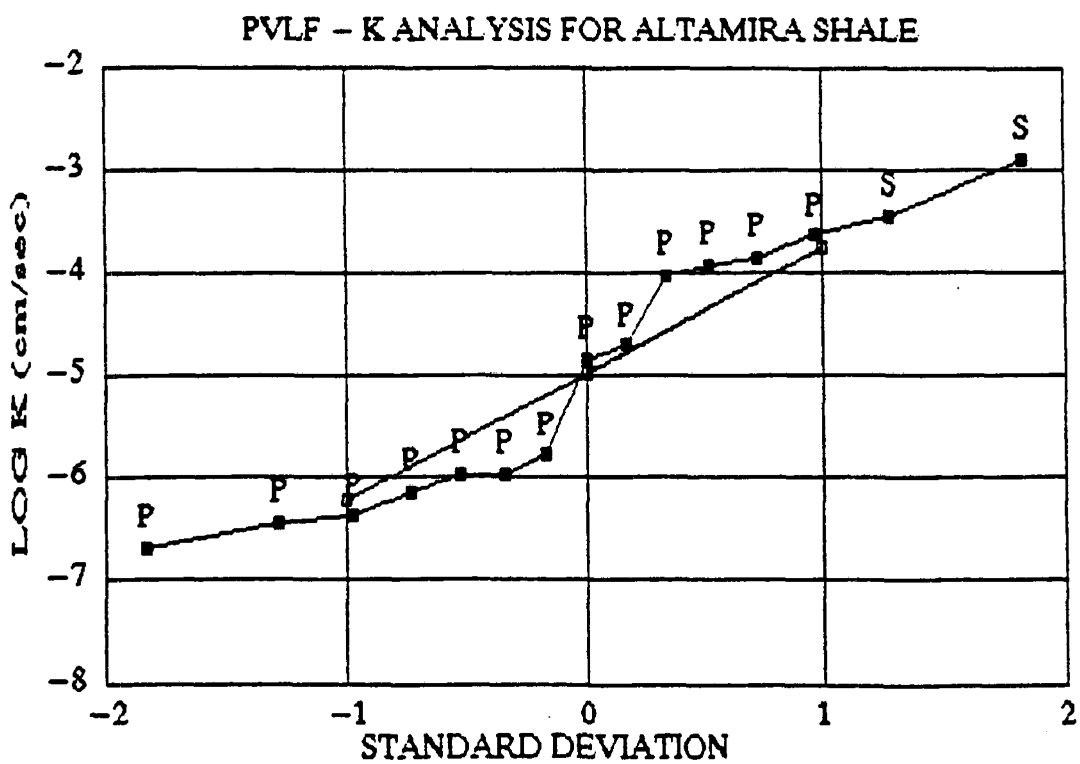

PALOS VERDES LANDFILL - 12482-009-128
STATISTICAL ANALYSIS OF K VALUES
REVISED BY TAJ 9/24/91

FILL - Qo

Test # (n)	Test Freq.	Standard Deviation	Log K (cm/sec)	K (cm/sec)	Test Type	Boring/ Well
1	0.0500	-1.646	-4.89	1.30E-05	S	M49A
2	0.1500	-1.038	-4.43	3.70E-05	S	M48A
3	0.2500	-0.676	-4.42	3.80E-05	S	M46A2
4	0.3500	-0.388	-4.38	4.20E-05	S	M25A
5	0.4500	-0.128	-4.26	5.50E-05	S	M23A
6	0.5500	0.124	-4.07	8.50E-05	S	M38A
7	0.6500	0.384	-3.91	1.24E-04	S	M37A
8	0.7500	0.672	-3.48	3.34E-04	S	M41A
9	0.8500	1.034	-2.92	1.20E-03	S	M36A
10	0.9500	1.642	-2.45	3.55E-03	S	M44A

0	ARITHMETIC MEAN LOG K	-3.920
1	ARITH. MEAN LOG K + 1 ST	-3.202
-1	ARITH. MEAN LOG K - 1 ST	-4.637
	GEOMETRIC MEAN K	1.18E-04
	GEO. MEAN K + 1 STD.	6.28E-04
	GEO MEAN K - 1 STD.	2.31E-05

S = Slug Test

PVLF – K ANALYSIS FOR FILL

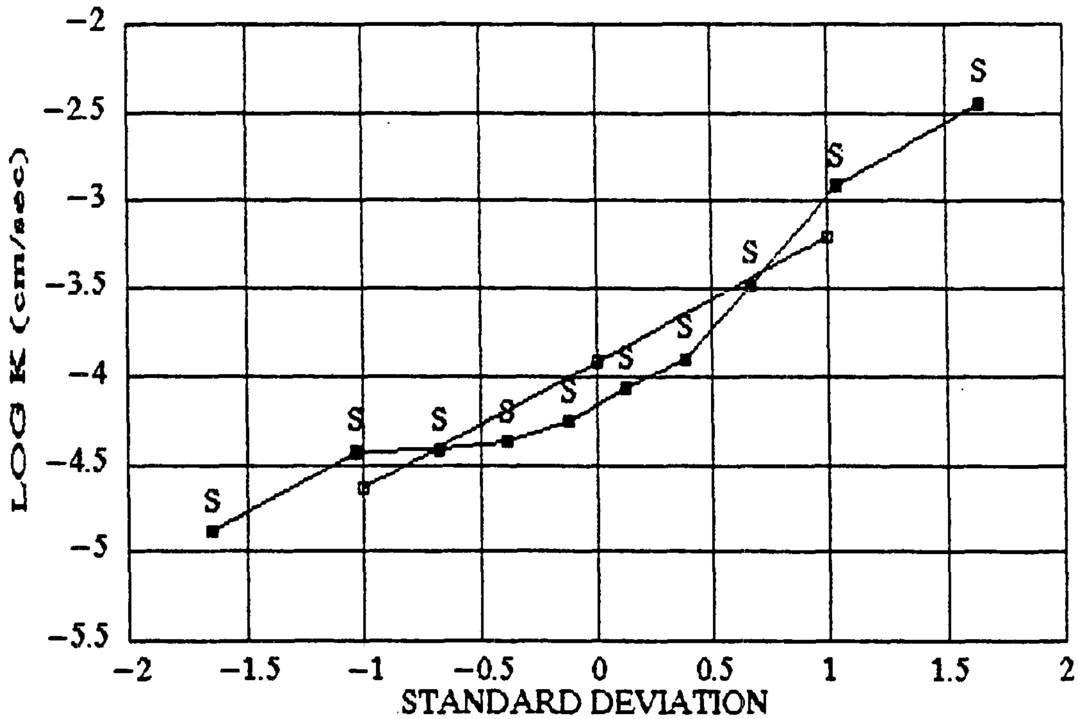

PALOS VERDES LANDFILL - 12482-009-128
STATISTICAL ANALYSIS OF K VALUES
REVISED BY TAJ 9/25/91

SAN PEDRO SAND - Qsp

Test (n)	Test Freq.	Standard Deviation	Log K (cm/sec)	K (cm/sec)	Test Type	Boring/ Well
1	0.0625	-1.536	-5.004	9.90E-06	S	M26A
2	0.1875	-0.89	-4.180	6.60E-05	A	RFB13/M52B
3	0.3125	-0.49	-3.921	1.20E-04	A	RFB4/M51B
4	0.4375	-0.16	-3.444	3.60E-04	L	RFB14
5	0.5625	0.156	-3.179	6.62E-04	L	RFB13/M52B
6	0.6875	0.486	-3.094	8.06E-04	L	RFB17
7	0.8125	0.886	-3.041	9.10E-04	L	RFB3/M50B
8	0.9375	1.532	-2.757	1.75E-03	A	RFB3/M50B

0	ARITHMETIC MEAN LOG K	-3.578
1	AR. MEAN LOG K + 1 STD.	-2.880
-1	AR. MEAN LOG K - 1 STD.	-4.275
	GEOMETRIC MEAN K	2.64E-04
	GEO. MEAN K + 1 STD.	1.32E-03
	GEO. MEAN K - 1 STD.	5.31E-05

A = Aquifer Test
L = Lab Test
S = Slug Test

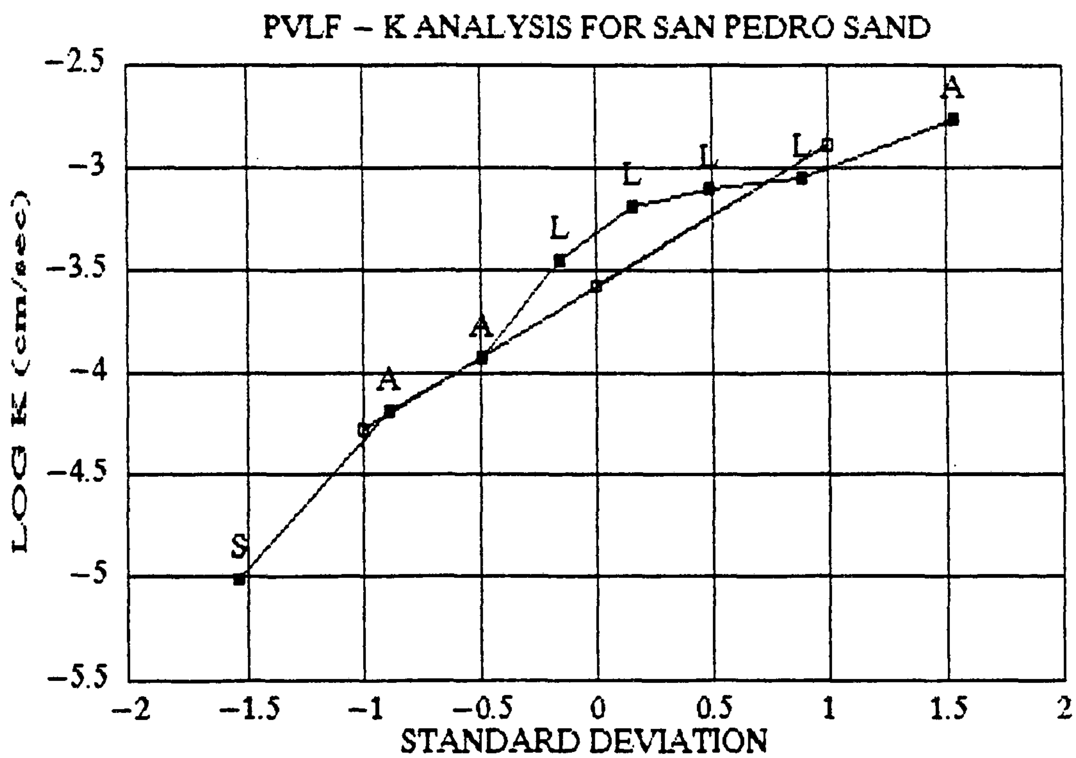

PALOS VERDES LANDFILL - 12482-009-128
STATISTICAL ANALYSIS OF K VALUES
REVISED BY TAJ 9/23/91

MALAGA MUDSTONE - Tm

Test # (n)	Test Freq.	Standard Deviation	Log K (cm/sec)	K (cm/sec)	Test Type	Boring/ Well
1	0.0217	-2.022	-7.96	1.10E-08	L	C-3
2	0.0652	-1.514	-7.77	1.70E-08	L	C-1
3	0.1087	-1.236	-7.60	2.50E-08	L	C-3
4	0.1522	-1.03	-7.36	4.40E-08	L	RFB 15
5	0.1957	-0.86	-7.21	6.10E-08	L	C-1
6	0.2391	-0.712	-7.21	6.16E-08	P	L3/M62B
7	0.2826	-0.578	-7.19	6.47E-08	P	L3/M62B
8	0.3261	-0.452	-7.14	7.23E-08	L	RFB 12
9	0.3696	-0.336	-6.98	1.05E-07	P	RFB 6
10	0.4130	-0.222	-6.92	1.21E-07	P	RFB 7
11	0.4565	-0.112	-6.79	1.61E-07	P	RFB 6
12	0.5000	-0.002	-6.58	2.63E-07	P	RFB 7
13	0.5435	0.108	-6.54	2.91E-07	P	RFB 12
14	0.5870	0.218	-6.34	4.57E-07	P	L3/M62B
15	0.6304	0.332	-6.20	6.30E-07	P	RFB 12
16	0.6739	0.448	-6.06	8.65E-07	P	RFB 32
17	0.7174	0.574	-5.96	1.10E-06	L	RFB 10
18	0.7609	0.708	-5.81	1.54E-06	P	RFB 12
19	0.8043	0.856	-5.01	9.77E-06	L	RFB 7
20	0.8478	1.026	-2.99	1.03E-03	S	M40A
21	0.8913	1.232	-2.55	2.79E-03	S	M34B
22	0.9348	1.51	-2.39	4.12E-03	S	M32B
23	0.9783	2.018	-2.35	4.50E-03	S	M39A

	0	ARITHMETIC MEAN LOG K	-6.039
L = Lab	1	AR. MEAN LOG K + 1 STD.	-4.313
P = Packer	-1	AR. MEAN LOG K - 1 STD.	-7.766
S = Slug		GEOMETRIC MEAN K	9.13E-07
		GEO. MEAN K + 1 STD.	4.87E-05
		GEO. MEAN K - 1 STD.	1.71E-08

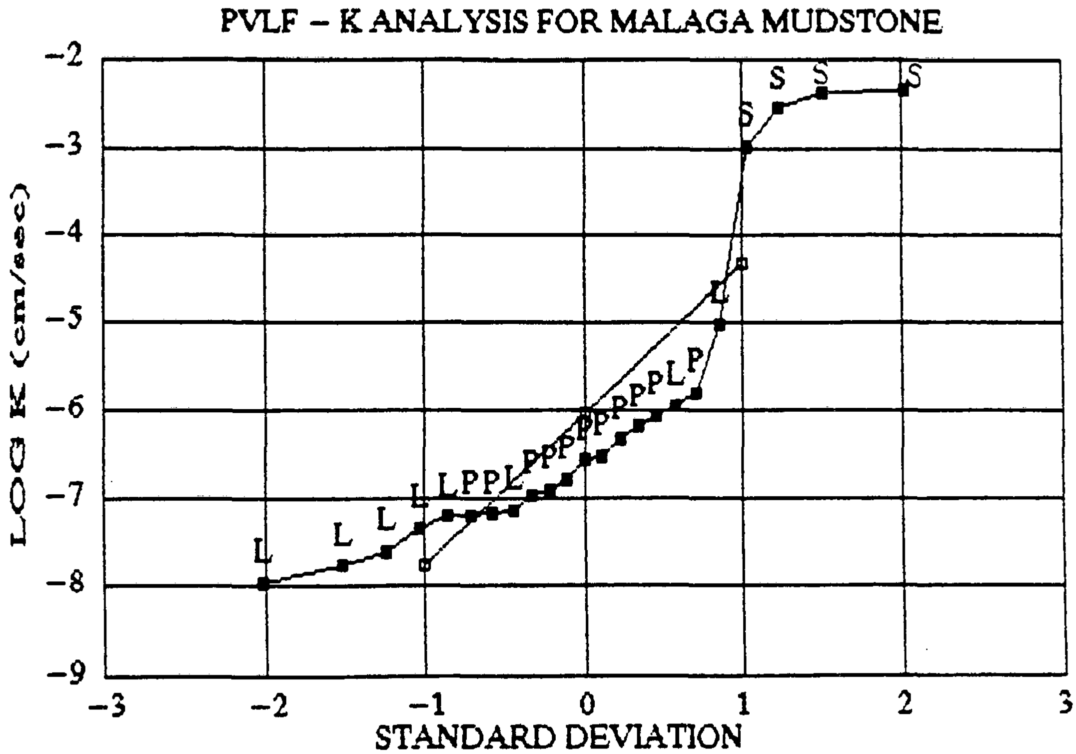

PVLF – K ANALYSIS FOR MALAGA MUDSTONE
LOG K (cm/sec)
STANDARD DEVIATION
−2
−3
−4
−5
−6
−7
−8
−9
−3
−2
−1
0
1
2
3

PALOS VERDES LANDFILL - 12482-009-128
STATISTICAL ANALYSIS OF K VALUES
REVISED BY TAJ 9/24/91

VALMONTE DIATOMITE - Tv

Test # (n)	Test Freq.	Standard Deviation	Log K (cm/sec)	K (cm/sec)	Test Type	Boring/ Well
1	0.0313	-1.864	-7.157	6.97E-08	P	RFB 7
2	0.0938	-1.32	-6.975	1.06E-07	P	RFB 11
3	0.1563	-1.012	-6.959	1.10E-07	P	RFB 19
4	0.2188	-0.778	-6.827	1.49E-07	P	RFB16/M53B
5	0.2813	-0.582	-6.783	1.65E-07	P	RFB 11
6	0.3438	-0.404	-6.706	1.97E-07	P	RFB 7
7	0.4063	-0.24	-6.633	2.33E-07	P	RFB 32
8	0.4688	-0.08	-6.295	5.07E-07	P	RFB 32
9	0.5313	0.076	-6.039	9.14E-07	P	RFB 11
10	0.5938	0.236	-5.818	1.52E-06	P	RFB24/M56B
11	0.6563	0.4	-5.350	4.47E-06	P	RFB 30A
12	0.7188	0.578	-5.184	6.55E-06	P	RFB 30A
13	0.7813	0.774	-3.886	1.30E-04	S	M24A
14	0.8438	1.008	-3.747	1.79E-04	P	RFB 19
15	0.9063	1.316	-3.359	4.38E-04	S	M42A
16	0.9688	1.86	-2.642	2.28E-03	S	M43A

0	ARITHMETIC MEAN LOG K	-5.647
1	AR. MEAN LOG K + 1 STD.	-4.224
-1	AR. MEAN LOG K - 1 STD.	-7.071
	GEOMETRIC MEAN K	2.12E-06
	GEO. MEAN K + 1 STD.	5.97E-05
	GEO. MEAN K - 1 STD.	8.49E-08

P = Packer Test
S = Slug Test

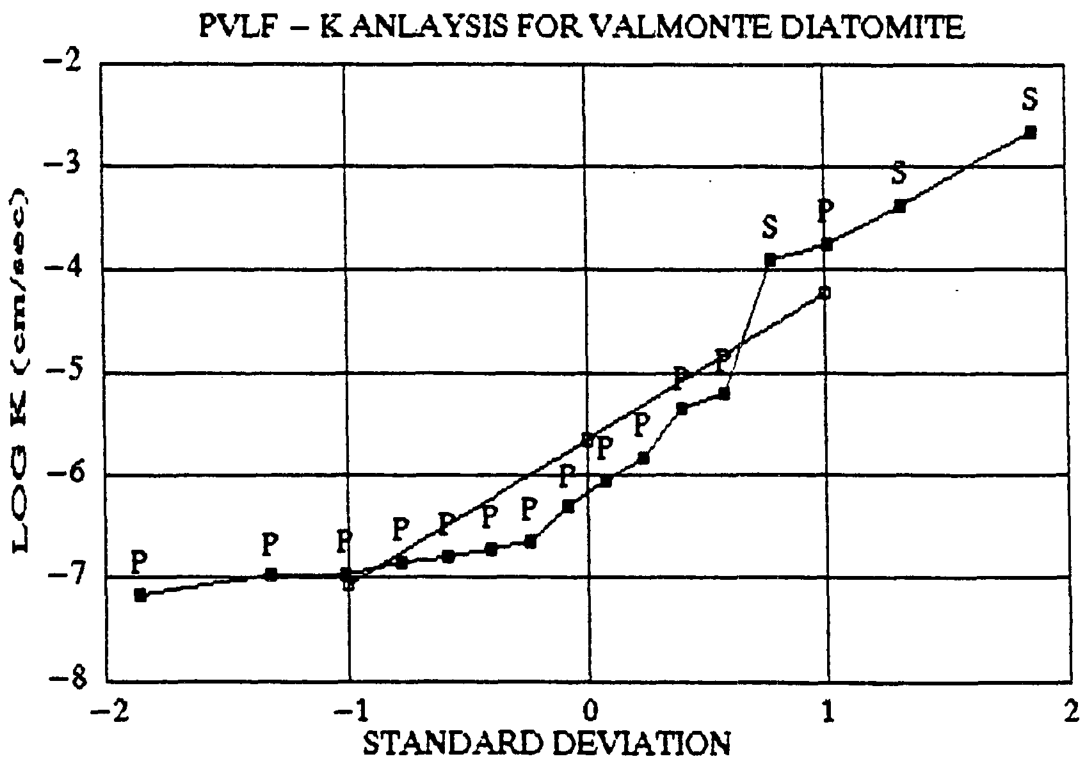

PALOS VERDES LANDFILL - 12482-009-128
STATISTICAL ANALYSIS OF K VALUES
REVISED BY TAJ 9/24/91

ALTAMIRA SHALE

Test # (n)	Test Freq.	Standard Deviation	Log K (cm/sec)	K (cm/sec)	Test Type	Boring/ Well
1	0.0333	-1.836	-6.68	2.09E-07	P	RFB 22
2	0.1000	-1.284	-6.44	3.64E-07	P	RFB 22
3	0.1667	-0.97	-6.37	4.22E-07	P	RFB25/M57B
4	0.2333	-0.73	-6.14	7.18E-07	P	RFB29/M60B
5	0.3000	-0.526	-5.97	1.08E-06	P	RFB 22
6	0.3667	-0.342	-5.96	1.10E-06	P	RFB25/M57B
7	0.4333	-0.17	-5.78	1.67E-06	P	RFB24/M56B
8	0.5000	-0.002	-4.84	1.45E-05	P	RFB25/M57B
9	0.5667	0.166	-4.70	2.00E-05	P	RFB 1
10	0.6333	0.338	-4.02	9.53E-05	P	RFB 1
11	0.7000	0.522	-3.91	1.24E-04	P	RFB 1
12	0.7667	0.726	-3.84	1.43E-04	P	RFB29/M60B
13	0.8333	0.966	-3.63	2.36E-04	P	RFB29/M60B
14	0.9000	1.28	-3.43	3.70E-04	S	M47B
15	0.9667	1.832	-2.89	1.30E-03	S	M45A2

0	ARITHMETIC MEAN LOG K	-4.973
1	AR. MEAN LOG K + 1 STD.	-3.736
-1	AR. MEAN LOG K - 1 STD.	-6.210
	GEOMETRIC MEAN K	1.06E-05
	GEO. MEAN K + 1 STD.	1.84E-04
	GEO. MEAN K - 1 STD.	6.17E-07

S = Slug Test
P = Packer Test

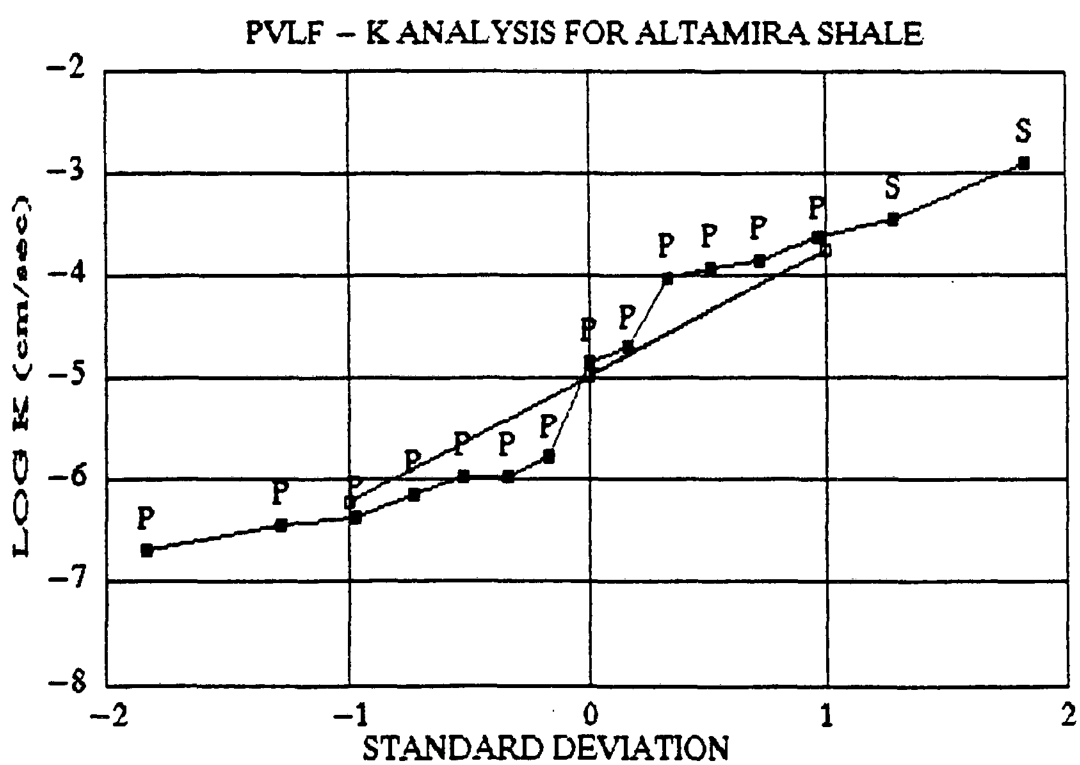

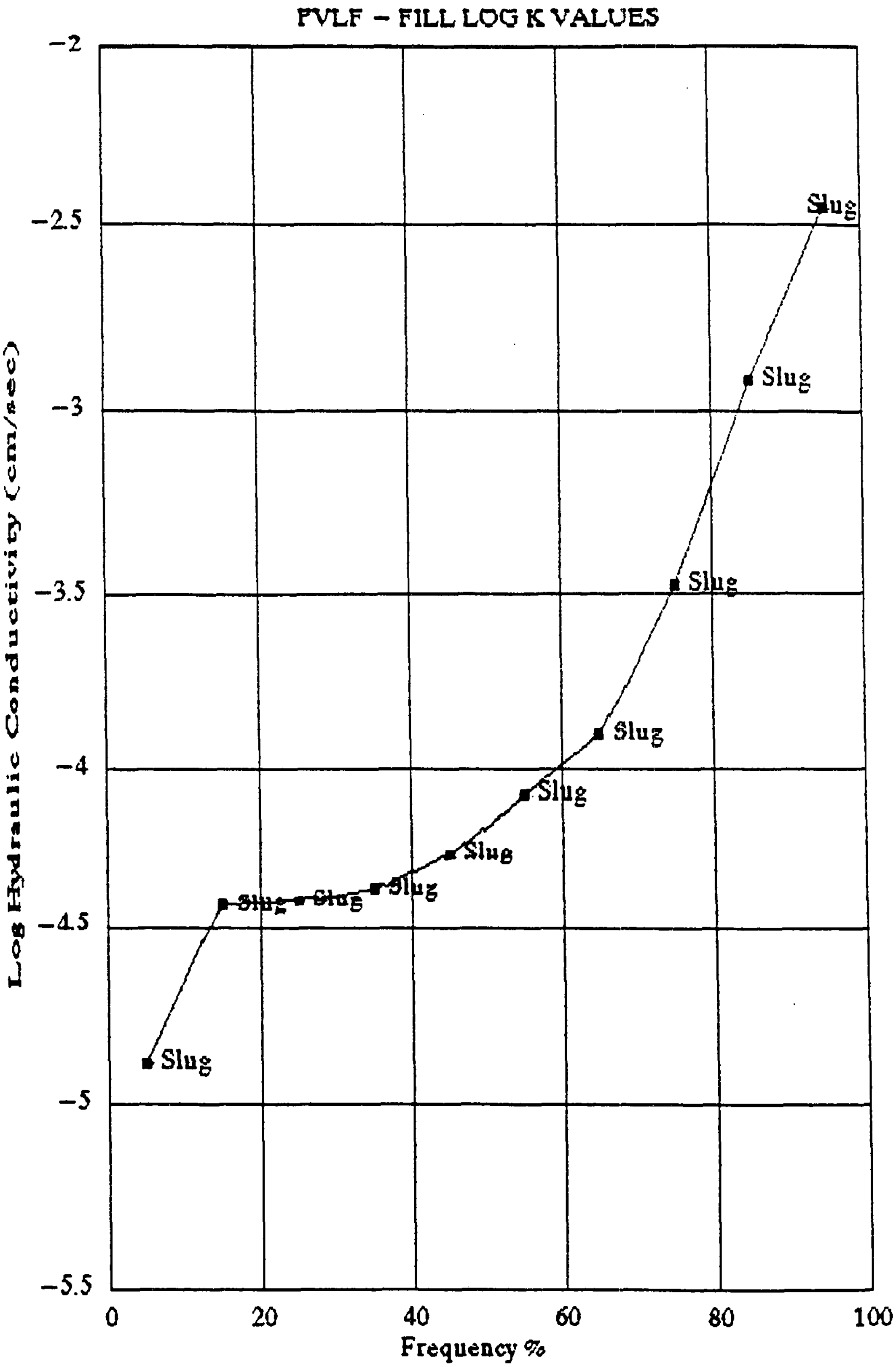

PVLF – FILL LOG K VALUES
Log Hydraulic Conductivity (cm/sec)
Frequency %
-2
-2.5
-3
-3.5
-4
-4.5
-5
-5.5
0
20
40
60
80
100
Slug

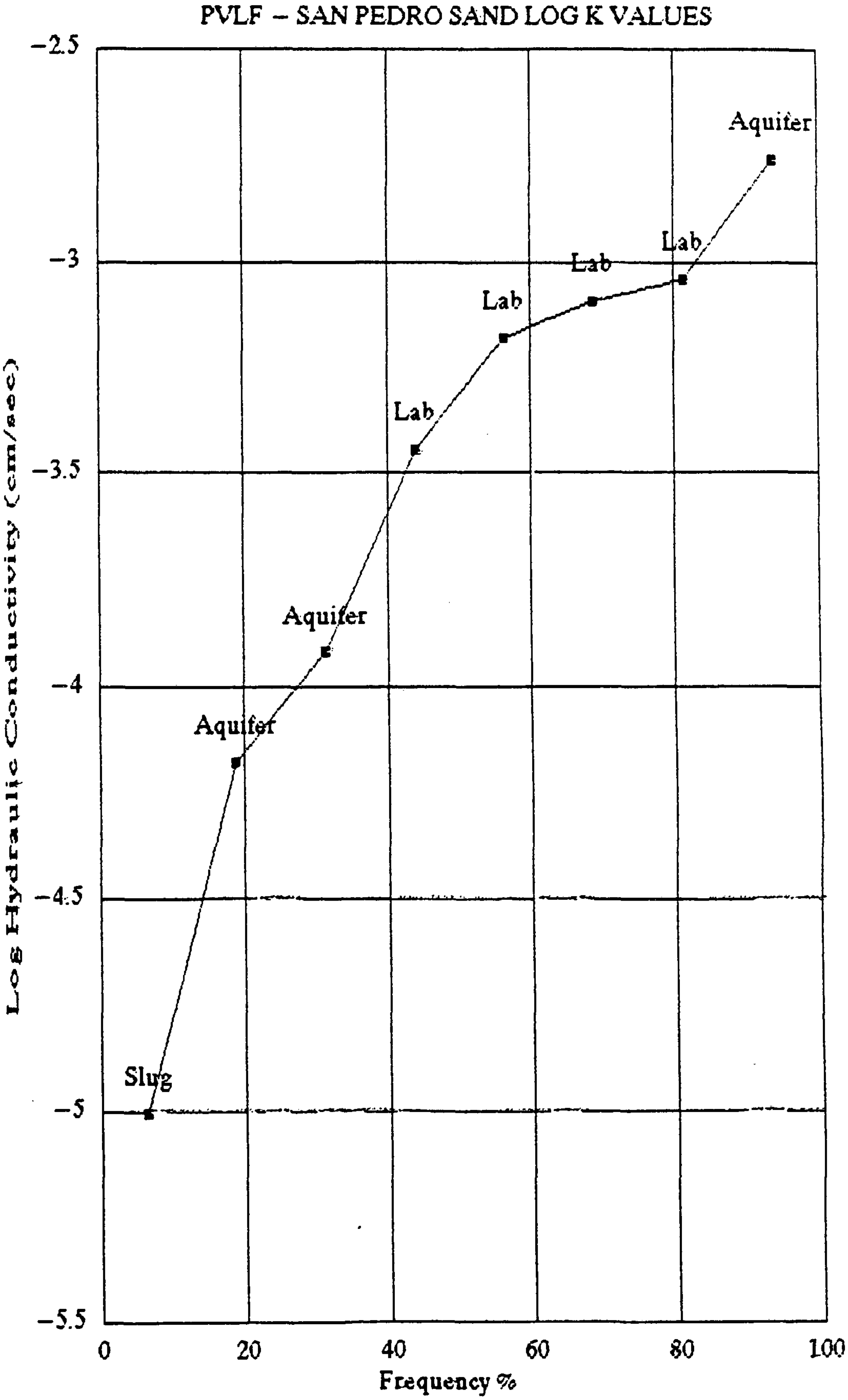
PVLF – SAN PEDRO SAND LOG K VALUES
Log Hydraulic Conductivity (cm/sec)
Frequency %
-2.5
-3
-3.5
-4
-4.5
-5
-5.5
0
20
40
60
80
100
Slug
Aquifer
Aquifer
Lab
Lab
Lab
Lab
Aquifer

FVLF – MALAGA MUDSTONE LOG K VALUES

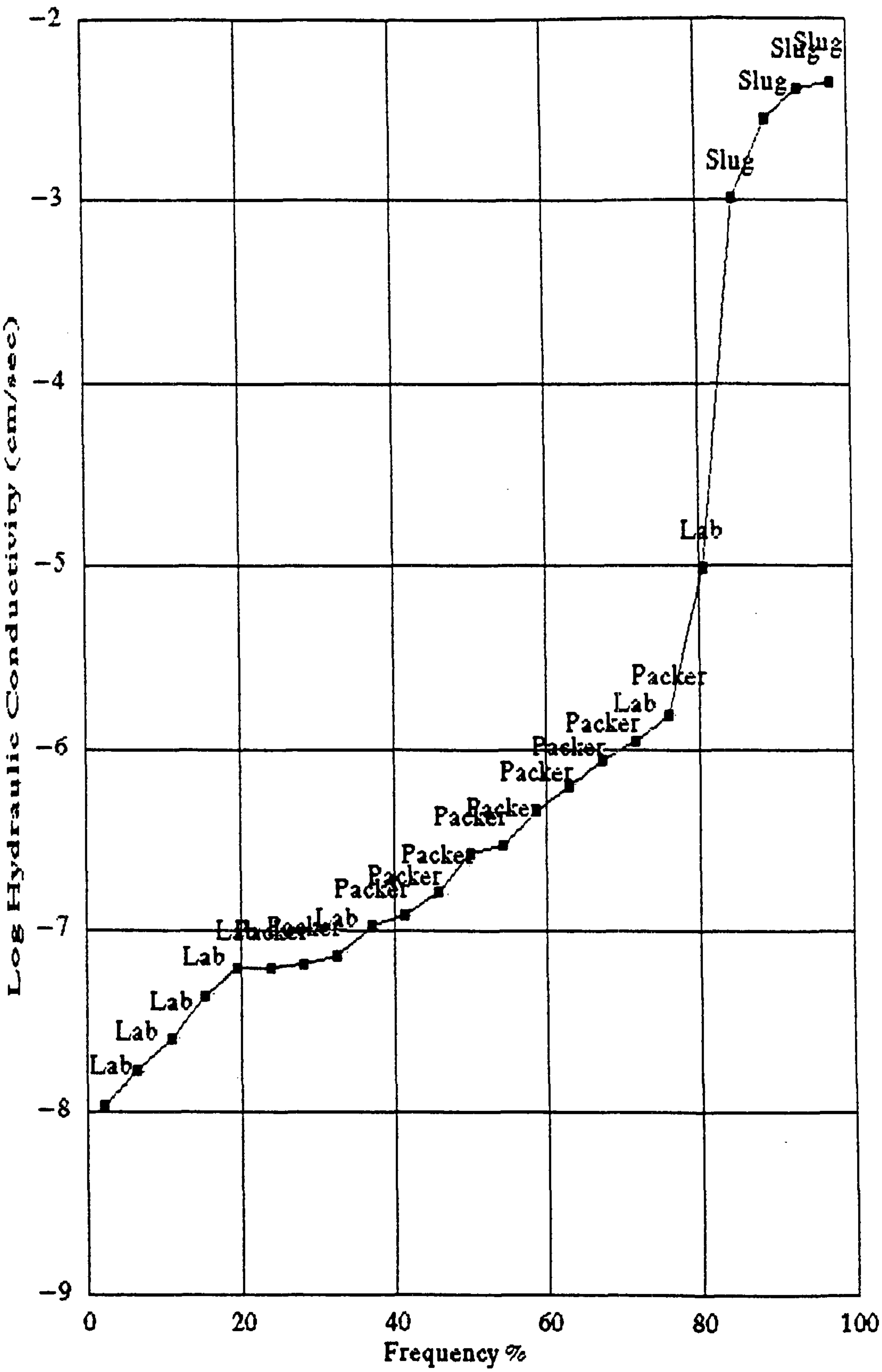

PVLF – VALMONTE DIATOMITE LOG K VALUES

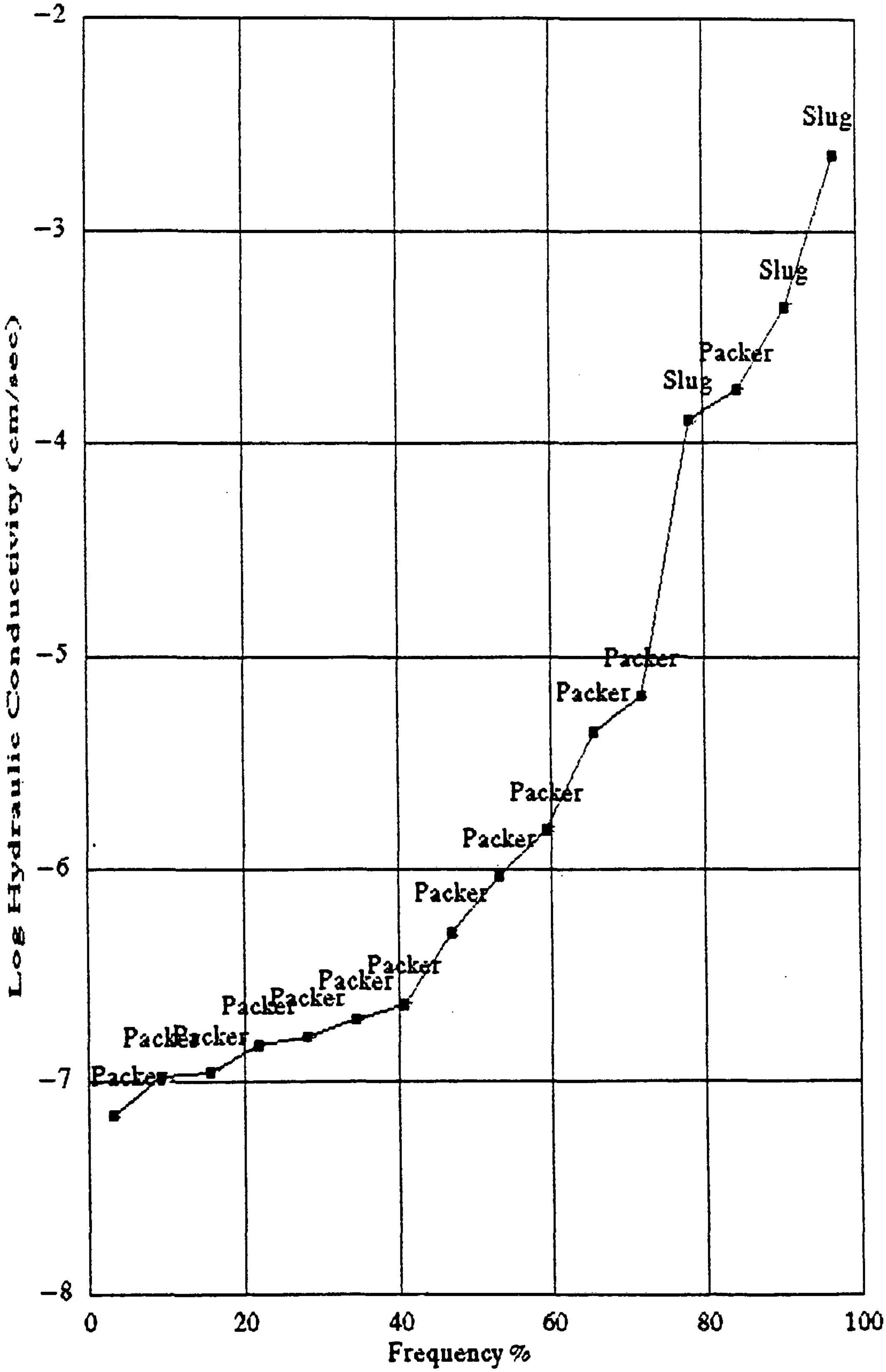

PVLF – ALTAMIRA SHALE LOG K VALUES

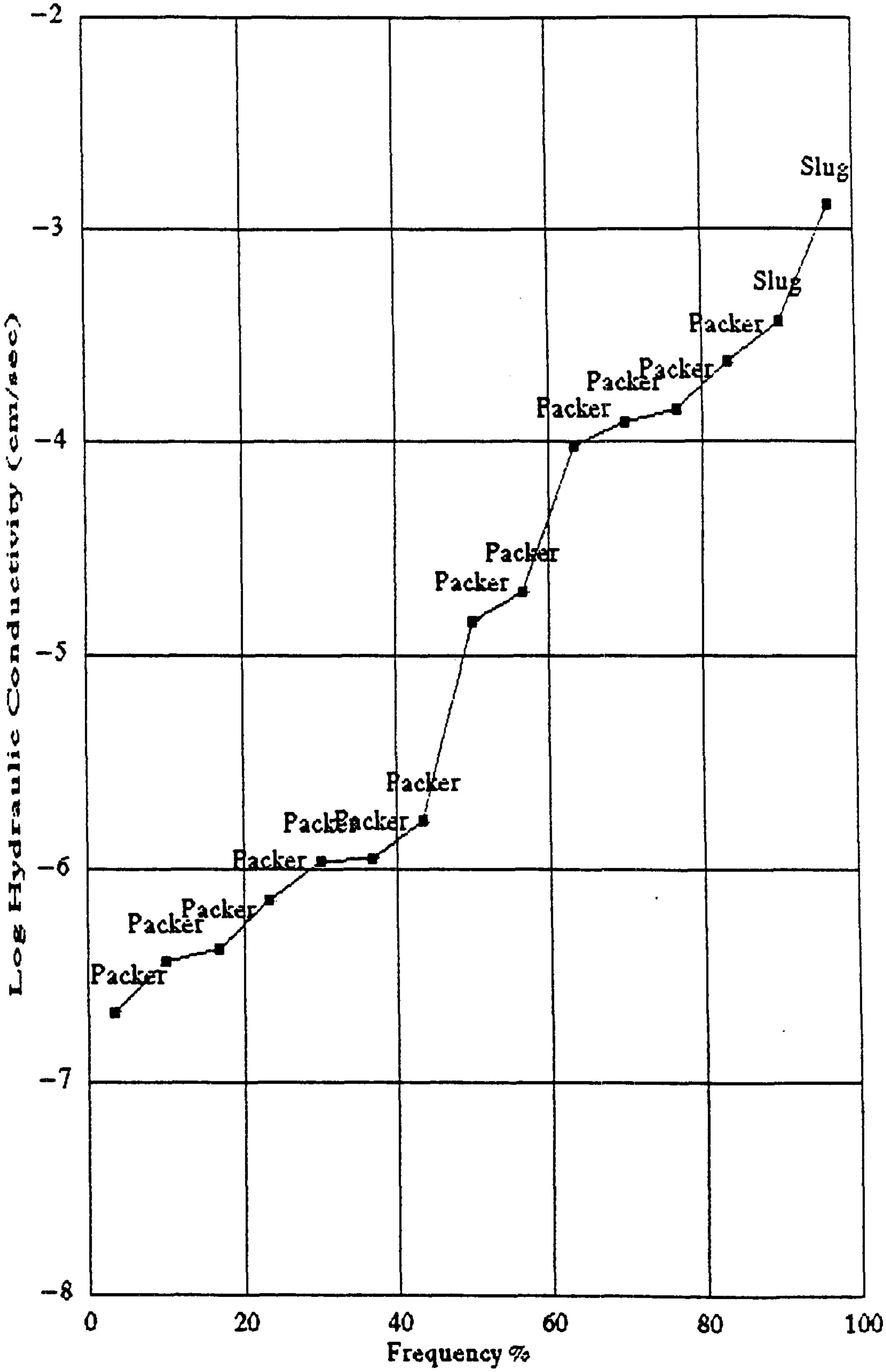

PALOS VERDES LANDFILL
ANALYSIS OF K VALUES BY DEPTH IN FORMATION

DATA FROM HERZOG VOLUMES I AND II

MALAGA MUDSTONE

BORING/ WELL #	DEPTH OF TEST BELOW TOP OF FM.	DESCRIPTION ON GEO. LOG	K (x10E-6 cm/sec)
RFB 11	7	Contact between Malaga and Valmonte. Highly fractured	0.17
RFB L3	10	Mudstone - fractures present	0.45
RFB 7	25	Mudstone, mod. to high. fract. closed, clean fract.	0.12
RFB 7	40	Contact between Malaga and Valmonte. No mention of fractures	0.25
RFB L3	45	Mudstone-Ashy, No mention of fract.	0.06
RFB 6	50	Mudstone w/ ash layers, sandstone laminae, no mention of fractures	0.11
RFB 6	60	Mudstone w/ minor ash. 5 ft. thick fracture zone.	0.16
RFB L3	60	Mudstone, open fractues, loss of drilling fluids	0.06
RFB 32	85	Mudstone/Dolostone w/ ash. Highly fractured	0.87
RFB 12	85	Mudstone, sl. to highly fract., ash	1.54
RFB 12	105	Mudstone, highly fract. w/ 2 preferred orientations, wood fragments	0.63
RFB 12	145	Mudstone w/ ash layers, fossiliferous moderately fractured	0.29

PALOS VERDES LANDFILL
ANALYSIS OF K VALUES BY DEPTH IN FORMATION

DATA FROM HERZOG VOLUMES I AND II

VALMONTE DIATOMITE

BORING/ WELL #	DEPTH OF TEST BELOW TOP OF FM.	DESCRIPTION ON GEO. LOG	K (x10E-6 cm/sec)
RFB 11	6	Contact between Malaga and Valmonte. Highly fractured	0.17
RFB 16	15	Siltstone - Highly fractured, ash	0.15
RFB 7	50	Mudstone & ash. No mention of fract	0.20
RFB 24	55	Shale/diatomite, sl. fractured	1.52
RFB 30A	55	Dolostone, chert, shale, no mention of fractures.	4.47
RFB 30A	60	Dolostone, chert, shale, no mention of fractures.	6.55
RFB 7	60	Diatomaceous mudstone & ash. Some silt. No mention of fractures	0.07
RFB 11	70	Diatomaceous siltstone, shells, ash. No mention of fractures.	0.91
RFB 32	85	Diatomaceous siltstone w/ ash. No mention of fractures.	0.51
RFB 11	110	Diatomaceous siltstone, shells, ash. Intensely fractures 5' below packer.	0.11
RFB 19	130	Through fault plane. Siltstone. med-highly fractured - tar filled.	1.79
RFB 19	165	Siltstone. Intensely fractured. Tar-filled.	0.11
RFB 32	190	Dolostone, Diatomaceous siltstone Massive. Ash. No mention of fract.	0.23

PALOS VERDES LANDFILL
ANALYSIS OF K VALUES BY DEPTH IN FORMATION

DATA FROM HERZOG VOLUMES I AND II

ALTAMIRA SHALE

BORING/ WELL #	DEPTH OF TEST BELOW TOP OF FM.	DESCRIPTION ON GEO. LOG	K (x10E-6 cm/sec)
RFB 24	5	Shale, diatomite, sl. fractured	1.67
RFB 1	20	Diatomaceous shale, highly fract. some clay, tar infilling	20.0
RFB 29	20	Diatomaceous shale. No mention of fractures.	236.0
RFB 25	40	Mudstone. Highly to intes. fract.	14.5
RFB 22	50	Cherty/tuff facies. med-high fract.	1.08
RFB 25	55	Mudstone. Highly fract, FeO Stains	0.42
RFB 22	70	Shale. Highly fractured.	0.36
RFB 1	75	Dolostone, intensely fract. w/ tar	95.3
RFB 29	80	Chert/dolomite/shale. Hard drilling No mention of fractures	0.72
RFB 1	85	Diatomaceous shale. Intensely fractured w/ tar filling	124.0
RFB 25	90	Ashy siltstone.No mention of fract.	1.10
RFB 22	95	Chert/tuff facies. Highly fractured w/ tar filling	0.21
RFB 29	120	Diatomaceous siltstone. Moderately fract. Loss of drilling fluid.	120.0

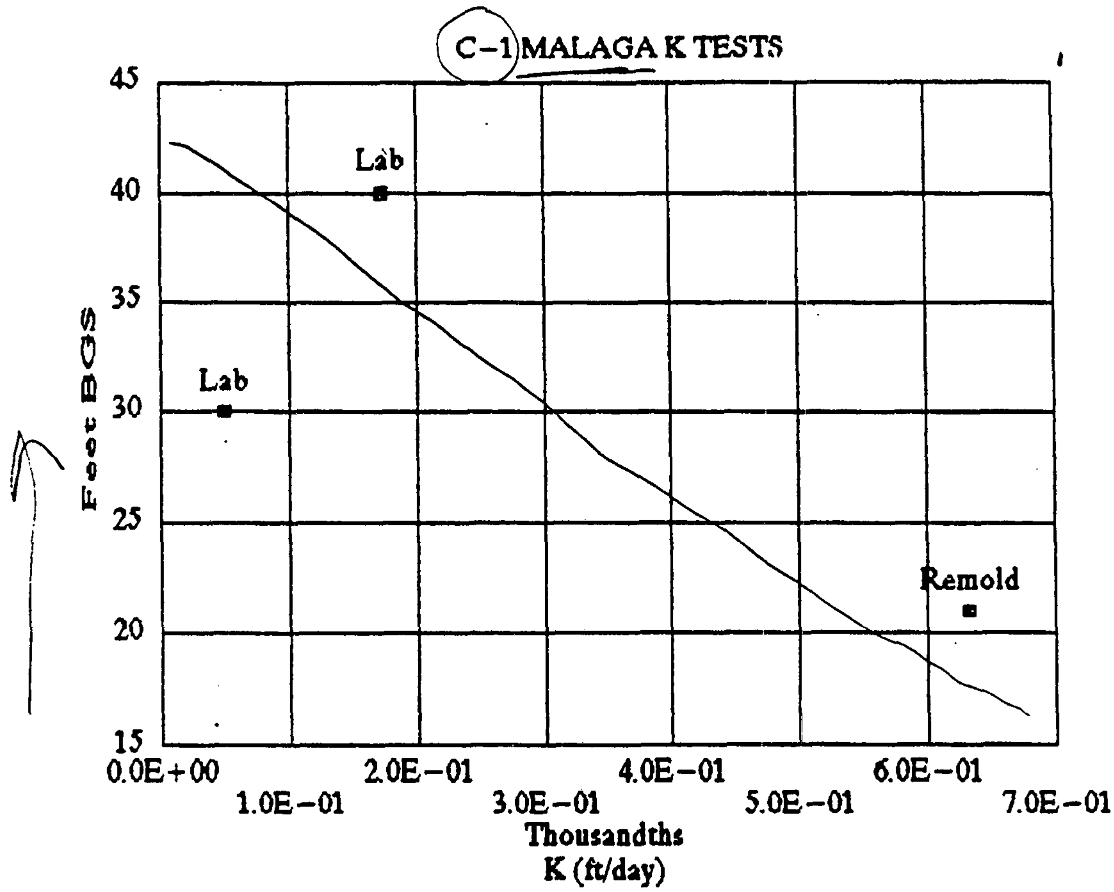
C-1 MALAGA K TESTS
Feet BGS
Lab
Lab
Remold
45
40
35
30
25
20
15
0.0E+00
1.0E-01
2.0E-01
3.0E-01
4.0E-01
5.0E-01
6.0E-01
7.0E-01
Thousandths
K (ft/day)

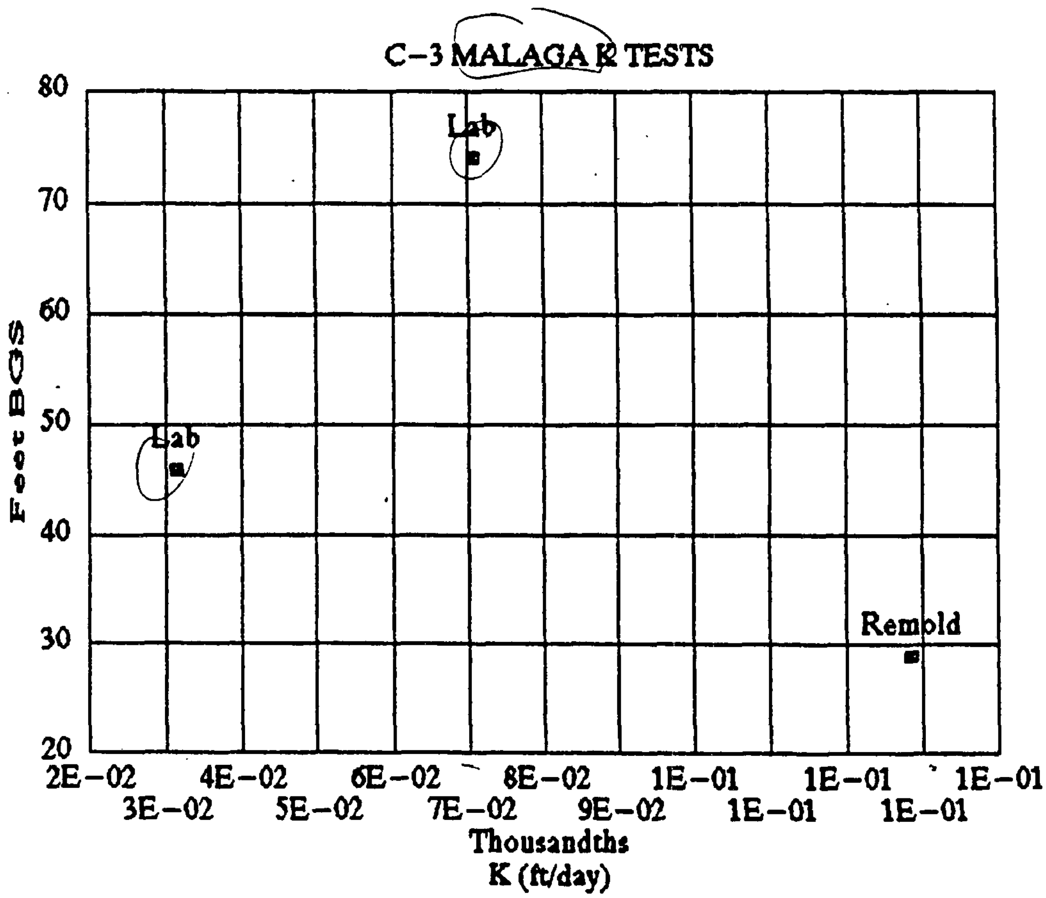
C-3 MALAGA K TESTS
Feet BGS
Lab
Lab
Remold
80
70
60
50
40
30
20
2E-02
3E-02
4E-02
5E-02
6E-02
7E-02
8E-02
9E-02
1E-01
1E-01
1E-01
1E-01
1E-01
Thousandths
K (ft/day)

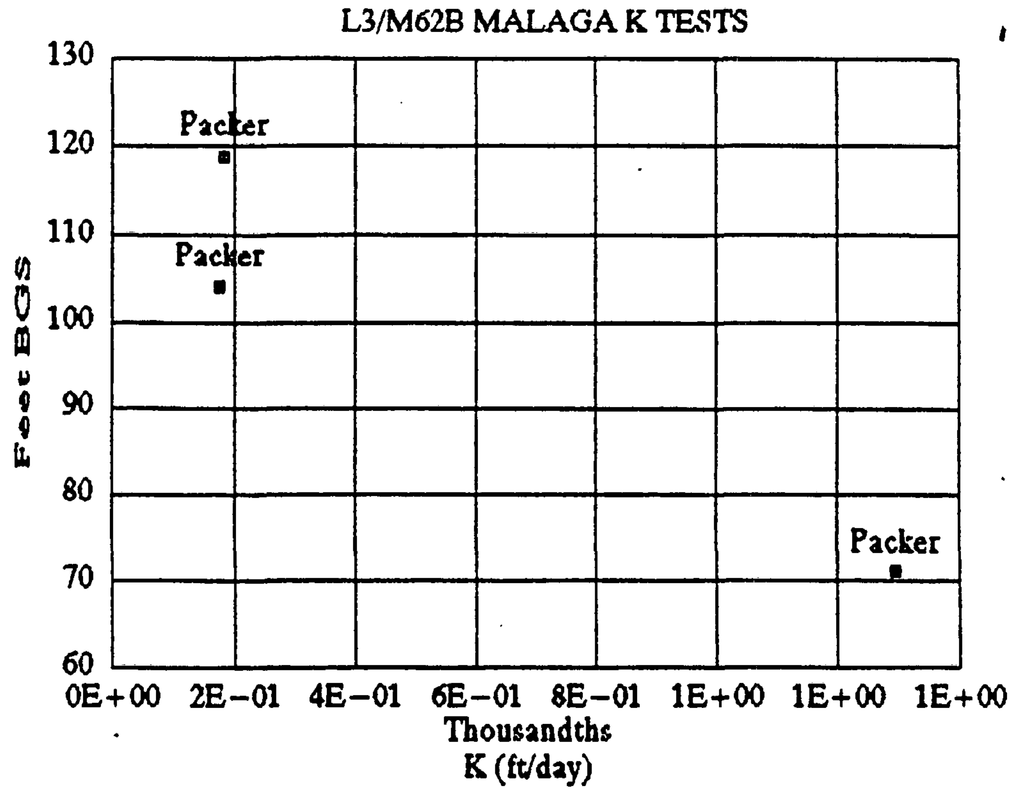
L3/M62B MALAGA K TESTS
130
120
110
100
90
80
70
60
Packer
Packer
Packer
Feet BGS
0E+00
2E−01
4E−01
6E−01
8E−01
1E+00
1E+00
1E+00
Thousandths
K (ft/day)

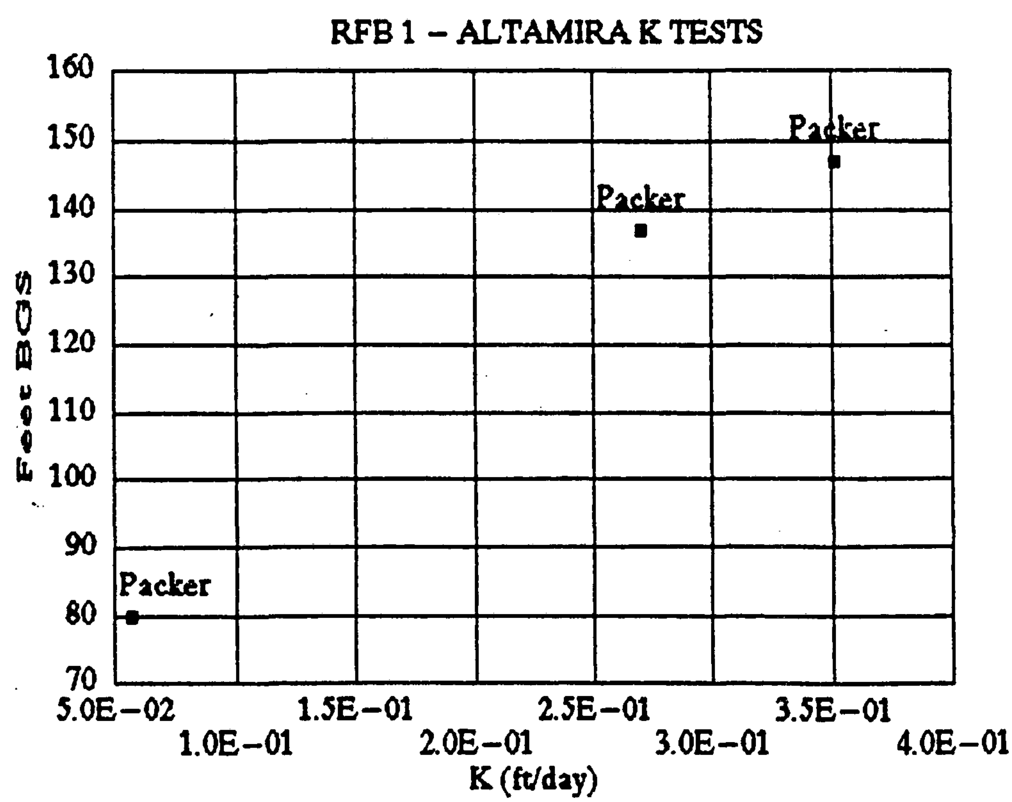
RFB 1 – ALTAMIRA K TESTS
160
150
140
130
120
110
100
90
80
70
Packer
Packer
Packer
Feet BGS
5.0E−02
1.0E−01
1.5E−01
2.0E−01
2.5E−01
3.0E−01
3.5E−01
4.0E−01
K (ft/day)

RFB 19 – VALMONTE K TESTS

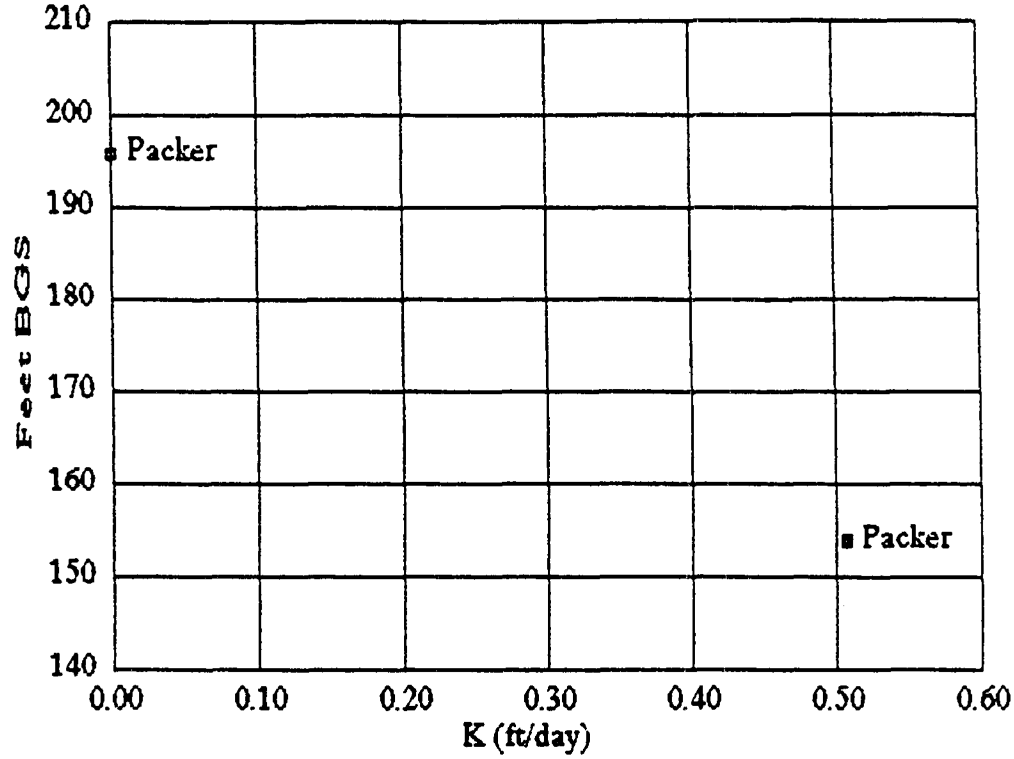

RFB 22 – ALTAMIRA K TESTS

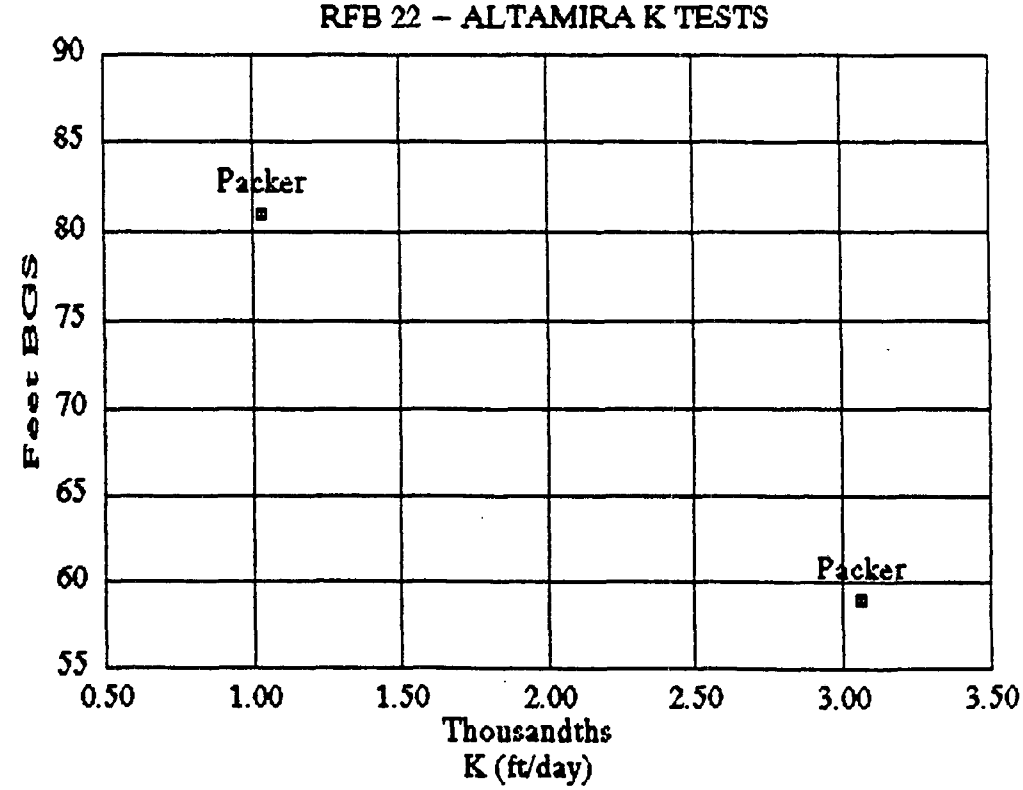

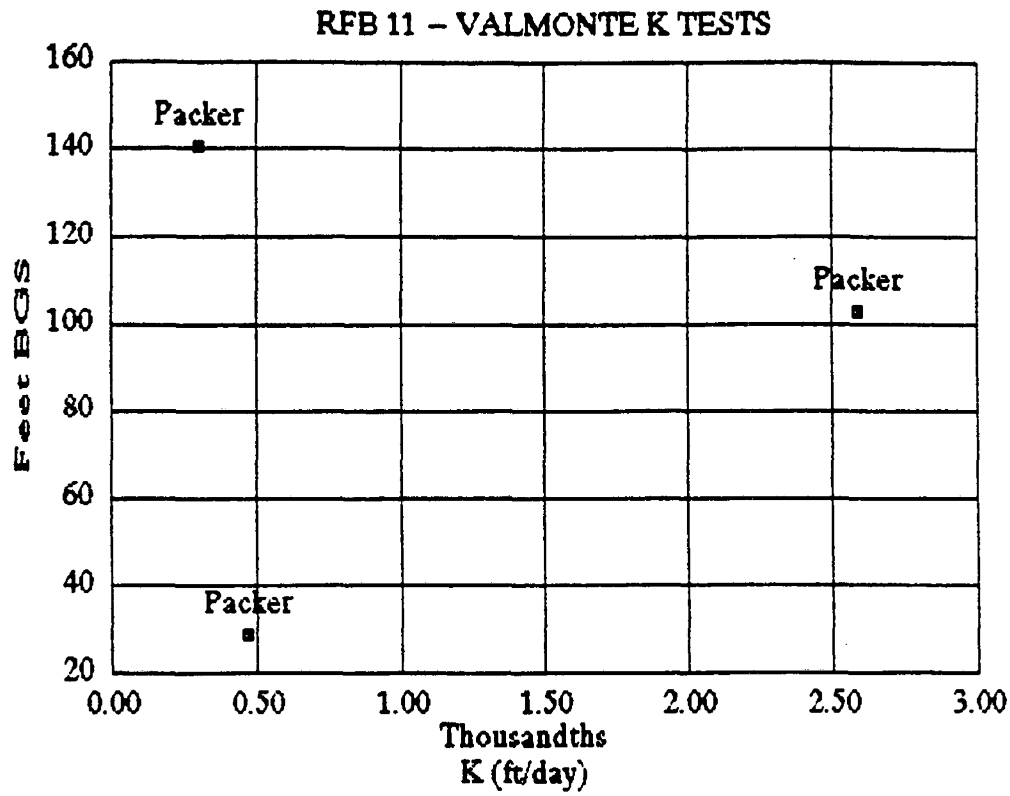

RFB 11 – VALMONTE K TESTS
Packer
Packer
Packer
Feet BGS
160
140
120
100
80
60
40
20
0.00
0.50
1.00
1.50
2.00
2.50
3.00
Thousandths
K (ft/day)

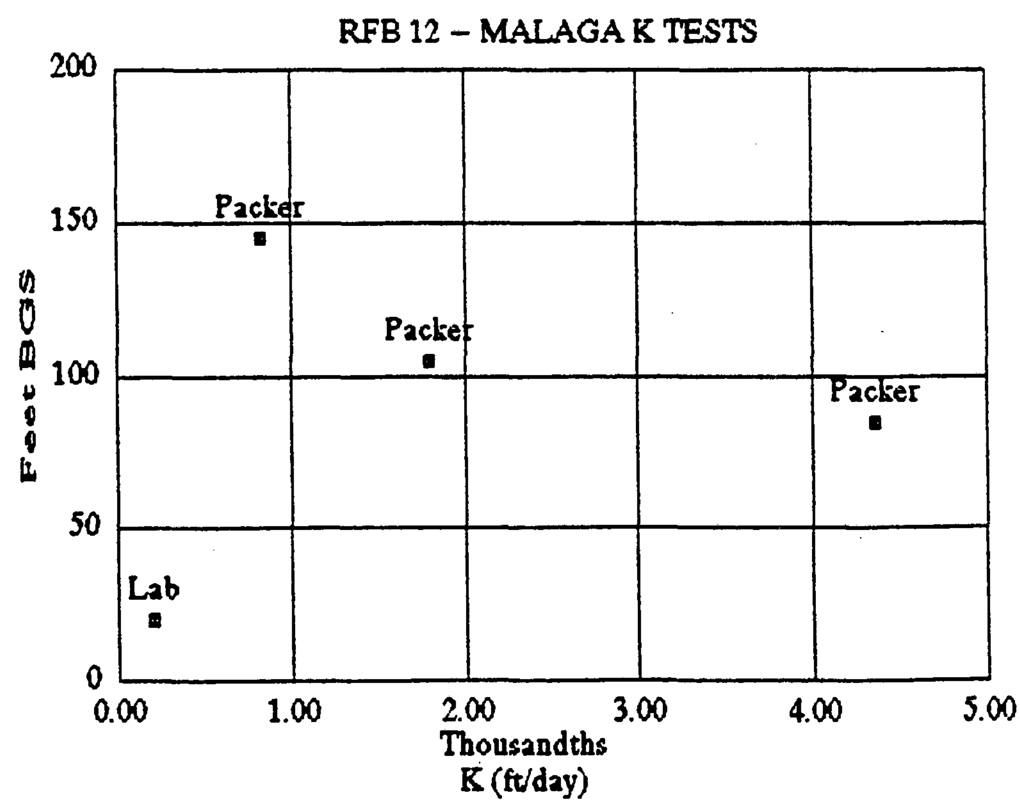

RFB 12 – MALAGA K TESTS
Packer
Packer
Packer
Lab
Feet BGS
200
150
100
50
0
0.00
1.00
2.00
3.00
4.00
5.00
Thousandths
K (ft/day)

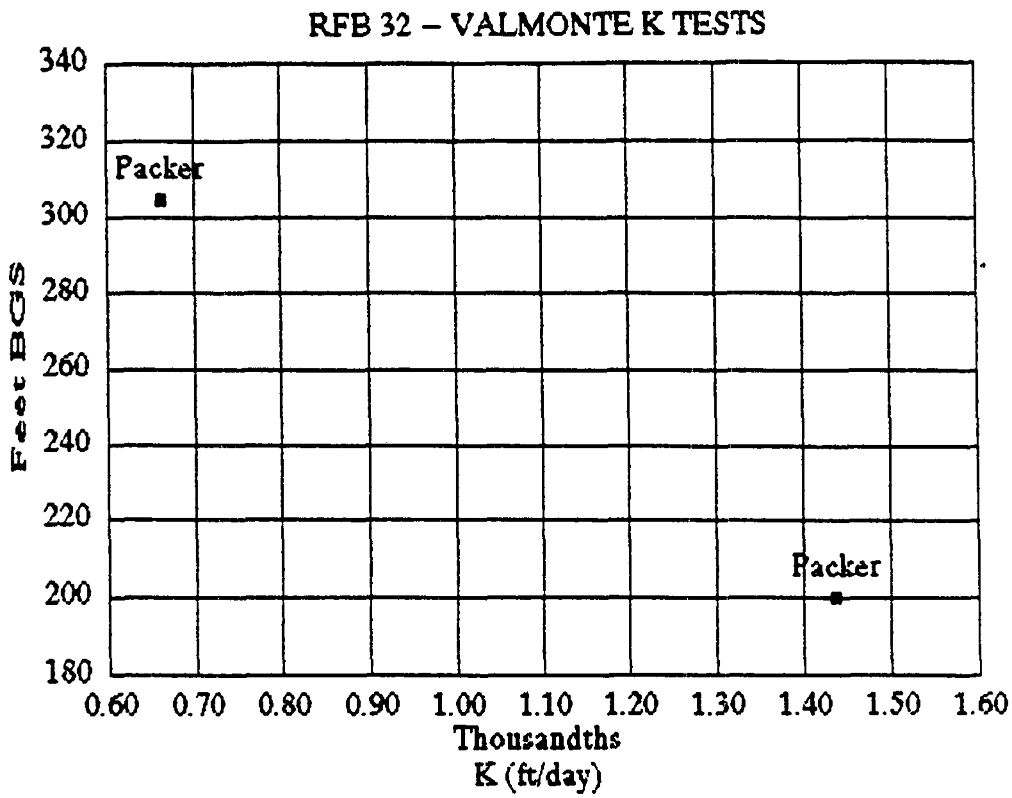
RFB 32 – VALMONTE K TESTS
Feet BGS
340
320
300
280
260
240
220
200
180
Packer
Packer
0.60
0.70
0.80
0.90
1.00
1.10
1.20
1.30
1.40
1.50
1.60
Thousandths
K (ft/day)

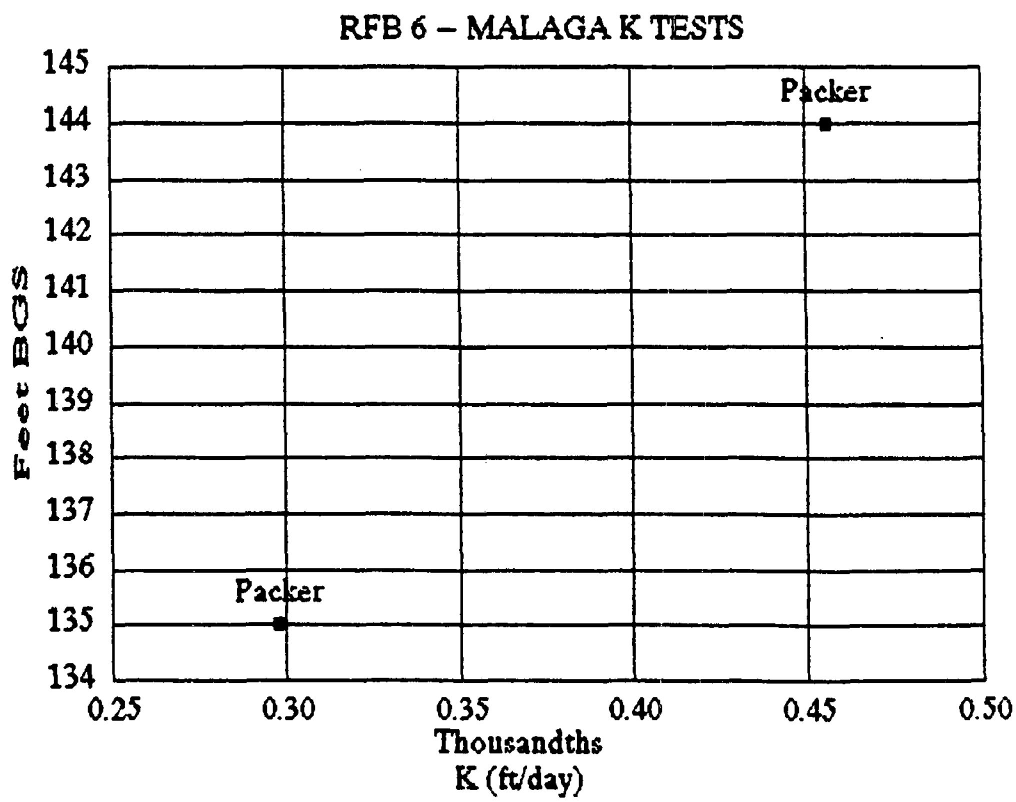
RFB 6 – MALAGA K TESTS
Feet BGS
145
144
143
142
141
140
139
138
137
136
135
134
Packer
Packer
0.25
0.30
0.35
0.40
0.45
0.50
Thousandths
K (ft/day)

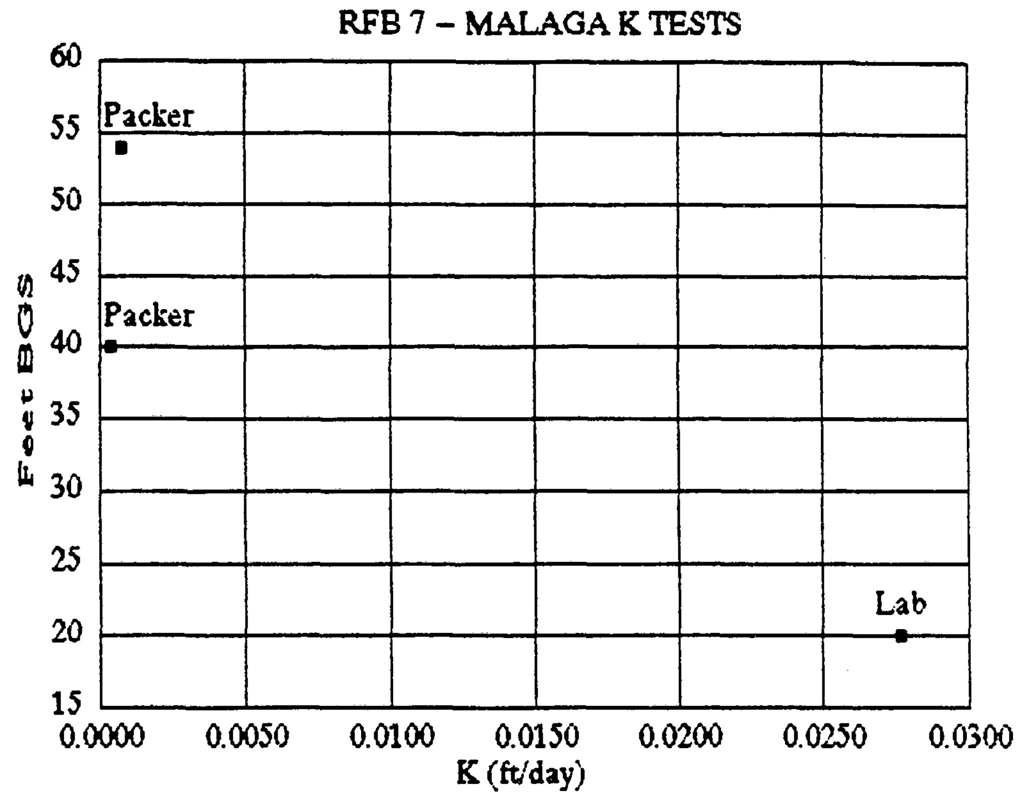

RFB 7 – MALAGA K TESTS
Feet BGS
60
55
50
45
40
35
30
25
20
15
Packer
Packer
Lab
0.0000
0.0050
0.0100
0.0150
0.0200
0.0250
0.0300
K (ft/day)

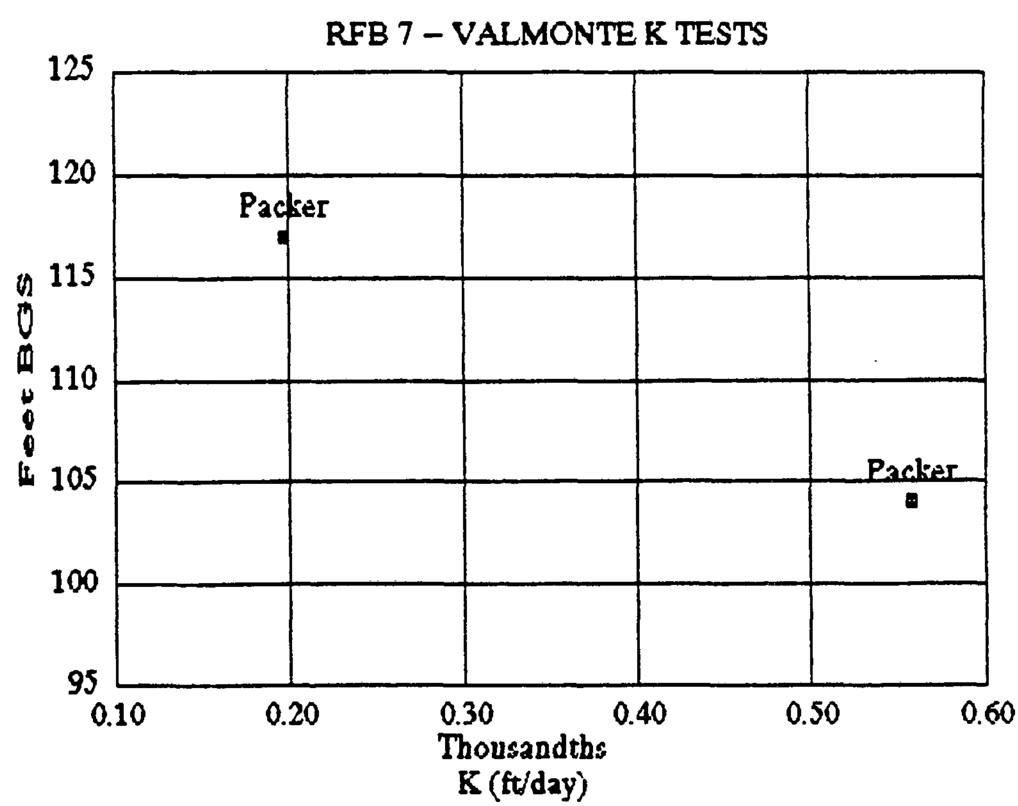

RFB 7 – VALMONTE K TESTS
Feet BGS
125
120
115
110
105
100
95
Packer
Packer
0.10
0.20
0.30
0.40
0.50
0.60
Thousandths
K (ft/day)

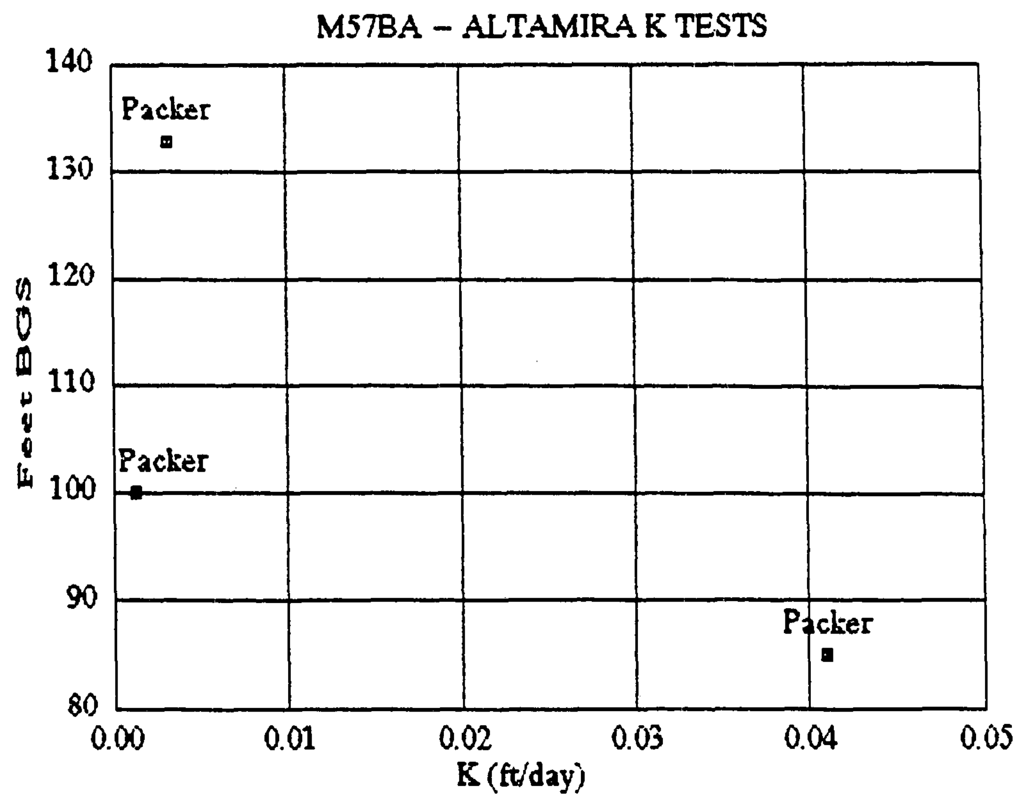

M57BA – ALTAMIRA K TESTS
Feet BGS
K (ft/day)
Packer
Packer
Packer
140
130
120
110
100
90
80
0.00
0.01
0.02
0.03
0.04
0.05

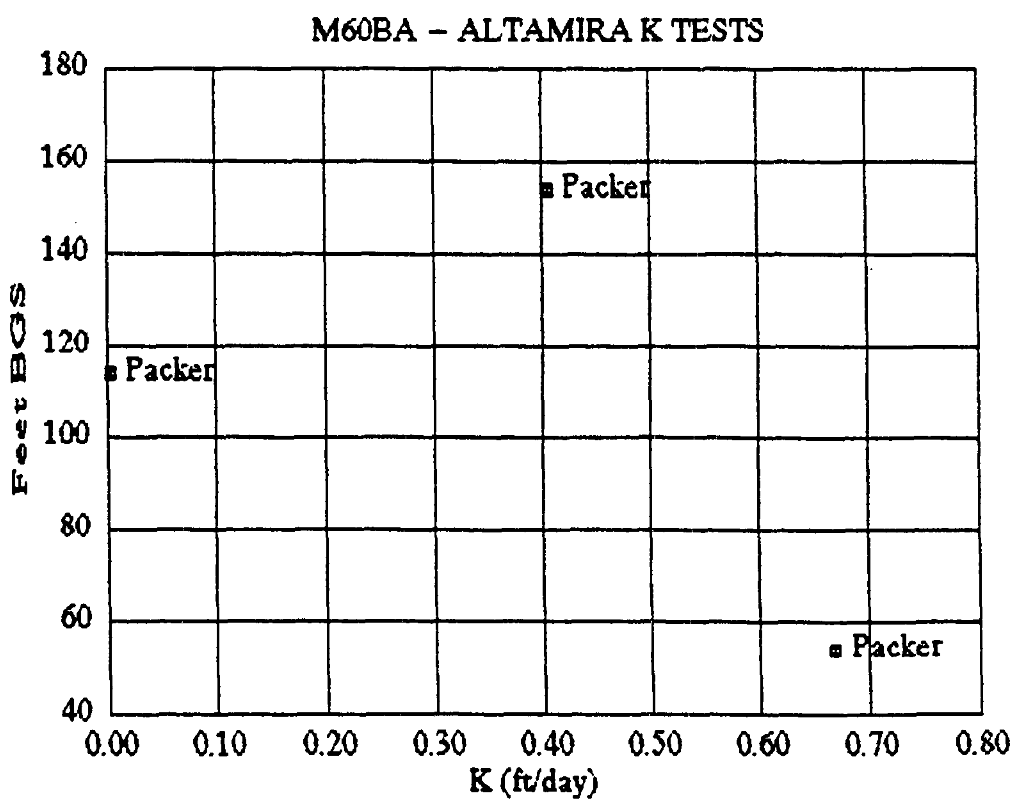

M60BA – ALTAMIRA K TESTS
Feet BGS
K (ft/day)
Packer
Packer
Packer
180
160
140
120
100
80
60
40
0.00
0.10
0.20
0.30
0.40
0.50
0.60
0.70
0.80

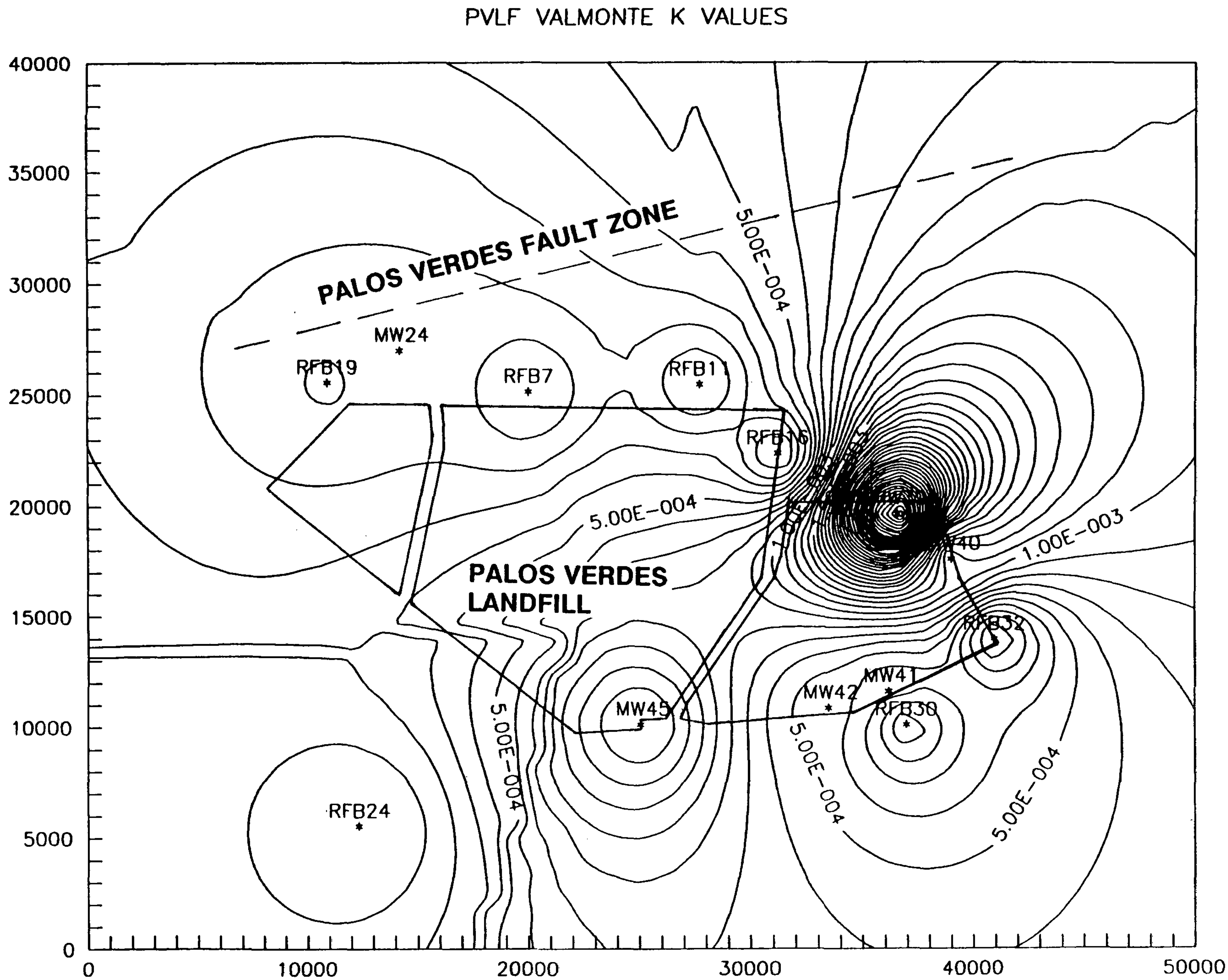
PVLF VALMONTE K VALUES
PALOS VERDES FAULT ZONE
PALOS VERDES LANDFILL
MW24
RFB19
RFB7
RFB11
RFB16
RFB32
MW41
MW42
RFB30
MW45
RFB24
5.00E-004
1.00E-003
0
5000
10000
15000
20000
25000
30000
35000
40000
50000

APPENDIX F

GLOSSARY OF SELECTED TECHNICAL TERMS

GLOSSARY OF SELECTED TECHNICAL TERMS

Absolute Maximum Residual: As applied in this text, the maximum difference between the model head and observed head for a given sensitivity case.

Adsorption: Adhesion of molecules (such as gases, solutes, or liquids) to the surfaces of solid bodies or liquids with which they are in contact.

Algebraic Mean: The sum of all variables in a data set divided by the number of variables.

Anthropogenic: Of or relating to the influence of human beings on nature. Of human origin.

Anticline: An arch of stratified rock in which the layers bend downward in opposite directions from the crest.

Anticlinorium: A series of anticlines and synclines so arranged structurally that together they form a general arch.

Aquifer: A water bearing layer of rock that will yield water in usable quantity to a well or spring.

Artesian Well: A well in which the water stands at some height above the aquifer due to internal pressure.

Biogenic: Produced by living organisms. Of biologic origin.

Calcareous: Resembling calcite or calcium carbonate especially in hardness and chemical composition. Consisting of or containing calcium carbonate.

Chert: A silicous, amorphous, biogenic rock resembling flint.

Conglomerate: A rock of fluvial origin composed of rounded fragments varying from small pebbles to large boulders in a finer grained matrix.

Correlation Coefficient: A measure of the strength of relationship between two variables. A perfect correlation equals 1.0.

Convection: The circular transfer of heat that occurs in a fluid at a nonuniform temperature owing to the variation of its density and the action of gravity.

Degrees of Freedom: A parameter in statistical analyses used as an index number to identify correct distributions to use.

Deposition: The laying down of potential rock forming material through the process of erosion; sedimentation.

GLOSSARY OF SELECTED TECHNICAL TERMS
(Continued)

Desorption: Removal of adsorbed material.

Diatomaceous Earth: A friable earthy deposit composed of nearly pure silica and consisting essentially of the frustules of microscopic signle-celled algae called diatoms.

Diatomite: A light friable siliceous material derived chiefly from diatom remains. Often used as filter material.

Diffusion: The spreading out of molecules, atoms, or ions into a vacuum, a fluid, or a porous medium, in a direction tending to equalize concentrations in all parts of the system.

Dolostone: A term for a sedimentary rock composed of fragmental, concretionary, or precipitated dolomite of organic or inorganic origin.

Feldspathic: Relating to or containing the mineral feldspar; used especially as a porcelain glaze.

Foraminiferal: Organisms that are foraminifers; marine rhizopods usually having calcareous shells.

Fossilferous: Containing fossils.

Geometric Mean: The n^{th} root of the product of all variables in a data set.

Glauconitic: Geologic material abundant in the mineral glauconite.

Gradient (hydraulic): The general slope of a water table. The level of equal hydraulic head in an aquifer.

Groundwater: That part of the subsurface water which is in the zone of saturation.

Gypsum: A widely distributed mineral consisting of hydrous calcium sulfate.

Hydraulic Head: The standing height above a datum (usually sea level) of a column of water in a well.

Hydrocarbon: A compound containing carbon and hydrogen. Commonly used in reference to fossil fuel deposits.

Hydrodynamic Dispersion: The extent to which a liquid substance introduced into a groundwater system spreads as it moves through the system.

GLOSSARY OF SELECTED TECHNICAL TERMS (Continued)

Hydrogeology: The branch of geology concerned with the movement and occurrence of groundwater.

Hydrology: Dealing with the properties, distribution, and circulation of water on and below the earth's surface and in the atmosphere.

Hydrostratigraphic Unit: Those geologic intervals, beds, formations, etc. that contain and transmit groundwater.

Lithologic: The physical characterization of a rock; the microscopic study and description of rocks.

Petroliferous: Containing or yielding petroleum.

Porous: Containing voids, or other openings which may or may not interconnect.

Radiolarian: Any of a large order (Radiolaria) of marine protozoans having a siliceous skeleton.

Recharge: The process by which water is adsorbed and is added to the zones of saturation.

Residual: As applied in this text, the difference between the model predicted head and the actual field measured head.

Schist: A metamorphic crystalline rock having closely foliated structure.

Sieve Analysis: Determination of the percent distribution of particle sizes by passing a measured sample of soil or sediment through standard sieves of various sizes.

Syncline: A trough of stratified rock in which the beds dip toward each other from either side.

APPENDIX G

HYDROGRAPHS OF SELECTED WELLS

WAITING FOR LACSD FIGURES

APPENDIX H

DISTRIBUTIONS OF HYDRAULIC CONDUCTIVITY AND POROSITY

PVLF - Initial Hyd Cond Distribution, Layer 1

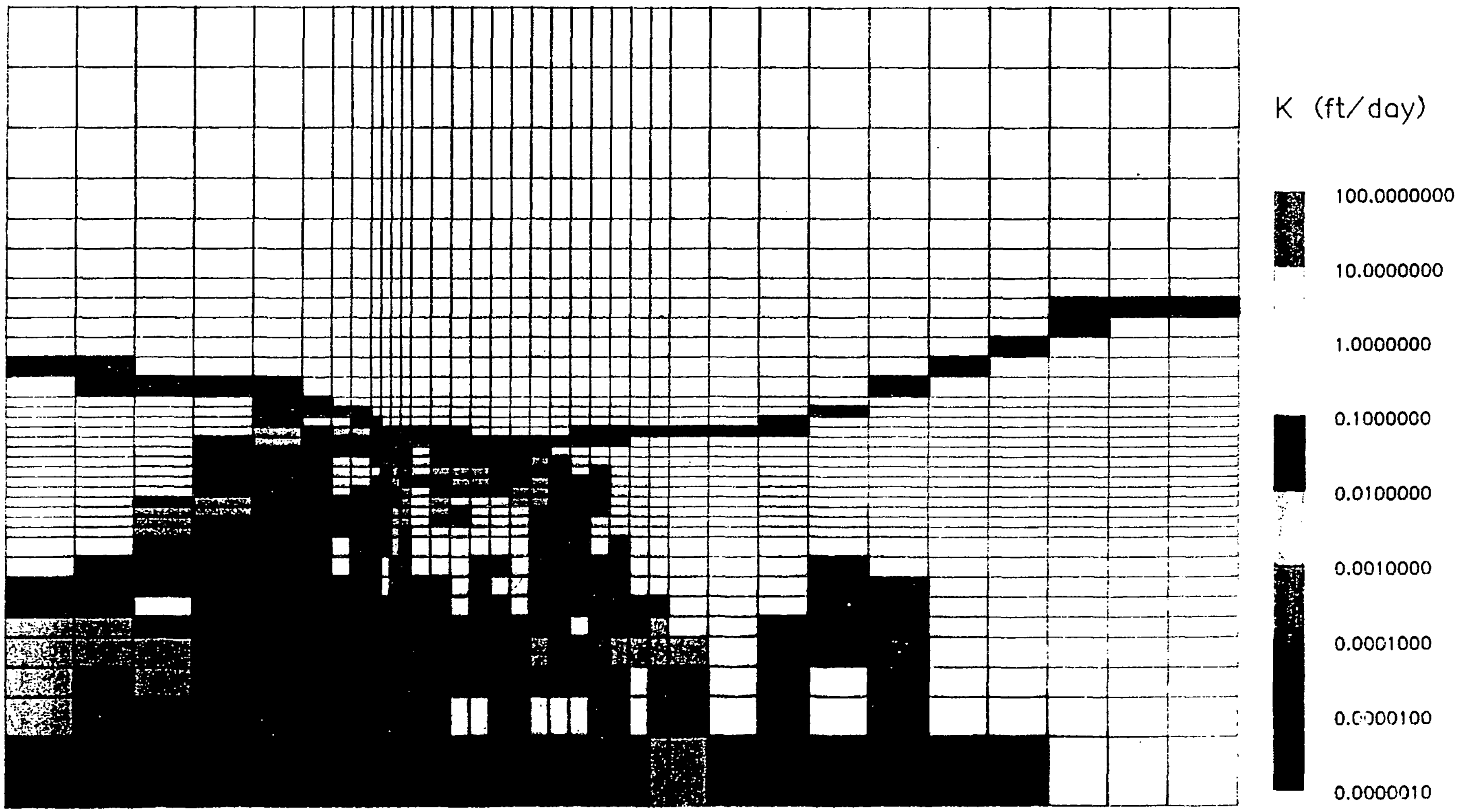

Figure H.1
INITIAL HYDRAULIC CONDUCTIVITY VALUES IN FINITE-DIFFERENCE CELLS, LAYER 1

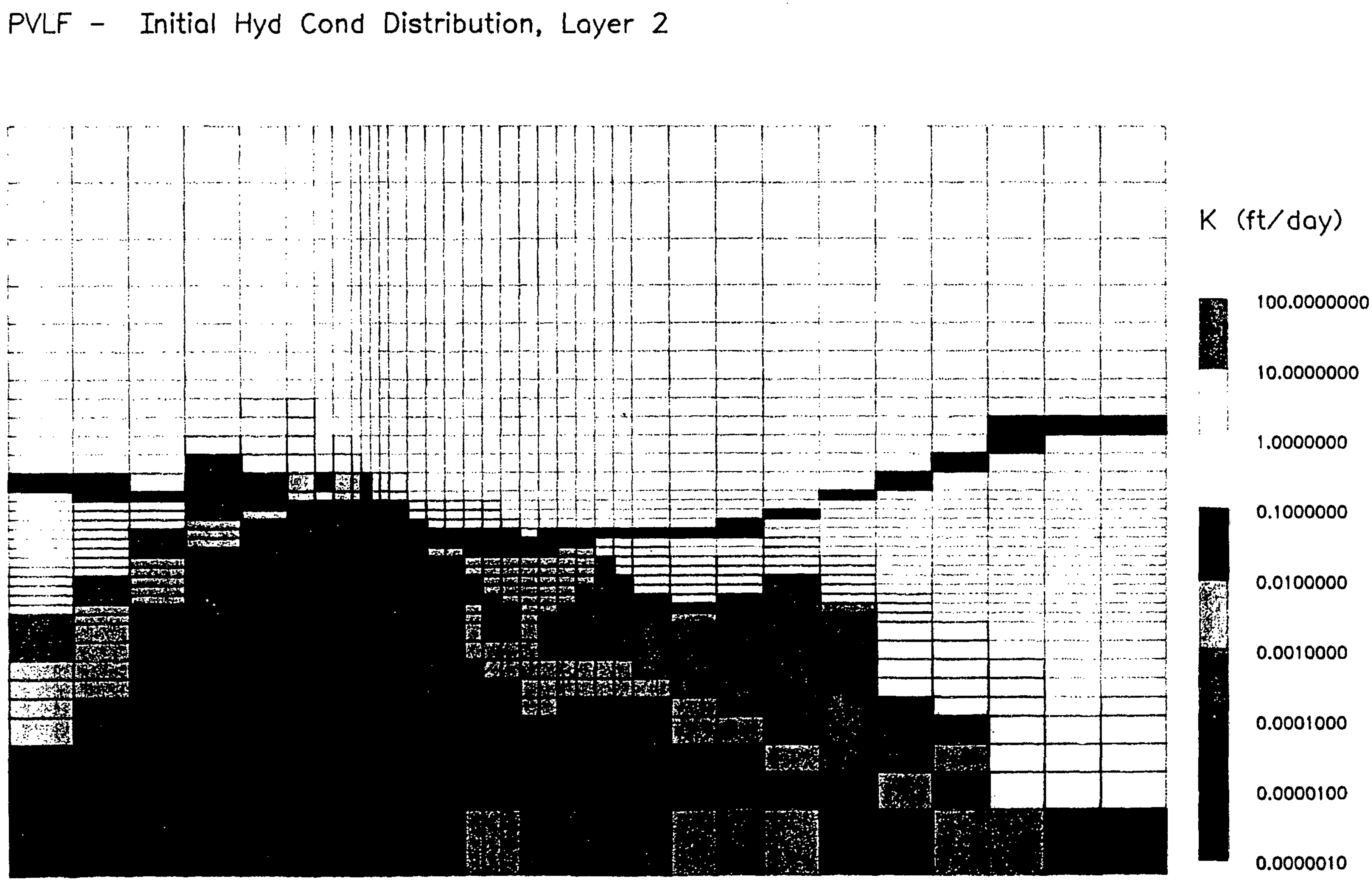

Figure H.2

INITIAL HYDRAULIC CONDUCTIVITY VALUES IN FINITE-DIFFERENCE CELLS, LAYER 2

PVLF - Initial Hyd Cond Distribution, Layer 3

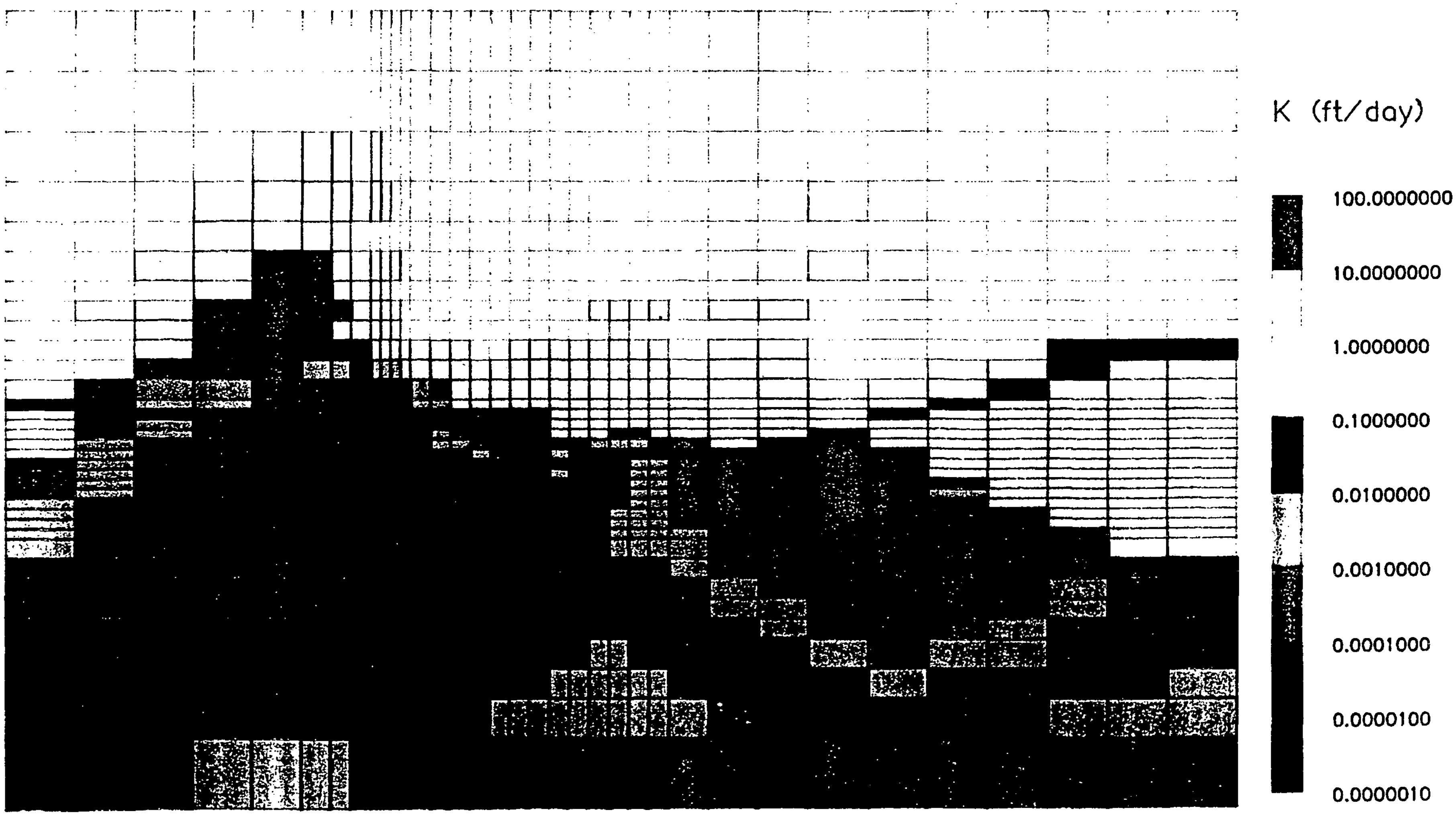

Figure H.3
INITIAL HYDRAULIC CONDUCTIVITY VALUES IN FINITE-DIFFERENCE CELLS, LAYER 3

PVLF - Calibrated Flow Model - Hyd Cond Distribution, Layer 1

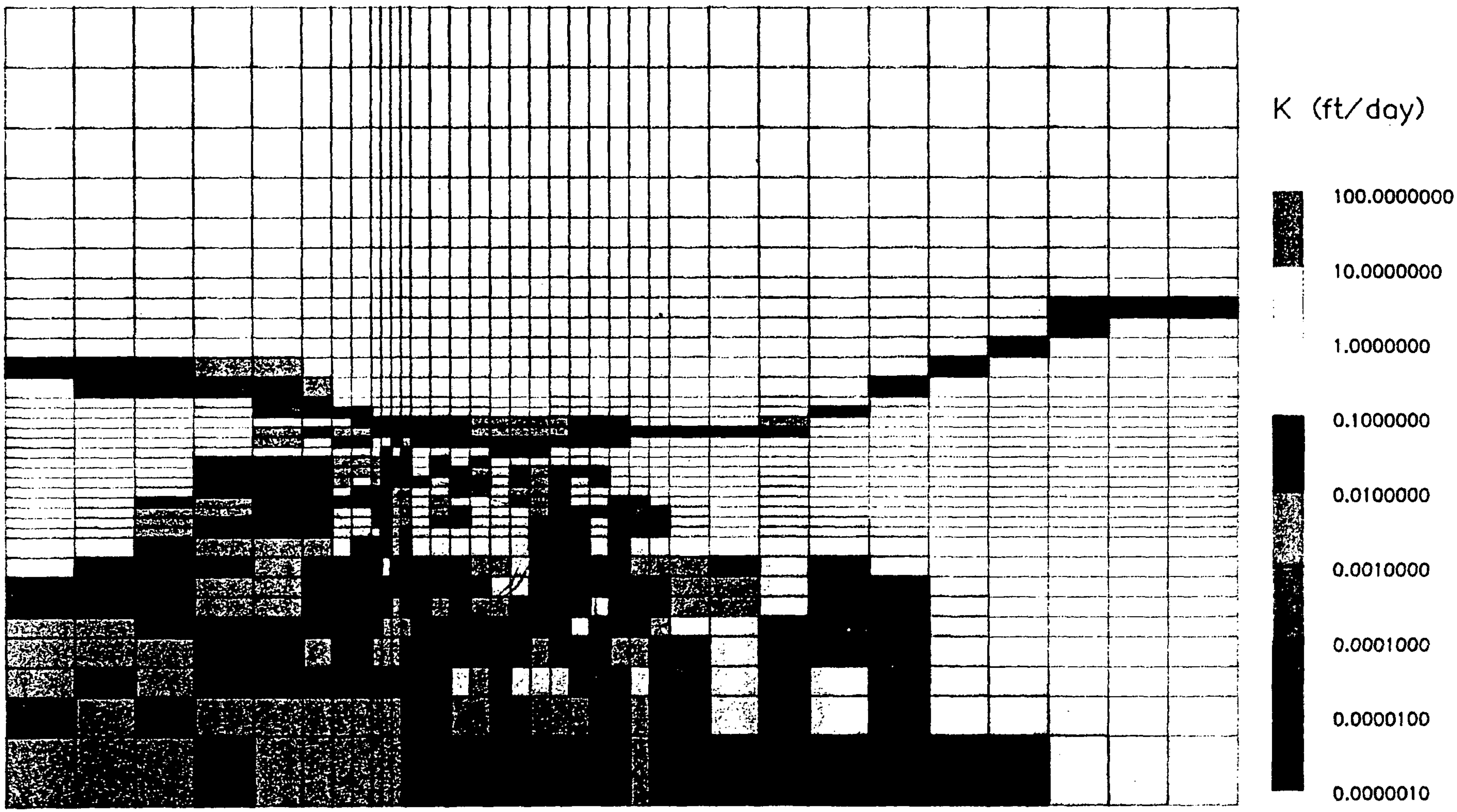

Figure H.4
CALIBRATED HYDRAULIC CONDUCTIVITY VALUES IN FINITE-DIFFERENCE CELLS, LAYER 1

PVLF - Calibrated Flow Model - Hyd Cond Distribution, Layer 2

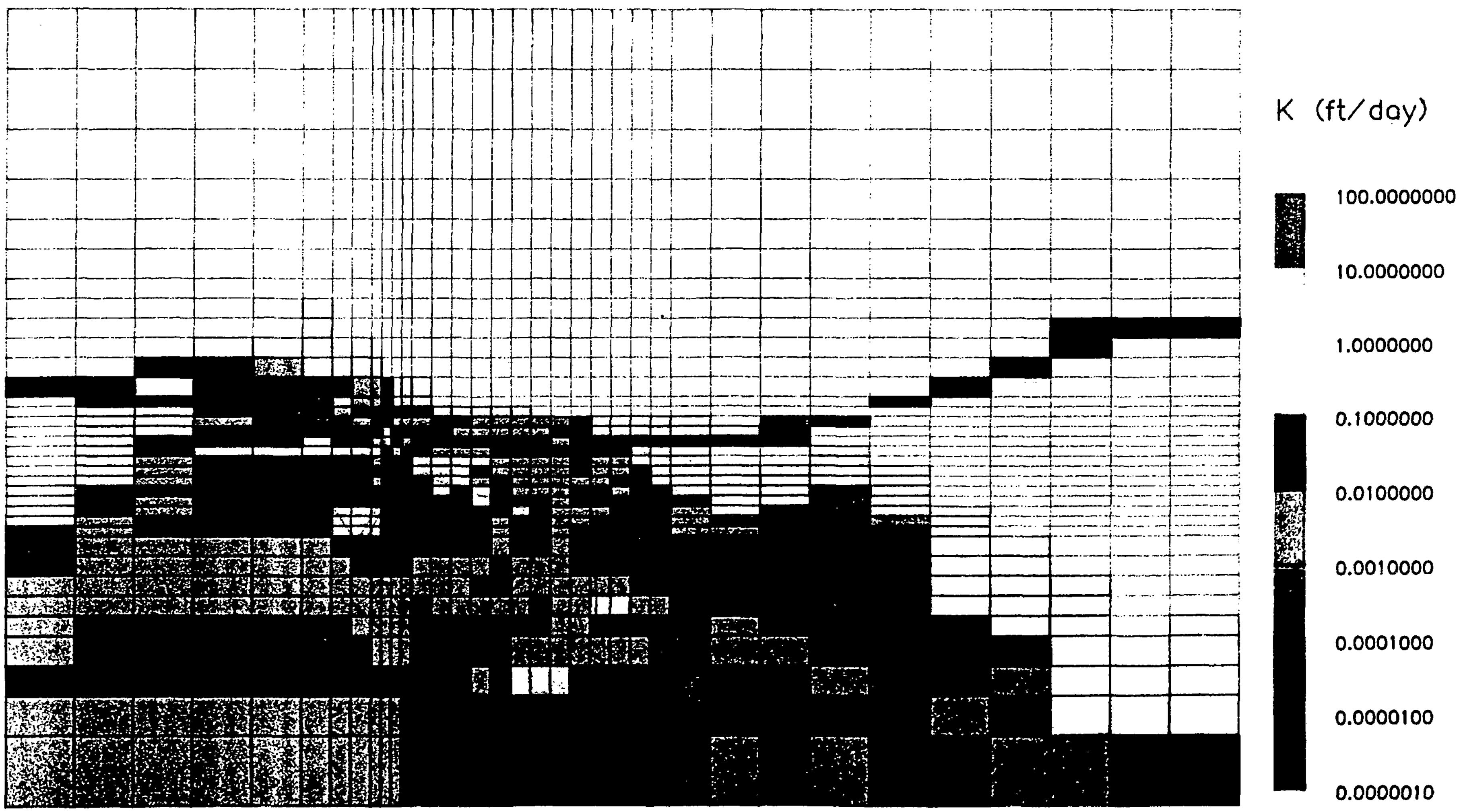

Figure H.5
CALIBRATED HYDRAULIC CONDUCT[illegible]Y VALUES IN FINITE-DIFFERENCE CE[illegible]S, LAYER 2

PVLF - Calibrated Flow Model - Hyd Cond Distribution, Layer 3

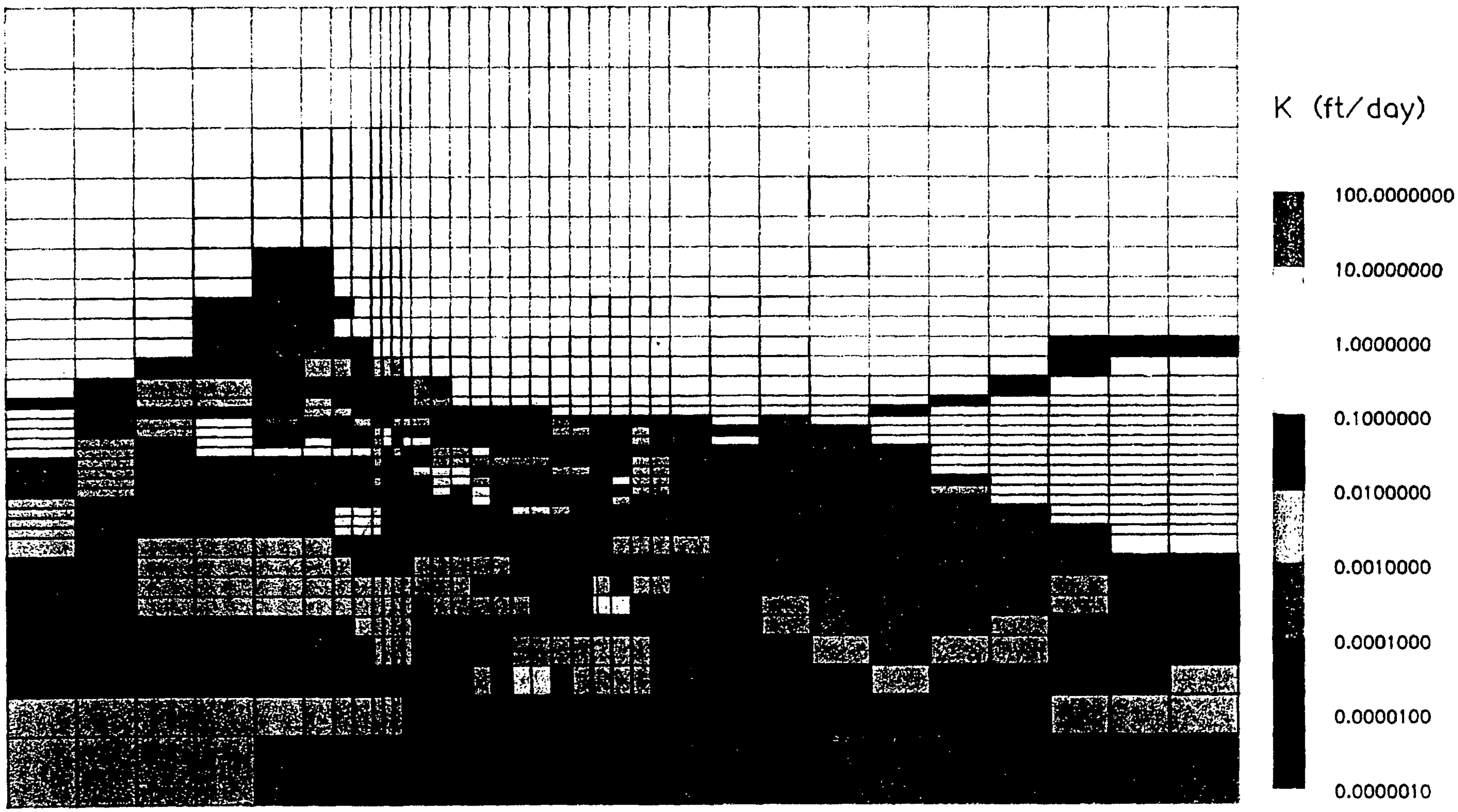

Figure H.6

CALIBRATED HYDRAULIC CONDUCTIVITY VALUES IN FINITE-DIFFERENCE CELLS, LAYER 3

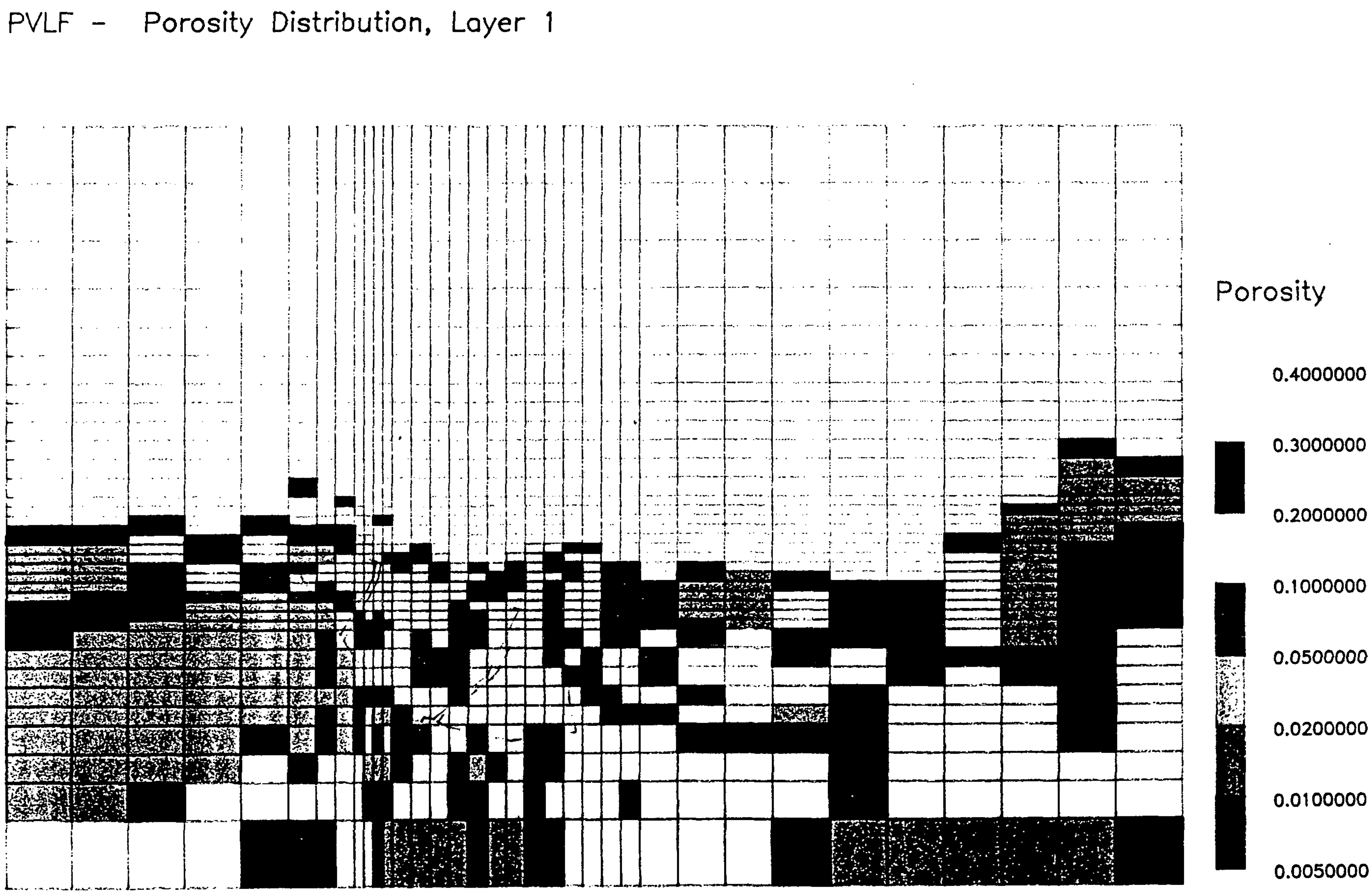

Figure H.7

POROSITY VALUES IN FINIT[E DI]FFERENCE C[EL]LS, LAYER 1

PVLF - Porosity Distribution, Layer 2

Figure H.8

POROSITY VALUES IN FINITE-DIFFERENCE CELLS, LAYER 2

PVLF - Porosity Distribution, Layer 3

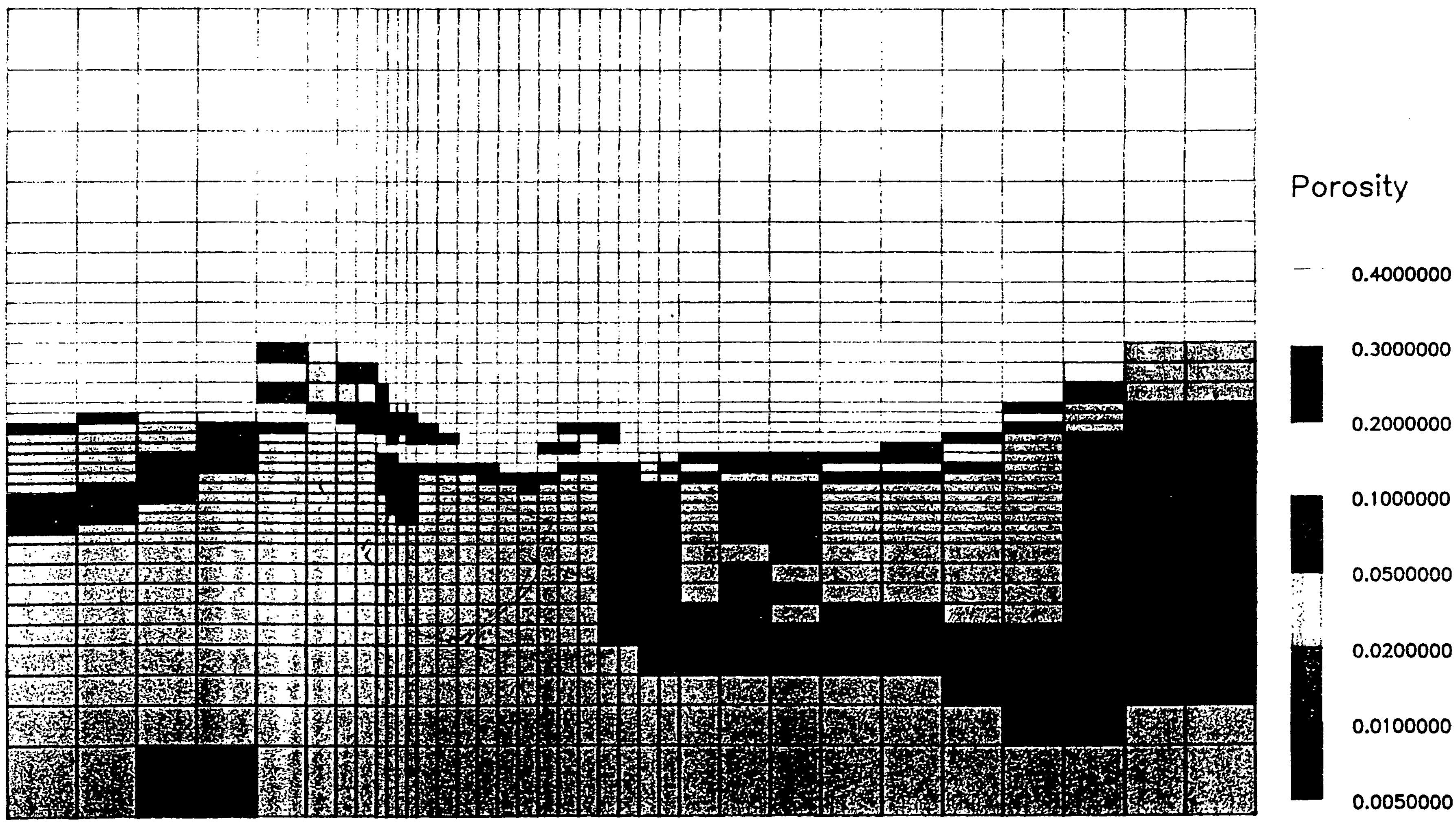

Figure H.9
POROSITY VALUES IN FINITE DIFFERENCE CELLS, LAYER 3

APPENDIX I

GRADIENT ACROSS THE PALOS VERDES LANDFILL

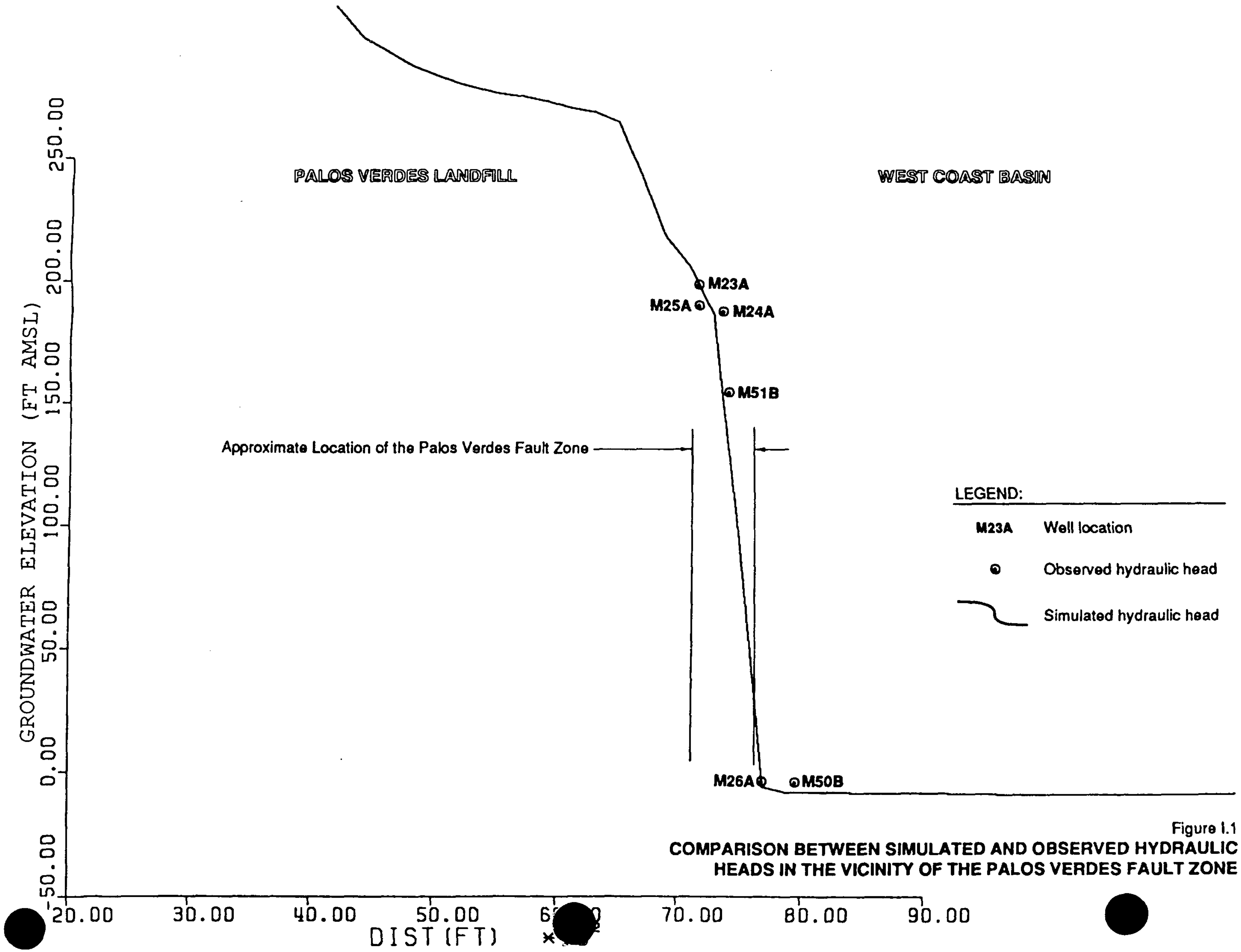

Figure I.1
COMPARISON BETWEEN SIMULATED AND OBSERVED HYDRAULIC HEADS IN THE VICINITY OF THE PALOS VERDES FAULT ZONE